



Development of nickel-catalyzed crosscoupling methodologies for the activation of carbon-oxygen bonds and α -arylation of acetone

Sary Abou Derhamine

► To cite this version:

Sary Abou Derhamine. Development of nickel-catalyzed crosscoupling methodologies for the activation of carbon-oxygen bonds and α -arylation of acetone. Catalysis. Université de Lyon, 2020. English. NNT : 2020LYSE1194 . tel-03351826

HAL Id: tel-03351826

<https://theses.hal.science/tel-03351826>

Submitted on 22 Sep 2021

HAL is a multi-disciplinary open access archive for the deposit and dissemination of scientific research documents, whether they are published or not. The documents may come from teaching and research institutions in France or abroad, or from public or private research centers.

L'archive ouverte pluridisciplinaire **HAL**, est destinée au dépôt et à la diffusion de documents scientifiques de niveau recherche, publiés ou non, émanant des établissements d'enseignement et de recherche français ou étrangers, des laboratoires publics ou privés.

N°d'ordre NNT : 2020LYSE1194



THESE de DOCTORAT DE L'UNIVERSITE DE LYON

opérée au sein de
l'Université Claude Bernard Lyon 1

Ecole Doctorale N° 206
Chimie, Procédés, Environnement

Spécialité de doctorat : Chimie
Discipline : Organométallique et catalyse

Soutenue publiquement le 2/11/2020, par :
ABOU DERHAMINE Sary

Couplages croisés catalysés au nickel : activation de liaisons carbone-oxygène et α -arylation de l'acétone

Devant le jury composé de :

ANDRIOLETTI, Bruno
BOUHADIR, Ghenwa
GRIMAUD, Laurence

Professeur, Univ. Lyon 1
MCF, Université Paul Sabatier, Toulouse
Directrice de Recherche CNRS, ENS Paris

Examineur
Rapporteuse
Rapporteuse

AMGOUNE, ABDERRAHMANE

Professeur, Univ. Lyon 1

Directeur de thèse

MONTEIRO, NUNO

Chargé de recherche, Univ. Lyon 1

Invité

N°d'ordre NNT : xxx



THESE de DOCTORAT DE L'UNIVERSITE DE LYON

opérée au sein de
l'Université Claude Bernard Lyon 1

Ecole Doctorale N° 206
Chimie, Procédés, Environnement

Spécialité de doctorat : Chemistry
Discipline : Organometallics and catalysis

Soutenue publiquement le 2/11/2020, par :
ABOU DERHAMINE Sary

Development of nickel-catalyzed cross-coupling methodologies for the activation of carbon-oxygen bonds and α -arylation of acetone

Devant le jury composé de :

ANDRIOLETTI, Bruno
BOUHADIR, Ghenwa
GRIMAUD, Laurence

Professeur, Univ. Lyon 1
MCF, Université Paul Sabatier, Toulouse
Directrice de Recherche CNRS, ENS Paris

Examineur
Rapporteuse
Rapporteuse

AMGOUNE, ABDERRAHMANE

Professeur, Univ. Lyon 1

Directeur de thèse

MONTEIRO, NUNO

Chargé de recherche, Univ. Lyon 1

Invité

UNIVERSITE CLAUDE BERNARD – LYON 1

Président de l'Université	M. Frédéric FLEURY
Président du Conseil Académique	M. Hamda BEN HADID
Vice-Président du Conseil d'Administration	M. Didier REVEL
Vice-Président du Conseil des Etudes et de la Vie Universitaire	M. Philippe CHEVALLIER
Vice-Président de la Commission de Recherche	M. Jean-François MORNEX
Directeur Général des Services	M. Damien VERHAEGHE

COMPOSANTES SANTE

Faculté de Médecine Lyon-Est –Claude Bernard	Doyen : M. Gilles RODE
Faculté de Médecine et Maïeutique Lyon Sud Charles. Mérieux	Doyenne : Mme Carole BURILLON
UFR d'Odontologie	Doyenne : Mme Dominique SEUX
Institut des Sciences Pharmaceutiques et Biologiques	Directrice : Mme Christine VINCIGUERRA
Institut des Sciences et Techniques de la Réadaptation	Directeur : M. Xavier PERRO
Département de Formation et Centre de Recherche en Biologie Humaine	Directrice: Mme Anne-Marie SCHOTT

COMPOSANTES & DEPARTEMENTS DE SCIENCES & TECHNOLOGIE

UFR Biosciences	Directrice : Mme Kathrin GIESELER
Département Génie Electrique et des Procédés (GEP)	Directrice : Mme Rosaria FERRIGNO
Département Informatique	Directeur : M. Behzad SHARIAT
Département Mécanique	Directeur : M. Marc BUFFAT
UFR -Faculté des Sciences	Directeur : M. Bruno ANDRIOLETTI
UFR (STAPS)	Directeur : M. Yannick VANPOULLE
Observatoire de Lyon	Directrice : Mme Isabelle DANIEL
Ecole Polytechnique Universitaire Lyon 1	Directeur : Emmanuel PERRIN
Ecole Supérieure de Chimie, Physique, Electronique (CPE Lyon)	Directeur : Gérard PIGNAULT
Institut Universitaire de Technologie de Lyon 1	Directeur : M. Christophe VITON
Institut de Science Financière et d'Assurances	Directeur : M. Nicolas LEBOISNE
ESPE	Administrateur Provisoire : M. Pierre CHAREYRON

Acknowledgments

It is a genuine pleasure to express my deep sense of thanks and gratitude to my supervisor Prof. **AMGOUNE** (Abder) for his guidance, kindness and continuous support. I sincerely appreciate and thank Dr. **MONTEIRO** Nuno and Dr. **BOUYSSI** Didier for their highly valuable advices and their excellent experimental training and discussions as well as providing us with an excellent scientific atmosphere that helped us working properly. My sincere appreciations for Dr. **TLILI** Anis for his daily scientific support, timely advices and motivations.

I owe a deep sense of gratitude for our Kind and respectful post-doc Dr. **KRACHKO** Tetiana for her timely suggestions, experimental help and fruitful discussions. In addition, I am thankful for all the members of my team Dr. Antonio **REINA TAPIA**, TALINE **KERACKIAN**, Hugo **Boddaert**, Florian **ORDIERA**, Eman **DOKMAK**, Corentin **Cruché**, Chloé **LHARDY**, Killian **ONIDA** and Louis **VERCHERE**.

I am also thankful for all the CCRMN and CCSM teams for their excellent NMR and HRMS services as well as ILM and Dr. **COMPAGNON** Isabelle for allowing us to use their Labs. I thank Solvias AG Company for their generous donations of Josiphos ligands and complexes.

I wish to greatly thank the French government for the financial support and for allowing us to conduct research at their institutions. A special thanks for the Lebanese university for teaching us how to be successful.

I wish to express my deepest thanks and sincere appreciations for my lovely wife for her encouragement, inspirations and for being always there for me, I can't thank you enough "odo". A special honorable thanks for my parents who raised me to this level and played a major role in shaping my future. Finally, I thank my brother, my sister, my friends and beloved ones for being my strongest power thanks a lot for your unconditional support and advices.

Résumé

Les travaux présentés dans cette thèse ont été réalisés à l'Institut de Chimie et Biochimie Moléculaires et Supramoléculaires, UMR 5246, Université Claude Bernard Lyon-1, sous la direction du Prof. AMGOUNE Abderrahmane et du Dr. MONTEIRO Nuno de septembre 2017 à octobre 2020.

La recherche présentée ci-après intitulée "Couplages croisés catalysés au nickel : activation de liaisons C-O et α -arylation de l'acétone" visait à développer et comprendre de nouvelles réactions de formation de liaisons carbone-carbone par catalyse au nickel. Ce travail se décompose en deux parties. La première partie se concentre sur l'activation de liaisons C_{Ar}-O des éthers aryliques et leur couplage avec divers nucléophiles organométalliques et non organométalliques (alcènes, alcynes... etc). Dans cette partie nous avons cherché, d'une part, à comprendre l'influence très particulière du ligand sur les performances catalytiques. D'autre part, nous avons développé un système catalytique dual nickel/aluminium qui s'est avéré très actif pour le couplage d'aryl éthers avec des esters boroniques.

Dans la deuxième partie, nous avons exploré l' α -arylation mono-sélective de l'acétone avec des chlorures d'aryle et des dérivés de phénol catalysée par le nickel. Un travail d'optimisation catalytique a d'abord été entrepris avec un système catalytique à base de nickel(0) supporté par un ligand diphosphine. Nous avons pu découvrir un système catalytique permettant le couplage d'une large sélection de chlorures d'aryle, ainsi que de dérivés de phénol. Nous avons ensuite entrepris des études mécanistiques (réaction stœchiométriques, caractérisation d'intermédiaires catalytiques, suivi RMN) qui nous ont permis de valider un processus redox à deux électrons Ni⁰/Ni^{II}. Ensuite, nous avons effectué une étude mécanistique approfondie pour vérifier toutes les voies d'inhibition

et de désactivation possibles qui pouvaient avoir lieu et expliquer la sélectivité observée. Finalement ces études nous ont aussi permis de mettre en lumière des performances catalytiques améliorées avec des catalyseurs de Nickel(II) stables à l'air et disponibles dans le commerce.

Abstract

The work presented in this dissertation was carried out at the Institut de Chimie et Biochimie Moléculaires et Supramoléculaires, UMR 5246, Claude Bernard university Lyon-1, under the guidance of Prof. AMGOUNE Abderrahmane and Dr. MONTEIRO Nuno from September 2017 to October 2020.

The research presented hereafter entitled "Development of nickel-catalyzed cross-coupling methodologies for the activation of carbon-oxygen bonds and α -arylation of acetone" aimed to develop and understand the formation of new C-C bonds under Ni-catalysis. It was decomposed in two parts. The First part focuses on the activation of C_{Ar}-O bonds of aryl ethers and coupling them with several organometallic and non-organometallic nucleophiles (alkenes, alkynes...etc). In this part, we aimed to understand the very particular influence of the ligand on the catalytic performance of the catalyst. In addition, we developed a dual nickel/aluminum catalytic system that proved very active for the coupling of aryl ethers with boronic esters.

In the second part, we explored the Nickel-catalyzed mono-selective α -arylation of acetone with aryl chlorides and phenol derivatives. Catalytic optimization work was first explored with a Nickel(0)-based catalytic system supported by a diphosphine ligand. We were able to discover a catalytic system allowing the coupling of a wide selection of aryl chlorides, as well as phenol derivatives. We then made mechanistic studies (stoichiometric studies, characterization of catalytic intermediates, NMR follow-up) that allowed us to validate a two-electron redox Ni⁰/Ni^{II} process. Next, we conducted an in-depth mechanistic study to verify all the possible inhibition and deactivation pathways that could occur as well as explaining the observed selectivity. Finally, these studies have also allowed us to discover an improved catalytic performance with an air-stable and commercially available Nickel(II) catalyst.

Table of contents

List of abbreviations	12
General experimental information.....	15
General introduction on nickel chemistry	19
1. Overview.....	19
2. Nickel v.s Palladium in cross-coupling catalysis	21
3. Elementary reactions with nickel.....	24
4. Catalytic cycles with Ni (Mechanisms)	28
5. Some recent applications of nickel in cross-coupling catalysis	29
6. Scope of the PhD work and organization of the manuscript.....	36
7. References	37

Part I

Dual Ni/Lewis acid catalytic system for the cross-coupling of aryl ethers

Introduction.....	45
--------------------------	-----------

Chapter I: State of the art of nickel-catalyzed cross-coupling of aryl ethers.

I. Carbon-Carbon bond formation.....	50
1. Cross-coupling with Grignard reagents	50
2. Cross-coupling with organolithium reagents	56
3. Cross-coupling with organolanthanides.....	58
4. Cross-coupling with organozincates	59
5. Cross-coupling with organoaluminium derivatives	60
6. Cross-coupling with organoboron derivatives	64
II. Carbon-Heteroatom bond formation.....	70
1. Carbon-Nitrogen bond formation: Cross-coupling with amines.....	70
2. Carbon-Boron bond formation: Borylation of aryl ethers	72
3. Carbon-Silicon bond formation: Silylation of aryl ethers.....	73
III. Reductive cleavage of C–O bond	76
IV. C-H arylation with aryl ethers derivatives	85
V. Cross-coupling reactions of vinylic and benzylic ethers	88
VI. Summary	90
VII. Research objective	95

1. Design of new ligands.....	95
2. LA assisted transformations.....	95
VIII. References	97

Chapter II: Investigations on Ni/Lewis acid catalyzed Suzuki-Miyaura reaction with aryl ethers.

I. Evaluation of new ligands.....	106
1. Introduction.....	106
2. Bidentate bis-NHC ligands	106
3. Monodentate ligands: electron rich phosphine with remote steric effects	109
4. Evaluation of ligands for nickel-catalyzed cross-coupling of aryl ethers with phenyl boronic esters.....	112
II. Computational investigations on the influence of phosphines on the C-O bond activation step.....	114
III. Lewis acid assisted Suzuki-Miyaura cross-coupling of aryl ethers	118
1. Introduction.....	118
2. Evaluation of Lewis acid co-catalysts for the nickel-catalyzed Suzuki-Miyaura cross-coupling of aryl ethers with ICy ligands	120
3. Evaluation of Lewis acids co-catalysts for the nickel-catalyzed Suzuki-Miyaura cross-coupling of aryl ethers with PCy ₃ ligand.....	125
4. Ligand screening assisted by Al(O ^t Bu) ₃	127
5. Scope of boronic esters with L.A.....	128
6. Scope of aryl ethers with L.A	129
IV. Computational studies.....	131
1. Starting mechanistic hypothesis.....	131
2. Influence of the Lewis acid co-catalyst	132
3. Transmetallation step	134
4. β -hydride elimination <i>v.s</i> Transmetallation	136
5. Alkylation <i>v.s</i> Transmetallation.....	137
6. Summary and Proposed mechanism	138
7. Computational details	139
V. Experimental part.....	141
VI. References.....	151

Chapter III: Investigations on Ni/Lewis acid catalyzed cross-coupling of aryl ethers with alkenes

I.	Introduction.....	157
II.	State of the art.....	157
1.	Heck-type cross-coupling reactions with phenol derivatives	157
2.	Difunctionalization of alkenes.....	159
3.	Research objective	161
III.	Investigations on Heck-type and difunctionalization reactions of aryl ethers.....	162
1.	Synthesis of model aryl ethers featuring pendant alkene moieties	162
2.	Catalytic studies.....	164
3.	Investigations on the difunctionalization of ether-tethered alkenes.....	168
IV.	Summary.....	180
V.	Experimental part.....	182
VI.	References.....	194

Part II

Nickel-Catalyzed Mono-Selective α -Arylation of Acetone with Aryl Chlorides and Phenol Derivatives

Introduction.....	200
--------------------------	------------

Chapter I: Bibliographic survey on transition metal catalyzed α -arylation of ketones

I.	Palladium-catalyzed α -arylation of substituted ketones	204
II.	Nickel-catalyzed α -arylation of substituted ketones.....	207
III.	Palladium-catalyzed α -arylation of acetone.....	218
IV.	Conclusion	220

Chapter II: Development of a nickel-catalyzed mono-selective α -arylation of acetone

I.	Objective and envisioned methodology with nickel.....	223
II.	Catalytic studies.....	224
1.	Screening of ligands.....	224
2.	Optimization experiments.....	226
3.	Screening of Ni ^{II} air stable complexes.....	228
III.	Scope of the reaction.....	229
1.	General scope with aryl chlorides.....	229
2.	Scope with Ni ^{II} pre-catalysts.....	231
3.	Reaction with phenol derivatives.....	232

4. Scope of ketones	234
IV. Mechanistic studies.....	237
1. Proposed mechanism and key questions.....	237
2. Nature and reactivity of Ni ⁰ active species	238
3. Thermal stability and reactivity of Ni ^{II} –aryl intermediates.....	242
4. Evaluation of catalytic competence of Ni ⁰ and Ni ^{II} intermediates.....	244
V. Summary.....	245
VI. Experimental part.....	247
VII. References.....	272
General conclusion and outlook	281

I. List of abbreviations

SET: Single Electron Transfer

HAA: Halogen Atom Abstraction

HAT: Hydrogen Atom Transfer

S_EAr: Electrophilic Aromatic Substitution

L: General ligand

L.A.: Lewis Acid

COD: 1,5-cyclooctadiene

acac: acetoacetate

SIPr: 1,3-Bis(2,6-di-*i*-propylphenyl)imidazolidin-2-ylidene

BBN: borabicylononane

IPrHCl: 1,3-Bis-(2,6-diisopropylphenyl)imidazolinium chloride

NHC: *N*-Heterocyclic Carbene

Ar: Generic aryl group

BDE: Bond dissociation energy

Cy: Cyclohexyl group

d: Day

dcype: 1,2-Bis(dicyclohexylphosphino)ethane

DFT: Density functional theory

Dipp: (2,6-Diisopropyl)phenyl group

DME: 1,2-Dimethoxyethane

Dppf: 1,1'-Bis(diphenylphosphino)ferrocene

Et: Ethyl group

EWG: Electron-withdrawing group

equiv: Equivalent

h: Hour

***i*Pr:** Isopropyl

IR: Infrared

Me: Methyl group

min: Minute

NMR: Nuclear magnetic resonance

OTf: Triflate

O.A: Oxidative addition

Ph: Phenyl

Pin: Pinacolborane

R: General alkyl group

RT: Room temperature

R.E: Reductive elimination

^tBu: tert-butyl group

tmeda: N,N,N',N'-tetramethylethane-1,2-diamine

TS: Transition state

T.M: Transmetallation

X: I, Br, Cl, F

XRD: X-ray diffraction

II. General experimental information

1. General information

All catalytic reactions and stoichiometric studies were carried out in an Argon filled glove box (JACOMEX) or by using standard Schlenk techniques. All solvents (acetone, toluene, dioxane, diethyl ether, THF, pentane...etc) were taken from an SPS solvent purification system or purchased extra dry from Sigma-Aldrich, Alfa-Aesar, or Fluorochem. Water was degassed by bubbling argon and all the other solvents were degassed by using freeze-pump-thaw technique three times. Deuterated solvents C_6D_6 , Acetone- D_6 , Toluene- D_8 , $CDCl_3$, and MeOD were degassed and stored over 4 Å activated molecular sieves.

The chemicals were purchased in reagent grade purity from Alfa-Aesar, Fluorochem, abcr GmbH TCI and Sigma-Aldrich. They were degassed for all catalytic tests and used without further purification for all standard organic reactions. Argon and Helium were purchased from Air Liquide.

a. NMR spectroscopy

Liquid state nuclear magnetic resonance spectrums of 1H , ^{11}B , ^{13}C , ^{19}F , and ^{31}P nuclei were recorded at RT using Bruker DRX 300, 400 or 500 MHz spectrometers. Chemical shifts (δ) are expressed in parts per million. 1H and ^{13}C chemical shifts are referenced to residual solvent signals. ^{19}F chemical shifts are relative to CFC_3 . Crude 1H and ^{19}F NMR yields were determined using 1,3,5-Trimethoxybenzene ($C_9H_{12}O_3$, 1H NMR δ 6.08 (3H, s, C_6H_3), 3.76 (9H, s, 1,3,5- CH_3)) and α,α,α -trifluorotoluene ($PhCF_3$, ^{19}F NMR δ -63.72 ppm) as internal standards. Spectra were reported as follows: chemical shift (δ ppm), integration, multiplicity (s=singlet, d=doublet, t=triplet, q=quartet, m=multiplet, br=broad), and coupling constants (reported in Hz). 1H and ^{13}C resonance signals were attributed by means of 2D COSY, HSQC, and HMBC experiments.

GENERAL INTRODUCTION

b. GC-MS analysis

GC-MS analyses were performed using Shimadzu GC-2010 Gas Chromatograph coupled to a GCMS-QP2010S mass spectrometer using helium as the carrier gas at a flow rate of 1.19 mL/min and an initial oven temperature of 60 °C. The column used was a Zebron 5ms (30 m length, 0.25 mm diameter and 0.25 µm thickness) lined with a mass (EI 0.7 kV) detection system. The injector temperature was 250 °C. The detector temperature was 250 °C. GC-MS yields were obtained by using dodecane as internal standard. Calibration curves of the organic compounds were plotted using at least 6 points at different concentrations. The plot was a straight line passing through the origin with $R^2 > 0.98$ and the yields were determined using (**Equation 1** and **Equation 2**). First, we get n_{exp} from equation 1 and we substitute it in equation 2 to get the yield.

Equation 1

$$\frac{A_{exp}}{A_{st}} = \frac{\Delta y}{\Delta x} \times \frac{n_{exp}}{n_{st}}$$

Equation 2

$$Yield_{exp} = \frac{n_{exp}}{n_{th}}$$

Where: A_{exp} = area of the product peak

A_{st} = area of the internal standard

n_{exp} = moles of the product experimentally

n_{st} = moles of the internal standard

n_{th} = moles of the product theoretically

$\Delta y/\Delta x$ = slope

GENERAL INTRODUCTION

c. HRMS

The high-resolution mass spectra (HRMS) were recorded by direct introduction in a positive and negative ion mode on a hybrid quadrupole time-of-flight mass spectrometer (MicroTOFQ-II, Bruker Daltonics, Bremen) with an Electrospray Ionization (ESI) ion source. The solutions were infused at 180 μ L/h. The mass range of the analysis was 50-1000 m/z and the calibration was done with sodium formate.

d. Column chromatography

Manual flash chromatographies were performed on silica gel (40-63 μ m) columns and automated high-resolution chromatography were performed by Combiflash^{RF} 150 Model.

e. Microwave

The microwave-assisted synthesis was carried out in an InitiatorTM single-mode microwave cavity producing controlled irradiation at 2.45 GHz (Biotage AB, Uppsala). The reactions were run in sealed vessels (0.5 to 20 mL) and magnetic stirring was used. A variable power source was employed (max 400 W) to reach the desired temperature and then to maintain it in the vessel during the programmed period.

f. X-ray diffraction

Single-crystal X-ray diffraction studies were carried out with a Gemini diffractometer and the related analysis software. An absorption correction based on the crystal faces was applied to the data sets (analytical). The structures were solved by direct methods using the SIR97 program, combined with Fourier difference syntheses and refined against F using reflections with $[I/\sigma(I) > 3]$ by using the CRYSTALS program. All atomic displacement parameters for non-hydrogen atoms were refined with anisotropic terms. The hydrogen atoms were theoretically located on the basis

GENERAL INTRODUCTION

of the conformation of the supporting atom and were refined by using the riding model. For each structure, the obtained Flack parameter value has been refined in order to show that the obtained value is close to 0, considering associated error value and not fixed to 0.

g. Theoretical calculations

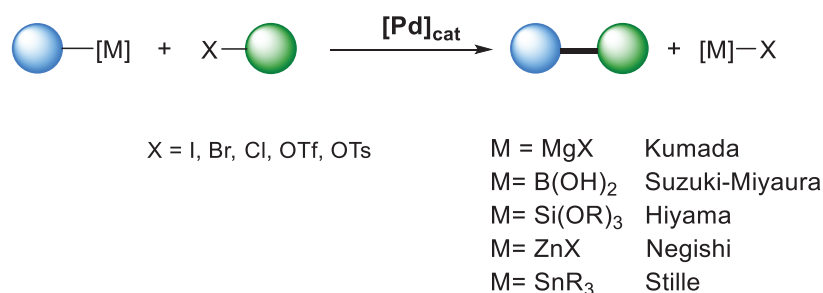
The computational studies was carried out by **Dr Miguel REINA** in the framework of a collaboration with the group of **Dr Lionel Perrin** within ICBMS. DFT calculations were carried out at the BP86-D3/def2TZVP-SDD//BP86-D3/6-31G(d)-SDD level of the theory and taking into account solvent effects (PCM toluene).

III. General introduction on nickel chemistry

1. Overview

In the area of organic chemistry, cross-coupling reactions represent one of the most powerful methodologies for the formation of carbon-carbon and carbon-heteroatom bonds.¹ After decades of research in this domain, several coupling transformations that seemed impossible by classical organic synthesis are feasible nowadays thanks to transition metal catalysts. This methodology makes a revolutionary change at the industrial and academic levels, finding its application in several domains far from pharmaceuticals and agrochemicals to conjugated polymers for material science and advanced materials.^{2,3} In 2010, Richard Heck, Ei-ichi Negishi, and Akira Suzuki were awarded the Noble Prize in chemistry for their outstanding work in this domain.^{4,5}

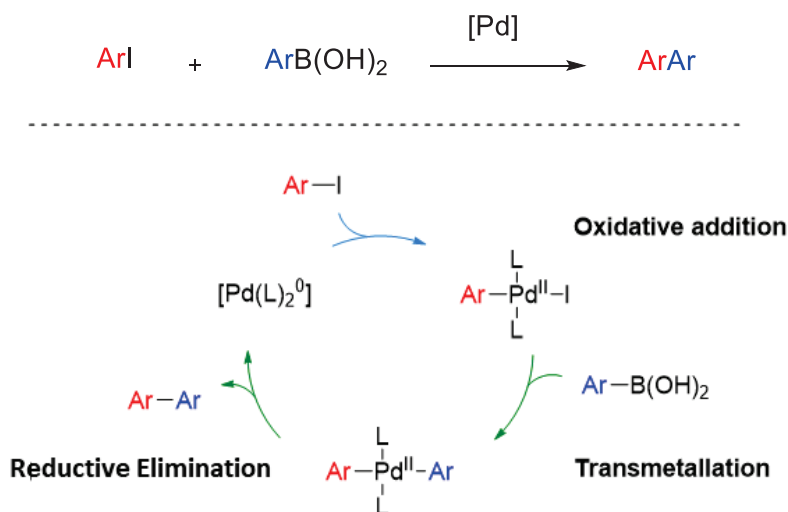
In the field of transition metal-catalyzed cross-couplings (**Scheme 1**), the Suzuki-Miyaura reaction is the most popular transformation.¹ The mild reaction conditions, commercial availability and stability of boronic acids, as well as the wide functional group compatibility make this coupling ideal for the preparation of high-value molecules. The Suzuki-Miyaura reaction is one of the most efficient transformations for the formation of $C_{sp^2}-C_{sp^2}$ bonds.²



Scheme 1: General scheme for cross-coupling reactions.

The Suzuki-Miyaura reaction involves the use of palladium catalysts and proceeds via a $\text{Pd}^0/\text{Pd}^{\text{II}}$ $2 e^-$ redox process (**Scheme 2**). The general mechanism of the reaction takes place through

three main elementary steps (i) oxidative addition (O.A), (ii) transmetallation (T.M), and (iii) reductive elimination (R.E).



Scheme 2: General mechanism for Suzuki-Miyaura reaction.

The advances of C-C bond cross-coupling inspired chemists to develop additional cross-coupling reactions like α -arylation, direct arylation by C-H activation, and decarboxylative couplings, which are of high interest.¹ Major advances were made in the last few decades. However, cross-coupling reactions of electrophiles beyond aryl halides, such as phenol derivatives or aryl fluorides are still premature.

Owing to their well-documented and predictable reactivity and selectivity, palladium-based catalysts dominate the field of transition metal-catalyzed cross-coupling reactions. After decades of research, other transition metals such as nickel, copper, iron, and cobalt were found to provide interesting reactivities in numerous transformations being a possible alternative to palladium.⁶ These first-row transition metals offer very interesting advantages due to their high abundance and low cost compared to second and third-row transition metals.

2. Nickel v.s Palladium in cross-coupling catalysis

One of the most promising alternative to palladium is nickel, which belongs to the same group and shares similar chemical properties since both of them are d^{10} transition metals. Nickel is much more abundant in the earth's crust than palladium as well as being about 2000 times less expensive than Pd and 10000 times less expensive than Pt as bulk metal.⁷ The ability of Ni to catalyze cross-coupling reactions was discovered much earlier than palladium in the early 1900s, but only recently, its potential was exploited.¹ Beyond the economic interest, nickel also features specific fundamental properties and reactivities. Various reaction mechanisms, complementary to those classically observed with palladium, have been shown to be achievable with nickel. Important progress was made in the last decade showing that Ni displays very interesting reactivities and selectivities in many catalytic transformations like hydrogenation, nucleophilic allylation, oligomerization, cycloisomerization and reductive couplings.⁸ The specific fundamental properties of nickel and their reactivity in catalytic cross-coupling reactions has been recently summarized in several reviews, highlighting the distinct mechanistic scenarios and unique transformations achievable with nickel catalysts.^{9,10,7}

In this section, a brief summary of the key differences between Pd and Ni catalysts as well as the characteristic properties and behavior of nickel species in the context of cross-coupling reactions will be presented.

a. Intrinsic properties of nickel vs. palladium

Nickel and palladium are both d^{10} transition metals but these two metals present distinctive properties and reactivities (**Table 1**).¹⁰ Regarding the accessible oxidation states with these metals, palladium has three main oxidation states **Pd⁰**, **Pd^{II}** and **Pd^{IV}** accessible in catalysis and mostly

two-electron oxidation processes via $\text{Pd}^0/\text{Pd}^{\text{II}}$ are operative with palladium catalysts. Nickel displays a broader palette of oxidation states going from Ni^0 , Ni^{I} , Ni^{II} , Ni^{III} to Ni^{IV} . As a consequence, the occurrence of two-electron redox processes as well as single electron transfer processes (SET) are easily achievable with nickel catalysts.¹⁰ The $\text{M}^{\text{II}}/\text{M}^0$ reduction potential is lower with nickel enabling the catalyst to be regenerated without the addition of an external reductant or base.

The electronegativity of palladium is much higher than nickel, making nickel more nucleophilic than palladium, which plays a significant role on the elementary steps. Nickel tends to be more reactive for oxidative addition, while palladium is more reactive towards reductive elimination.

Table 1: Comparative physical and chemical properties of palladium and nickel.

Properties	Pd	Ni
oxidation states	$\text{Pd}^0/\text{Pd}^{\text{II}}/\text{Pd}^{\text{IV}}$	$\text{Ni}^0/\text{Ni}^{\text{I}}/\text{Ni}^{\text{II}}/\text{Ni}^{\text{III}}$
Mechanisms	2 e ⁻ redox process	2 e ⁻ redox + SET process
Reduction potential E^0/V for $\text{M}^{\text{II}}/\text{M}^0$	0.951	-0.257
Electronegativity	2.2	1.8
Nucleophilicity	Less nucleophilic	More nucleophilic
Elementary steps	Facile R.E	Facile O.A
Metal-Ligand bond	Longer Pd-L bonds	Shorter Ni-L bonds
BDE of [M]-C bond (kcal/mol)	$\text{BDE}_{\text{Pd-C}} = 48.3\text{--}55.2$	$\text{BDE}_{\text{Ni-C}} = 38.0\text{--}51.1$
Atomic radius (pm)	169	149

b. Ligand binding and stability

The cleavage of the metal-ligand is very important in catalysis in order to exchange ligands and access lower ligated complexes. Ni-ligand bond is usually shorter than Pd-ligand bond. The

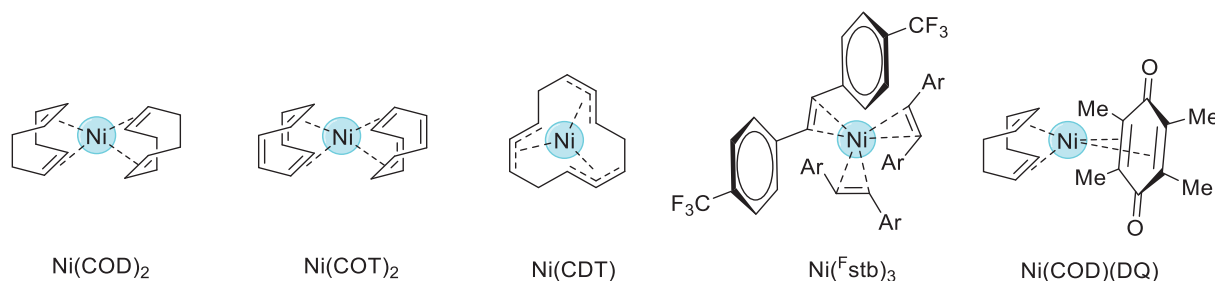
metal-phosphine bond was evaluated with M^{II} and M^0 species. For $M^{II}L_2X_2$ complexes the dissociation of the Ni–P bond is easier [Ni–P (24.5 kcal/mol) < Pd–P (32.1 kcal/mol)]. However, with M^0L_2 complexes the Ni–P bond is stronger [Pd–P (33.6 kcal/mol) < Ni–P (39.7 kcal/mol)]. This indicates that the dissociation of phosphines is easily accessible with Ni^{II} complexes, whereas the Ni–P bond becomes much stronger and stable with Ni^0 species. In addition, the binding of alkenes and alkynes to nickel is much stronger ($\Delta E = 34.3$ and 41.6 kcal/mol, respectively) compared to palladium ($\Delta E = 16.1$ – 23.7 kcal/mol). The BDE of the metal-carbon sigma bond is generally weaker with nickel, making it more reactive than palladium (**Table 1**). Additionally, the homolytic cleavage of the M–C bond is also easier with nickel allowing the contribution of SET processes in nickel catalysis.^{10,11}

In addition, Ni atomic size is 24% smaller than Pd, and as a consequence, the same ligand will occupy more buried volume around Ni than Pd (more steric hindrance). This higher steric hindrance and occupied volume around Ni may render substrate binding and subsequent O.A more difficult. For that reason, most of the ligands used with Pd are unreactive with Ni, preventing O.A to take place due to steric hindrance.¹²

c. Sources of nickel precursors

Even though several Ni^{II} pre-catalysts are commercially available, Ni^0 sources are very limited due to their high instability. The major Ni^0 source is bis(cyclooctadiene)nickel(0) $Ni(COD)_2$ which is predominantly used in catalysis. Interestingly, few Ni^0 complexes were reported as alternatives to $Ni(COD)_2$, such as bis(cyclooctatetraene)nickel(0) $Ni(COT)_2$ and bis(cyclododeca-1,5,9-triene)nickel(0) $Ni(CDT)_2$, but they are highly unstable. More recently, two air-stable Ni^0 complexes were reported: $Ni^0(F^t\text{sb})_3$ using *p*-CF₃-stilbene ligands and $Ni(COD)(DQ)$

stabilized by duroquinone.^{13,14} They seem very promising as interesting alternatives to $\text{Ni}(\text{COD})_2$, and $\text{Ni}(\text{COD})(\text{DQ})$ is now commercially available (**Scheme 3**).

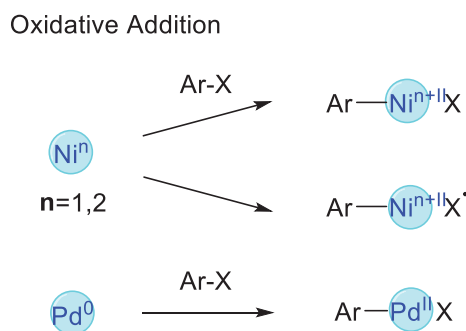


Scheme 3: Sources of Ni^0 precursors. $\text{Ar} = p\text{-CF}_3\text{-phenyl}$.

3. Elementary reactions with nickel

a. Oxidative addition

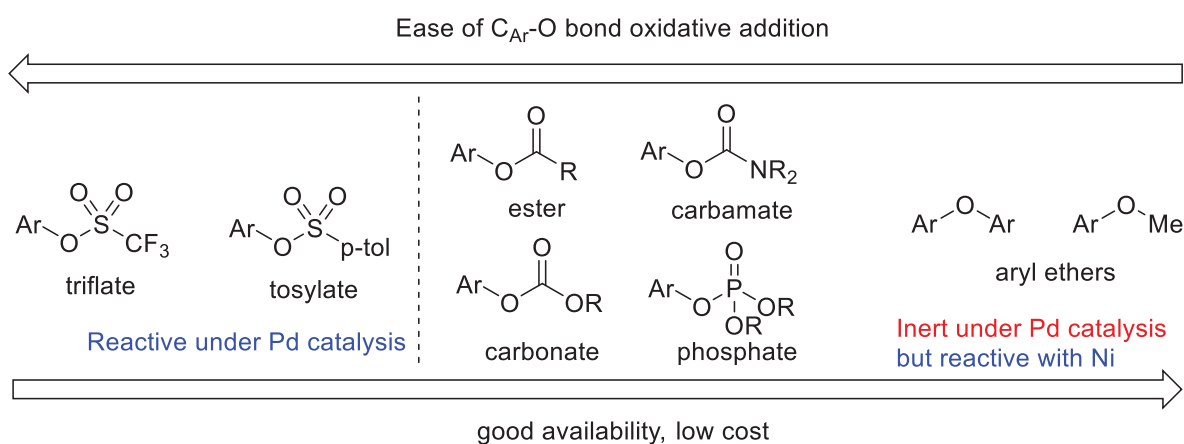
Oxidative addition is usually the step that initiates the catalytic cycle, where $[\text{Ni}(\text{L})_2^n]$ catalyst makes insertion in between Ar-X bond and forms the Ni^{n+II} O.A intermediate (**Scheme 4**). Since nickel provides ready access to diverse oxidation states ranging from Ni^0 to Ni^{IV} , it can make O.A from Ni^0 or Ni^I pre-catalysts through the two-electron pathways $\text{Ni}^0/\text{Ni}^{II}$ and $\text{Ni}^I/\text{Ni}^{III}$, respectively. In contrast, palladium can only make O.A via the $\text{Pd}^0/\text{Pd}^{II}$ pathway.^{15,11,7}



Scheme 4: Oxidative addition with Ni and Pd .

This transformation is controlled by several factors, mainly the electronic factor, the electron density on the metallic center, and the nature of the metal, ligand, and substrate. In general, when the metallic center is richer in electrons the oxidative addition becomes easier. In addition, since O.A needs the transfer of two electrons from the metallic center to the substrate, the more the metallic center is willing to give those electrons (more nucleophilic) the easier the oxidative addition will be. Since nickel is much more nucleophilic than palladium, the O.A with nickel becomes much easier enabling the activation of stronger bonds.

With respect to the substrate, the more electrophilic the substrate the easier the O.A will be. In contrast, the stronger the C-X bond, the harder the oxidative addition is, making several electrophiles like aryl ethers and aryl fluorides highly challenging for cross-coupling reaction due to the robustness, high strength and elevated dissociation energies of C_{aryl}-OMe and C_{aryl}-F bonds. These challenging substrates which are of high synthetic interest are much more reactive (if not only) under Ni catalysis (**Scheme 5**).¹⁶



Scheme 5: Comparison of Ni and Pd reactivities toward challenging substrates as a function of substrate availability and price

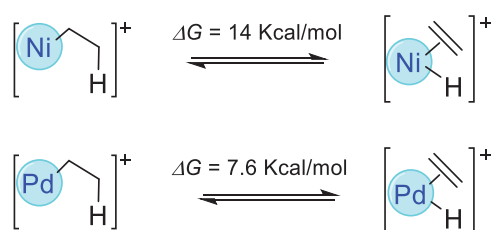
In addition, the nature of the ligands and their ability to donate and accept electrons through their orbitals have a significant effect in improving the nucleophilicity of the metallic center, and

so, the more σ -donating and less π -accepting ligands like NHC's, are usually the best ligands for O.A with nickel.

b. Transmetallation and β -Hydride elimination

Transmetallation reaction is the exchange of the organic moiety from the organometallic coupling partner (e.g, ArMgX) to the metallic center by the halide (**Scheme 6**). This reaction is usually irreversible and does not change the oxidation state, electronic count and coordination numbers of the metallic center. While transmetallation for aryl groups is common with palladium, the transfer of alkyl groups is much more challenging due to the high propensity of Pd to undergo β -hydride elimination giving a new reduced byproduct (**Scheme 6**). Interestingly, β -hydride elimination Gibbs free energy is much higher with nickel than palladium (by 7 kcal/mol) making nickel more efficient for the transmetallation and coupling of alkyl moieties by minimizing the β -hydride elimination deactivation pathway.¹⁷

β -hydride Elimination



Scheme 6: β -Hydride elimination with Ni and Pd.

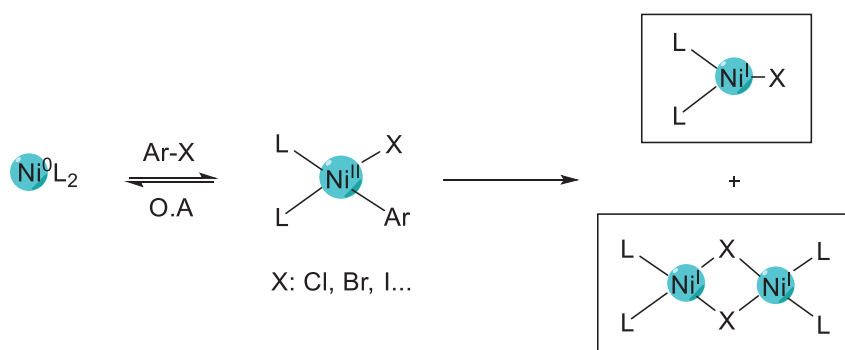
c. Reductive elimination

Reductive elimination is the last step in catalytic cycles, where a $[\text{Ni}^{\text{II}}(\text{L})_2\text{ArAr}]$ intermediate forms the $\text{C}_{\text{Ar}}-\text{C}_{\text{Ar}}$ bond by releasing the valuable molecule and regenerating the active catalyst. Reductive elimination is usually more favored with palladium than nickel because of its higher electrophilicity. However, the electronic factors have a minor effect on R.E. In fact, it is

predominantly favored by the steric hindrance and bulkiness of the ligand that forces R.E to take place to release the strain. In addition, the higher the energy of the new bond formed (stronger and more stable bond) the easier the R.E will be. Since the energy of the formation of $C_{Ar}-C_{Ar}$ bond is very high, in addition to its aromatic nature and electron conjugation, its high stability will be the driving force for reductive elimination.

d. Comproportionation reactions

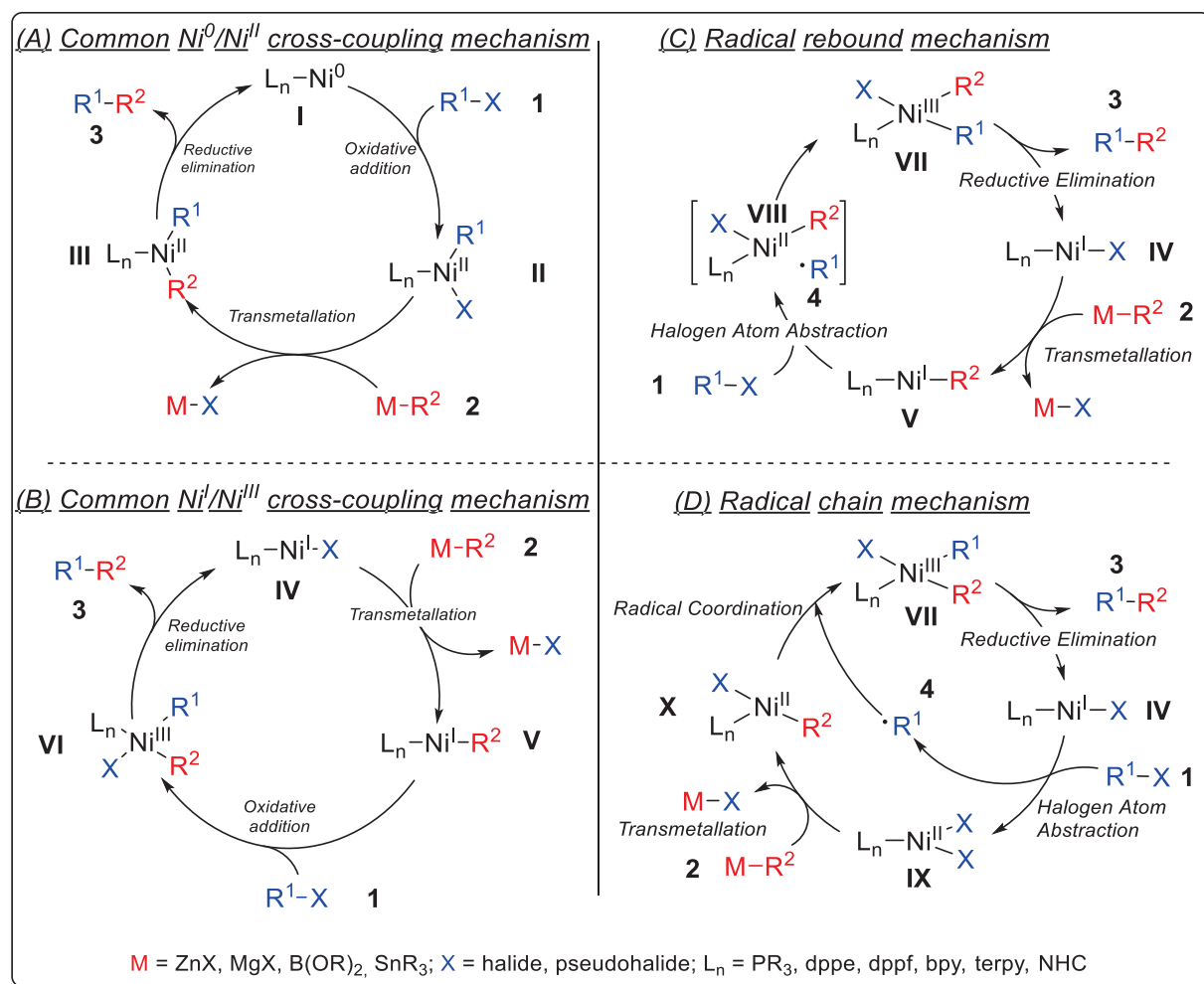
After the formation of the oxidative addition complex, comproportionation instead of transmetallation represents one of the main deactivation pathways leading usually to the formation of unreactive Ni^I species (**Scheme 7**).¹⁸ The comproportionation rate is determined by the stability and bulkiness of the ligand and their effect in stabilizing the oxidative addition intermediate. In general, the decomposition rate is lower with bulky and bidentate ligands for which the steric bulkiness of the ligand favors direct transmetallation.¹⁹ In addition, ortho-substituted substrates disfavor the formation of Ni^I species due to the steric hindrance and repulsion exerted by the two ortho substituted groups.²⁰ Moreover, the temperature plays a critical role in accelerating the decomposition, several complexes like $(dppf)Ni^{II}Cl(Ph)$ and $(BINAP)Ni^{II}Cl(Ph)$ comproportionate overtime even at room temperature.^{18,21}



Scheme 7: Formation of Ni^I species by comproportionation of the O.A Ni^{II} complex.

4. Catalytic cycles with Ni (Mechanisms)

The SET process extends nickel reactivity to radical transformations, such as Halogen Atom Abstraction (HAA) and Radical Coordination, allowing for a rich array of mechanisms.²² Common cross-coupling mechanisms include two-electron pathways via $\text{Ni}^0/\text{Ni}^{\text{II}}$ and $\text{Ni}^{\text{I}}/\text{Ni}^{\text{III}}$ (Scheme 8-A/B).



Scheme 8: Common $\text{Ni}^0/\text{Ni}^{\text{II}}$, $\text{Ni}^{\text{I}}/\text{Ni}^{\text{III}}$ cross-coupling mechanisms and common single electron nickel cross-coupling mechanisms.

For $\text{Ni}^0/\text{Ni}^{\text{II}}$ mechanism (Scheme 8-A), the catalytic cycle starts with oxidative addition of the C-X bond to Ni^0 (I) to form $\text{R}^1\text{Ni}^{\text{II}}\text{X}$ species (II), followed by a transmetalation step with M-

R^2 (**2**) to give $R^1Ni^{II}R^2$ (**III**), and is then ended by reductive elimination to afford the cross-coupling product and recycle the active Ni^0 (**I**) catalyst. For Ni^I/Ni^{III} mechanism (**Scheme 8-B**), the cycle starts from Ni^I (**IV**). From there, two sequences of events can happen: either transmetallation with $M-R^2$ (**2**) then oxidative addition of R^1-X (**1**) and reductive elimination, or oxidative addition of R^1-X (**1**) then transmetallation with $M-R^2$ (**2**) and reductive elimination to give the cross-coupling product and regenerate the catalytic Ni^I species (**IV**).

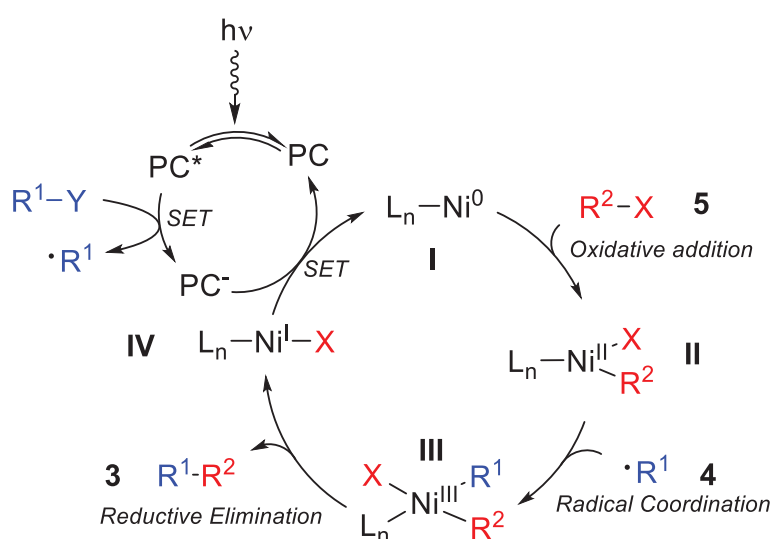
As β -H elimination is limited for Ni-Alkyl complexes, it allows cross-coupling reactions with Csp^3 electrophiles. They often involve Ni^I species, *N*-coordinating ligands and alkyl radicals generated through SET pathways. Two possible mechanisms were encountered. The radical rebound mechanism (**Scheme 8-C**) consists of direct transmetallation of the catalytic Ni^I-X (**IV**) with $M-R^2$ (**2**). The given Ni^I-R^2 (**V**) species then performs a Halogen Atom Abstraction on R^1-X (**1**), delivering a $R^2Ni^{II}X$ (**VIII**) intermediate and an organic radical $R^{1\cdot}$ (**4**). This radical then combines with the previously mentioned nickel complex to give the final catalytic species $R^1R^2Ni^{III}X$ (**VI**), closing the cycle by reductive elimination to afford the cross-coupling product and Ni^I-X (**IV**). In the alternative radical chain mechanism (**Scheme 8-D**) Halogen Atom Abstraction occurs first to generate $Ni^{II}-X$ (**IX**) and $R^{1\cdot}$ radical (**VIII**). In this case, the alkyl radical adds to the Ni^{II} species (**IX**) after transmetallation.¹¹

5. Some recent applications of nickel in cross-coupling catalysis

a. Ni/Photoredox catalysis

The capacity of nickel intermediates to readily react with radicals opened completely new possibilities for the development of cross-coupling reactions. One representative example is the development of Ni/photoredox catalysis. Complementary from a mechanistic point of view, nickel

and photoredox catalyses have proven efficient combined together.²³ The advent of photocatalysis, with generation of radicals under mild conditions, has logically conducted to the merging of these two catalysis fields to perform efficient and original cross-coupling reactions. Those reactions generally proceed as follows: a nickel catalyst (**I**) undergoes both oxidative addition of a C-X bond (where X = Cl, Br, I, F, N) and radical combination to give a $R^1R^2NiXL_n$ (**III**) species where n= 0 or 1. The latter then undergoes reductive elimination to give the desired product (**3**) (**Scheme 9**).



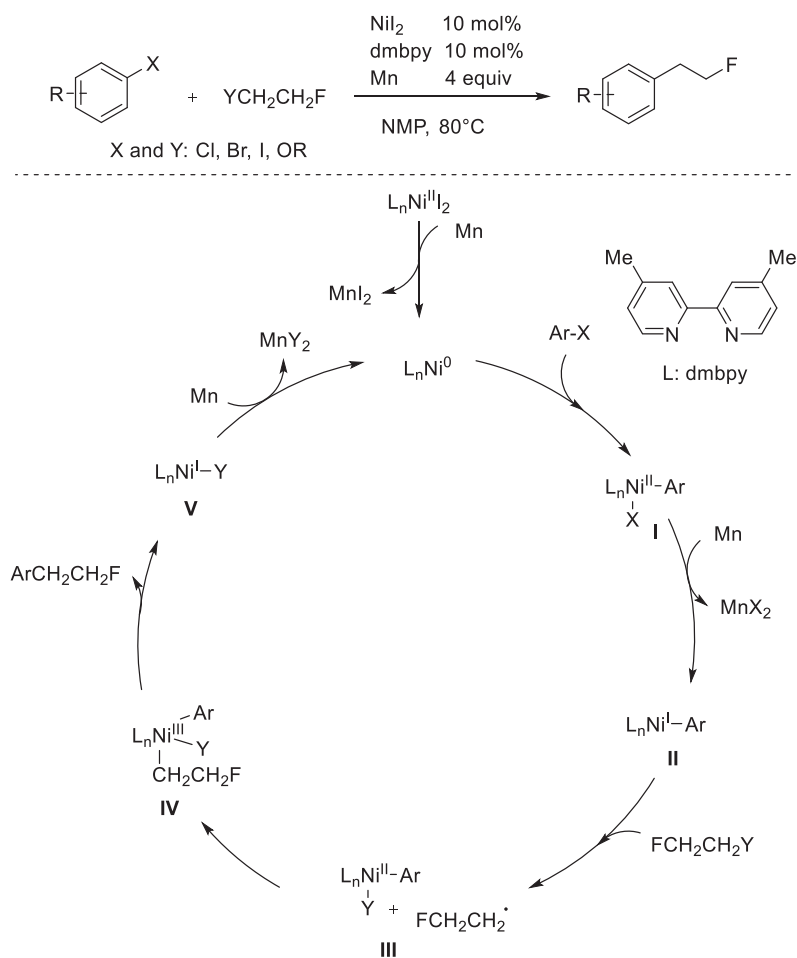
Scheme 9: General mechanism for dual nickel/photoredox catalysis.

The cooperative Ni/photoredox catalysis is one of the main cross-coupling methodologies that benefits from the ability of Ni to interact with radicals and access several oxidation states. Several photocatalysts were proven efficient with nickel. They can be organic molecules, or metal-centered complexes such as $[Ir(dF(CF_3)ppy)_2(dtbbpy)]PF_6$ and $[Ru(bpy)_3]Cl_2$ with redox potentials in the excited state varying from +0.77 V to +1.35 V.²⁴ Several leading authors like MacMillan, Doyle, and Molander reported many interesting cross-coupling transformations in this domain in the last two decades.^{25,26,27,24}

b. Reductive coupling

Nickel-catalyzed reductive cross-coupling was developed as a versatile and feasible synthetic methodology for selective C-C bond formation. The use of cheap and readily available electrophiles avoids the multistep synthesis and enrollment of organometallic reagents. In general, a nickel catalyst is involved in combination to a metallic reductant (e.g, Zn, Mn, Mg...) enabling the functionalization of alkyl, alkenyl and aryl groups. One of the main applications of Ni-catalyzed reductive cross-coupling is the "cross-electrophile coupling" which gained a lot of interest recently and was explored through several seminal studies by the groups of Weix, MacMillan, Gong, and Reisman.^{28,29,30,31}

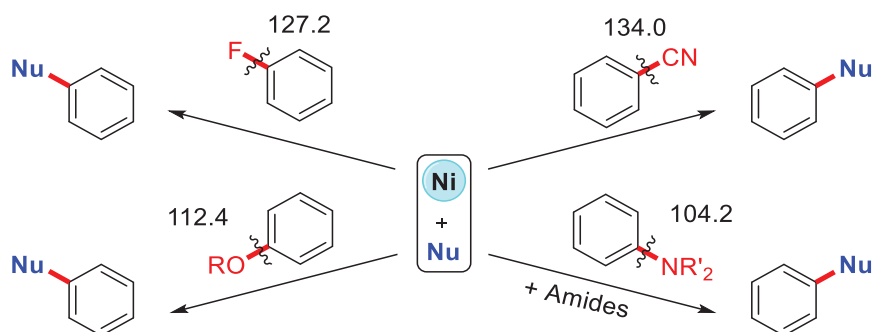
An interesting example of cross-electrophile coupling of organohalides and phenol derivatives was reported recently.³² The reaction is catalyzed by the combination of NiI_2 and dmbpy (4,4'-dimethyl-2,2'-bipyridine) ligand in the presence of a large excess of manganese that is used as a reductant (**Scheme 10**). First, the L_nNiI_2 complex is reduced to L_nNi^0 by the action of manganese, followed by the oxidative addition of Ar-X generating intermediate $\text{L}_n\text{Ni}^{\text{II}}(\text{Ar})(\text{X})$ (**I**) that is reduced by Mn, affording the $\text{L}_n\text{Ni}^{\text{I}}\text{Ar}$ (**II**) species. Then, $\text{L}_n\text{Ni}^{\text{I}}\text{Ar}$ undergoes another oxidative addition of $\text{FCH}_2\text{CH}_2\text{Y}$ involving a halogen atom abstraction and a radical cage-rebound process, delivering the Ni^{III} intermediate (**IV**). The latter subsequently undergoes reductive elimination, releasing the valuable $\text{ArCH}_2\text{CH}_2\text{F}$ product and $\text{L}_n\text{Ni}^{\text{I}}\text{Y}$ (**V**) species that is reduced back again to L_nNi^0 by the action of manganese.



Scheme 10: Proposed mechanism for nickel-catalyzed cross-electrophile couplings.

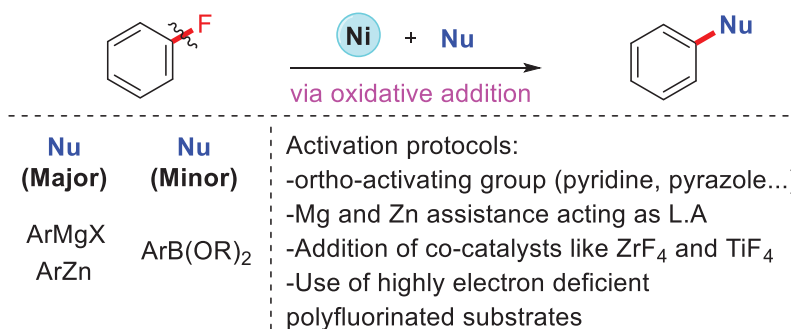
c. Nickel-catalyzed cross coupling of unconventional electrophiles

The strong nucleophilic character of nickel can promote the activation of several challenging bonds such as $\text{C}_{\text{aryl}}\text{-F}$, $\text{C}_{\text{aryl}}\text{-CN}$, $\text{C}_{\text{aryl}}\text{-NR}'_2$ and $\text{C}_{\text{aryl}}\text{-OR}$ (**Scheme 11**). These are very strong bonds with high bond dissociation energies beyond 100 Kcal/mol.³³



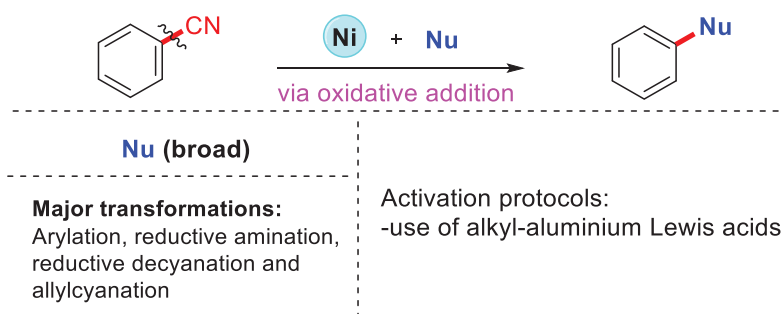
Scheme 11: Nickel-catalyzed cross-coupling of challenging bonds. $R=R'=H$ (values of BDE are given in Kcal/mol).³³

The cross-coupling of aryl fluorides is reported predominantly with organomagnesium or organozinc reagents with few examples using mild nucleophiles like organoborons or amines (**Scheme 12**).^{34,35,36,37} The activation relies on two pathways. The first, using an ortho-activating group like pyridine, pyrazole or quinolone that promotes C–F bond activation by chelating to Ni and stabilizing the catalyst. The next protocol is achieved by the assistance of magnesium and zinc ions acting as Lewis acids and activating the C–F bond. However, with mild nucleophiles like organoborons the activation is usually accomplished by using metal fluoride co-catalysts like ZrF_4 and TiF_4 that act as a fluoride donor and interact with the nucleophile forming a more reactive transmetallating species. In the case of organoborons, a more reactive tetra-coordinated borate species is formed. Of note, the use of poly-fluorinated substrates forms highly electron-deficient electrophiles that become much more reactive than mono-aryl fluorides and could be activated even with palladium under mild conditions.^{38,39} The mechanism is reported to take place via a classical oxidative addition pathway even with the strong nucleophiles.^{34,36}



Scheme 12: Nickel-catalyzed cross-coupling of aryl fluorides.

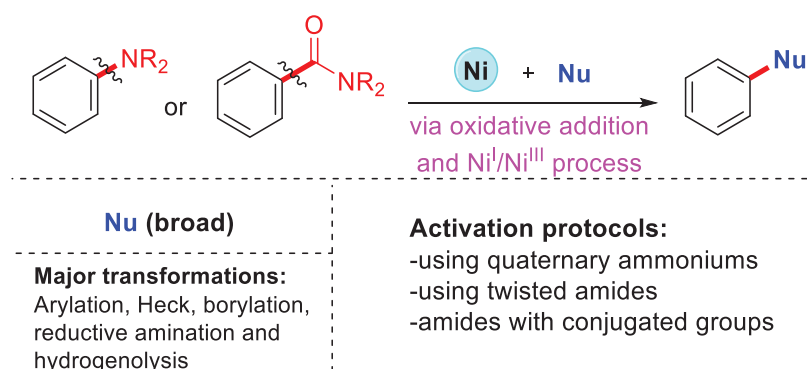
Benzonitriles can be coupled also with organomagnesiums and organozincs.^{40,41} Suzuki-Miyaura cross-coupling of aryl nitriles was reported by Shi in 2009.⁴² In addition, reductive amination and reductive decyanation was reported later on.⁴³ Maiti reported decyanation with tetramethyldisiloxane (TMDSO) as a hydride source and then a more greener method was established with di-hydrogen as a reductant.^{44,45} Nakao and Hiyama reported several regio- and stereoselective allylcyanation of alkynes and show that the addition of alkyl-aluminium Lewis acids has a dramatic effect on the activation of C-CN bond and accelerating the reaction rate.^{46,47} The general mechanism involves a classical oxidative addition pathway (**Scheme 13**).



Scheme 13: Nickel-catalyzed cross-coupling of aryl nitriles.

Direct cross-coupling of aniline derivatives is very challenging and was established only recently with boronic esters.⁴⁸ In general, C-N bond activation is achieved by forming a more

reactive species like quaternary ammoniums.^{49,50} Activated amides gained a lot of interest for carbonylative and decarbonylative cross-couplings via C-N bond activation using pre-activated twisted amides as well as amides with conjugated groups where the activation is driven by resonance disruption. In addition, the cross-coupling of electron-deficient phthalimides and ortho-chelating pyrazole amides was effectively assisted by chelation to nickel.^{51,52,53} These activated amides extend the reactivity for arylative and Heck cross-coupling transformations along with borylation, reductive amination and hydrogenolysis. They also proved to be highly effective on weakening the C-N bond where many of the substrates like tosyl amides and glutarimides become active under Pd catalysis.^{54,55,56} The mechanism usually proceeds via oxidative addition. However, a $\text{Ni}^{\text{I}}/\text{Ni}^{\text{III}}$ process was reported for cross-coupling of anilines with boronic esters (**Scheme 14**).⁴⁸



Scheme 14: Nickel-catalyzed cross-coupling of amines and amides.

6. Scope of the PhD work and organization of the manuscript

Nickel has been shown to afford several complementary properties and reactivities compared to palladium and to allow very unique transformations. In the general context of cross-coupling reactions, we were motivated to explore and understand the reactivity of nickel catalysts for the activation and functionalization of unconventional electrophiles. The PhD manuscript is divided in two parts, with each part dedicated to the development and understanding of a nickel catalyzed cross-coupling reaction.

In Part I, we were particularly interested to gain some knowledge in the parameters governing the crucial C-O bond activation step of aryl ethers with nickel. This part is organized around three main chapters. In the first chapter we describe a comprehensive state of the art of the recent developments on nickel-catalyzed cross-coupling of aryl ethers with a focus on mechanistic discussions. In the following chapters we disclose our investigations on the influence of ligand and Lewis acid co-catalysts in the nickel-catalyzed cross-coupling of arylothers with boronate esters (Chapter 2) and with alkenes (chapter 3).

The second part of the manuscript (Part 2) describes our work on the development of a nickel-catalyzed arylation of acetone using aryl halides and phenol derivatives and contains two main chapters. The first chapter summarizes the relevant reports disclosing catalytic arylation of ketones with nickel and the very few reports on palladium-catalyzed arylation of acetone. Then, we discuss in details our results on the synthetic development and mechanistic studies of a new nickel-catalyzed reaction with acetone.

7. References

- (1) Johansson Seechurn, C. C. C.; Kitching, M. O.; Colacot, T. J.; Snieckus, V. Palladium-Catalyzed Cross-Coupling: A Historical Contextual Perspective to the 2010 Nobel Prize. *Angew. Chem. Int. Ed.* **2012**, *51* (21), 5062–5085.
- (2) Magano, J.; Dunetz, J. R. Large-Scale Applications of Transition Metal-Catalyzed Couplings for the Synthesis of Pharmaceuticals. *Chem. Rev.* **2011**, *111* (3), 2177–2250.
- (3) Verheyen, L.; Leysen, P.; Van Den Eede, M. P.; Ceunen, W.; Hardeman, T.; Koeckelberghs, G. Advances in the Controlled Polymerization of Conjugated Polymers. *Polymer (Guildf)*. **2017**, *108*, 521–546.
- (4) Heck, K. F.; Nolley, J. P. Palladium-Catalyzed Vinylic Hydrogen Substitution Reactions with Aryl, Benzyl, and Styryl Halides. *J. Org. Chem.* **1972**, *37* (14), 2320–2322.
- (5) Suzuki, A. Cross-Coupling Reactions of Organoboranes: An Easy Way to Construct C-C Bonds (Nobel Lecture). *Angew. Chem. Int. Ed.* **2011**, *50* (30), 6723–6733.
- (6) Knochel, P.; Thaler, T.; Diene, C. Pd-, Ni-, Fe-, and Co-Catalyzed Cross-Couplings Using Functionalized Zn-, Mg-, Fe-, and in-Organometallics. *Isr. J. Chem.* **2010**, *50* (5–6), 547–557.
- (7) Tasker, S. Z.; Standley, E. A.; Jamison, T. F. Recent Advances in Homogeneous Nickel Catalysis. *Nature* **2014**, *509* (7500), 299–309.
- (8) Ackermann, L.; Cavalcanti, L. N.; Cera, G.; Chatani, N.; Correa, A.; Janine, C.; Gaydou, Y. D. M.; Gong, H.; Guerinot, A.; Itami, K.; et al. *Ni- and Fe-Based Cross-Coupling Reactions*; 2017; Vol. 35.
- (9) Diccianni, J.; Lin, Q.; Diao, T. Mechanisms of Nickel-Catalyzed Coupling Reactions and Applications in Alkene Functionalization. *Acc. Chem. Res.* **2020**, *53* (4), 906–919.

- (10) Ananikov, V. P. Nickel: The “Spirited Horse” of Transition Metal Catalysis. *ACS Catal.* **2015**, 5 (3), 1964–1971.
- (11) Diccianni, J. B.; Diao, T. Mechanisms of Nickel-Catalyzed Cross-Coupling Reactions. *Trends Chem.* **2019**, 1 (9), 830–844.
- (12) Wu, K.; Doyle, A. G. Parameterization of Phosphine Ligands Demonstrates Enhancement of Nickel Catalysis via Remote Steric Effects. *Nat. Chem.* **2017**, 9 (8), 779–784.
- (13) Nattmann, L.; Saeb, R.; Nöthling, N.; Cornella, J. An Air-Stable Binary Ni(0)–Olefin Catalyst. *Nat. Catal.* **2020**, 3 (1), 6–13.
- (14) Tran, V. T.; Li, Z.; Apolinar, O.; Derosa, J.; Joannou, M. V.; Wisniewski, S. R.; Eastgate, M. D.; Engle, K. M. Ni(COD)(DQ): An Air-Stable 18-Electron Nickel(0)–Olefin Precatalyst. *Angew. Chem. Int. Ed.* **2020**, 59 (19), 7409–7413.
- (15) Ananikov, V. P. Nickel: The “Spirited Horse” of Transition Metal Catalysis. *ACS Catal.* **2015**, 5 (3), 1964–1971.
- (16) Tobisu, M.; Chatani, N. Nickel-Catalyzed Cross-Coupling Reactions of Unreactive Phenolic Electrophiles via C–O Bond Activation. *Top. Curr. Chem.* **2016**, 374 (4), 1–28.
- (17) Cornella, J.; Gómez-Bengoa, E.; Martin, R. Combined Experimental and Theoretical Study on the Reductive Cleavage of Inert C–O Bonds with Silanes: Ruling out a Classical Ni(0)/Ni(II) Catalytic Couple and Evidence for Ni(I) Intermediates. *J. Am. Chem. Soc.* **2013**, 135 (5), 1997–2009.
- (18) Yin, G.; Kalvet, I.; Englert, U.; Schoenebeck, F. Fundamental Studies and Development of Nickel-Catalyzed Trifluoromethylthiolation of Aryl Chlorides: Active Catalytic Species and Key Roles of Ligand and Traceless MeCN Additive Revealed. *J. Am. Chem. Soc.* **2015**, 137 (12), 4164–4172.

- (19) Kalvet, I.; Guo, Q.; Tizzard, G. J.; Schoenebeck, F. When Weaker Can Be Tougher: The Role of Oxidation State (I) in P- vs N-Ligand-Derived Ni-Catalyzed Trifluoromethylthiolation of Aryl Halides. *ACS Catal.* **2017**, *7* (3), 2126–2132.
- (20) Bajo, S.; Laidlaw, G.; Kennedy, A. R.; Sproules, S.; Nelson, D. J. Oxidative Addition of Aryl Electrophiles to a Prototypical Nickel(0) Complex: Mechanism and Structure/Reactivity Relationships. *Organometallics* **2017**, *36* (8), 1662–1672.
- (21) Ge, S.; Green, R. A.; Hartwig, J. F. Controlling First-Row Catalysts: Amination of Aryl and Heteroaryl Chlorides and Bromides with Primary Aliphatic Amines Catalyzed by a BINAP-Ligated Single-Component Ni(0) Complex. *J. Am. Chem. Soc.* **2014**, *136* (4), 1617–1627.
- (22) Diccianni, J. B.; Diao, T. Mechanisms of Nickel-Catalyzed Cross-Coupling Reactions. *Trends Chem.* **2019**, *1* (9), 830–844.
- (23) Zuo, Z.; Ahneman, D. T.; Chu, L.; Terrett, J. A.; Doyle, A. G.; MacMillan, D. W. C. Merging Photoredox with Nickel Catalysis: Coupling of α -Carboxyl Sp³-Carbons with Aryl Halides. *Science*. **2014**, *345* (6195), 437–440.
- (24) Milligan, J. A.; Phelan, J. P.; Badir, S. O.; Molander, G. A. Alkyl Carbon–Carbon Bond Formation by Nickel/Photoredox Cross-Coupling. *Angew. Chem. Int. Ed.* **2019**, *58* (19), 6152–6163.
- (25) Badir, S. O.; Molander, G. A. Developments in Photoredox/Nickel Dual-Catalyzed 1,2-Difunctionalizations. *Chem* **2020**, *6* (6), 1327–1339.
- (26) Tellis, J. C.; Kelly, C. B.; Primer, D. N.; Jouffroy, M.; Patel, N. R.; Molander, G. A. Single-Electron Transmetalation via Photoredox/Nickel Dual Catalysis: Unlocking a New Paradigm for Sp³-Sp² Cross-Coupling. *Acc. Chem. Res.* **2016**, *49* (7), 1429–1439.
- (27) Matsui, J. K.; Lang, S. B.; Heitz, D. R.; Molander, G. A. Photoredox-Mediated Routes to

- Radicals: The Value of Catalytic Radical Generation in Synthetic Methods Development. *ACS Catal.* **2017**, 7 (4), 2563–2575.
- (28) Knappke, C. E. I.; Grupe, S.; Gärtner, D.; Corpet, M.; Gosmini, C.; Jacobi Von Wangelin, A. Reductive Cross-Coupling Reactions between Two Electrophiles. *Chem. Eur. J.* **2014**, 20 (23), 6828–6842.
- (29) Weix, D. J. Methods and Mechanisms for Cross-Electrophile Coupling of Csp² Halides with Alkyl Electrophiles. *Acc. Chem. Res.* **2015**, 48 (6), 1767–1775.
- (30) Kim, S.; Goldfogel, M. J.; Gilbert, M. M.; Weix, D. J. Nickel-Catalyzed Cross-Electrophile Coupling of Aryl Chlorides with Primary Alkyl Chlorides. *J. Am. Chem. Soc.* **2020**, 142 (22), 9902–9907.
- (31) Ackerman, L. K. G.; Lovell, M. M.; Weix, D. J. Multimetallic Catalysed Cross-Coupling of Aryl Bromides with Aryl Triflates. *Nature* **2015**, 524 (7566), 454–457.
- (32) Yang, Y.; Luo, G.; Li, Y.; Tong, X.; He, M.; Zeng, H.; Jiang, Y.; Liu, Y.; Zheng, Y. Nickel-Catalyzed Reductive Coupling for Transforming Unactivated Aryl Electrophiles into B-Fluoroethylarenes. *Chem. Asian J.* **2020**, 15 (1), 156–162.
- (33) Blanksby, S. J.; Ellison, G. B. Bond Dissociation Energies of Organic Molecules. *Acc. Chem. Res.* **2003**, 36 (4), 255–263.
- (34) Yoshikai, N.; Mashima, H.; Nakamura, E. Nickel-Catalyzed Cross-Coupling Reaction of Aryl Fluorides and Chlorides with Grignard Reagents under Nickel/Magnesium Bimetallic Cooperation. *J. Am. Chem. Soc.* **2005**, 127 (51), 17978–17979.
- (35) Guo, H.; Kong, F.; Kanno, K. I.; He, J.; Nakajima, K.; Takahashi, T. Early Transition Metal-Catalyzed Cross-Coupling Reaction of Aryl Fluorides with a Phenethyl Grignard Reagent Accompanied by Rearrangement of the Phenethyl Group. *Organometallics* **2006**, 25 (8),

2045–2048.

- (36) Tobisu, M.; Xu, T.; Shimasaki, T.; Chatani, N. Nickel-Catalyzed Suzuki-Miyaura Reaction of Aryl Fluorides. *J. Am. Chem. Soc.* **2011**, *133* (48), 19505–19511.
- (37) Harada, T.; Ueda, Y.; Iwai, T.; Sawamura, M. Nickel-Catalyzed Amination of Aryl Fluorides with Primary Amines. *Chem. Commun.* **2018**, *54* (14), 1718–1721.
- (38) Amii, H.; Uneyama, K. C-F Bond Activation in Organic Synthesis. *Chem. Rev.* **2009**, *109* (5), 2119–2183.
- (39) Braun, T.; Wehmeier, F. C-F Bond Activation of Highly Fluorinated Molecules at Rhodium: From Model Reactions to Catalysis. *Eur. J. Inorg. Chem.* **2011**, *2011* (5), 613–625.
- (40) Miller, J. A.; Dankwardt, J. W. Nickel Catalyzed Cross-Coupling of Modified Alkyl and Alkenyl Grignard Reagents with Aryl- and Heteroaryl Nitriles: Activation of the C-CN Bond. *Tetrahedron Lett.* **2003**, *44* (9), 1907–1910.
- (41) Penney, J. M.; Miller, J. A. Alkynylation of Benzonitriles via Nickel Catalyzed C-C Bond Activation. *Tetrahedron Lett.* **2004**, *45* (25), 4989–4992.
- (42) Yu, D. G.; Yu, M.; Guan, B. T.; Li, B. J.; Zheng, Y.; Wu, Z. H.; Shi, Z. J. Carbon - Carbon Formation via Ni-Catalyzed Suzuki - Miyaura Coupling through C - CN Bond Cleavage of Aryl Nitrile. *Org. Lett.* **2009**, *11* (15), 3374–3377.
- (43) Miller, J. A.; Dankwardt, J. W.; Penney, J. M. Nickel Catalyzed Cross-Coupling and Amination Reactions of Aryl Nitriles. *Synthesis (Stuttg.)* **2003**, *2003* (11), 1643–1648.
- (44) Patra, T.; Agasti, S.; Akanksha, A.; Maiti, D. Nickel-Catalyzed Decyanation of Inert Carbon-Cyano Bonds. *Chem. Commun.* **2013**, *49* (1), 69–71.
- (45) Patra, T.; Agasti, S.; Modak, A.; Maiti, D. Nickel-Catalyzed Hydrogenolysis of Unactivated Carbon–Cyano Bonds. *Chem. Commun.* **2013**, *49* (75), 8362–8364.

- (46) Nakao, Y.; Yada, A.; Ebata, S.; Hiyama, T. A Dramatic Effect of Lewis-Acid Catalysts on Nickel-Catalyzed Carbocyanation of Alkynes. *J. Am. Chem. Soc.* **2007**, *129* (9), 2428–2429.
- (47) Yada, A.; Yukawa, T.; Idei, H.; Nakao, Y.; Hiyama, T. Nickel/Lewis Acid-Catalyzed Carbocyanation of Alkynes Using Acetonitrile and Substituted Acetonitriles. *Bull. Chem. Soc. Jpn.* **2010**, *83* (6), 619–634.
- (48) Cao, Z. C.; Xie, S. J.; Fang, H.; Shi, Z. J. Ni-Catalyzed Cross-Coupling of Dimethyl Aryl Amines with Arylboronic Esters under Reductive Conditions. *J. Am. Chem. Soc.* **2018**, *140* (42), 13575–13579.
- (49) Blakey, S. B.; MacMillan, D. W. C. The First Suzuki Cross-Couplings of Aryltrimethylammonium Salts. *J. Am. Chem. Soc.* **2003**, *125* (20), 6046–6047.
- (50) Xie, L. G.; Wang, Z. X. Nickel-Catalyzed Cross-Coupling of Aryltrimethylammonium Iodides with Organozinc Reagents. *Angew. Chem. Int. Ed.* **2011**, *50* (21), 4901–4904.
- (51) Takise, R.; Muto, K.; Yamaguchi, J. Cross-Coupling of Aromatic Esters and Amides. *Chem. Soc. Rev.* **2017**, *46* (19), 5864–5888.
- (52) Meng, G.; Shi, S.; Szostak, M. Cross-Coupling of Amides by N-C Bond Activation. *Synlett* **2016**, *27* (18), 2530–2540.
- (53) Dander, J. E.; Garg, N. K. Breaking Amides Using Nickel Catalysis. *ACS Catal.* **2017**, *7* (2), 1413–1423.
- (54) Guo, L.; Rueping, M. Decarbonylative Cross-Couplings: Nickel Catalyzed Functional Group Interconversion Strategies for the Construction of Complex Organic Molecules. *Acc. Chem. Res.* **2018**, *51* (5), 1185–1195.
- (55) Shi, S.; Nolan, S. P.; Szostak, M. Well-Defined Palladium(II)-NHC Precatalysts for Cross-Coupling Reactions of Amides and Esters by Selective N-C/O-C Cleavage. *Acc. Chem. Res.*

2018, *51* (10), 2589–2599.

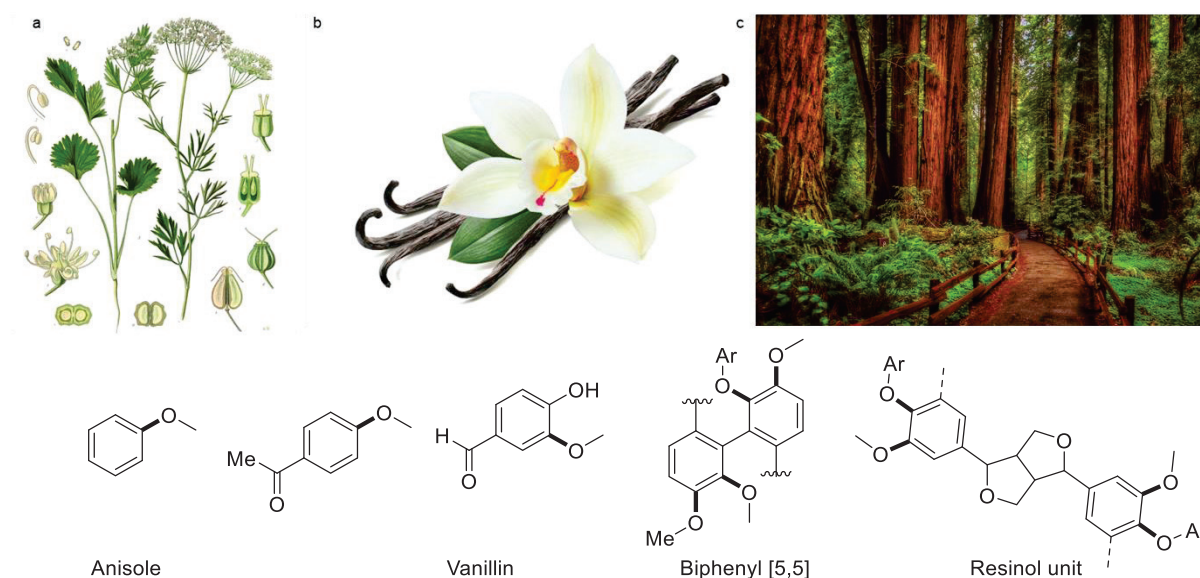
- (56) Reina, A.; Krachko, T.; Onida, K.; Bouyssi, D.; Jeanneau, E.; Monteiro, N.; Amgoune, A. Development and Mechanistic Investigations of a Base-Free Suzuki-Miyaura Cross-Coupling of α,α -Difluoroacetamides via C-N Bond Cleavage. *ACS Catal.* **2020**, *10* (3), 2189–2197.

Part I:

***Dual Ni/Lewis acid catalytic system for
the cross-coupling of aryl ethers***

I. Introduction

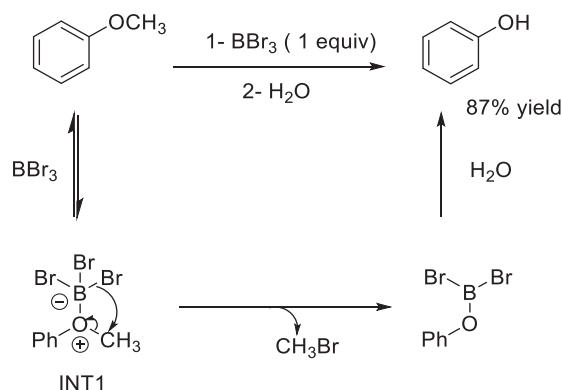
Phenols are the most abundant aromatic feedstock from the coal-based chemical industry and they can be easily obtained from several natural sources at low costs.¹ Among Phenol derivatives, aryl ethers constitute one of the basic units of lignin, a major component of biomass (**Scheme 1**).²



Scheme 1: Natural abundance of aryl ethers, ^aAnise plant, ^bvanilla plant, ^cMajor structural units of lignin from wood.

Aryl ethers are very stable compounds featuring a very robust $C_{Ar}-OMe$ bond (Energy of dissociation around 102.6 kcal/mol for anisole).³ The transformations of aryl ethers have been limited to combustion, pyrolysis and conversion to phenols. This latter reaction that essentially applies to aryl methyl ethers requires the use of a very reactive Lewis acid like BBr_3 ⁴ to activate the $C_{Ar}-OMe$ bond towards hydrolysis. The mechanism for this transformation, as proposed by Silva,⁵ proceeds through a unimolecular process which most likely occurs for branched aryl ethers since they can stabilize the carbocation better than the methoxy group (**Scheme 2**). First, BBr_3 coordinates to the ether oxygen and forms intermediate INT1 which follows an intramolecular

transformation to PhOBr_2 by releasing MeBr . Then PhOBr_2 reacts with water to give phenol in a high yield (87%).



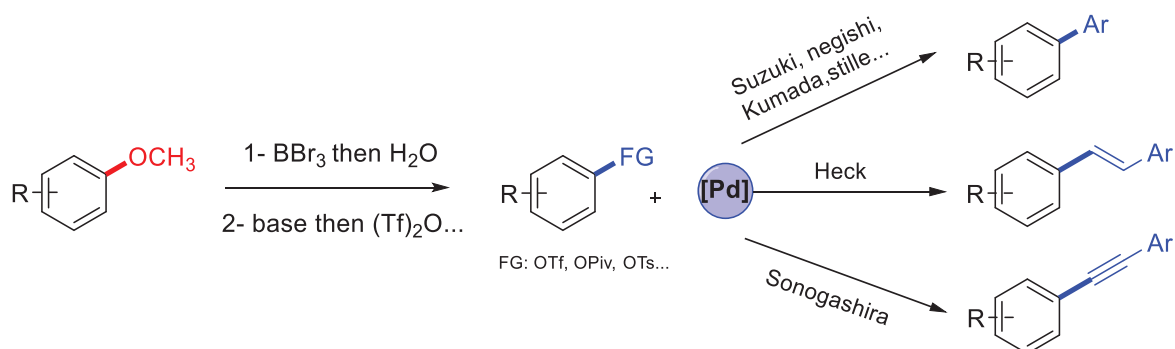
Scheme 2: Unimolecular mechanism proposed for the BBr_3 -promoted demethylation of aryl methyl ethers.

Aryl ethers have also attracted interest in the context of cross-coupling reaction for the preparation of aromatic compounds, which are the basic building blocks of many pharmaceuticals, electronics, agrochemicals, and dyes.^{6,7,8} Since the pioneering works in transition metal-catalyzed cross-coupling reaction in the 1970's,^{9,10,11} tremendous efforts have been made to synthesize and functionalize aromatic compounds. In this area, aryl halides are the most popular electrophilic partners, but their high cost, low accessibility, particularly for aryl bromides and aryl iodides, and concerns in terms of toxicity of halide waste generated as a by-product have limited their application in industries.¹² Since then, the search for more economical and environmentally friendly alternatives began. In this objective, phenol derivatives appeared as interesting candidates for the development of more sustainable synthetic methodologies to high-value added aromatic compounds.

However, the direct functionalization of aryl ethers via $\text{C}_{\text{Ar}}\text{-OMe}$ bond activation is challenging due to the high activation energy required for $\text{C}_{\text{Ar}}\text{-OMe}$ cleavage and the low propensity of methoxy residue to act as a leaving group.

Palladium catalysts classically used in cross-coupling reactions with aryl halides were shown inactive for the cross-coupling of aryl ethers or phenols. To overcome these challenges, indirect cross-coupling strategies involving multistep procedures have been initially developed.

The use of aryl ethers using traditional cross-coupling methods with palladium catalysts involved a general three-step procedure (**Scheme 3**).¹³



Scheme 3: Classical three-step procedure for aryl ether cross-coupling.

The aryl methyl ether is first demethylated, and the phenol moiety is then activated, for example by the triflate (trifluoromethanesulfonyl) group (until now the $C_{Ar}-O$ bond is untouched).⁴ The third step involves a transition metal-catalyzed cross-coupling of phenol triflate which serves as an excellent electrophile for coupling.¹⁴

In contrast, direct cross-coupling reaction of ethers have been shown to be possible using nickel catalysis in the late 1970s.¹⁵ Since then, these reactions have remained essentially restricted to C–C bond-forming transformations using highly reactive organometallic reagents, but very rapid developments have appeared within the last decade of research. Today, the range of nucleophiles that can be coupled with aryl ethers has been expanded significantly.^{1,2}

This part of the manuscript will be dedicated to our investigations in nickel catalyzed cross coupling of aryl ethers with boron derivatives and with alkenes. In the first chapter, a state of the art of the main achievements in the area of nickel catalyzed cross-coupling of aryl ethers will be

presented. It is organized according to the nature of bond formation reaction and will contain key mechanistic information collected over the last few years. In the second chapter, our work on the development and investigations of a dual Ni/Al catalytic system for the cross-coupling of aryl ethers with boronic esters will be discussed. In the third chapter, the investigation of intramolecular coupling of aryl ether with alkenes will be presented.

Chapter I:

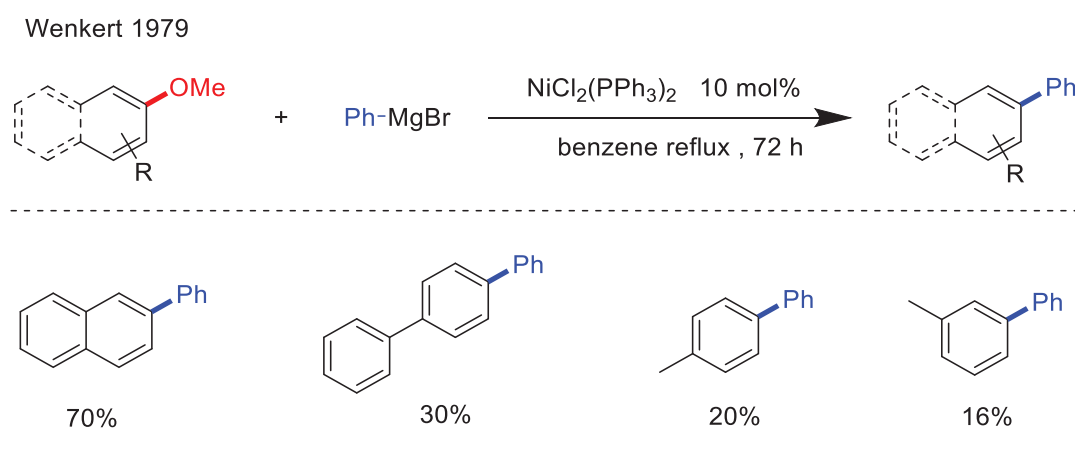
State of the art of the nickel-catalyzed cross-coupling of aryl ethers.

I. Nickel-catalyzed cross-coupling of aryl ethers: Carbon-Carbon bond formation

1. Cross-coupling with Grignard reagents

a. Coupling with ArMgX

The first example of transition metal-catalyzed cross-coupling of aryl ethers dates back to 1979.¹⁵ Wenkert described the cross-coupling of aryl methyl ethers with Grignard reagents as nucleophilic partners catalyzed by $\text{NiCl}_2(\text{PPh}_3)_2$ (**Scheme 4**). The scope of the reaction was very limited.^{15,16} Methoxynaphthalene and π -extended electrophiles appeared to be more reactive than simple anisole derivatives. This trend is always observed in catalysis and known as the “naphthalene problem”. It could be attributed to the formation of π -arene-Ni intermediates that are more stable and form easier with π -extended systems.² Alkyl Grignard reagents having a beta-hydrogen like EtMgBr lead to reduction rather than C–C bond formation through C–OMe bond cleavage.



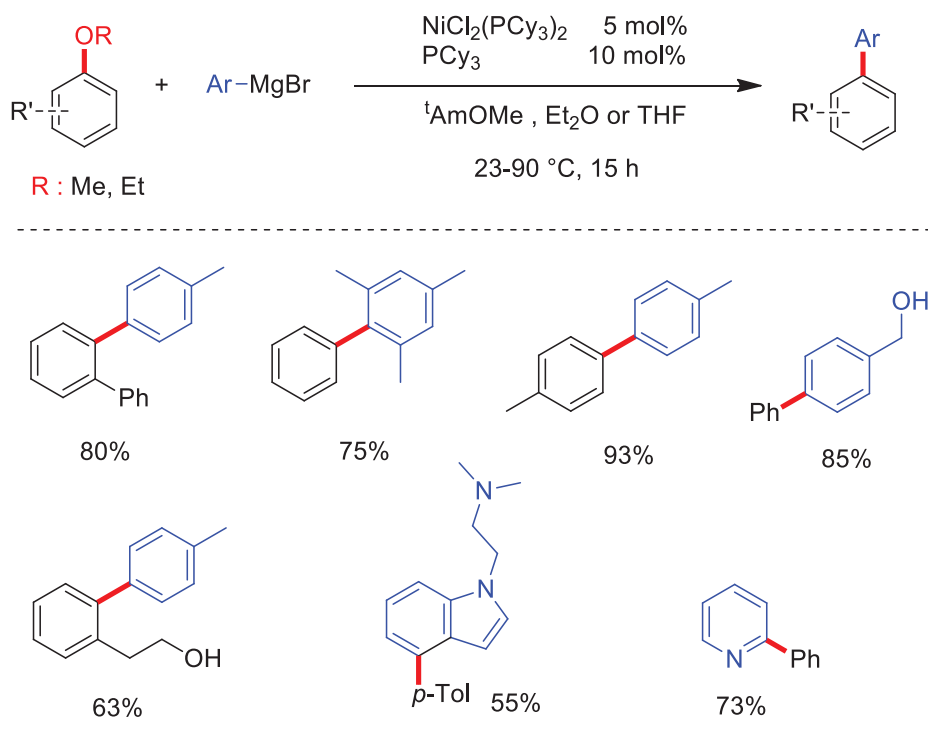
Scheme 4: Ni-catalyzed Kumada-Tamao-Corriu cross-coupling of aryl ethers with PhMgBr.

At that time, the work of Suzuki, published the same year,¹⁷ on palladium-catalyzed cross-coupling of aryl halides with organoboron reagents has attracted most of the attention from the scientific community. Pd-catalyzed cross-couplings discovered in the 70's dominated the research in this field, and the seminal work of Wenkert remained unexploited for 25 years.

In 2004, Dankwardt re-examined the pioneering work of Wenkert by exploring the effect of different phosphine ligands in combination with $\text{NiCl}_2(\text{PPh}_3)_2$ catalyst on the arylation of aryl ethers with ArMgX .¹⁸ Electron-rich alkyl phosphines were shown to be more reactive than aromatic ones. A trend between the ligand cone angle and the catalytic reactivity has been observed. Phosphines with intermediate cone angles have shown the highest reactivity, with PCy_3 (tricyclohexylphosphine) being the most efficient ligand for this transformation. Non-polar solvents afforded much better results than polar solvents. This effect was explained by the deleterious presence of the MgBr(OMe) adduct formed *in-situ*, which was proposed to poison the catalytically active species. In fact, this adduct is insoluble and precipitates instantaneously in non-polar solvents.

The scope of the reaction using these conditions significantly extends that of the previous methodology. Interestingly, anisole derivatives lacking π -extended rings were found to be suitable substrates under these conditions (**Scheme 5**). Besides, microwave irradiation could significantly reduce the time of the reaction down to 30 min.

Dankwardt 2004



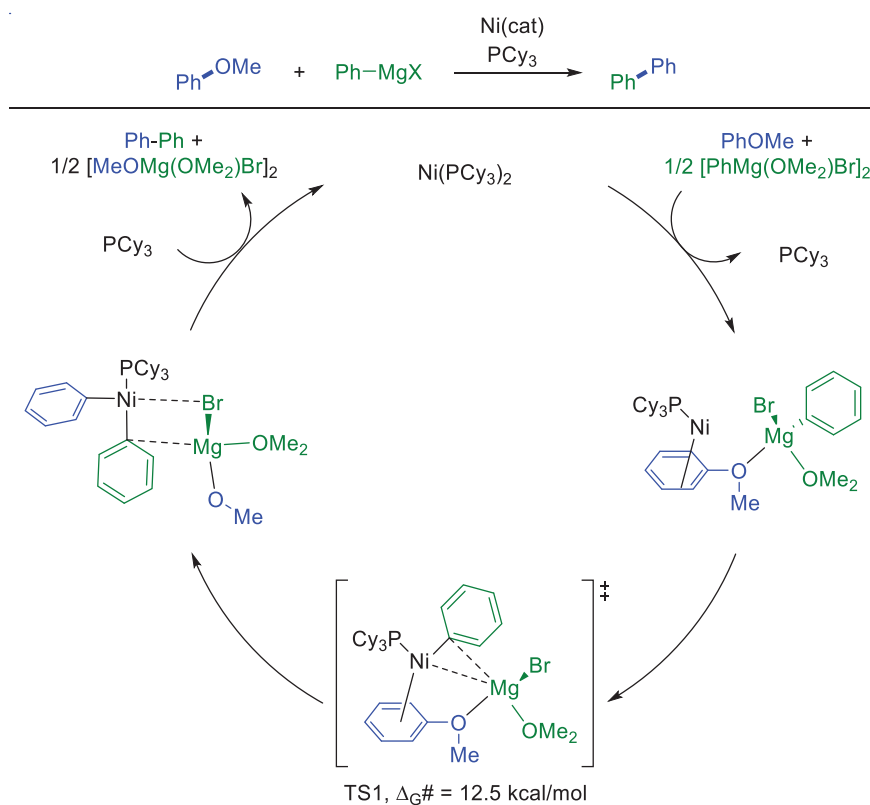
Scheme 5: Cross-coupling of aryl ethers with aryl Grignard reagents as developed by Dankwardt in 2004.

The main drawback of this system is the use of Grignard reagent as a transmetalation agent, which is very reactive and functional group intolerant limiting its use for late-stage synthesis.

The mechanism of the reaction was investigated in 2015 by Uchiyama through computational studies.¹⁹ Based on DFT calculations, the authors proposed the following pathway as the most probable mechanism (**Scheme 6**). First, the strongly donating PCy₃ ligands displace the labile COD groups forming Ni(PCy₃)₂ complex, followed by coordination of Ni to the π -extended system. The activation of the C–OMe bond takes place smoothly via a five-membered transition state through a push-pull effect, where Mg acts as a Lewis acid weakening the C–OMe bond, and the highly nucleophilic Ni “ate” complex inserts into the bond (TS1). The associated activation energy

is only 12.7 kcal/mol, in line with the experimental observation that the coupling of ArMgX proceeds smoothly under mild conditions. It is worth noting that this activation takes place through a concerted mechanism and without the formation of $\text{Ph-Ni}^{\text{II}}\text{-OMe}$ complex. MeOMgBr is then released, and reductive elimination liberates the thermodynamically stable biphenyl product. The oxidative addition of the C-OMe bond to Ni^0 species was also computed, but it was found to be kinetically ($\Delta G^\ddagger = 37$ kcal/mol) and thermodynamically unfavorable ($\Delta G = 14$ kcal/mol).

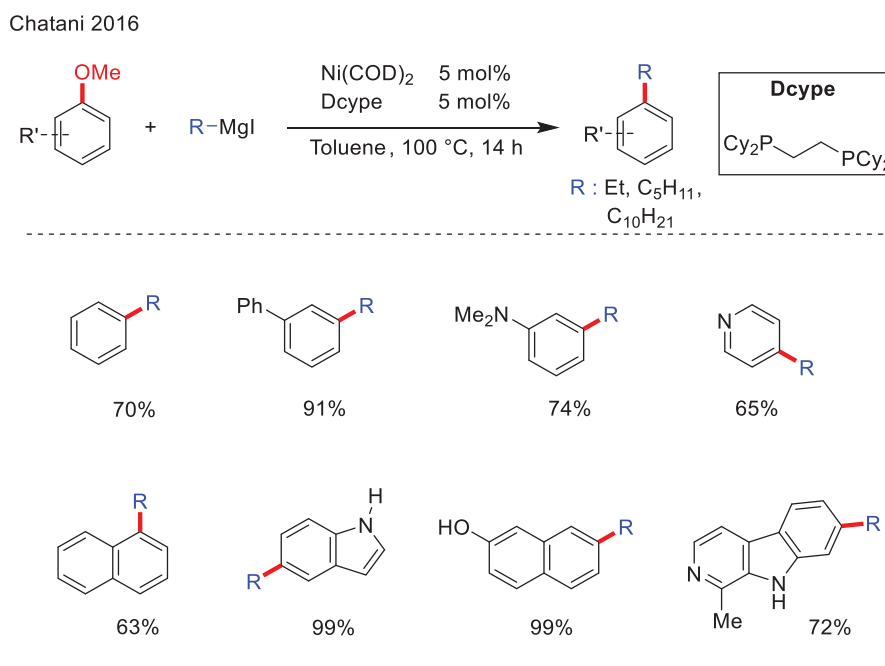
DFT calculations were also carried out with Pd instead of Ni under the same conditions. A transition state with a very high associated activation barrier of 38 kcal/mol was located for the C–O bond activation, in line with the lack of experimental reactivity.



Scheme 6: Proposed mechanism for the cross-coupling of anisole with Grignard reagents.

b. Coupling with alkylMgX

More recently, alkyl Grignard reagents were also found to be reactive for alkylative cross-couplings of aryl ethers. Chatani reported an effective alkylation strategy with AlkMgI , catalyzed by Ni(COD)_2 and Dcype (1,2-Bis(dicyclohexylphosphino)ethane) ligand.²⁰ NHC ligands, ICy (1,3-Dicyclohexyl-1,3-dihydro-2H-imidazol-2-ylidene) and IPr (1,3-Diisopropyl-1,3-dihydro-2H-imidazol-2-ylidene), as well as PCy_3 were unreactive under these conditions. In the case of PCy_3 , naphthalene (11%) was formed as a by-product indicating that β -hydride elimination might take place, which could be avoided using bidentate ligands. Among several di-phosphines, Dcype showed the best reactivity. This strategy shows a unique capability of activating a broad scope of anisole derivatives. In addition, even simple anisole provided good reaction yield (70%) (**Scheme 7**).



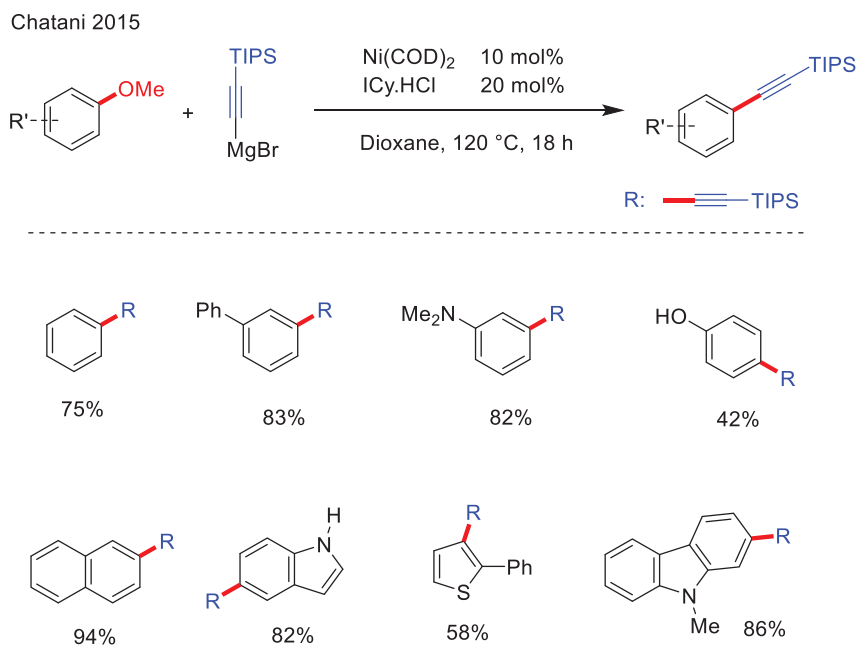
Scheme 7: Scope for alkylative cross-coupling with RMgI .

The reaction proceeds without β -hydride elimination and the halide on Grignard reagent was shown to have a significant impact on the reactivity. Iodo magnesium derivatives are the most reactive, while chloro and bromo derivatives display low reactivity. However, good reactivities were recovered upon addition of MgI_2 salt (1 equiv).

The reaction was first proposed to proceed via oxidative addition of the C–OMe bond assisted by coordination of MgI_2 to the methoxy group, but monitoring by ^{31}P -NMR a mixture of $\text{Ni}(\text{COD})_2$ (1 equiv), dcype (1 equiv), MgI_2 (2 equiv), and methoxynaphthalene (2 equiv) in toluene- d^8 at 80 °C for 14 h did not show any reactivity, indicating that the presence of RMgI is essential for the activation, and suggesting that the activation also proceeds via Nickel “ate” complex as proposed with aryl Grignard reagents.

c. Coupling with alkynylMgX

The first alkynylative cross-coupling of aryl ethers with Grignard reagents was reported by Chatani in 2015²¹ catalyzed by $\text{Ni}(\text{COD})_2$ and NHC ligands. PCy_3 ligand was totally inactive but a variety of alkyl NHC ligands proved effective, with 1,3-dicyclohexylimidazolium chloride offering the best results. The scope was broad, enabling the activation of simple anisole (75%) and a variety of anisole derivatives in very good yields (**scheme 8**).



Scheme 8: Scope for alkynylative cross-coupling with *TIPSMgBr*.

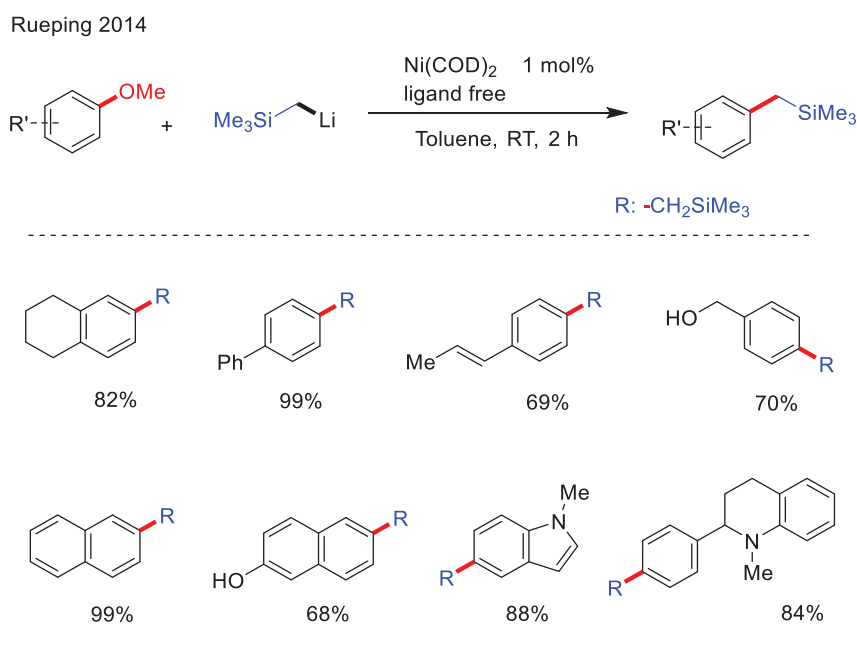
Screening a variety of alkynyl magnesium reagents, it was shown that the triisopropylsilyl ether (TIPS) group is essential for the reaction to proceed efficiently. The bulkier alkynyl moieties display higher reactivity, probably because they inhibit the interaction of the alkyne moiety with the metallic center. No mechanistic studies or mechanisms were proposed but the activation via Nickel “ate” complex is the most common mechanism with RMgX nucleophiles.

2. Cross-coupling with organolithium reagents

a. Coupling with alkyl lithium

An interesting alkylation method using $\text{LiCH}_2\text{SiMe}_3$ as organolithium reagent was discovered by Rueping in 2014.²² It is worth to mention that organomagnesium species showed lower reactivity under the same conditions. Ni(COD)_2 is an active catalyst but the air-stable $\text{NiCl}_2(\text{PCy}_3)_2$ could also be used with a comparable activity. The reaction was carried out at room temperature for 1.5 – 2 hours. In contrast to all previous methods, the ligand is not required for the reaction.

$\text{Ni}(\text{COD})_2$ (1 mol%) alone without any ligand gives the same result as with 2-5 mol% of PCy_3 . Toluene is the best solvent, but the reaction can also be conducted in polar solvents without affecting significantly the yield. The scope was broad with good to excellent yields (**Scheme 9**).



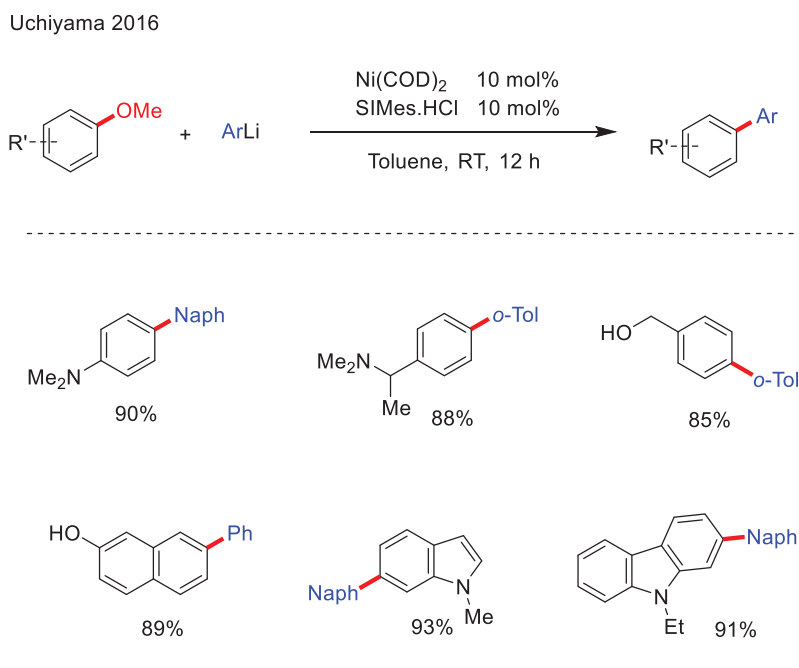
Scheme 9: Scope for alkylative cross-coupling with $\text{LiCH}_2\text{SiMe}_3$.

No mechanistic studies have been carried out. However, having reactivity in the absence of the ligand poses plenty of questions about the mechanism, because the ligand plays a major role in all the previously reported mechanisms. It was proposed that a classical cycle via oxidative addition might take place.

b. Coupling with aryllithium

Another study using organolithium reagents for the arylation of aryl ethers was reported by Uchiyama in 2016,²³ catalyzed by $\text{Ni}(\text{COD})_2$ under very mild conditions. The reaction can be carried out at room temperature using $\text{Ni}(\text{COD})_2$ alone without any additional ligand. No marked

improvement was found by adding any ligand, including PCy₃ and ICy, with the exception of SIMes NHC ligand that proved to be slightly more efficient. The scope was broad, enabling the activation of many aryl ethers and some anisole derivatives (**Scheme 10**).



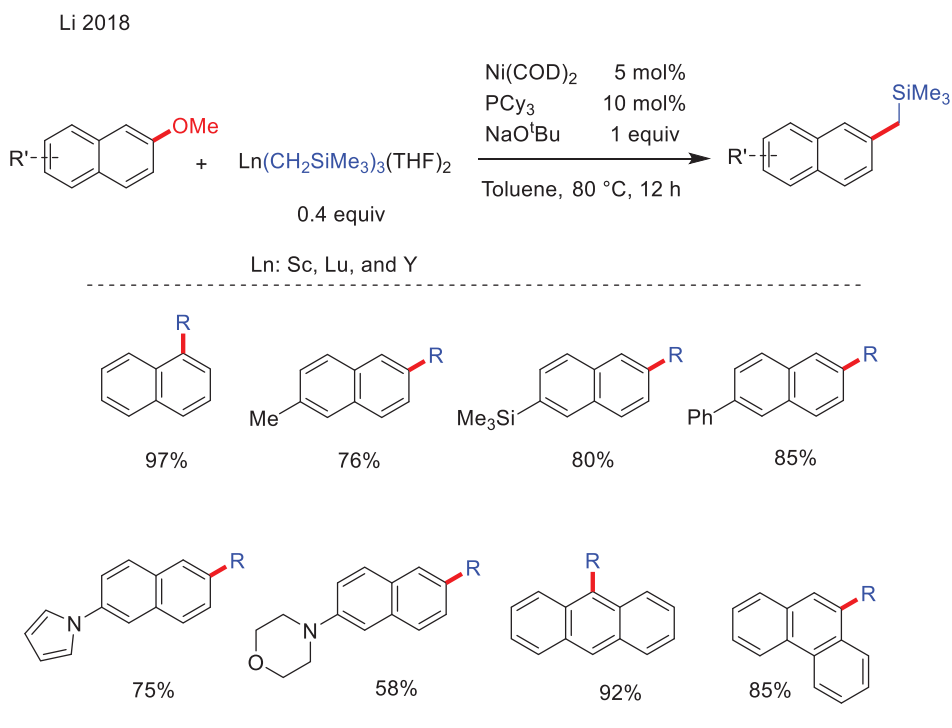
Scheme 10: Scope for cross-coupling arylation with ArLi.

The main interest of organolithium reagents lies in their remarkable reactivity allowing Ni(COD)₂ to catalyze the reaction without the need for any ligand. The mechanism was investigated later on by the group of Uchiyama using DFT calculations. A pathway very similar to that observed with RMgX was proposed, via the formation of an “ate” complex, which proceeds with a five-membered TS with an activation barrier of 19.4 kcal/mol.²⁴

3. Cross-coupling with organolanthanides

Li & al. recently reported the cross-coupling of aryl ethers with organolanthanide compounds, Ln(CH₂SiMe₃)₃(THF)₂ (Ln = Sc, Lu, Y), as nucleophilic coupling partners catalyzed by

the combination of $\text{Ni}(\text{COD})_2$ and PCy_3 ligand.²⁵ Among several phosphines and NHC's, PCy_3 showed the best reactivity. It is worth to mention that the reaction also proceeds without ligand albeit with lower yields. The scope of aryl ethers was limited to π -extended systems (**Scheme 11**).



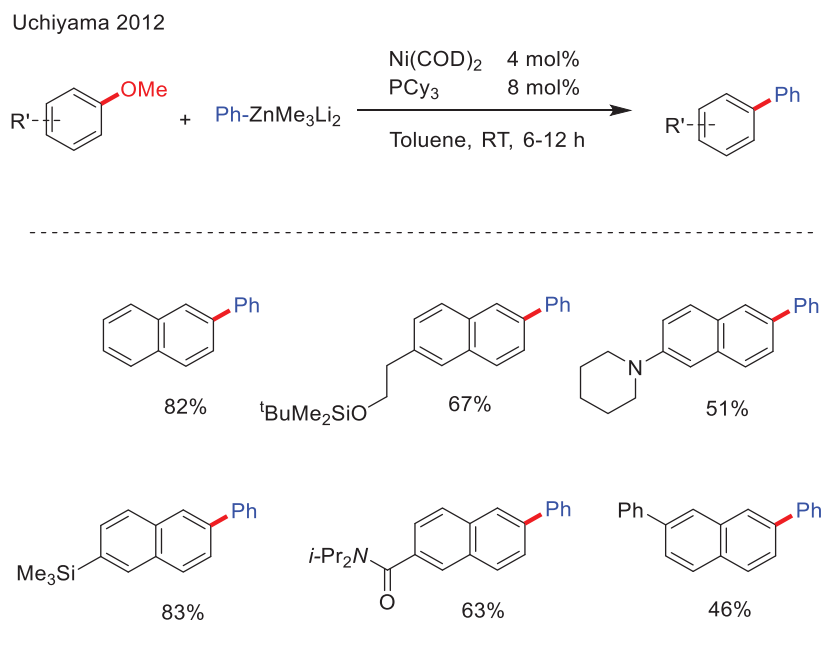
Scheme 11: Scope for cross-coupling alkylation with lanthanides.

A classical $\text{Ni}^0/\text{Ni}^{\text{II}}$ pathway was proposed, where the oxidative addition takes place via a three-membered TS, which is assisted by the coordination of the lanthanide to the methoxy group acting as a Lewis acid.

4. Cross-coupling with organozincates

The first Negishi cross-coupling reaction of aryl ethers with organozinc species was explored by Uchiyama in 2012,²⁶ catalyzed by $\text{Ni}(\text{COD})_2$ and PCy_3 ligand. The first attempts showed that classical organozinc species and lithium mono-anionic organozincate are totally inactive. However, lithium di-anionic organozincate showed high activity at room temperature (**Scheme**

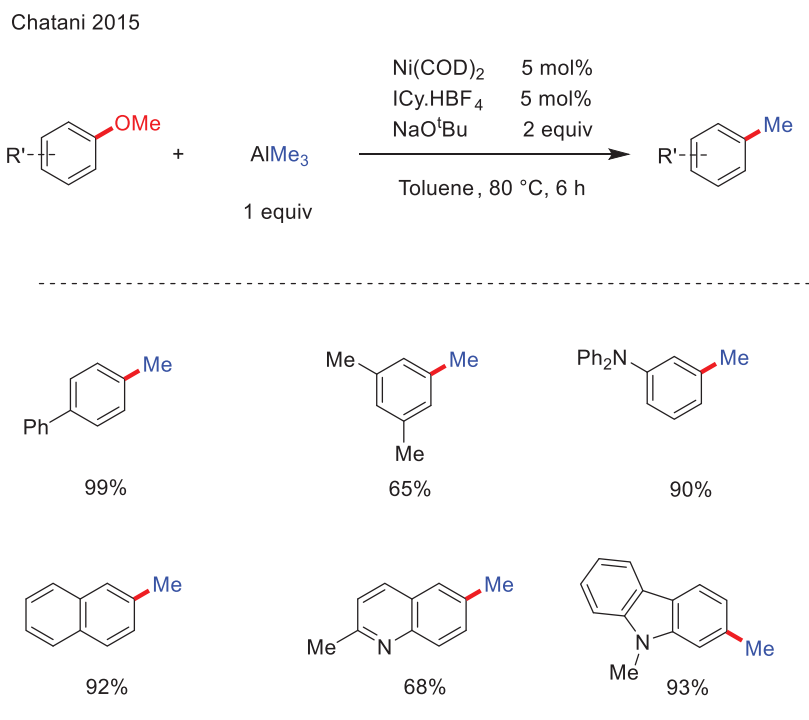
12). A mechanism very similar to that observed with RMgX partners, via “ate” complex, was proposed based on DFT calculations.²⁴



Scheme 12: Scope for cross-coupling arylation with lithium di-anionic organozincate.

5. Cross-coupling with organoaluminium derivatives

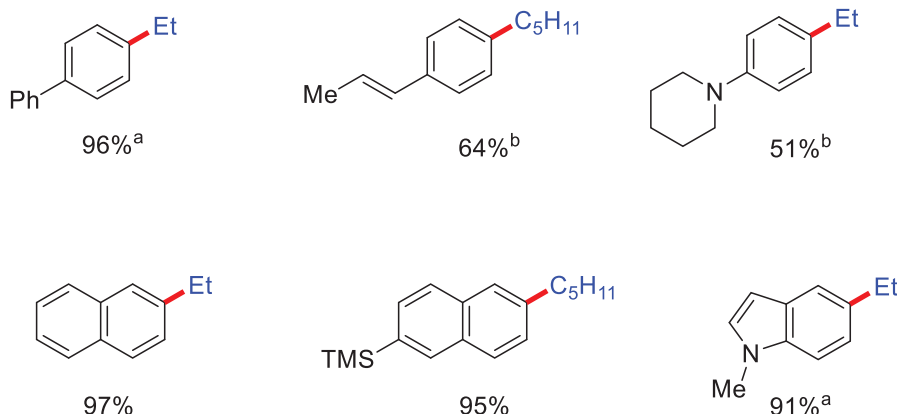
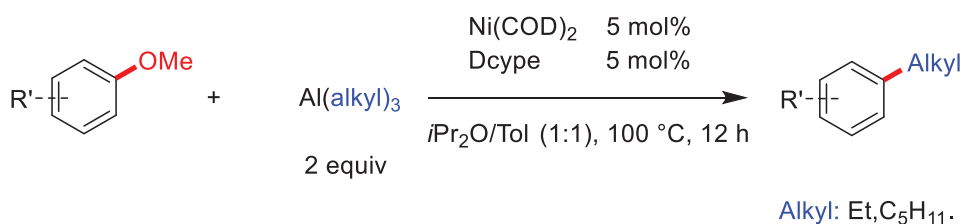
Methylation of anisole derivatives was reported with AlMe_3 using Ni(COD)_2 and NHC ligand.²⁷ ICy was shown to be the most efficient ligand. The scope was broad under mild conditions with the ability to activate some simple anisole derivatives (**Scheme 13**).



Scheme 13: Scope for cross-coupling methylation with AlMe_3 .

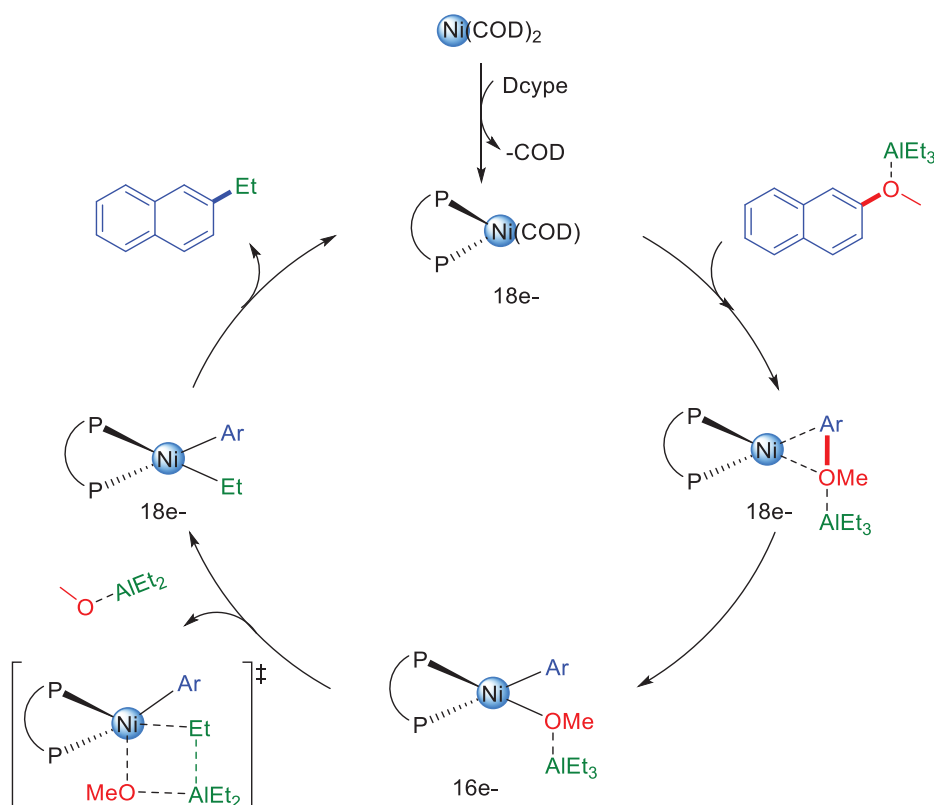
Later on, Rueping & al. reported that the best catalytic system for the introduction of higher alkyl chains was Ni(COD)_2 in combination with 1,2-Bis(dicyclohexylphosphino)ethane ligand.²⁸ Various ligands were screened, including mono- and bis-phosphines as well as NHCs, but only Dcype ligand was shown to be efficient. The coupling reaction proceeds without β -Hydride elimination, but was limited to activated anisole derivatives (**Scheme 14**).

Rueping 2016



Scheme 14: Scope for cross-coupling alkylation with Al(alkyl)₃.^[a] at 120 °C, 72 h. ^[b] at 140 °C, 72 h.

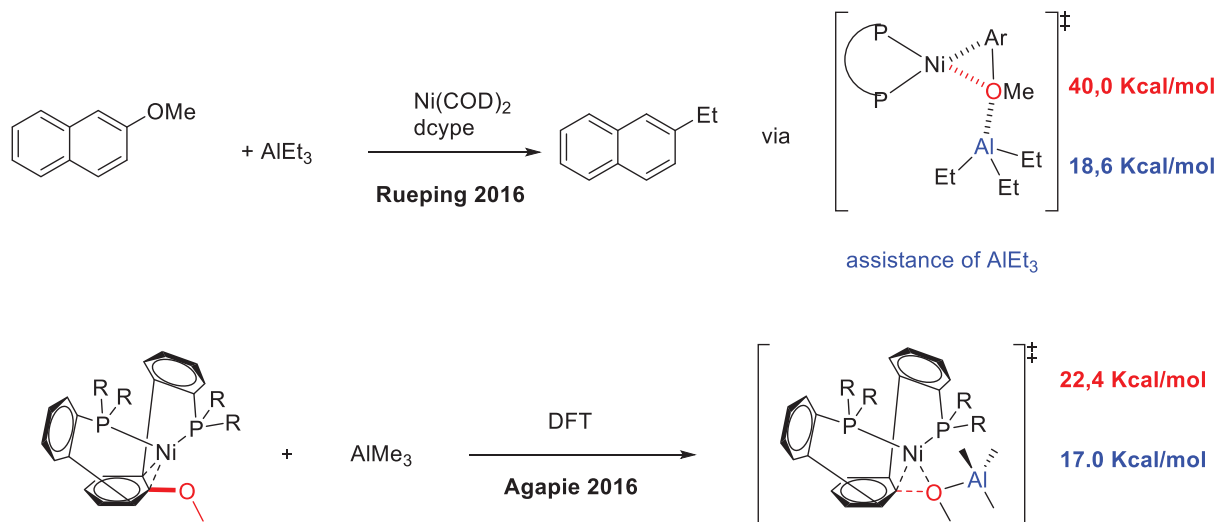
The Lewis acidic character of the organoaluminium compounds limits the tolerance towards functional groups like carbonyl, amine and hydroxyl groups. The mechanism of the reaction was proposed to take place via oxidative addition of the C–OMe bond assisted by the coordination of AlR₃ to the methoxy group with a reasonable activation barrier of 18.6 kcal/mol (**Scheme 15**). Subsequent transmetallation occurs through a four-membered transition state with an activation barrier of 19 kcal/mol. Then reductive elimination takes place releasing the valuable product and regenerating the catalyst.



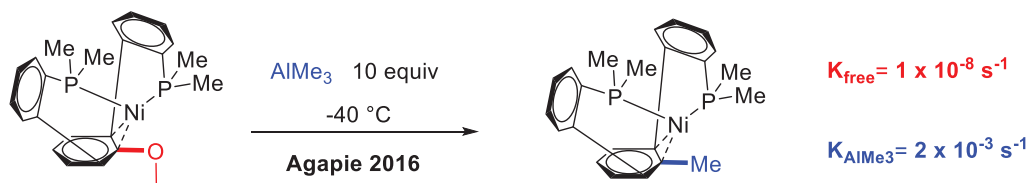
Scheme 15: Proposed mechanism for alkylative cross-coupling with AlR_3 .

The assistance of $AlEt_3$ was able to reduce the activation energy from 40.0 kcal/mol to 18.6 kcal/mol (**Scheme 16**). NMR spectroscopic studies were carried out to provide evidence for the coordination of $AlEt_3$ with methoxynaphthalene. A significant shift of the ^{27}Al NMR resonance of $AlEt_3$ from 158 to 181 ppm was observed upon reaction with the aryl ether. Also, the 1H -NMR shifts of the methoxy group, as well as those of CH_2 and CH_3 of the $AlEt_3$ were shifted indicating the coordination of $AlEt_3$ to the methoxy group. Besides this study, Agapie & al. investigated the effect of $AlMe_3$ addition in the intramolecular C–OMe bond cleavage with nickel. The reaction of $Ni(COD)_2$ with bisphosphine ligands incorporating an anisole moiety was investigated using computational and experimental tools.²⁹ DFT calculations indicated that the assistance of $AlMe_3$ lowers the activation barrier of the oxidative addition step (**scheme 16**). Kinetic studies also indicated a

dramatic effect of AlMe_3 concentration, the reaction rate being increased around 10^5 folds from that without AlMe_3 (**Scheme 17**).



Scheme 16: AlR_3 assistance in the transition states. $R=\text{Me}$.

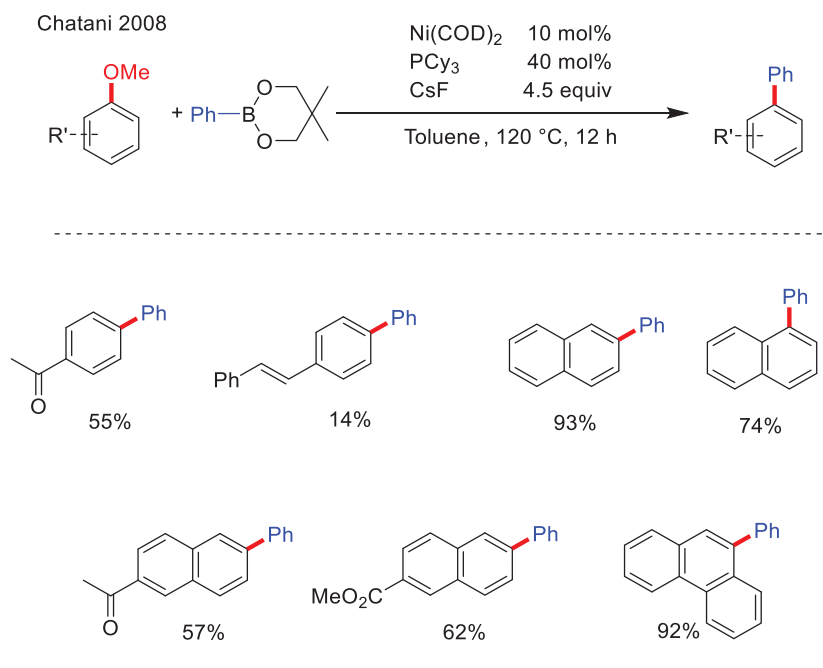


Scheme 17: Kinetic effect of AlMe_3 .

6. Cross-couplings with organoboron derivatives

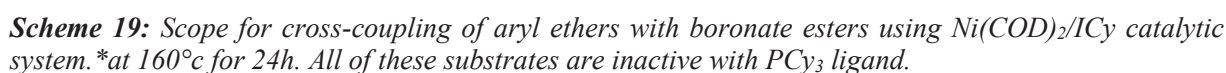
Organoboron reagents were used by the group of Chatani in 2008 as mild nucleophiles in a modified Suzuki strategy for the cross-coupling with aryl ethers using $\text{Ni}(\text{COD})_2$ and PCy_3 ligand as catalytic system.³⁰ The first attempts showed that borates and boronic acids were totally inactive, but boronic esters were excellent partners for this reaction. The base was essential for the reaction to proceed, and the best results were obtained in the presence of a large excess of CsF (4.5 equiv). Several mono- and bis-phosphine ligands as well as $\text{IPr}\cdot\text{HCl}$ were also examined, but all these

ligands were totally ineffective, PCy_3 being the only active ligand. The scope was narrow and limited to naphthyl derivatives, anisoles being totally unreactive (**Scheme 18**).

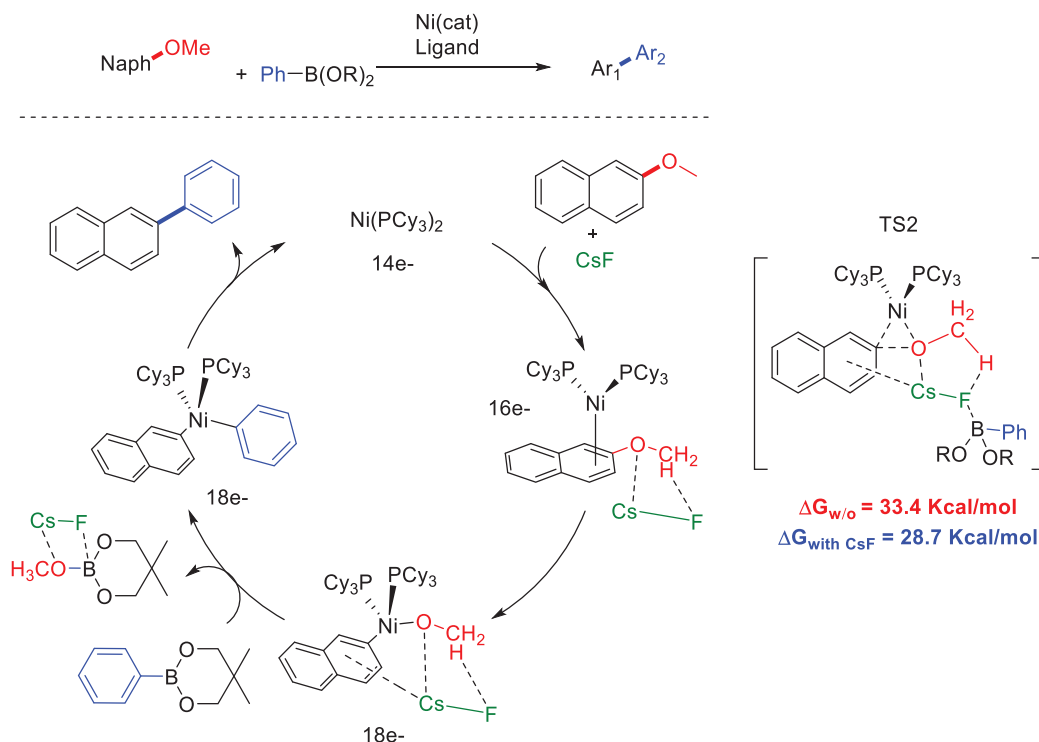


Scheme 18: Scope for cross-coupling arylation with boronate esters using $\text{Ni(COD)}_2/\text{PCy}_3$ catalytic system.

In 2014, Chatani & al. reported a more efficient catalytic system for the arylation of aryl and benzylic ethers.³¹ They explored several NHCs for catalysis. It appeared that the scope of ligands is extremely limited and only ICy is active, all other NHC ligands are inactive. The reaction proceeds well in the presence of 2 equivalents of CsF (**Scheme 19**), but later they observed in another study that the reaction can be done even without CsF .³² It is worth of note that PCy_3 was not active with these electrophiles.³⁰



In 2017, a mechanistic study on Ni-catalyzed cross-coupling of ArOMe with ArB(OR)₂ combining experimental and computational investigations indicated that the mechanism takes place via Ni⁰/Ni^{II} pathway involving oxidative addition of the C–OMe bond (**Scheme 20**).³² First, the strongly donating PCy₃ ligands replace the labile COD groups, followed by η² coordination of naphthyl ether to nickel forming the 16e[−] Ni⁰ complex. Then, oxidative addition of the C–OMe bond generates the 18e[−] Ni^{II} complex. The oxidative addition is shown to be assisted by the action of CsF and aryl boronic ester which interacts with nickel forming a quaternary complex that decreases the activation barrier of the transition state by 4.7 kcal/mol (TS2). This explains why the use of CsF is essential for the reaction to take place.



Scheme 20: Proposed mechanism for the Ni/PCy₃-catalyzed cross-coupling of aryl ethers with boronate esters assisted by CsF.

Calculations were carried out for bis-ligated NiL₂ and mono-ligated NiL species. The oxidative addition step was found to be energetically more favorable for NiL₂ species, but transmetalation step is more favorable for the NiL species. One PCy₃ should dissociate from the oxidative addition complex before transmetalation, this might explain why bidentate ligands are not suitable for this transformation. Transmetalation takes place with NiL complex via a four-membered transition state, followed by reductive elimination that regenerates the 14e⁻ Ni⁰ complex. β-hydride elimination was found to not compete with transmetalation because it is energetically less favored.

With ICy ligands, the oxidative addition was found to be energetically accessible without the aid of CsF because the Nickel-ICy bonds are stronger and therefore stabilize the O.A transition state, thus lowering the activation barrier of the oxidative addition step. Oxidative addition is the

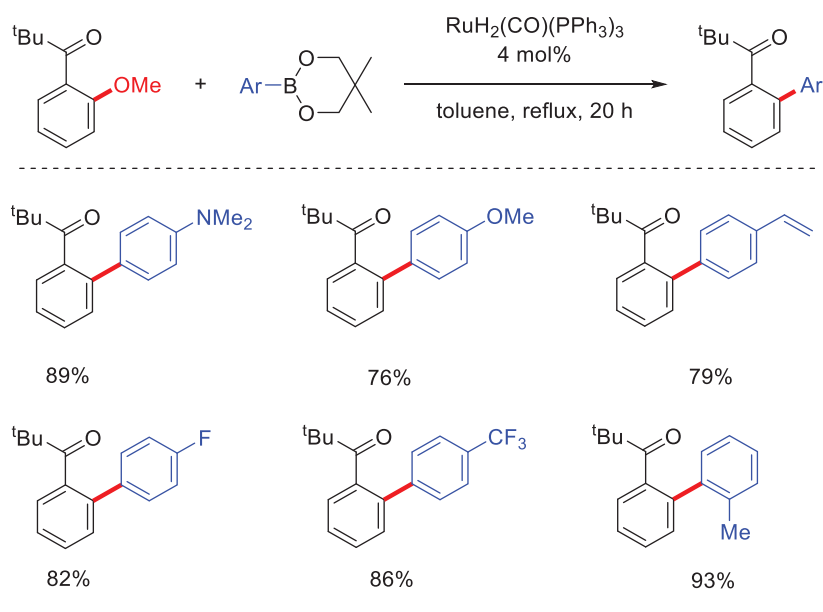
rate-determining step in this reaction and the driving force of this transformation is the high-energy release from the formation of $C_{Ar}-C_{Ar}$ bond.

The advantages of the Ni/ICy system compared to Ni/PCy₃ are the broader scope, the ability to activate challenging electrophiles like anisole derivatives and having ICy active even in the absence of the base. DFT calculations also showed that the activation barrier of the C-O bond oxidative addition with ICy is lower than that with PCy₃, as well as having a stronger binding to Ni with the carbene moiety which helps stabilizing the catalytic intermediates.³²

It is worth to mention that this type of coupling has been shown earlier to be catalyzed by ruthenium complexes by Murai in 2004.³³ The catalytic system based on $RuH_2(CO)(PPh_3)_3$ was efficient for the coupling of various organoboranes, but proved effective only with (*ortho*)-carbonyl substituted aryl ethers (**Scheme 21**).

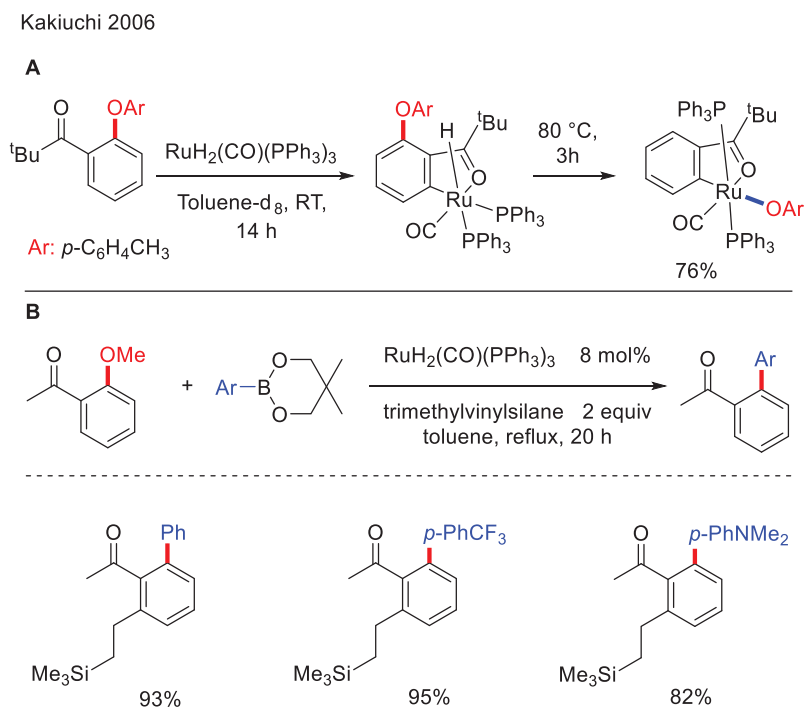
A classical Ru^0/Ru^{II} pathway was proposed. The oxidative addition is assisted by carbonyl chelation to ruthenium, which plays a critical role in C-OMe activation. The oxidative addition is followed by transmetallation with the boronate ester and reductive elimination. Even though, $RuH_2(CO)(PPh_3)_3$ catalyst is well known to promote C-H activation of acetophenone derivatives,³⁴ a high selectivity for C-OMe vs. C-H activation has been observed at high temperatures.

Murai 2004



Scheme 21: Scope for ruthenium-catalyzed cross-coupling of aryl ethers with organoboron reagents.

Later on, Kakiuchi & al. reported the isolation of the oxidative addition complex with Ruthenium (**Scheme 22-A**).³⁵ Mechanistic studies showed that C–H bond activation could be achieved at room temperature forming the ruthenium hydride complex which was well characterized by ¹H and ³¹P-NMR (a doublet at –5.97 ppm in ¹H-NMR, and the two phosphines observed at 35.49 and 39.85 ppm in ³¹P-NMR). On the other hand, heating the hydride complex at 80 °C for 3 h generates the oxidative addition complex of C–OAr bond that was isolated and characterized by X-ray crystallography. This strategy was further used for synergetic CH/CO cross-coupling of vinyl silanes and boronate esters with an excellent chemoselectivity (**Scheme 22-B**). Recently, it was reported using DFT calculations that the mechanism takes place via Ru(II)/Ru(IV) redox process which is more energetically favorable than Ru(0)/Ru(II) process and proceeds via a classical two electrons redox pathway.³⁶



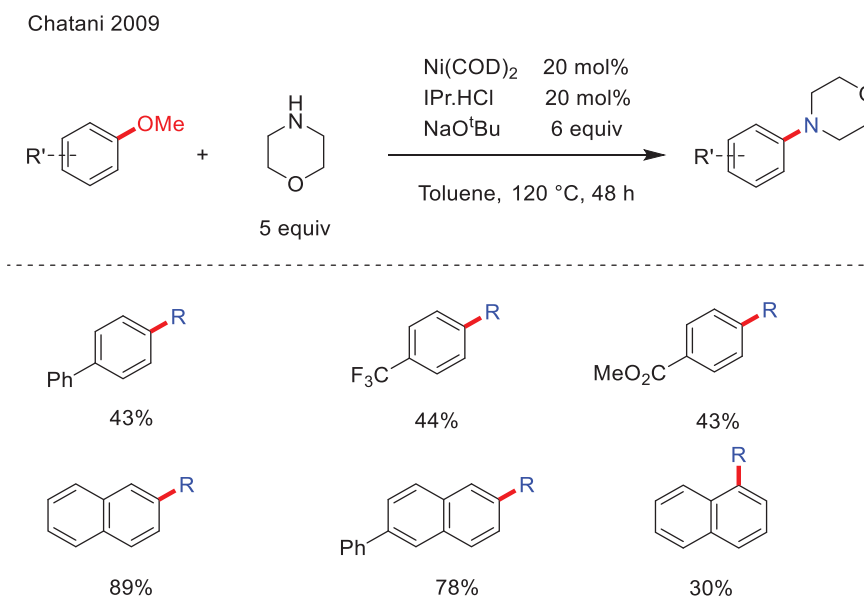
Scheme 22: Synthesis of the oxidative addition complex of C-OAr bond with ruthenium (A). The scope for cross-coupling of vinylsilanes and organoboronates with o-methoxyacetophenone (B).

II. Carbon-heteroatom bond formation

1. Carbon-Nitrogen bond formation: Cross-coupling with amines

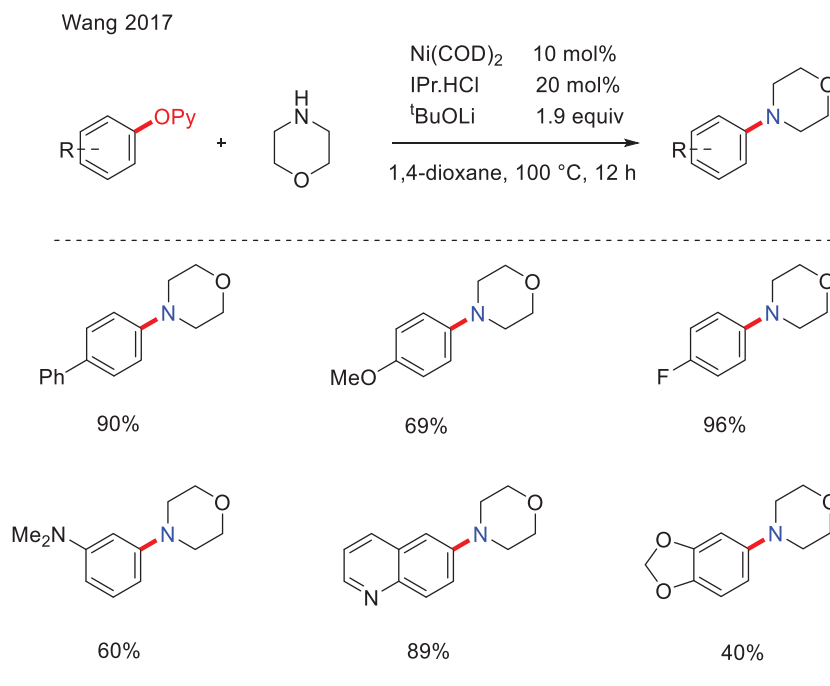
In 2009, Chatani examined the reactivity of amines as potential nucleophiles, and reported the reductive amination of aryl ethers.³⁷ The transformation was catalyzed by $\text{Ni}(\text{COD})_2$ and IPr was the ligand of choice among several other NHCs and phosphine ligands. This system was able to promote the reaction of various cyclic and acyclic amines with good yields. It appeared that increasing the cycle size has a negative impact on the yield, which could be attributed to steric hindrance. This method has several limitations. For instance, primary amines and anilines did not participate in the reaction. In addition, among the series of anisole derivatives tested, only those having electron-withdrawing groups proved effective electrophilic partners for the reaction.

(**Scheme 23**). Generally, the scope is narrow and the reaction conditions are harsh (6 equiv of base, 5 equiv of amines, 20 mol% of $[\text{Ni}^0]$, 48 h ...).



Scheme 23: Scope for cross-coupling amination of aryl ethers. $R = \text{Morpholine}$.

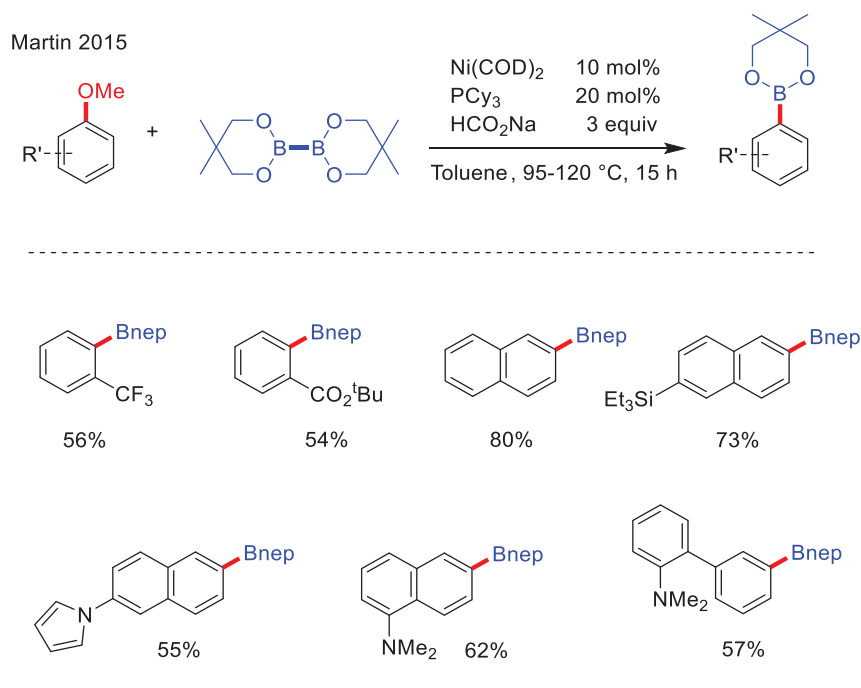
A similar catalytic system reported by Wang in 2017 was used for cross-coupling amination of aryl 2-pyridyl ethers where the reactivity was limited to only NHC ligands.³⁸ Since aryl 2-pyridyl ethers are much more reactive than aryl ethers, the scope was broader and the transformation was achieved under milder conditions (**Scheme 24**). A classical mechanism was expected to take place via a $\text{Ni}^0/\text{Ni}^{\text{II}}$ pathway involving oxidative addition of the C–OPy bond.



Scheme 24: Scope for cross-coupling amination of aryl 2-pyridyl ethers.

2. Carbon-Boron bond formation: Borylation of aryl ethers

Ni-catalyzed borylation of aryl ethers was reported by Martin in 2015.³⁹ The reaction is catalyzed by $\text{Ni(COD)}_2/\text{PCy}_3$ system using diboranes, $\text{B}_2(\text{OR})_4$, as borylating reagents. The borylation reaction works only with PCy_3 and ICy ligands as observed for the cross-coupling with ArB(OR)_2 . The scope was good enabling the activation of a variety of substrates (**Scheme 25**).

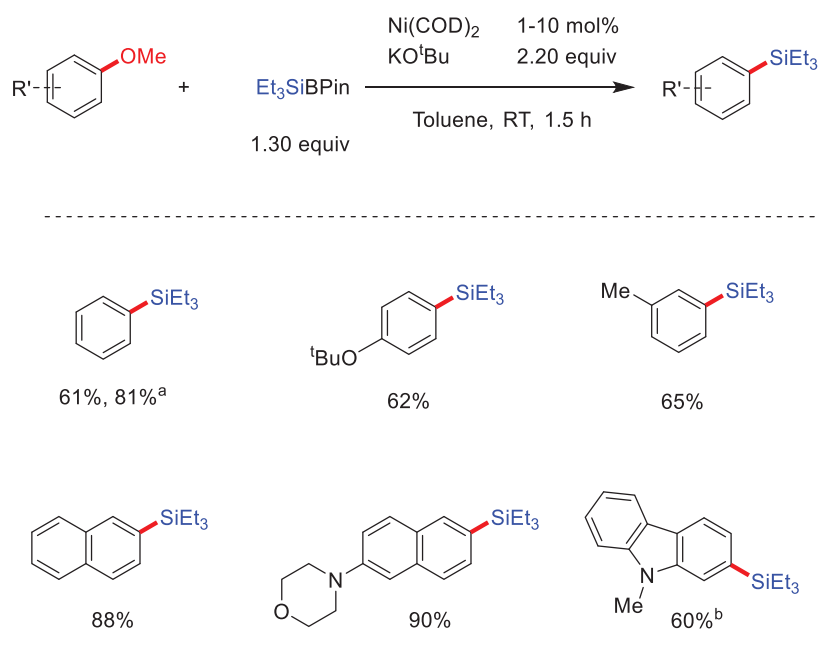


Scheme 25: Scope for borylative cross-coupling. Bnep = 5,5-dimethyl-1,3,2-dioxaborolane.

3. Carbon-Silicon bond formation: Silylation of aryl ethers

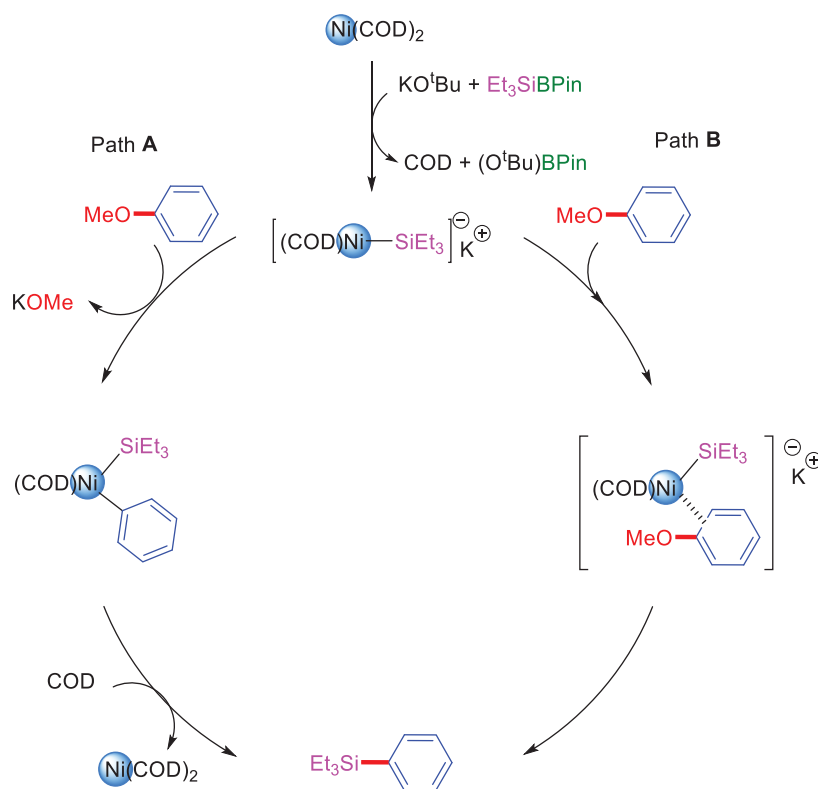
Nickel-catalyzed silylative cross-coupling was reported under mild and ligand-free conditions by the group of Martin.⁴⁰ The reaction was carried out using Ni(COD)_2 as a catalyst, excess of KO^tBu (6.5 equiv) as a base, and Et_3SiBPin as the silylating reagent. Screening of bases revealed that only KO^tBu provided fruitful results. The base survey indicated that the potassium counter ion plays an important role (NaO^tBu was inactive). Moreover, KOMe , KHMDs or KF were also not reactive, indicating that a balance of nucleophilicity and steric bulk of the base may be required. The *ipso*-silylation reaction proceeded well with several naphthyl ethers and anisole derivatives (Scheme 26).

Martin 2016



Scheme 26: Scope for silylative cross-coupling. ^a Et_3SiBPin (2.0 equiv), KO^tBu (6.50 equiv). ^b Et_3SiBPin (1.75 equiv), KO^tBu (4.50 equiv).

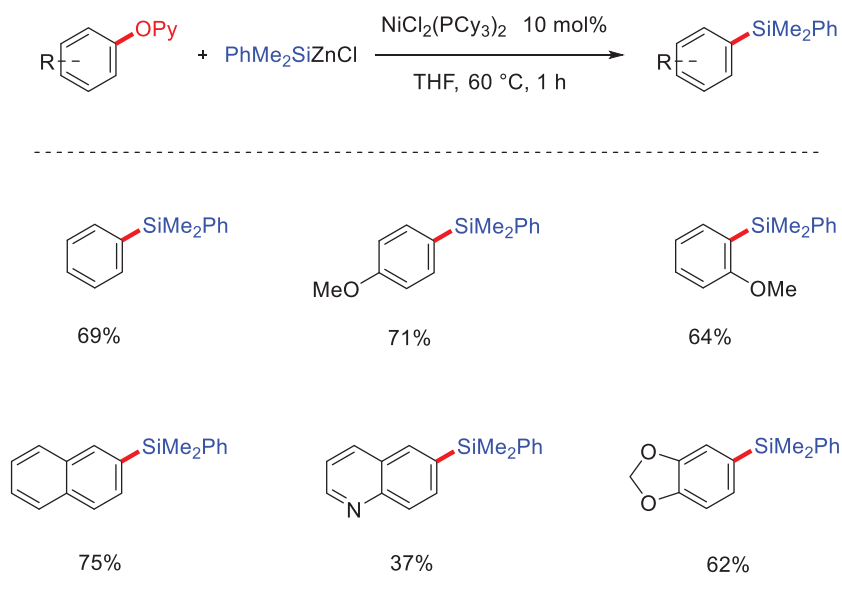
In preliminary mechanistic studies, the authors carried out a series of experiments to rule out the occurrence of heterogeneous or single electron transfer processes. The mildness of the reaction conditions (reaction proceeds even at 0 °C) and the activity in the absence of ligand suggest that a $\text{Ni}^0/\text{Ni}^{\text{II}}$ pathway via the direct oxidative addition of $\text{Ni}(\text{COD})_2$ to C–OMe bond is also unlikely. In contrast, the participation of silyl anionic species, generated *in situ* in the presence of KO^tBu , could be corroborated. Based on these experiments, the authors proposed the involvement of a silyl Ni^0 “ate” complex $[(\text{COD})\text{Ni}(\text{SiEt}_3)]^-\cdot\text{K}^+$ that could participate either in a nucleophilic aromatic substitution or in a pathway via *non-classical* oxidative addition of the Ni “ate” complex (scheme 27).



Scheme 27: Proposed mechanism for silylative cross-coupling of aryl ethers with Et_3SiH .

The silylative cross-coupling of aryl 2-pyridyl ethers was reported by Wang in 2019⁴¹ using $\text{NiCl}_2(\text{PCy}_3)_2$ complex as catalyst and $\text{PhMe}_2\text{SiZnCl}$ as the silylating reagent. Of note, $\text{NiCl}_2(\text{PCy}_3)_2$ was critical for this transformation, with minor reactivity observed with other Ni^{II} complexes possessing several mono and bidentate phosphine ligands (e.g; PPh_3 , PMe_3 , dppp and dppf). The scope was wide encompassing various electron-poor and electron-rich substrates (**Scheme 28**). Two mechanisms were proposed, either via classical oxidative addition of C–OPy bond or by the formation of Ni "ate" complexes such as $[\text{PhMe}_2\text{SiNi}(\text{PCy}_3)_2]^- \text{ZnCl}^+$ and $[\text{PhMe}_2\text{SiNi}(\text{PCy}_3)(\text{COD})]^- \text{ZnCl}^+$.

Wang 2019

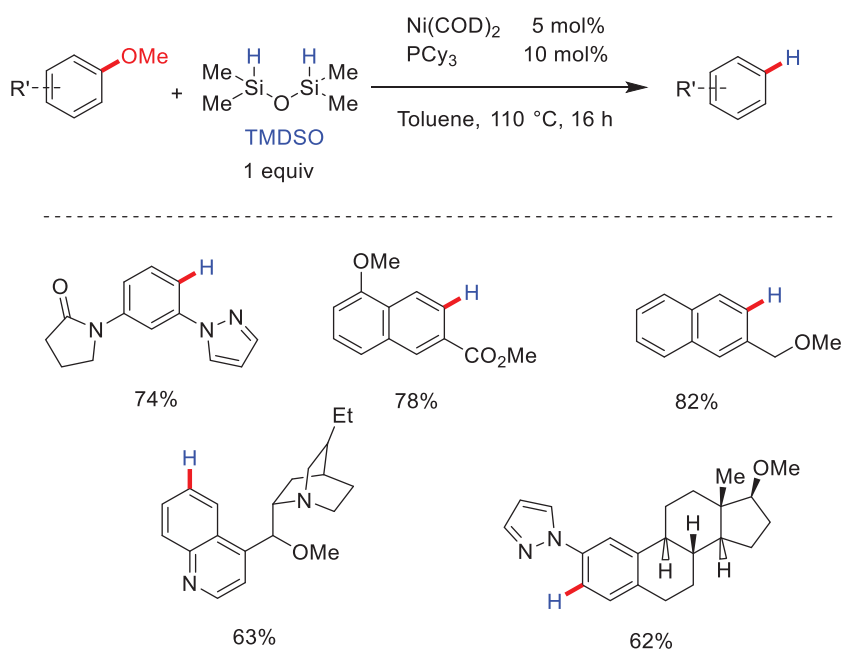


Scheme 28: Scope for silylative cross-coupling of aryl 2-pyridyl ethers.

III. Reductive cleavage of C–O bond

In 2010, the group of Martin discovered that aryl ethers could undergo catalytic hydrogenolysis by C–OMe bond cleavage using $\text{Ni}(\text{COD})_2 / \text{PCy}_3$ catalytic system and tetramethyl disiloxane (TMDSO) as a hydride source.⁴² Among several phosphines, only PCy_3 ligand was active for catalysis. The reaction did not work in the absence of nickel catalysts indicating that the activation of the C–OMe bond by nickel was required. Deuterium labeling experiments with D-TMDSO clearly showed that this species acts as a hydride source. The method is mild and can be used for late-stage synthesis. The scope was large but included mainly methoxynaphthalenes, with anisole derivatives remaining essentially unreactive (**Scheme 29**).

Martin 2010

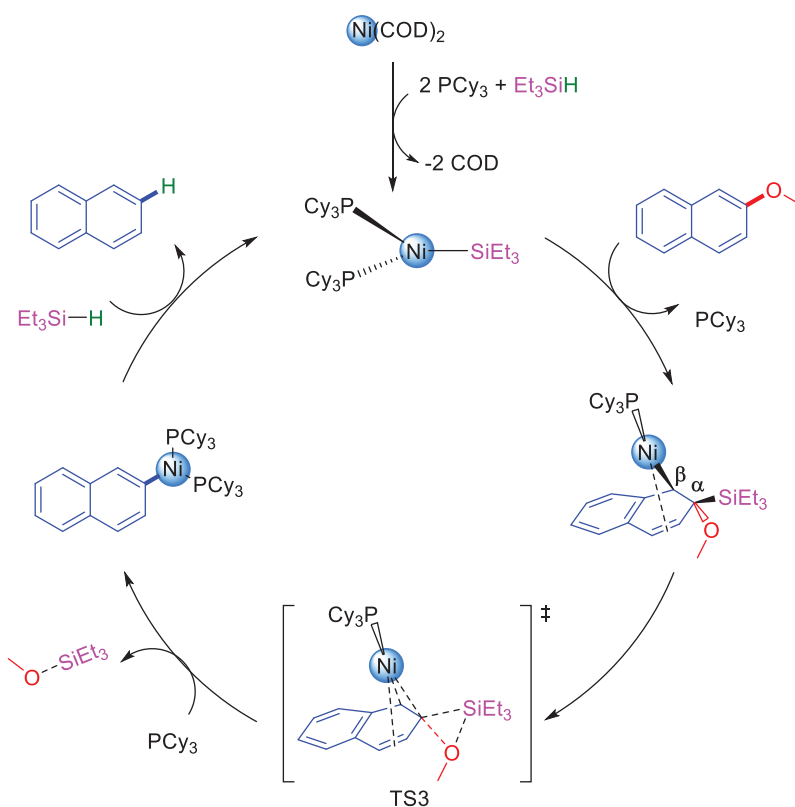


Scheme 29: Scope for cross-coupling hydrogenolysis with TMDSO.

Independently, Chatani & al. published a similar work in 2011.⁴³ It was found that many hydrosilane species can act as hydride donors. The best reductant was found to be $HSiMe(OMe)_2$ due to its high Lewis acidity which can improve the σ -bond metathesis (σ -CAM) of C–OMe bond by strengthening the Si–OMe interaction in the transition state. Deuterated studies indicate also that $HSiMe(OMe)_2$ acts as a hydride source and the hydride is not coming from the methoxy group or solvent.

The group of Martin conducted thorough mechanistic studies combining experimental and theoretical investigations. In contrast to previous reports, a Ni^0/Ni^{II} pathway involving oxidative addition of Ar–OMe to Ni^0 was shown to be unlikely in this case. The authors proposed that the mechanism takes place via a Ni^I pathway (**Scheme 30**).⁴⁴ In this mechanism, $(PCy_3)_2Ni^I-SiEt_3$ is the active catalyst that initiates the catalytic cycle by η^2 -C–OMe coordination and migratory insertion of the naphthyl group forming the benzylic Ni^I complex. This was followed by the migration

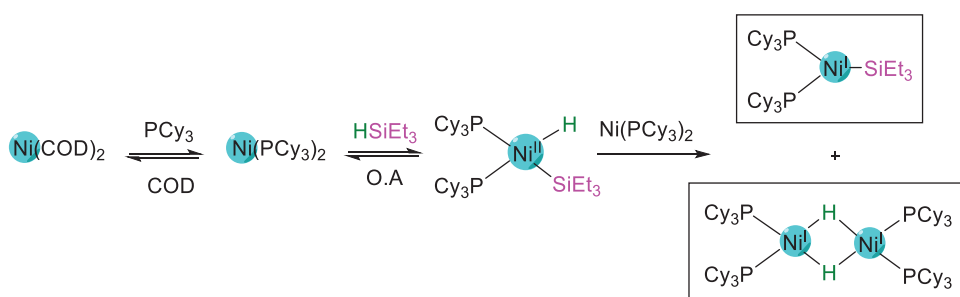
of Ni^{I} species from the β to α position combined with the elimination of $(\text{OMe})\text{SiEt}_3$ via a three-membered transition state (TS3). Finally, the $(\text{PCy}_3)_2\text{Ni}^{\text{I}}(\text{naphthyl})$ complex undergoes σ -bond metathesis with Et_3SiH forming naphthalene and regenerating the catalyst. The rate-determining step in this reaction is the migratory insertion to naphthalene and not the C–OMe activation having a barrier of 32.9 kcal/mol.



Scheme 30: Proposed mechanism for reductive hydrogenolysis of methoxynaphthalene with Et_3SiH via Ni^{I} species.

NMR monitoring of the reaction showed rapid consumption of the reactants without the formation of any intermediates detectable by ^1H -NMR or ^{29}Si -NMR. The reaction was also monitored by IR spectroscopy indicating the decreasing of the characteristic Si–H bond at 812 cm^{-1} of HSiEt_3 with an induction period. The ^1H NMR of the reaction crude showed a signal at -15.8 ppm

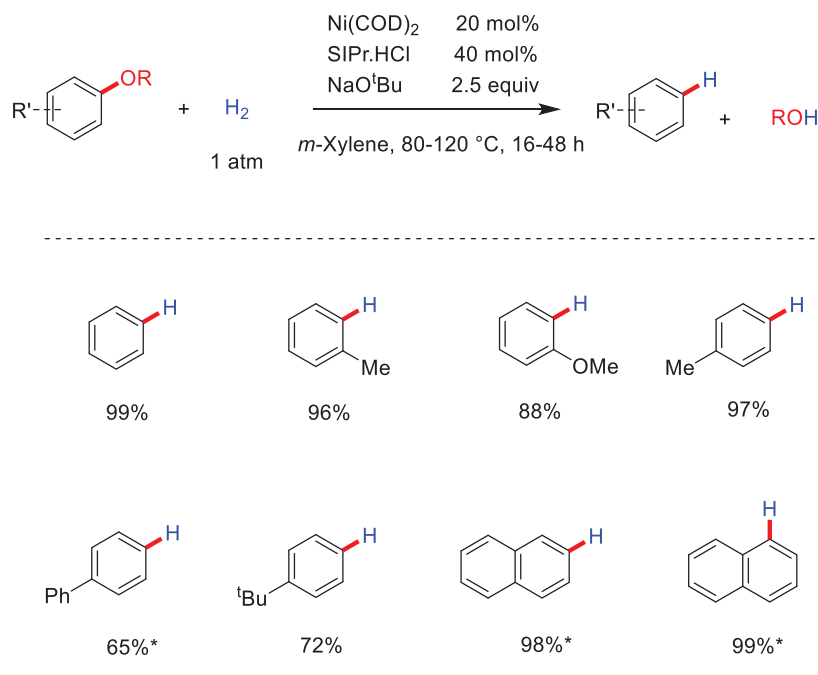
which corresponds to a nickel hydride complex. In addition, EPR spectroscopy identified the presence of a characteristic signal for Ni^{I} species during the induction period and also after the formation of the product. These results indicate the presence of paramagnetic Ni^{I} intermediates that are most likely generated by comproportionation. Therefore, the $(\text{PCy}_3)_2\text{Ni}^{\text{I}}\text{-SiEt}_3$ intermediate was proposed to be generated *in situ* from a disproportionation reaction between $(\text{PCy}_3)_2\text{Ni}^0$ and $(\text{PCy}_3)_2\text{Ni}^{\text{II}}(\text{SiEt}_3)\text{H}$ issued from oxidative addition of HSiEt_3 to $(\text{PCy}_3)_2\text{Ni}^0$ (**Scheme 31**). The disproportionation generates another Ni^{I} -hydride complex that is not active for catalysis.



Scheme 31: Mechanism for the formation of Ni^{I} species by disproportionation from Ni^{II} complex.

Another hydrogenolysis transformation was reported by the Hartwig group in 2011 using hydrogen gas (1 atm) as a hydride source.⁴⁵ The reaction is catalyzed by $\text{Ni}(\text{COD})_2$ and NHC ligands. The use of PCy_3 as ligand did not afford the desired product. Instead, cyclohexane and cyclohexene were formed, indicating that Cy-P bond cleavage takes place, dissociating the active catalyst. Among several NHC ligands, SIPr (1,3-Bis(2,6-di-*i*-propylphenyl)imidazolidin-2-ylidene) is the best ligand.

Hartwig 2011



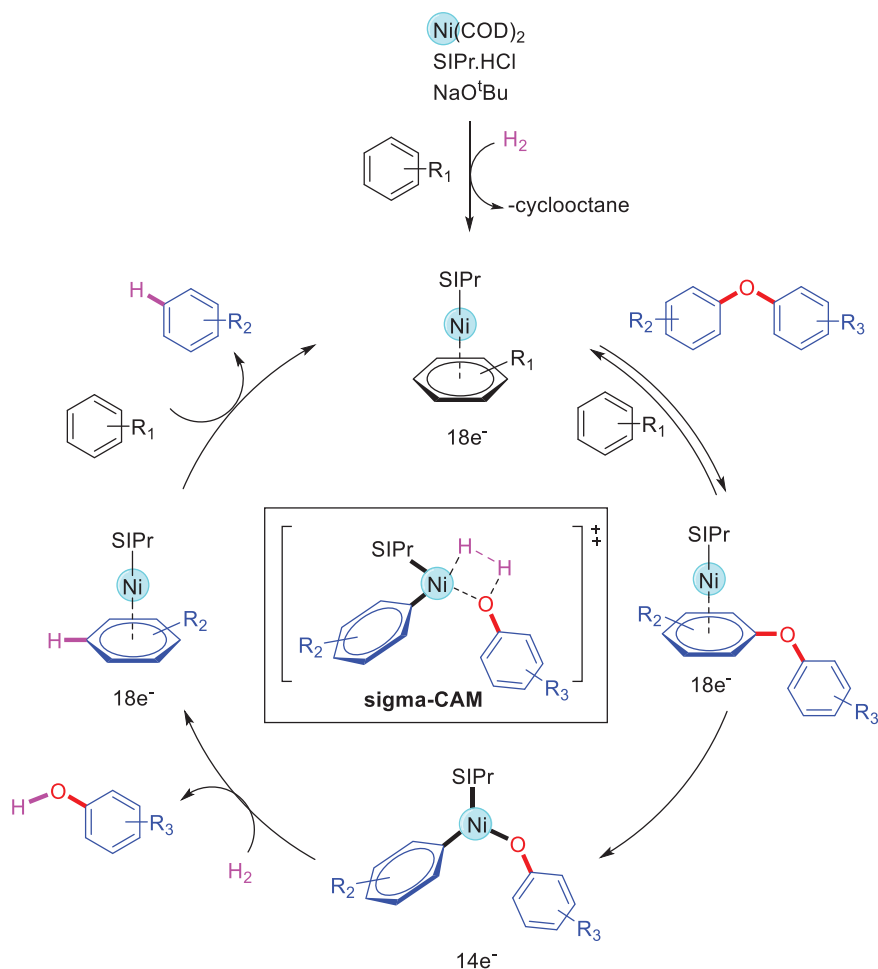
Scheme 32: Scope for hydrogenolysis with hydrogen gas. *R = Me, with 1 equiv AlMe₃. All other R groups are symmetrical.

Interestingly, the addition of 1 equivalent of AlMe₃ improved the yield of the reaction. The scope was broad, encompassing various aryl ethers having different substituent groups with good to excellent yields (**Scheme 32**). Aryl substrates bearing electron-withdrawing groups reacted more readily than those having electron-donating groups. A competition reaction between methoxy and diphenyl ethers showed a better reactivity for the latter.

This methodology takes hydrogenolysis of aryl ethers to a whole new level, owing to its selectivity, mildness, and cost-efficiency with high atom economy. It can be used as an industrial process for biomass conversion and lignin reduction, as an alternative to technologies using high pressures and temperatures with heterogeneous catalysts which are totally unselective giving rise to several by-products.⁴⁶

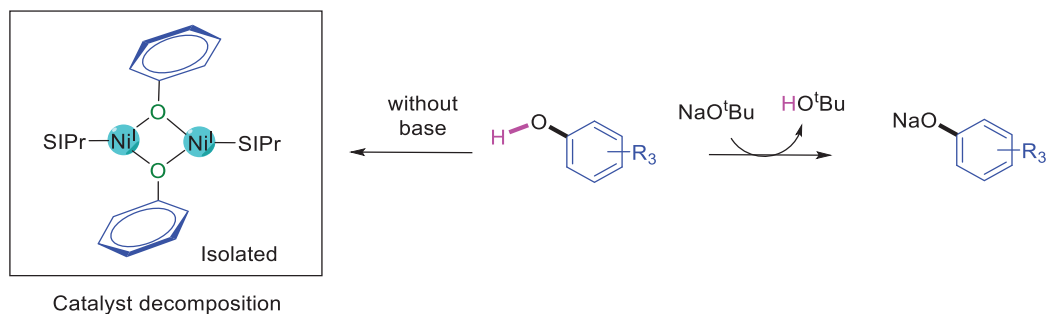
In 2016, a theoretical study reported by Chung suggested that the activation of di-aryl ethers is accomplished via an anionic Ni^0 pathway.⁴⁷ After the formation of the precatalyst $(\text{SIPr})\text{Ni}(\text{COD})$ in the presence of an excess of NaO^tBu (2.5 equiv), the butoxide group attacks the metallic center forming an anionic nickel species $[(\text{SIPr})\text{Ni}(\text{O}^t\text{Bu})]^- \cdot \text{Na}^+$. The anionic species is more nucleophilic and facilitates a smooth oxidative addition of PhOPh forming $[(\text{SIPr})\text{Ni}(\text{O}^t\text{Bu})(\text{Ph})(\text{OPh})]^- \cdot \text{Na}^+$ complex. This was followed by dissociation of phenoxide group and coordination of dihydrogen where a σ -bond metathesis (σ -CAM) takes place generating the nickel-hydride complex $[(\text{SIPr})\text{Ni}(\text{H})(\text{Ph})]$ and releasing butanol. Finally, the reductive elimination takes place from the hydride complex combined with an attack of another butoxide regenerating the initial anionic catalyst and releasing the valuable reduced product.

However, the group of Hartwig thoroughly investigated the mechanism of the reaction in 2017. The isolation of several key intermediates, and kinetic studies led to the proposition of a mechanism involving classical $\text{Ni}^0/\text{Ni}^{\text{II}}$ pathway (**Scheme 33**).⁴⁸ Initially, a $(\text{SIPr})\text{Ni}^0(\eta^6\text{-C}_6\text{D}_6)$ species is formed by π -coordination of the solvent to nickel as indicated by ^1H NMR and UV-vis spectroscopy. Then, the solvent is replaced by the di-aryl ether substrate to form an $\eta^6(\text{PhOPh})\text{Ni}^0$ intermediate that has been isolated and characterized by X-ray diffraction analysis. This is followed by oxidative addition of the C-OPh bond to Ni^0 , which was established as the rate determining step with an associated barrier of 26 kcal/mol. Then, dihydrogen undergoes a complex-assisted σ -bond metathesis (σ -CAM) with $\text{Ni}^{\text{II}}\text{-OAr}$ intermediate via a four-membered transition state, followed by reductive elimination that liberates phenol and generates a new $(\text{SIPr})\text{Ni}^0(\eta^6\text{-aryl})$ species. Solvent-assisted release of the arene restarts the catalytic cycle.



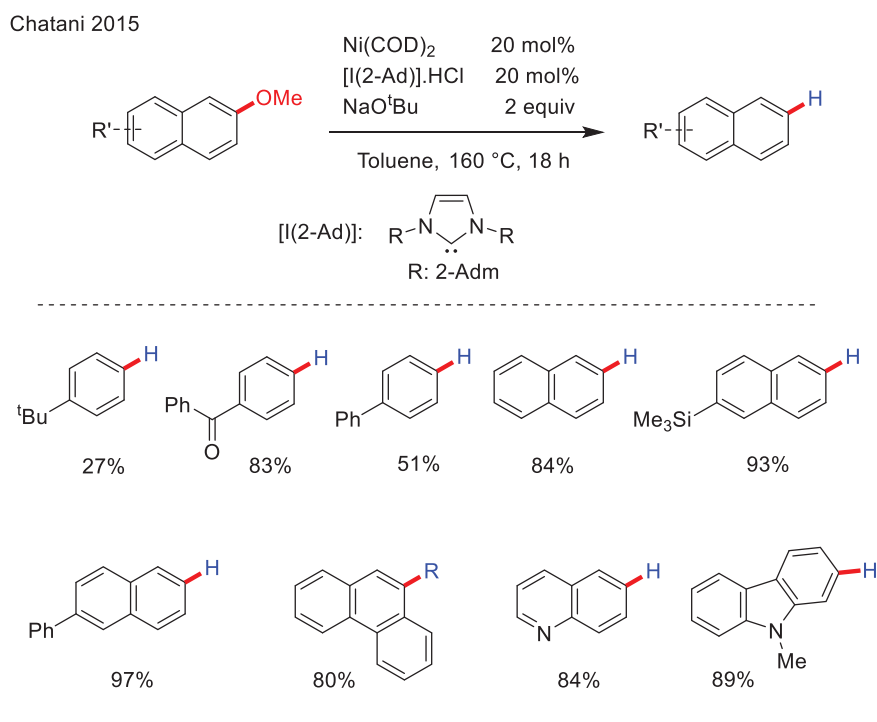
Scheme 33: Proposed mechanism for the reductive hydrogenolysis of di-aryl ethers with hydrogen. Ar-R_1 =solvent or C_6D_6 .

The authors showed that the base does not play any role in the oxidative addition step. Instead, the base has been shown to play a key role by preventing catalyst decomposition. Without the presence of the base, the released phenol compound reacts with nickel to form an unreactive Ni^{I} di-hydroxy species which was isolated and characterized by X-ray diffraction analysis. The base is proposed to react with the released phenol to form a phenoxide species and thus prevent from catalyst decomposition to Ni^{I} species (**Scheme 34**).



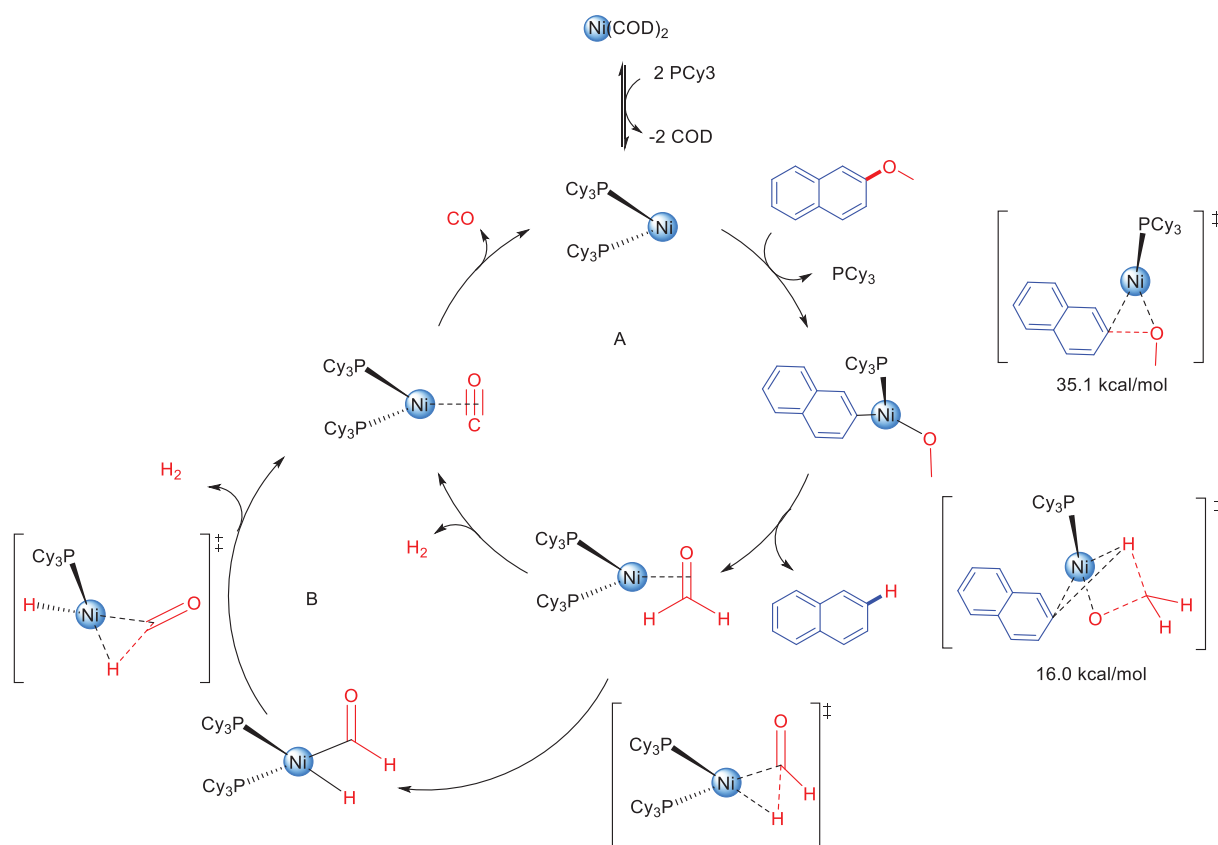
Scheme 34: The role of the base in the hydrogenolysis of diaryl ethers.

The group of Chatani showed recently that reductive cleavage could take place in the absence of any external reductant using NaO^tBu as sole reagent in the presence of Ni(COD)₂/NHC ligand [I(2-Ad)] as catalyst system (**Scheme 35**).⁴⁹ PCy₃ and SIPr which are the most effective ligands for hydrogenolysis with silanes and dihydrogen showed poor reactivity. Deuterium labeling experiments indicated that the hydrogen is delivered directly from the methoxy group.



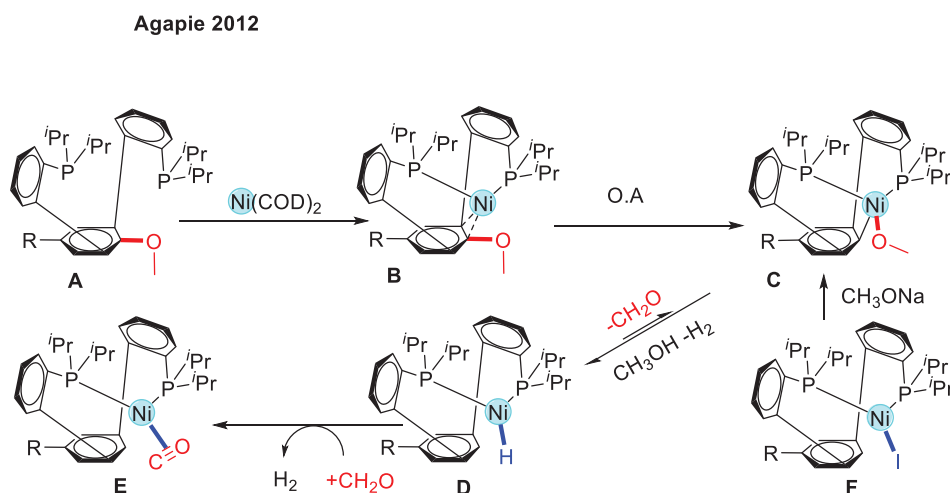
Scheme 35: Scope of the hydrogenolysis reaction without external reductant.

In the course of their investigations on hydrogenolysis of ethers with silanes, the group of Martin computed a reaction pathway that could account for the formation of naphthalene without external reductant (**Scheme 36**).⁴⁴ After coordination of the substrate, oxidative addition takes place via a three-membered transition state with an activation barrier of 35.1 kcal/mol, then β -hydride elimination of the coordinated methoxy group would generate the Ni^0 (formaldehyde) intermediate and release naphthalene. The Ni^0 (formaldehyde) intermediate undergoes oxidative addition of the C–H bond of formaldehyde followed by α -elimination to give Ni^0 (carbonyl) complex and dihydrogen (**Scheme 36**).



Scheme 36: Proposed mechanism for the reductive hydrogenolysis of di-aryl ethers without external reductant.

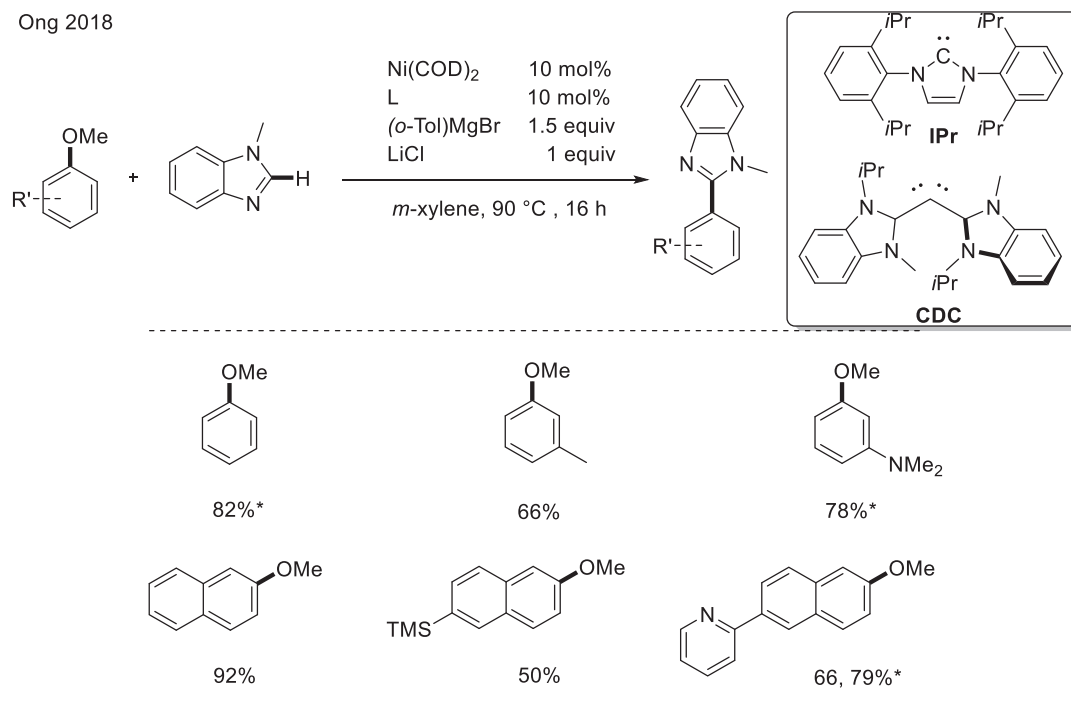
The group of Agapie also showed that a similar process could take place with Ni(diphosphine) complexes.⁵⁰ Remarkably, a Ni⁰ complex with a methoxyarene bound in an η^2 manner was isolated (**Scheme 37-B**). Heating of the complex **B** for 12 h at 45 °C while monitoring by ¹H NMR led to the formation of new species with NMR signals characteristic of Ni-methoxide complex **C** that has been independently prepared from complex **F**. This species is not stable and undergoes β -hydride elimination to give the Ni-hydride complex **D**, followed by an α -elimination forming Ni⁰(carbonyl) complex with generation of dihydrogen.



Scheme 37: Stoichiometric intramolecular cleavage of C–OMe bond.

IV. C-H arylation with aryl ethers derivatives

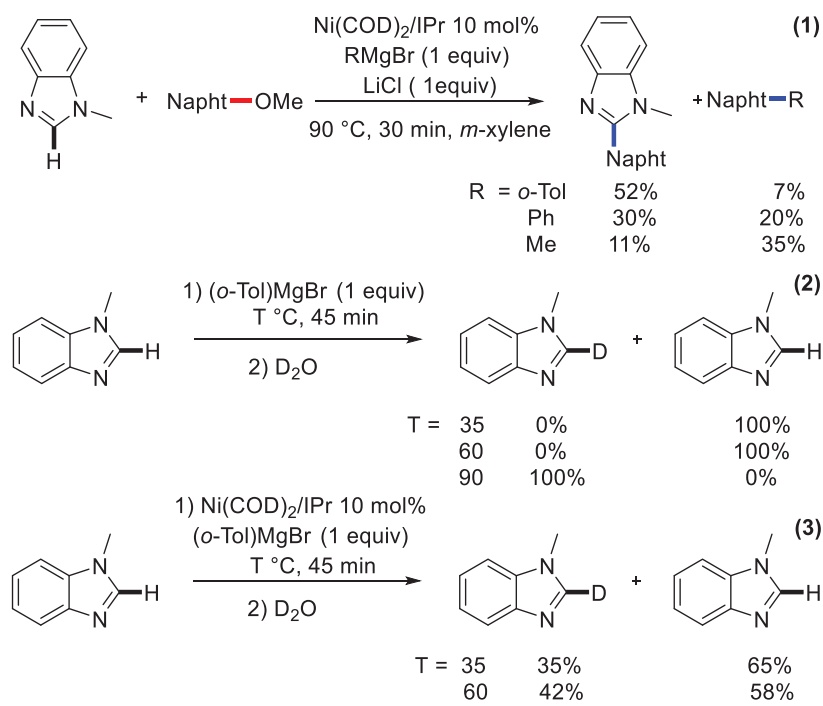
In 2018, the group of Ong reported the cross-coupling of aryl ethers with 1-methylbenzimidazole.⁵¹ The reaction is carried out using a combination of Ni(COD)₂ and IPr-NHC, in the presence of an excess of (*o*-Tol)MgBr. Several phosphines and NHC's were effective with carbodicyclobene (CDC) being superior to IPr-NHC ligand. The scope was broad enabling the activation of various aryl ethers including anisole derivatives (**Scheme 38**).



Scheme 38: Scope for cross-coupling of aryl ethers with 1-methylbenzimidazole. *with CDC.

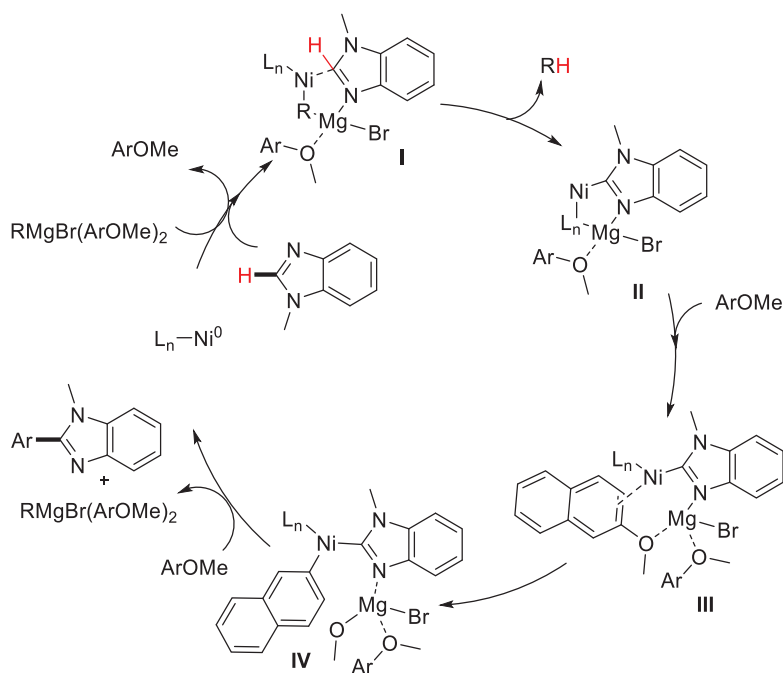
Even though ArMgBr reagents are well known to readily arylate the C-OMe bond under similar conditions,¹² the reaction was very selective towards the arylation of benzimidazole with minor amount of bi-aryl by-product. The selectivity toward CO/CH arylation was further enhanced by using bulky Grignard reagents (**Scheme 39.1**).

In order to further understand the role of $(o\text{-Tol})\text{MgBr}$, deuterium labeling experiments were conducted indicating that ArMgBr is enrolled in the deprotonation of azole and probably to form (azole) MgBr adduct *in situ* (**Scheme 39.2**). The deprotonation was observed only at 90 °C, however, the addition of Ni(COD)_2 to the medium makes the deprotonation possible at much lower temperatures (**Scheme 39.3**). These outcomes clearly highlight the importance of both nickel and Grignard reagent and their cooperation in assisting C–H bond activation.



Scheme 39: Mechanistic studies on $ArMgBr$ role.

The addition of radical scavengers like TEMPO had a negative impact on the yield pointing toward the involvement of radical species in the process. However, no EPR signal was detected all over the reaction at ambient and low temperatures, suggesting that two electrons redox process is more reasonable (**Scheme 40**). Starting from L_nNi^0 , the deprotonation was shown to be assisted by the cooperation of $RMgBr$, 1-methylbenzimidazole and methoxynaphthalene which interact with nickel forming a quaternary complex **I**, followed by the release of $R-H$ and the formation of complex **II**. The coordination of methoxynaphthalene to **II** generates complex **III** that undergoes a L.A promoted oxidative addition of the CO-Me bond aided by magnesium coordination forming complex **IV**. Subsequently, reductive elimination of **IV** takes place while releasing the valuable product and restoring the active catalyst.

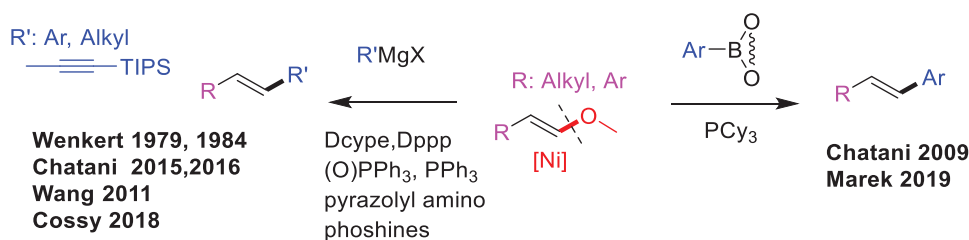


Scheme 40: Proposed mechanism for the tandem CO/CH cross-coupling of aryl ethers with azoles. $R = \text{Tol}$.

Imperatively, the cooperative effect between RMgBr and nickel is fundamental for enabling the C–O/C–H cleavage, and a more sterically demanding Grignard reagent is additionally critical to suppress the side products in this reaction like Ar-R , azole- R and homocoupling product. More strikingly, in contrast to what was reported before, DFT calculations shows that the rate-determining step in this reaction is reductive elimination and not oxidative addition.

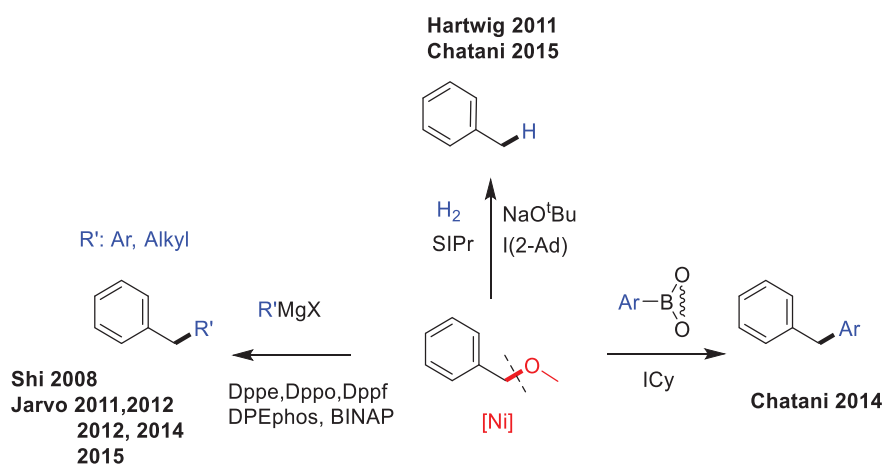
V. Cross-coupling reactions of vinylic and benzylic ethers

Several cross-coupling reactions of vinylic ethers were reported like arylations with boronate esters,^{52,53} alkylations and arylations with Grignard reagents, and few examples of alkynylations (Scheme 41).^{20,15,16,54,55,21}



Scheme 41: Ni-catalyzed cross-couplings of vinylic ethers.

Benzylic ethers have also been used as interesting substrates for similar transformations, most of them being stereoselective.^{31,56,57,58,59,60} Additionally, few examples are reported on their use for hydrogenolysis (**Scheme 42**).^{45,49}

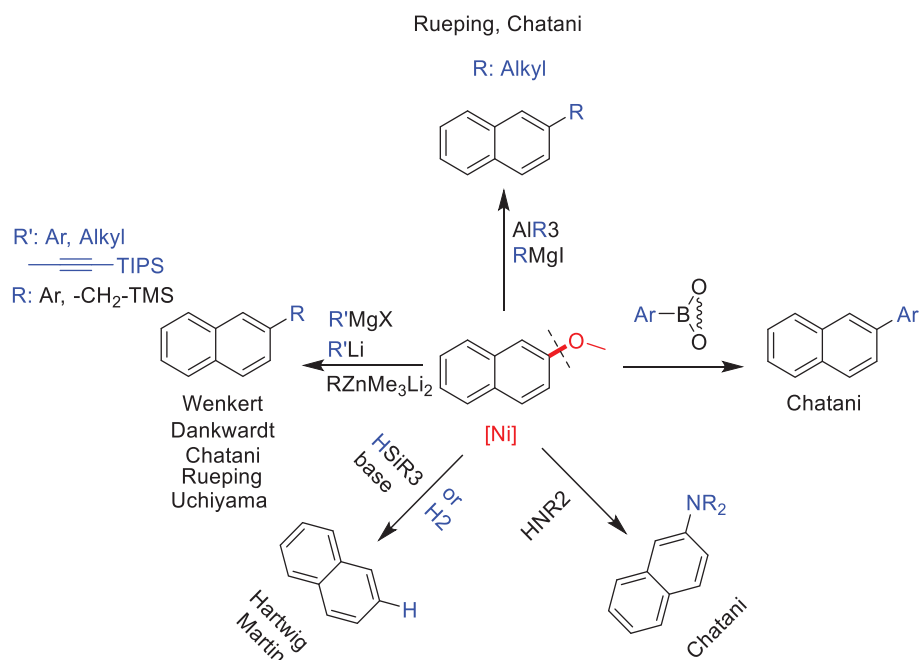


Scheme 42: Ni-catalyzed cross-couplings of benzylic ethers.

The activation of aryl ethers is much more difficult than vinylic and benzylic ethers due to the conjugation caused by the aryl group and the high bond dissociation energy of the C–OMe bond. In general, most of the catalytic systems used for aryl ethers are active for vinylic and benzylic ethers. In contrast, only a few systems that are used for benzylic and vinylic ethers can activate aryl ethers. The general scope and the scope of active ligands are broader than those of aryl ethers and several new bi-dentate ligands are active, including chiral ligands that are used for stereospecific synthesis.

VI. Summary

The seminal work of Dandkwart inspired chemists to explore other active nucleophilic partners for cross-coupling of aryl ethers. Several C–C bond forming reactions were reported, including arylation, alkylation, methylation,²⁷ and alkynylation (**Scheme 43**). In addition, C-heteroatom bond-forming processes were also developed for borylation,³⁹ silylation,⁴⁰ amination, as well as reductive C–O bond cleavage processes.⁶¹



Scheme 43: State of the art for the major cross-coupling transformations of aryl ethers.

In general, relatively few ligands were shown to be reactive for the functionalization of aryl ethers. Furthermore, the scope of active ligands is somehow related to the type of nucleophile used. With strong nucleophiles, such as Grignard or organolithium reagents, the cross-coupling reactions have been shown to proceed quite well with several phosphines and NHC ligands (**Table 1**). The ligand is even not required for the coupling of organolithiums. While unsaturated organo-

metallic reagents (e.g: ArMgX , $\text{ArZnMe}_3\text{Li}_2$, alkynyl- MgX) and AlMe_3 work better with monodentate ligands, alkyl metallics like alkyl MgI and AlR_3 ($\text{R} \neq \text{Me}$) work only with bidentate ligands. Bidentate ligands are essential for alkylative cross-coupling in order to saturate the vacant sites of the catalyst and inhibit β -hydride elimination.

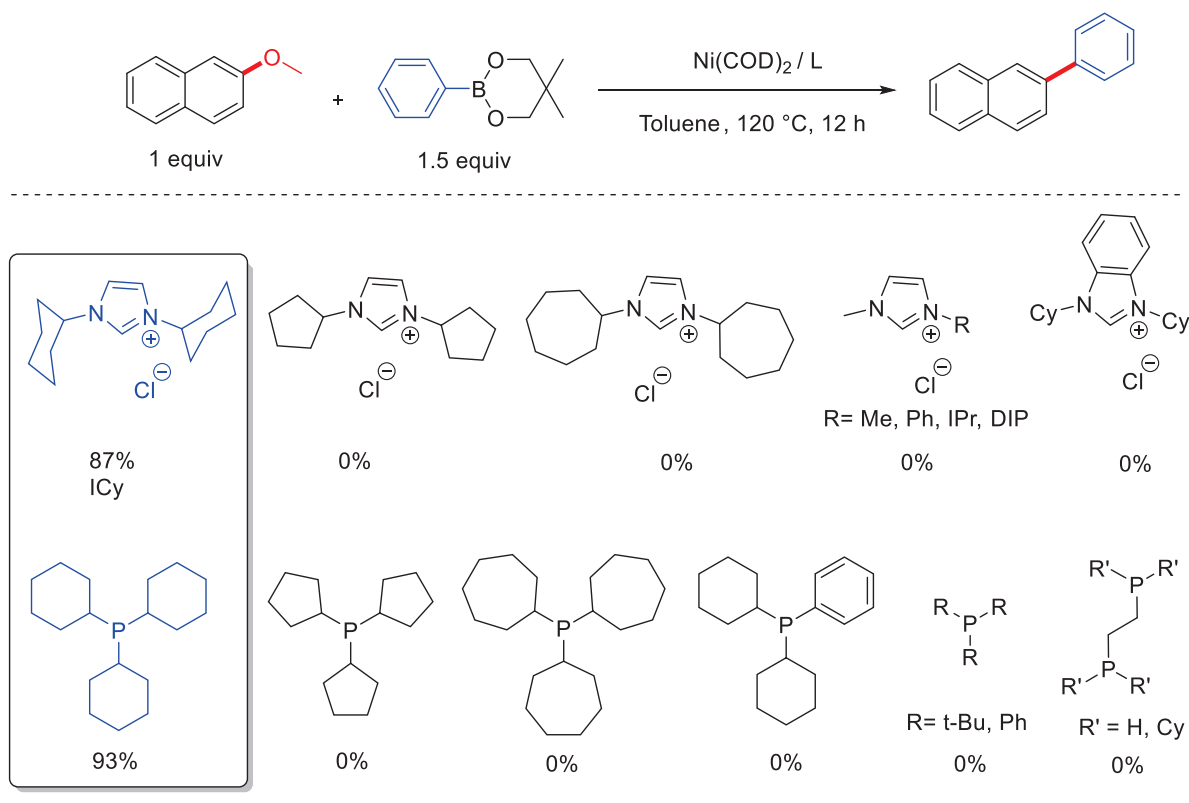
For hydrogenolysis, the ligand is highly dependent on the reductant used. For example, PCy_3 is critical for processes based on the use of silanes as reductants, while all phosphines including PCy_3 are not active when dihydrogen is involved. Otherwise, several NHC ligands are also active, with SIPr being the most efficient. Reductions performed in the absence of reductant are poorly effective using either PCy_3 or SIPr as ligands. A bulkier ligand like Adm-NHC is required probably to enhance reductive elimination.

Table 1: Critical data analysis with trends of reactivities of the nucleophiles w.r.t ligands.

Type	nucleophile	ligand	Only active ligand?
Strong nucleophiles	Very strong (ArLi , RLi)	Ligand free SIMes	No
	Non-alkylative (ArMgX , $\text{ArZnMe}_3\text{Li}_2$, Alkynyl MgX)	Monodentate (PPh_3 , PCy_3 , $\text{ICy}\dots$)	No
	Alkylative (Alkyl MgI , AlR_3)	Bidentate (Dcype)	AlR_3 : Yes RMgI : limited to bidentate ligands
	Highly L.A ($\text{Ln}(\text{CH}_2\text{SiMe}_3)_3(\text{THF})_2$)	PCy_3	No
Hydrogenolysis	Silanes	PCy_3	Yes
	Hydrogen	SIPr	Limited to NHCs
	none	Adm-NHC	Almost
Mild nucleophiles	Amines	IPr-NHC	Almost
	ArB(OR)_2 - $\text{B}_2(\text{OR})_4$	PCy_3 / ICy	yes

Moving for milder systems the ligand becomes more and more dependent on the nucleophile used. For example, with boronate esters only PCy₃ and ICy are effective. For amines, minor reactivities were observed with several ligands even under harsh conditions, with IPr-NHC being the most reactive ligand.

In general, the information on the structure/activity relationship of nickel-based catalysts for these cross-coupling transformations is scarce. This is in striking contrast to the tremendous knowledge on ligand design accumulated over the past two decades for palladium-catalyzed cross-couplings reactions.⁶ It appears that direct transfer of this knowledge to nickel catalysis is far from straightforward. Indeed, several phosphine and carbene-based ligands very efficient in palladium cross-coupling catalysis are not reactive with nickel catalysis. PCy₃ and ICy ligands are by far the most used ligands for the cross-coupling of aryl ethers, and they have been shown to even display unique reactivities with many nucleophiles. Intriguingly, even very subtle ligand modifications, such as using cyclopentyl or cycloheptyl instead of cyclohexyl substituents, or using alkyl groups and phenyl generally result in complete suppression of activity (**Scheme 44**). Important efforts directed to clear identification of the key parameters governing the reactivity of nickel in catalytic C–O bond functionalization of aryl ethers are highly required to unveil the synthetic potential of this methodology.



*Scheme 44: Ligand problem and limits.*²

Regarding the mechanisms (**Table 2**), the activation was generally proposed to proceed via oxidative addition in the case of mild nucleophiles like RB(OR)_2 and $\text{B}_2(\text{OR})_4$. In contrast, for strong nucleophiles having weak Lewis acid character, like ArMgX , ArLi , and $\text{ArZnMe}_3\text{Li}_2$, the activation is always achieved via nickel “ate” complex. The high nucleophilicity of these reagents favors the transfer of the anionic motifs to Ni and the formation of Ni “ate” complexes.

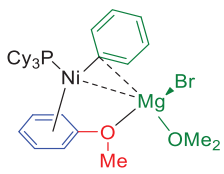
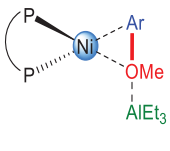
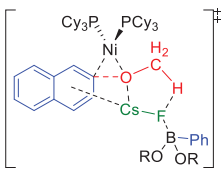
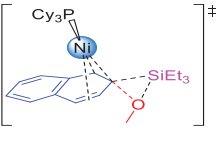
The polarity and the strength of the σ -donation from the phenyl anion in Ph-[M] (M: Mg, Li, Zn) to the Ni⁰ in the “ate” complexes are very important for the catalyst and have a very important role in stabilizing this intermediate.²⁴ Comparing the strength of the σ -donation for Ph-[M] (M: Mg, Li, Zn) could explain why arylzincs, displaying the weakest σ -bond donation, are not active in catalysis. The polarity and strength of the donation could be dramatically enhanced by

changing the anionic character of the organometallic partner and this is what makes the difference between arylzincs and $\text{ArZnMe}_3\text{Li}_2$.

The Lewis acidity of the reagents could also play a major role in their reactivity by coordinating to oxygen and weakening the C–OMe bond, thus facilitating its activation. However, the weak Lewis acidity of ArMgX , ArLi , or $\text{ArZnMe}_3\text{Li}_2$, and their coordination to the methoxy group cannot promote oxidative addition by itself; it was computed to decrease only slightly the O.A barrier.¹⁹ In contrast, coordination of strong Lewis acids like AlR_3 and LnR_3 can significantly reduce the O.A barrier and promote C–OMe bond activation by oxidative addition.^{28,25}

For hydrogenolysis, two mechanisms were proposed, either via classical oxidative addition using NHC ligands which are reported to be efficient in reductions with dihydrogen⁴⁸ and base,⁴⁹ or via Ni^{I} species followed by σ -bond metathesis, as reported by Martin for reductions with silanes using PCy_3 ligand.⁴² Both mechanisms were validated by isolating some key intermediates. This illustrates the large changes in mechanism that could be caused by small modifications in the catalytic system and the reagents used.

Table 2: Critical data analysis for the mechanisms depending on the nucleophile properties and type.

Nucleophile	ArMgX , ArLi , $\text{ArZnMe}_3\text{Li}_2$	AlR_3 and LnR_3	RB(OR)_2 , $\text{B}_2(\text{OR})_4$	Silanes
Nucleophilicity	+++	-	Mild	
Lewis acidity	-	+++		
Intermediate				
Mechanism	via Ni "ate"	via O.A	via O.A	via Ni^{I}

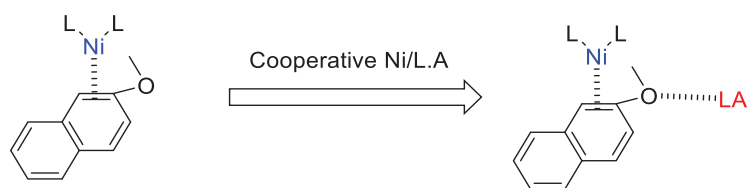
VII. Research objective

1. Design of new ligands

The state of the art on the cross-coupling reactions with aryl ethers emphasized the lack of knowledge concerning the key role of the ancillary ligand in the activation and functionalization of the C–OMe bond. We have seen that only ICy and PCy₃ are the active ligands with organoborons. In addition, the exact mechanism for the key C–O bond activation step is still under debate and seems to depend on subtle parameters that have not been clearly understood yet. So what is the key role of the ligand in the cross-coupling reaction of aryl ethers with aryl boronates? In addition, can the oxidative addition of the C–OMe bond be an operative process for the cross-coupling of aryl ethers with mild nucleophiles? Based on that, we decided to test other well-designed NHC and phosphine ligands that have been shown to feature interesting reactivities with nickel for the activation and functionalization of strong bonds.

2. LA assisted transformations

It has been shown previously that aryl ethers are highly challenging to activate. This is because of the extremely high dissociation energy of the C–OMe bond (beyond 100 kcal/mol), which makes the O.A nearly impossible. There are several ways to assist O.A, either by increasing the nucleophilicity of the metallic center, which is achieved by the action of the ligand and discussed in the previous part, or by weakening the C–OMe bond. However, can the use of a cooperative Ni/L.A. system (**Scheme 45**) where the Lewis acid coordinates to OMe-group weaken it and assist oxidative addition?



Scheme 45: Cooperative Ni/LA system.

VIII. References

- (1) Zeng, H.; Qiu, Z.; Domínguez-Huerta, A.; Hearne, Z.; Chen, Z.; Li, C. J. An Adventure in Sustainable Cross-Coupling of Phenols and Derivatives via Carbon-Oxygen Bond Cleavage. *ACS Catal.* **2017**, 7 (1), 510–519.
- (2) Tobisu, M.; Chatani, N. Cross-Couplings Using Aryl Ethers via C-O Bond Activation Enabled by Nickel Catalysts. *Acc. Chem. Res.* **2015**, 48 (6), 1717–1726.
- (3) Nowakowska, M.; Herbinet, O.; Dufour, A.; Glaude, P. A. Detailed Kinetic Study of Anisole Pyrolysis and Oxidation to Understand Tar Formation during Biomass Combustion and Gasification. *Combust. Flame* **2014**, 161 (6), 1474–1488.
- (4) Williard, P. G.; Fryhle, C. B. Boron Trihalide-Methyl Sulfide Complexes as Convenient Reagents for Dealkylation of Aryl Ethers. *Tetrahedron Lett.* **1980**, 21 (39), 3731–3734.
- (5) Sousa, C.; Silva, P. J. BBr₃-Assisted Cleavage of Most Ethers Does Not Follow the Commonly Assumed Mechanism. *Eur. J. Org. Chem.* **2013**, No. 23, 5195–5199.
- (6) Ackermann, L.; Cavalcanti, L. N.; Cera, G.; Chatani, N.; Correa, A.; Janine, C.; Gaydou, Y. D. M.; Gong, H.; Guerinot, A.; Itami, K.; et al. *Ni- and Fe-Based Cross-Coupling Reactions*; 2017; Vol. 35.
- (7) Hassan, J.; Sévignon, M.; Gozzi, C.; Schulz, E.; Lemaire, M. Aryl-Aryl Bond Formation One Century after the Discovery of the Ullmann Reaction. *Chem. Rev.* **2002**, 102 (5), 1359–1469.
- (8) McElroy, W. T.; DeShong, P. Synthesis of the CD-Ring of the Anticancer Agent Streptonigrin: Studies of Aryl-Aryl Coupling Methodologies. *Tetrahedron* **2006**, 62 (29), 6945–6954.
- (9) de Meijere, A.; Bräse, S.; Oestreich, M. *Metal Catalyzed Cross-Coupling Reactions and*

- More*; de Meijere, A., Bräse, S., Oestreich, M., Eds.; Wiley-VCH Verlag: Weinheim, Germany, 2013; Vol. 3.
- (10) Miyaura, N.; Buchwald, S. L. *Cross-Coupling Reactions : A Practical Guide*; Springer, 2002.
- (11) Magano, J.; Dunetz, J. R. Large-Scale Applications of Transition Metal-Catalyzed Couplings for the Synthesis of Pharmaceuticals. *Chem. Rev.* **2011**, *111* (3), 2177–2250.
- (12) Cornella, J.; Zarate, C.; Martin, R. Metal-Catalyzed Activation of Ethers via C-O Bond Cleavage: A New Strategy for Molecular Diversity. *Chem. Soc. Rev.* **2014**, *43* (23), 8081–8097.
- (13) Mesganaw, T.; Garg, N. K. Ni- and Fe-Catalyzed Cross-Coupling Reactions of Phenol Derivatives. *Org. Process Res. Dev.* **2013**, *17* (1), 29–39.
- (14) Oh-e, T.; Miyaura, N.; Suzuki, A. Palladium-Catalyzed Cross-Coupling Reaction of Organoboron Compounds with Organic Triflates. *J. Org. Chem.* **1993**, *58* (8), 2201–2208.
- (15) Wenkert, E.; Michelotti, E. L.; Swindell, C. S. Nickel-Induced Conversion of Carbon-Oxygen into Carbon-Carbon Bonds. One-Step Transformations of Enol Ethers into Olefins and Aryl Ethers into Biaryls. *J. Am. Chem. Soc.* **1979**, *101* (8), 2246–2247.
- (16) Wenkert, E.; Michelotti, E. L.; Swindell, C. S.; Tingoli, M. Transformation of Carbon-Oxygen into Carbon-Carbon Bonds Mediated by Low-Valent Nickel Species. *J. Org. Chem.* **1984**, *49* (25), 4894–4899.
- (17) Norio Miyaura and Akira Suzuki. Stereoselective Synthesis of Arylated (E) -Alkenes by the Reaction of Alk-1 -Enylboranes with Aryl Halides in the Presence of Palladium Catalyst. *J.C.S. Chem. Comm* **1979**, 590 (866), 866–867.
- (18) Dankwardt, J. W. Nickel-Catalyzed Cross-Coupling of Aryl Grignard Reagents with

- Aromatic Alkyl Ethers: An Efficient Synthesis of Unsymmetrical Biaryls. *Angew. Chem. Int. Ed.* **2004**, *43*, 2428–2432.
- (19) Ogawa, H.; Minami, H.; Ozaki, T.; Komagawa, S.; Wang, C.; Uchiyama, M. How and Why Does Ni⁰ Promote Smooth Etheric C–O Bond Cleavage and C–C Bond Formation? A Theoretical Study. *Chem. Eur. J.* **2015**, *21* (40), 13904–13908.
- (20) Tobisu, M.; Takahira, T.; Morioka, T.; Chatani, N. Nickel-Catalyzed Alkylative Cross-Coupling of Anisoles with Grignard Reagents via C–O Bond Activation. *J. Am. Chem. Soc.* **2016**, *138* (21), 6711–6714.
- (21) Tobisu, M.; Takahira, T.; Ohtsuki, A.; Chatani, N. Nickel-Catalyzed Alkynylation of Anisoles via C–O Bond Cleavage. *Org. Lett.* **2015**, *17* (3), 680–683.
- (22) Leiendecker, M.; Hsiao, C. C.; Guo, L.; Alandini, N.; Rueping, M. Metal-Catalyzed Dealkoxylation of Aryl Ethers by Employing a Functionalized Nucleophile. *Angew. Chem. Int. Ed.* **2014**, *53* (47), 12912–12915.
- (23) Yang, Z. K.; Wang, D. Y.; Minami, H.; Ogawa, H.; Ozaki, T.; Saito, T.; Miyamoto, K.; Wang, C.; Uchiyama, M. Cross-Coupling of Organolithium with Ethers or Aryl Ammonium Salts by C–O or C–N Bond Cleavage. *Chem. Eur. J.* **2016**, *22* (44), 15693–15699.
- (24) Kojima, K.; Yang, Z.-K.; Wang, C.; Uchiyama, M. Etheral C–O Bond Cleavage Mediated by Ni(0)-Ate Complex: A DFT Study. *Chem. Pharm. Bull. (Tokyo)*. **2017**, *65* (9), 862–868.
- (25) Yan, X.; Yang, F.; Cai, G.; Meng, Q.; Li, X. Nickel(0)-Catalyzed Inert C–O Bond Functionalization: Organo Rare-Earth Metal Complex as the Coupling Partner. *Org. Lett.* **2018**, *20* (3), 624–627.
- (26) Wang, C.; Ozaki, T.; Takita, R.; Uchiyama, M. Aryl Ether as a Negishi Coupling Partner:

- An Approach for Constructing C-C Bonds under Mild Conditions. *Chem. Eur. J.* **2012**, *18* (12), 3482–3485.
- (27) Morioka, T.; Nishizawa, A.; Nakamura, K.; Tobisu, M.; Chatani, N. Nickel-Catalyzed Cross-Coupling of Anisole Derivatives with Trimethylaluminum through the Cleavage of Carbonoxygen Bonds. *Chem. Lett.* **2015**, *44* (12), 1729–1731.
- (28) Liu, X.; Hsiao, C. C.; Kalvet, I.; Leiendecker, M.; Guo, L.; Schoenebeck, F.; Rueping, M. Lewis Acid Assisted Nickel-Catalyzed Cross-Coupling of Aryl Methyl Ethers by C-O Bond-Cleaving Alkylation: Prevention of Undesired β -Hydride Elimination. *Angew. Chem. Int. Ed.* **2016**, *55* (20), 6093–6098.
- (29) Kelley, P.; Edouard, G. A.; Lin, S.; Agapie, T. Lewis Acid Accelerated Aryl Ether Bond Cleavage with Nickel: Orders of Magnitude Rate Enhancement Using AlMe_3 . *Chem. Eur. J.* **2016**, *22* (48), 17173–17176.
- (30) Tobisu, M.; Shimasaki, T.; Chatani, N. Nickel-Catalyzed Cross-Coupling of Aryl Methyl Ethers with Aryl Boronic Esters. *Angew. Chem. Int. Ed.* **2008**, *47* (26), 4866–4869.
- (31) Tobisu, M.; Yasutome, A.; Kinuta, H.; Nakamura, K.; Chatani, N. 1,3-Dicyclohexylimidazol-2-Ylidene As a Superior Ligand for the Nickel-Catalyzed Cross-Couplings of Aryl and Benzyl Methyl Ethers With Organoboron Reagents. *Org. Lett.* **2014**, *16* (21), 5572–5575.
- (32) Schwarzer, M. C.; Konno, R.; Hojo, T.; Ohtsuki, A.; Nakamura, K.; Yasutome, A.; Takahashi, H.; Shimasaki, T.; Tobisu, M.; Chatani, N. Combined Theoretical and Experimental Studies of Nickel-Catalyzed Cross-Coupling of Methoxyarenes with Arylboronic Esters via C-O Bond Cleavage. *J. Am. Chem. Soc.* **2017**, *139* (30), 10347–10358.

- (33) Kakiuchi, F.; Usui, M.; Ueno, S.; Chatani, N.; Murai, S. Ruthenium-Catalyzed Functionalization of Aryl Carbon-Oxygen Bonds in Aromatic Ethers with Organoboron Compounds. *J. Am. Chem. Soc.* **2004**, *126* (9), 2706–2707.
- (34) Kakiuchi, F.; Matsuura, Y.; Kan, S.; Chatani, N. A $\text{RuH}_2(\text{CO})(\text{PPh}_3)_3$ -Catalyzed Regioselective Arylation of Aromatic Ketones with Arylboronates via Carbon-Hydrogen Bond Cleavage. *J. Am. Chem. Soc.* **2005**, *127* (16), 5936–5945.
- (35) Ueno, S.; Mizushima, E.; Chatani, N.; Kakiuchi, F. Direct Observation of the Oxidative Addition of the Aryl Carbon-Oxygen Bond to a Ruthenium Complex and Consideration of the Relative Reactivity between Aryl Carbon-Oxygen and Aryl Carbon-Hydrogen Bonds. *J. Am. Chem. Soc.* **2006**, *128* (51), 16516–16517.
- (36) Lau, S.; Ward, B.; Zhou, X.; White, A. J. P.; Casely, I. J.; MacGregor, S. A.; Crimmin, M. R. Mild sp^2 Carbon-Oxygen Bond Activation by an Isolable Ruthenium(II) Bis(Dinitrogen) Complex: Experiment and Theory. *Organometallics* **2017**, *36* (18), 3654–3663.
- (37) Tobisu, M.; Shimasaki, T.; Chatani, N. Ni^0 -Catalyzed Direct Amination of Anisoles Involving the Cleavage of Carbon–Oxygen Bonds. *Chem. Lett.* **2009**, *38* (7), 710–711.
- (38) Li, J.; Wang, Z. X. Nickel-Catalyzed Amination of Aryl 2-Pyridyl Ethers via Cleavage of the Carbon-Oxygen Bond. *Org. Lett.* **2017**, *19* (14), 3723–3726.
- (39) Zarate, C.; Manzano, R.; Martin, R. Ipso- Borylation of Aryl Ethers via Ni-Catalyzed C-OMe Cleavage. *J. Am. Chem. Soc.* **2015**, *137* (21), 6754–6757.
- (40) Zarate, C.; Nakajima, M.; Martin, R. A Mild and Ligand-Free Ni-Catalyzed Silylation via C-OMe Cleavage. *J. Am. Chem. Soc.* **2017**, *139* (3), 1191–1197.
- (41) Kong, Y.; Wang, Z. Nickel-Catalyzed Reaction of Aryl 2-Pyridyl Ethers with Silylzinc Chlorides: Silylation of Aryl 2-Pyridyl Ethers via Cleavage of the Carbon–Oxygen Bond.

- Adv. Synth. Catal.* **2019**, 361 (23), 5440–5448.
- (42) Álvarez-Bercedo, P.; Martín, R. Ni-Catalyzed Reduction of Inert C–O Bonds: A New Strategy for Using Aryl Ethers as Easily Removable Directing Groups. *J. Am. Chem. Soc.* **2010**, 132 (49), 17352–17353.
- (43) Tobisu, M.; Yamakawa, K.; Shimasaki, T.; Chatani, N. Nickel-Catalyzed Reductive Cleavage of Aryl–Oxygen Bonds in Alkoxy- and Pivaloxyarenes Using Hydrosilanes as a Mild Reducing Agent. *Chem. Commun.* **2011**, 47 (10), 2946–2948.
- (44) Cornella, J.; Gómez-Bengoa, E.; Martín, R. Combined Experimental and Theoretical Study on the Reductive Cleavage of Inert C–O Bonds with Silanes: Ruling out a Classical Ni(0)/Ni(II) Catalytic Couple and Evidence for Ni(I) Intermediates. *J. Am. Chem. Soc.* **2013**, 135 (5), 1997–2009.
- (45) Alexey G. Sergeev, J. F. H. Selective, Nickel-Catalyzed Hydrogenolysis of Aryl Ethers. *Science*. **2011**, 332 (6028), 439–443.
- (46) Wang, M.; Zhao, Y.; Mei, D.; Bullock, R. M.; Gutiérrez, O. Y.; Camaioni, D. M.; Lercher, J. A. The Critical Role of Reductive Steps in the Nickel-Catalyzed Hydrogenolysis and Hydrolysis of Aryl Ether C–O Bonds. *Angew. Chem. Int. Ed.* **2020**, 59 (4), 1445–1449.
- (47) Xu, L.; Chung, L. W.; Wu, Y. D. Mechanism of Ni–NHC Catalyzed Hydrogenolysis of Aryl Ethers: Roles of the Excess Base. *ACS Catal.* **2016**, 6 (1), 483–493.
- (48) Saper, N. I.; Hartwig, J. F. Mechanistic Investigations of the Hydrogenolysis of Diaryl Ethers Catalyzed by Nickel Complexes of N-Heterocyclic Carbene Ligands. *J. Am. Chem. Soc.* **2017**, 139 (48), 17667–17676.
- (49) Tobisu, M.; Morioka, T.; Ohtsuki, A.; Chatani, N. Nickel-Catalyzed Reductive Cleavage of Aryl Alkyl Ethers to Arenes in Absence of External Reductant. *Chem. Sci.* **2015**, 6 (6),

3410–3414.

- (50) Kelley, P.; Lin, S.; Edouard, G.; Day, M. W.; Agapie, T. Nickel-Mediated Hydrogenolysis of C–O Bonds of Aryl Ethers: What Is the Source of the Hydrogen? *J. Am. Chem. Soc.* **2012**, *134* (12), 5480–5483.
- (51) Zhao, L.; Ong, T. Nickel-Catalyzed Heteroarenes Cross Coupling via Tandem C–H/C–O Activation. *ACS Catal.* **2018**, *8*, 11368–11376.
- (52) Shimasaki, T.; Konno, Y.; Tobisu, M.; Chatani, N. Nickel-Catalyzed Cross-Coupling Reaction of Alkenyl Methyl Ethers with Aryl Boronic Esters. *Org. Lett.* **2009**, *11* (21), 4890–4892.
- (53) Ho, G. M.; Sommer, H.; Marek, I. Highly E-Selective, Stereoconvergent Nickel-Catalyzed Suzuki-Miyaura Cross-Coupling of Alkenyl Ethers. *Org. Lett.* **2019**, *21* (8), 2913–2917.
- (54) Hostier, T.; Neouchy, Z.; Ferey, V.; Gomez Pardo, D.; Cossy, J. Nickel-Catalyzed System for the Cross-Coupling of Alkenyl Methyl Ethers with Grignard Reagents under Mild Conditions. *Org. Lett.* **2018**, *20* (7), 1815–1818.
- (55) Xie, L.-G.; Wang, Z.-X. Cross-Coupling of Aryl/Alkenyl Ethers with Aryl Grignard Reagents through Nickel-Catalyzed C–O Activation. *Chem. Eur. J.* **2011**, *17* (18), 4972–4975.
- (56) Guan, B. T.; Xiang, S. K.; Wang, B. Q.; Sun, Z. P.; Wang, Y.; Zhao, K. Q.; Shi, Z. J. Direct Benzylic Alkylation via Ni-Catalyzed Selective Benzylic Sp³C–O Activation. *J. Am. Chem. Soc.* **2008**, *130* (11), 3268–3269.
- (57) Yonova, I. M.; Johnson, A. G.; Osborne, C. A.; Moore, C. E.; Morrisette, N. S.; Jarvo, E. R. Stereospecific Nickel-Catalyzed Cross-Coupling Reactions of Alkyl Grignard Reagents and Identification of Selective Anti-Breast-Cancer Agents. *Angew. Chem. Int. Ed.* **2014**, *53*

- (9), 2422–2427.
- (58) Taylor, B. L. H.; Harris, M. R.; Jarvo, E. R. Synthesis of Enantioenriched Triarylmethanes by Stereospecific Cross-Coupling Reactions. *Angew. Chem. Int. Ed.* **2012**, *51* (31), 7790–7793.
- (59) Greene, M. A.; Yonova, I. M.; Williams, F. J.; Jarvo, E. R. Traceless Directing Group for Stereospecific Nickel-Catalyzed Alkyl-Alkyl Cross-Coupling Reactions. *Org. Lett.* **2012**, *14* (16), 4293–4296.
- (60) Taylor, B. L. H.; Swift, E. C.; Waetzig, J. D.; Jarvo, E. R. Stereospecific Nickel-Catalyzed Cross-Coupling Reactions of Alkyl Ethers: Enantioselective Synthesis of Diarylethanes. *J. Am. Chem. Soc.* **2011**, *133* (3), 389–391.
- (61) Nakamura, K.; Tobisu, M.; Chatani, N. Nickel-Catalyzed Formal Homocoupling of Methoxyarenes for the Synthesis of Symmetrical Biaryls via C-O Bond Cleavage. *Org. Lett.* **2015**, *17* (24), 6142–6145.

Chapter II:

*Investigations on Ni/Lewis acid catalyzed Suzuki-
Miyaura reaction with aryl ethers*

I. Evaluation of new ligands

1. Introduction

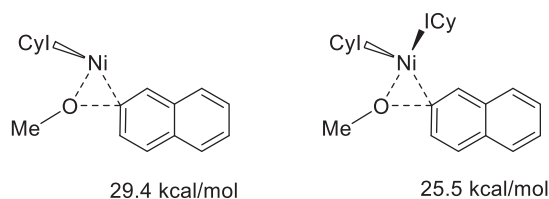
In a first instance, we wanted to further examine how the nature of the ancillary ligand may influence the reactivity of nickel for the cross-coupling of aryl ethers with mild nucleophiles. We focused our attention on the Suzuki-Miyaura cross-coupling of aryl ethers developed by the group of Chatani.¹ As discussed in the previous section, two types of ligands have shown high efficiency for this reaction, 1,3-dicyclohexylimidazol-2-ylidene (ICy) and tricyclohexylphosphine (PCy₃). Both ligands were shown to feature appropriate steric and electronic parameters. The stronger electron donating ICy ligand has been shown to be generally more reactive for cross-coupling with aryl boronates than PCy₃.²

Taking into account these observations, we were willing to explore two types of ligands that have been recently shown to feature interesting electronic and steric properties for the activation and functionalization of robust bonds, namely (i) bidentate bis-NHC ligands and (ii) phosphines with remote steric bulk.

2. Bidentate bis-NHC ligands

a. Properties and reactivity with nickel

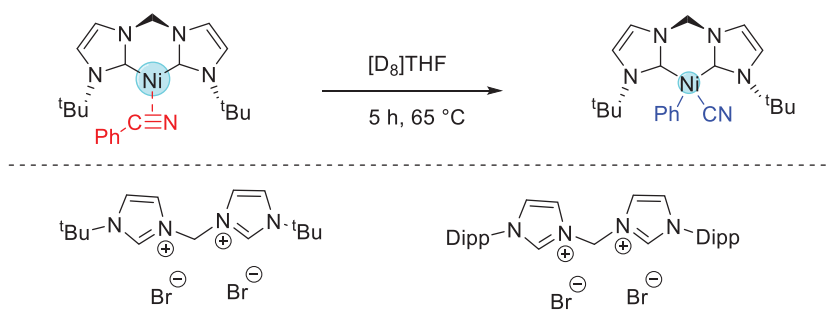
During their mechanistic investigations on nickel-catalyzed cross-coupling of aryl ethers with aryl boronates, the group of Chatani reported, using DFT calculations, that bis-ligated NiL₂ species (L = ICy or PCy₃) are more reactive for the oxidative addition of C-O bond with an associated activation barrier 4 kcal/mol lower than that of monoligated nickel species NiL (Scheme 46).³ They conclude that in the catalytic conditions, using an excess of ligands vs. nickel, the formation of bis-ligated Ni⁰ species may be favored.



Scheme 46: energetic values associated to the C-O bond of activation of aryl ether with mono- and bis-ligated (NHC)Ni species.

Based on these observations, we decided to prepare and evaluate the catalytic activity of bidentate NHC ligands, to further favor the bis-chelation. In this case, we also envisioned that the bite angle of the bidentate ligands might be an additional parameter that could improve the reactivity of nickel for the C-O bond activation. The bite angle has a very important role in the performance and activity of the catalyst.⁴ This role is expressed in terms of stabilization or destabilization of crucial intermediates involved in the transformation. The use of di-coordinate nickel complexes with a small bite angle should significantly improve the interaction of the metal with aryl ethers by raising the HOMO of nickel complex and thereby increasing its back-donation properties.⁵ We focused our attention to small bite angle bis-NHC ligands with methylene bridge.

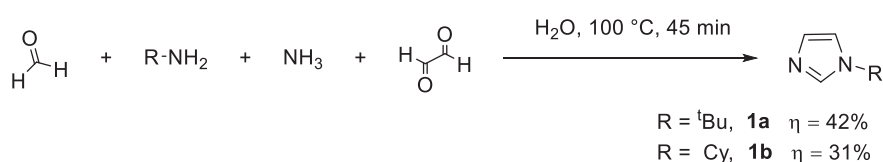
This type of ligands have been recently shown by the group of Hoffmann to confer remarkable reactivity to Ni^0 for the C-CN bond oxidative addition of benzonitrile (**Scheme 47**).⁶ These ligands are made as salts, which can be deprotonated later to give the corresponding naked bis-carbenes.



Scheme 47: Activation of Ph-CN bond at $\text{Ni}(0)$ bis-NHC complexes as reported by Hoffmann & al.. Dipp = 2,6-diisopropylphenyl.

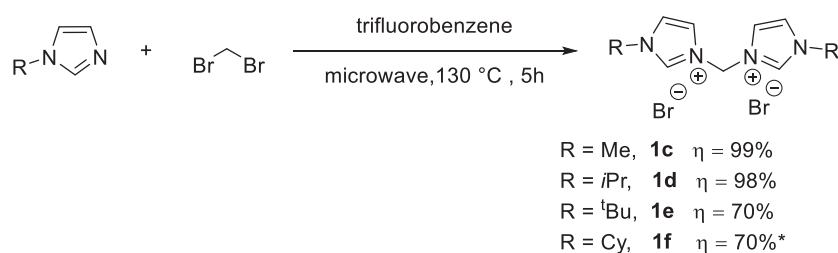
b. Synthesis and characterization of bis-NHC ligands synthesis

Inspired by the report of Hoffmann and coworkers, we synthesized the substituted imidazoles and their corresponding bis-imidazolium salts. First (*tert*-butyl)-1*H*-imidazole (**1a**) and 1-cyclohexyl-1*H*-imidazole (**1b**) were synthesized according to published procedures.⁷ The combination of formaldehyde, primary amines, ammonia and glyoxal in water afforded the substituted imidazoles in moderate yields (**Scheme 48**).



Scheme 48: Synthesis of substituted imidazoles according to Streubel's procedure.⁷

Subsequently, bis-imidazolium salts Bis-NHC^{Me} (**1c**), Bis-NHC^{*i*Pr} (**1d**), Bis-NHC^{*t*Bu} (**1e**) and Bis-NHC^{Cy} (**1f**) were prepared by microwave-assisted S_N2 reactions of the corresponding imidazoles with dibromomethane (**Scheme 49**).⁶ These ligands were directly tested in combination with Ni(COD)₂ for S.M cross-coupling of ArOMe (see next section 1.4)

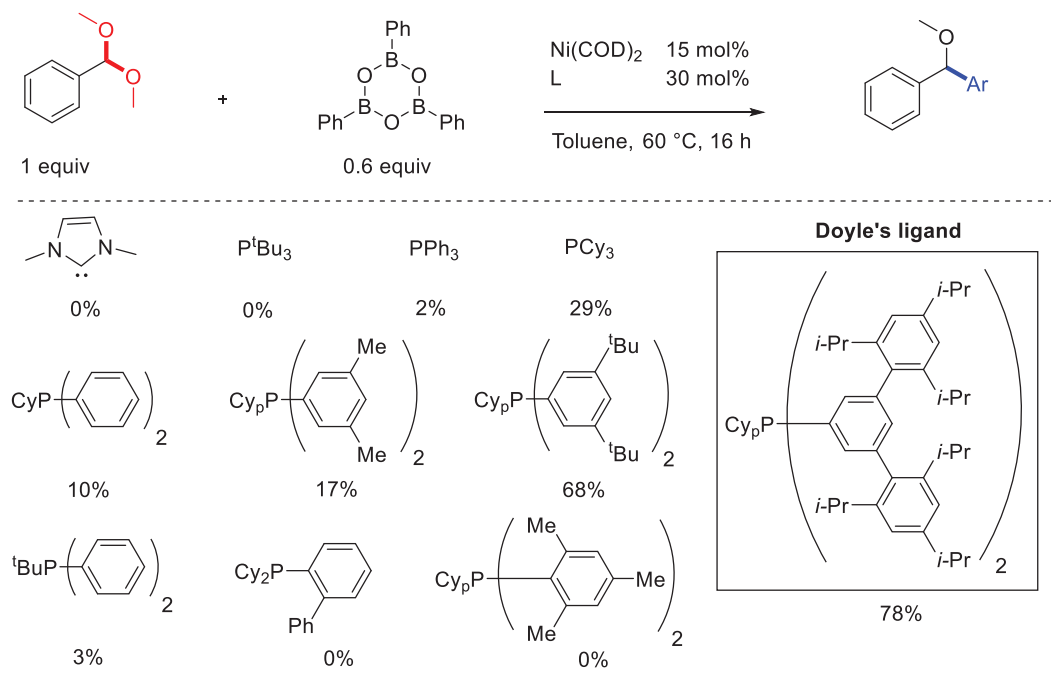


Scheme 49: Synthesis of several substituted bis-imidazolium salts according to published procedures.⁶
 *prepared as diiodide salt.

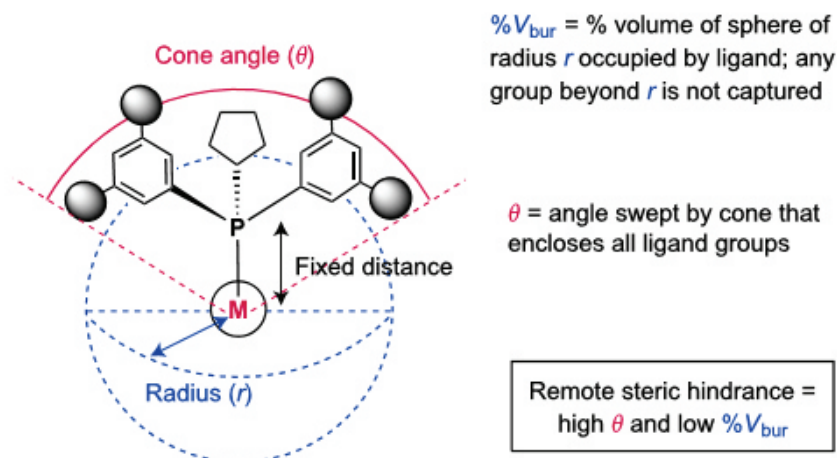
3. Monodentate ligands: electron rich phosphine with remote steric effects

a. Properties and applications in nickel catalyzed cross-coupling reactions

In 2017, the group of Doyle reported a thorough study on the key parameters controlling the reactivity of phosphine ligands used in nickel catalysis and demonstrated that phosphine ligands featuring steric hindrance at remote position from the nickel center may significantly enhance its reactivity in catalysis.⁸ Based on theoretical calculations and mathematical modeling they investigated the key influence of physical parameters like electronic and steric factors for Ni-catalyzed cross-coupling arylation of acetals with boronic acids (**Scheme 50**). They found that electronic factor did not play a significant role. In contrast, the steric factor was found to play a key role on the reactivity. The steric hindrance of the ligands were defined by two physical parameters: the buried volume which is the volume occupied by the ligand around the metallic center and the cone angle which is the angle made by the furthestmost groups of the ligand (**Scheme 51**).



Scheme 50: Ligands scope for Ni-catalyzed cross-coupling arylation of acetals with boronic acids. Cy_P = cyclopentyl.



Scheme 51: Remote steric bulkiness model.⁹

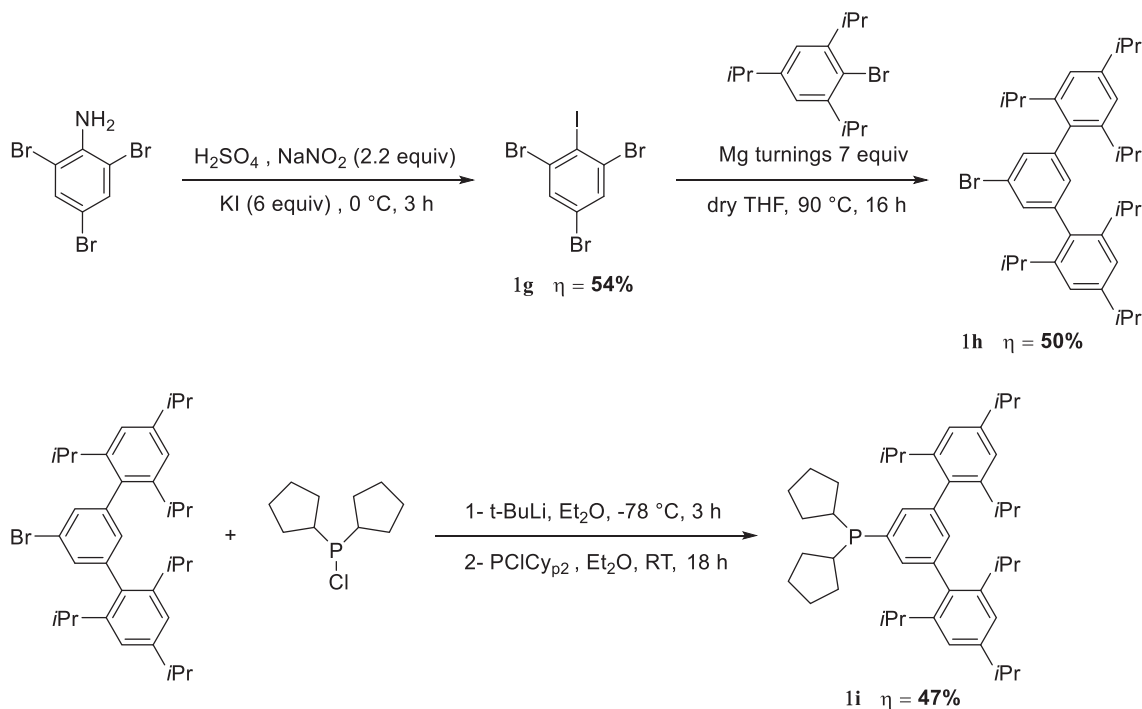
In this context, they found that ligands having small buried volume around the metallic center in addition to large cone angles, displayed the highest reactivity in catalysis for cross-coupling arylation of acetals with boronic acids. In fact, bulky ligands are needed for reductive elimination and the bulkier the ligand the easier R.E will be. However, when the ligand is bulky it occupies more buried volume around the metallic center preventing the substrate from approaching and thus rendering oxidative addition from taking place. This effect is much more significant with nickel than with palladium, because Ni is smaller than Pd. In addition, Ni-P bonds are shorter than Pd-P bonds. One way to solve this problem is to design ligands that are very bulky but at the same time far from the metallic center. In this way, the substrate can coordinate easily to nickel and at the same time the bulkiness of the ligand will improve R.E. This new ligand design approach was defined as “Remote Steric Hindrance”.

The remote steric hindrance principle was highly effective in several nickel-catalyzed processes. They demonstrated that dicyclopentyl(2,2'',4,4'',6,6''-hexaisopropyl-[1,1':3',1''-terphenyl]-5'-yl)phosphane (Doyle's ligand, **1i**) is a ligand matching this criteria. It showed a unique reactivity

for cross-coupling arylation of acetals with boronic acids as well as Suzuki-Miyaura cross-coupling of tertiary benzylic and allylic sulfones with arylboroxines¹⁰. Since aryl-dimethoxymethyl acetals are relatively indistinguishable from aryl ethers we envisioned that this ligand might clear up the problem with aryl ethers.

b. Synthesis of Doyle's ligand

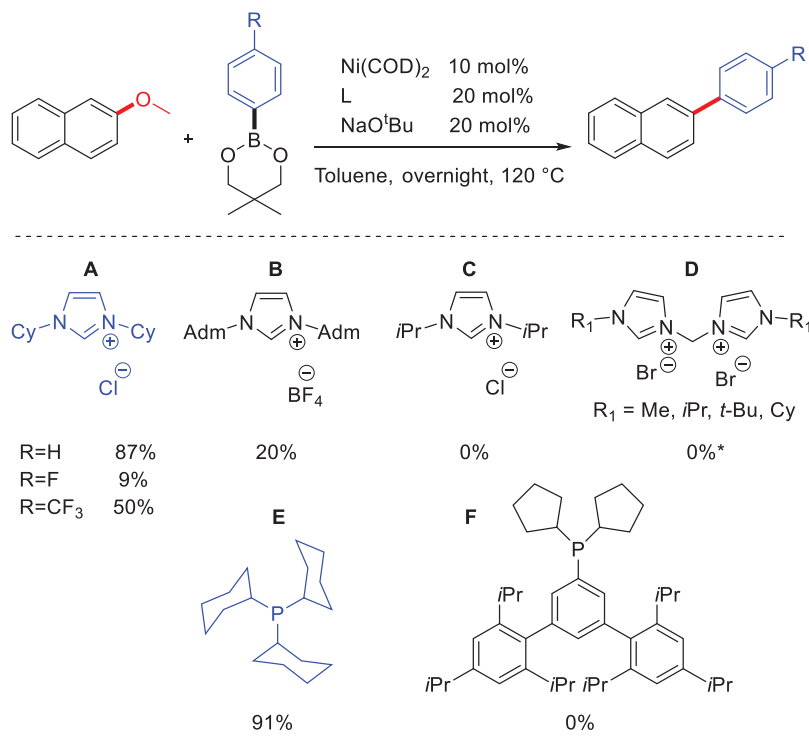
The synthesis of dicyclopentyl(2,2'',4,4'',6,6''-hexaisopropyl-[1,1':3',1''-terphenyl]-5'-yl)phosphane (**1i**) ligand requires a multi-step procedure (**Scheme 52**).⁹ The reaction of 2,4,6-tribromoaniline with the *in situ* generated nitrous acid forms the aryl diazonium ion that reacts with potassium iodide via nucleophilic substitution forming 1,3,5-tribromo-2-iodobenzene (**1g**). Coupling of **1g** with the *in situ* prepared Grignard reagent of 2-bromo-1,3,5-triisopropylbenzene affords 5'-bromo-2,2'',4,4'',6,6''-hexaisopropyl-1,1':3',1''-terphenyl (**1h**). Bromine-lithium exchange of **1h** by t-BuLi takes place followed by a nucleophilic attack on chlorodicyclopentylphosphane forming **1i** in good yields.⁹



Scheme 52: Synthesis of **1i** according to published procedure. Characteristic signal of **1i** = ^{31}P -NMR (122 MHz, Benzene- d_6) δ -0.34.

4. Evaluation of ligands for nickel-catalyzed cross-coupling of aryl ethers with phenyl boronic esters

As preliminary experiments, we tried to reproduce the results reported by Chatani with ICy and PCy₃ ligands as a control experiment using methoxynaphthalene (1 equiv), phenyl boronic ester (1.5 equiv), Ni(COD)₂ (10 mol%), ICy.HCl (20 mol%) and NaO^tBu (20 mol%) in toluene (1.5 mL) overnight at 120°C, and the same system with PCy₃ (40 mol%) and CsF (4.5 equiv). The results were nicely reproduced (**Scheme 53-A**). We have seen in the previous chapter that several NHC's were screened and they were totally unreactive (**Scheme 44, chapter 1**). Therefore, we selected some new monodentate NHC's at 20 mol% loading. Among them, only adamantyl-NHC showed a minor reactivity giving only 20% yield (**Scheme 53-B**).



Scheme 53: Evaluation of several mono and bidentate ligands. Reactions performed with Ni(COD)_2 (10 mol%), NHC's (20 mol%), NaOtBu (20 mol%), methoxynaphthalene (1 equiv), ArB(OR)_2 (1.5 equiv) or with phosphines L (40 mol%) using CsF (4.5 equiv) instead of NaOtBu . Yields were determined by ^{19}F -NMR spectroscopy using PhCF_3 as internal standard, or by GCMS. * L (10 mol%), $R = \text{H}, \text{CF}_3$.

Then we tried to probe the reactivity of the synthesized Bis-NHC ligands with different substituents (Me, *i*Pr, ^tBu, Cy) at 10 mol% loading but they proved totally unreactive (**Scheme 53-D**), even though the cyclohexyl-Bis-NHC is very close to ICy as well as sharing the cyclohexyl group with the only two reactive ligands ICy and PCy₃. Unfortunately, **1i** was also unreactive under these conditions.

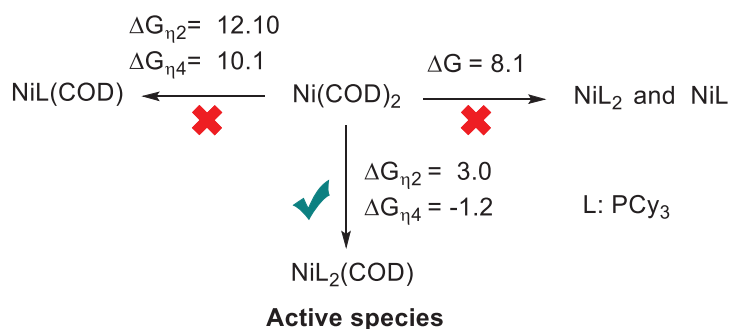
These results clearly show how much challenging and difficult is the activation of aryl ethers. The “on-off” effect in addition to these unexplained failures led us to investigate another activation pathway. In the absence of any rational, blind screening of myriads of ligands would be time consuming, and we thus preferred to focus on L.A assisted cross-couplings.

II. Computational investigations on the influence of phosphines on the C-O bond activation step

Influence of the ligand on the C-O bond activation step

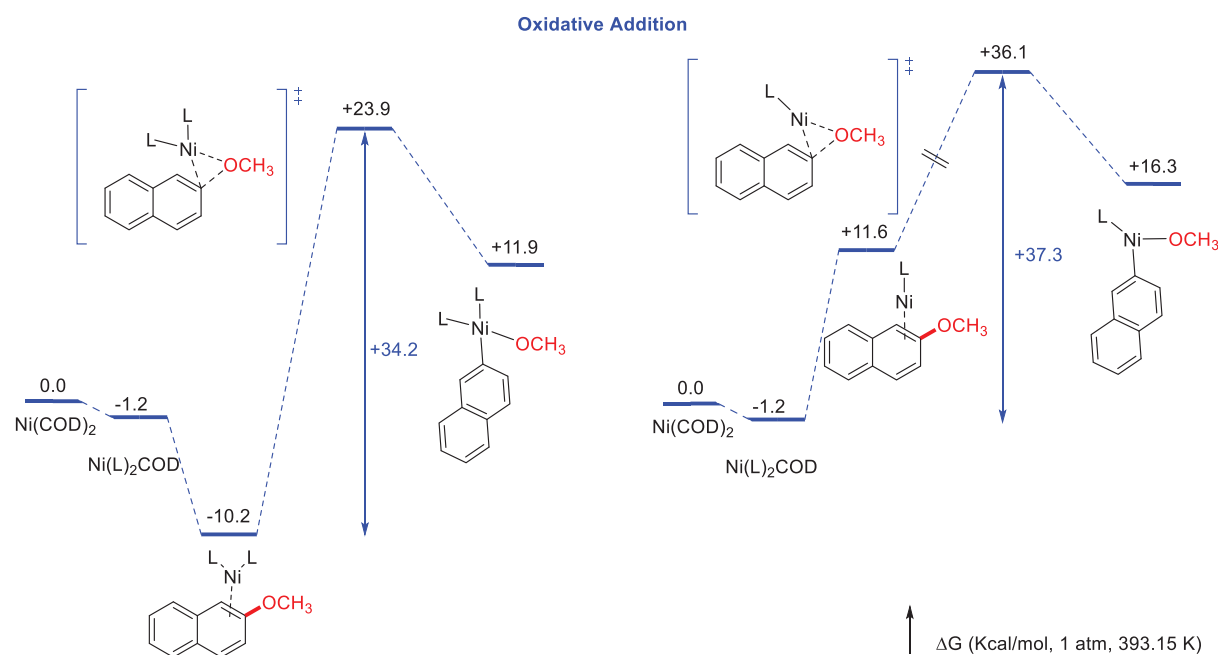
We first investigated the oxidative addition step by analyzing the influence of the nature of the phosphine ligand and ligation number on the reaction profile for the oxidative addition of methoxynaphthalene starting from $\text{Ni}(\text{COD})_2$ and PCy_3 ligands. DFT calculations were carried out at the BP86-D3/def2TZVP-SDD//BP86-D3/6-31G(d)-SDD level of theory. Solvation by toluene were taken into accounts by the implicit PCM solvent model (see Computational Details).

The first step of the reaction should involve the displacement of COD ligands by phosphines. The dissociation of COD by 2 equivalents of PCy_3 has been shown experimentally by the group of Martin to be a non-trivial process.¹¹ The dissociation of one or two COD ligands by PCy_3 to form nickel(0) species ligated by either one or two phosphines was evaluated (**Scheme 54**). The formation of putative $\text{Ni}(\text{PCy}_3)$ and $\text{Ni}(\text{PCy}_3)_2$ species is an endergonic process. The same observation is made for the formation of $(\text{COD})\text{Ni}(\text{PCy}_3)$ species (+10-12 kcal/mol). In contrast, the formation of $(\text{COD})\text{Ni}(\text{PCy}_3)_2$ species is slightly exergonic ($\Delta G = -1.2$ kcal/mol for κ^4 coordination of COD). This suggests that this species is most likely the starting point of the reaction.



Scheme 54: Speciation and associated Gibbs energies of several pre-catalytic species.

Then the displacement of COD from $(\text{COD})\text{Ni}(\text{PCy}_3)_2$ by methoxynaphthalene to form the $(\text{PCy}_3)_2\text{Ni}(\text{ArOMe})$ adduct is computed as an exergonic step ($\Delta G = -10.2$ kcal/mol). The subsequent oxidative addition proceeds with a very high activation barrier ($\Delta G^\ddagger = 34.2$ kcal/mol) and is found to be thermodynamically unfavorable (**Scheme 55**). A similar energetic pathway has been reported by Tobisu, Chatani and Mori ($\Delta G^\ddagger = 33.7$ kcal/mol).³ The reaction pathway involving the dissociation of COD and one PCy_3 ligand is found to be even less energetically favorable (**Scheme 55**).



Scheme 55: Gibbs free energy profile computed with a solvent (PCM model: toluene) at the BP86-D3/def2TZVP-SDD//BP86-D3/6-31G(d)-SDD level of theory for the O.A. of naphthyl-OMe by the monoligated and bis-ligated Ni^0 -PCy₃ complexes.

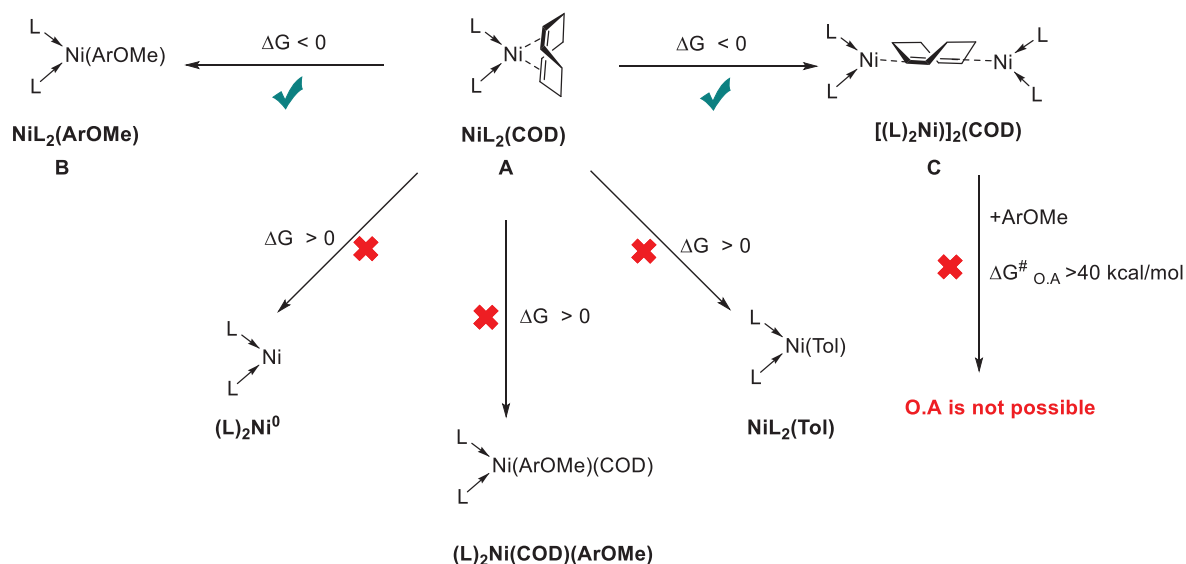
We have also evaluated both reaction pathways with other phosphines (**Table 3**), and very similar results have been obtained with all phosphines examined. The reaction pathway with bisphosphine nickel(0) species is energetically more favorable in all cases, and the oxidative addition barrier is very similar to that observed with PCy₃ ligands. As a reminder, only PCy₃ ligand was experimentally active for the arylation of aryl ethers with ArB(OR)_2 , and usually 0.2 to 0.4 equiv of the ligand are used.

Table 3: Gibbs free energy computed with a solvent (PCM model: toluene) at the BP86-D3/def2TZVP-SDD//BP86-D3/6-31G(d)-SDD level of theory for the O.A. starting from $\text{NiL}_2(\text{COD})$ as the active species with different phosphine ligands.

Ligand	Bisphosphine species				Monophosphine species			
	INT-1	TS-1	INT-2	ΔG^\ddagger	INT-1	TS-1	INT-2	ΔG^\ddagger
PCy _p	3.7	36.2	24.3	36.2	16.8	35.9	15.4	35.9
PCy ₃	-10.2	23.9	11.9	34.2	11.6	36.1	16.3	37.3
PPh ₃	-2.4	28.3	16.3	34.0	18.3	41.5	21.0	47.3
P(<i>i</i> Pr) ₃	10.2	31.5	17.0	31.5	12.9	38.8	19.4	38.9
PMe ₃	5.1	32.9	12.2	35.3	17.1	41.4	20.3	43.7

In contrast with the experimental observations, these results do not hint at significant differences between PCy₃ and other phosphine ligands. We hypothesized that the absence of activity with other ligands, as observed experimentally, may result from the formation of totally inactive species. Starting from L₂Ni(COD) species, we examined all the possible species that may be formed in the presence of naphthyl ether in toluene as solvent (**Table 4**).

Table 4: Gibbs free energy computed with a solvent (PCM model: toluene) at the BP86-D3/def2TZVP-SDD//BP86-D3/6-31G(d)-SDD level of theory for all the possible combinations of the active species evaluated with different Ni ligated phosphine complexes.



Ligand	L ₂ Ni(ArOMe)	L ₂ Ni	L ₂ Ni(COD)(ArOMe)	L ₂ Ni(ArOMe)	[L ₂ Ni(COD)] ₂
PCy ₃	-2.82	2.92	4.65	7.19	-14.22
PCy ₃	-9.00	9.33	-2.12	3.38	-3.11
PPh ₃	3.37	18.04	5.32	12.79	-20.21
P(<i>i</i> Pr) ₃	3.62	-	-	-	-12.53
PMe ₃	7.47	-	-	-	-14.24

Among the different conceivable species, only the formation of L₂Ni(ArOMe) adduct (**B**) and the dimeric species with a bridging coordination of COD, [(L₂Ni)]₂(COD) (**C**), are computed as thermodynamically favorable processes (**Table 4**). Furthermore, the formation of the dimeric

species **C** was the most thermodynamically favorable reaction for all the phosphine ligands, except for PCy₃. The oxidative addition of naphthyl ether to compounds **C** was found to be an endergonic process with a prohibitively high activation barrier ($\Delta G^\ddagger \geq 40$ kcal/mol). In contrast, for PCy₃ ligand, the formation of the naphthyl ether adduct **B** is favored over the dimeric species **C**.

These results suggest that the dimeric species **C**, which is mostly favored with all phosphines evaluated, except for PCy₃, is a thermodynamic sink from which oxidative addition is not possible. Although not completely clear at this stage, PCy₃ ligands may feature the adequate electronic and steric properties to allow the selective formation of the L₂(Ni)(ArOMe) species.

III. Lewis acid assisted Suzuki-Miyaura cross-coupling of aryl ethers

1. Introduction

As already discussed in the previous chapter, the nature of the nucleophile has been shown to significantly affect the reaction conditions and the scope of the cross-coupling reaction with aryl ethers. For instance, the scope of the cross-coupling with Grignard reagents and alkyl aluminums is much broader and the reactions proceed under milder conditions than with milder nucleophiles such as boronic esters. While different mechanistic scenarios have been proposed, the participation of the nucleophilic partner for the key C-O bond activation step, via Lewis acidic coordination to the methoxy moiety, is often suggested. For example, in the cross-coupling arylation with Grignard reagents, Uchiyama suggested the assistance of Mg in the concerted activation step via Nickel “ate” complex formation, where Mg acts as L.A, weakening the C-O bond (**Scheme 6, chapter 1**).¹² In the context of cross-coupling alkylation with alkyl aluminums, Rueping reported that alkyl

aluminum can significantly reduce the activation barrier for the C-O bond oxidative addition (from 40 kcal/mol to 18.6 kcal/mol) (**Scheme 16, chapter 1**).¹³ In addition, the group of Agapie reported a stoichiometric study indicating the significant acceleration of C-O bond activation of aryl ether in the presence of AlMe₃ (**Scheme 17, chapter 1**).¹⁴ The group of Hartwig also observed that the addition of stoichiometric amount of AlMe₃ in reductive cleavage cross-coupling, significantly increases the rate of nickel-catalyzed hydrogenolysis of diphenylethers (**Scheme 32, chapter 1**).¹⁵

For the arylation cross-coupling reaction of methoxyarenes with boronic esters, Chatani and Tobisu proposed that CsF may also assist the activation of the C-O bond by forming a quaternary adduct in which the Lewis acidic Cs atom coordinates to oxygen. The associated activation barrier has been found to be lower in energy compared to that without this pre-coordination, albeit at a lower extent (4.2 kcal/mol lower in energy)³ (**Scheme 20, chapter 1**).

These studies indicate that Lewis acid assistance may be envisioned as a strategy to enhance the reactivity of nickel catalysts for the cross-coupling of aryl ethers with mild nucleophiles. However, the Lewis acid has never been used as co-catalyst to promote the cross-coupling of aryl ethers. We were thus motivated to explore the reactivity of nickel/Lewis acid catalytic systems for these cross-coupling reactions and investigate the impact of Lewis acids with two types of ligands (ICy and PCy₃). Of note, the group of Chatani reported that the addition of several Lewis acidic additives, such as Mg, Zn and Li salts had detrimental effects on the Suzuki-Miyaura cross-coupling of methoxyarenes. However, the Lewis acids were added in stoichiometric amount, which may lead to decomposition pathways.^{1,16}

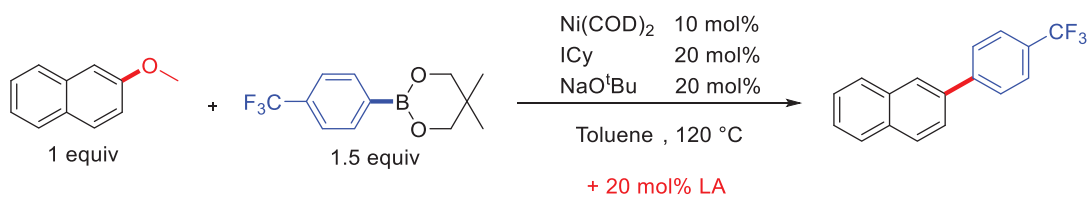
2. Evaluation of Lewis acid co-catalysts for the nickel-catalyzed Suzuki-Miyaura cross-coupling of aryl ethers with ICy ligands

a. screening of Lewis acids

To investigate the influence of Lewis acid co-catalysts in the cross-coupling of aryl ethers, we examined the prototypical Suzuki-Miyaura reaction. Aryl boronate esters bearing $-\text{CF}_3$ substituents were selected to allow ^{19}F NMR spectroscopy monitoring. The reaction was first carried out under the reaction conditions described by Chatani & al (Entry 1, **Table 5**).³ The coupling product was obtained in 51% yield after 12 h of reaction at 120 °C. Then, the addition of several Lewis acids as co-catalysts was evaluated.

We started with the addition of $\text{Al}(\text{O}^i\text{Bu})_3$ as co-catalyst at 20 mol% loading. In the presence of the Lewis acid, the reaction was quantitative, affording the coupling product in 88% yield after 3h (Entry 2, **Table 5**). Under the same conditions, the reaction yield is only 14% without $\text{Al}(\text{O}^i\text{Bu})_3$. This clearly supports the beneficial impact of $\text{Al}(\text{O}^i\text{Bu})_3$ as a co-catalyst, which is in line with what was observed by Nakao in the arylcyanation of alkynes where the reaction was significantly accelerated by using aluminum-based Lewis acids.^{17,18}

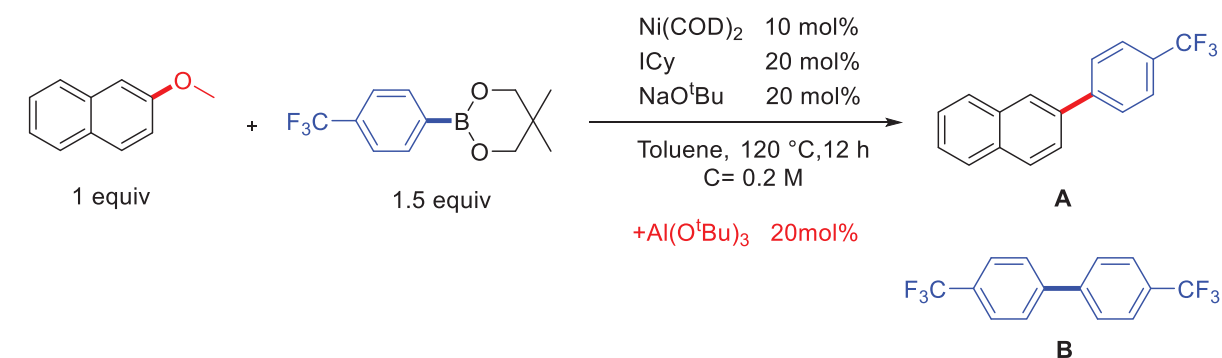
However, when strong Lewis acids like AlCl_3 , BF_3 or BBr_3 were added as co-catalysts, no reaction was observed. Only decomposition to black metallic nickel is observed in these cases (Entries 3-5, **Table 5**). The same observations were made using metal triflates as Lewis acids (Entries 6-8, **Table 5**). On the other hand, alkyl boron BET_3 proved very effective, while AlMe_3 showed only little performance at 20 mol% loading. It is worth of note that alkylation was not observed under these conditions (Entries 9-10, **Table 5**). Finally, a selection of other metal alkoxides and salts (entries 11-16, **Table 5**) were shown to have a negative effect on the yield.

Table 5: Screening of Lewis acid scope with ICy ligand.^[a]

Entry	Lewis acid	Yield after 3h	Yield after 12h
1	none	14%	51%
2	$\text{Al(O}^t\text{Bu)}_3$	88%	100%
3	AlCl_3	-	1%
4	BF_3	0%	-
5	BBr_3	0%	-
6	Y(OTf)_3	-	0%
7	Al(OTf)_3	1%	-
8	Zn(OTf)_2	-	0%
9	BEt_3	84%	-
10	AlMe_3	35%	-
11	B(OMe)_3	28%	-
12	$\text{Zr(O}^t\text{Bu)}_4$	12%	-
13	$\text{Y(O}^i\text{Pr)}_3$	12%	-
14	Ag(OAc)	0%	-
15	ZrCl_4	1%	1%
16	LiCl	1%	-

^[a] Reactions performed with Ni(COD)_2 (10 mol%), ICy (20 mol%), NaO^tBu (20 mol%), methoxynaphthalene (1 equiv), $(p\text{-PhCF}_3)\text{B(OR)}_2$ (1.5 equiv), Lewis acid (20 mol%). Yields were determined by ^{19}F -NMR spectroscopy using PhCF_3 as internal standard.

With the positive result observed in the presence of catalytic amounts of $\text{Al(O}^t\text{Bu)}_3$ in hand, we re-evaluated several reaction parameters for optimization. The effect of reaction conditions on the production of organoboron homocoupling side-product was also observed (**Table 6**).

Table 6: Optimizing reaction conditions.^[a]

Entry	Deviation from standard conditions	Yield (%) for A	Yield (%) for B
0	-	100	12
1	1 equiv boronate instead of 1.5 equiv	43	4
2	5 mol% Ni(COD)_2 instead of 10 mol%	47	4
3	100 °C instead of 120 °C	43	9
4	80 °C instead of 120 °C	7	2
5	3 h instead of 12 h	88	4
6	30 min MW at 120 °C instead of 12 h	27	6
7	30 min MW at 150 °C instead of 12 h	51	5

^[a] Reactions performed with Ni(COD)_2 (5-10 mol%), ICy (20 mol%), NaO^tBu (20 mol%), methoxynaphthalene (1 equiv), (p- PhCF_3) B(OR)_2 (1-1.5 equiv). Yields were determined by ^{19}F -NMR spectroscopy using PhCF_3 as internal standard, and by GCMS.

The yield of the reaction was significantly reduced when stoichiometric amount of boronate ester was used instead of 1.5 equivalent. The same observation was made when the catalytic loading was reduced to 5 mol% (entries 1-2, **Table 6**). Of note, a high temperature is still required to reach quantitative yield, even in the presence of the Lewis acid co-catalyst. Decreasing the temperature to 100 °C reduces the yield by half, while at 80 °C only minor reactivity was observed (entries 3-4, **Table 6**). With respect to reaction time, the L.A can significantly reduce the time down to 3 h with minor reduction of the yield. Interestingly, under microwave irradiation, it can deliver up to 51% yield in only 30 min (entries 6-8, **Table 6**).

It emerges from this study that the Lewis acid has a clear beneficial effect on the rate of the reaction. Lowering the reaction temperature can significantly decrease the yield due to the high activation energy of aryl ethers that requires high internal energy in the medium which is achieved

by heating. The optimal conditions for this transformation are the following: Ni(COD)_2 (10 mol%), ICy.HCl (20 mol%), NaO^tBu (20 mol%), $\text{Al(O}^t\text{Bu)}_3$ (20 mol%), aryl ethers (1 equiv) and boronate ester (1.5 equiv) in toluene (1.5 ml) at 120 °C. Excess of boronate ester is essential for the reaction to take place efficiently due to homocoupling side-reactions in the presence of transition metals.¹⁹ In addition, we always observe homocoupling in the reactions and its amount is higher in the presence of L.A.

b. Effect of Lewis acid loading

Then, we examined the influence of the Lewis acid loading with different aluminium species: $\text{Al(O}^t\text{Bu)}_3$, AlMe_3 and MAD (methylaluminum bis(2,6-di-tert-butyl-4-methylphenoxide)) (Table 7).

Table 7: Effect of the Lewis acid loading on the reaction yield. ^[a]

Entry	L.A (mol%)	$\text{Al(O}^t\text{Bu)}_3$ (% yield)	AlMe_3 (% yield)	MAD (% yield)
1	100	0	-	-
2	50	9	-	-
3	20	88	35%	5%
4	10	80	100%	90%
5	5	-	91%	-
6	0	51	51%	51%

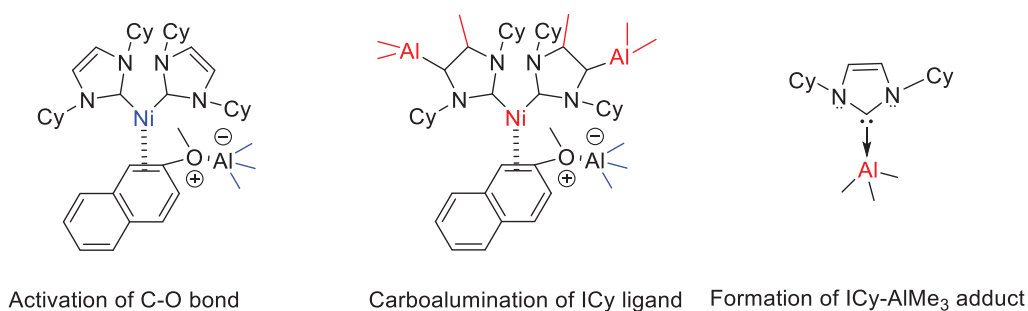
^[a] Reactions performed with Ni(COD)_2 (10 mol%), ICy (20 mol%), NaO^tBu (20 mol%), methoxynaphthalene (1 equiv), $(p\text{-PhCF}_3)\text{B(OR)}_2$ (1.5 equiv), Lewis acid (x mol%). Yields were determined by ^{19}F NMR spectroscopy using PhCF_3 as internal standard, and by GCMS.

The addition of a stoichiometric amount of $\text{Al(O}^t\text{Bu)}_3$ totally inhibits the reaction (entry 1, Table 7), in line with what was previously observed by the group of Chatani.¹ It appears also that the reaction is quenched at high Lewis acid loading (entry 2, Table 7).

When using AlMe_3 as co-catalyst, a low reaction yield is observed at 20 mol% loading (entry 3, **Table 7**), while a very high yield is observed at 10 mol% loading (entry 4, **Table 7**), which is even higher than that obtained with $\text{Al}(\text{O}^t\text{Bu})_3$ at 10 mol% (entry 4, **Table 7**).

In addition, in contrast with the results from Rueping's group, methylative cross-coupling was not observed when using AlMe_3 under these conditions (entries 3-5, **Table 7**).¹³ Thus, AlMe_3 acts selectively on assisting the O.A rather than in alkylating the naphthyl ether. Based on the above results, it appears that ICy ligand is highly sensitive to L.A loading: while 20 mol% of $\text{Al}(\text{O}^t\text{Bu})_3$ give quantitative yields, 50 to 100 mol% loadings proved detrimental to the reaction. In addition, each L.A has its own optimum loading. For instance, $\text{Al}(\text{O}^t\text{Bu})_3$ works best at 20 mol% loading, while 10 mol% is the optimum loading for AlMe_3 . In fact, the stronger the L.A, the more sensitive it will be; and in the case of AlMe_3 , the yield is highly reduced to only 35% at 20 mol% loading, while quantitative yields are reached at 10 mol% loading.

Several side reactions between the Lewis acid and the catalytic system may be envisioned to explain the absence of catalytic activity at high L.A loading (**Scheme 56**).

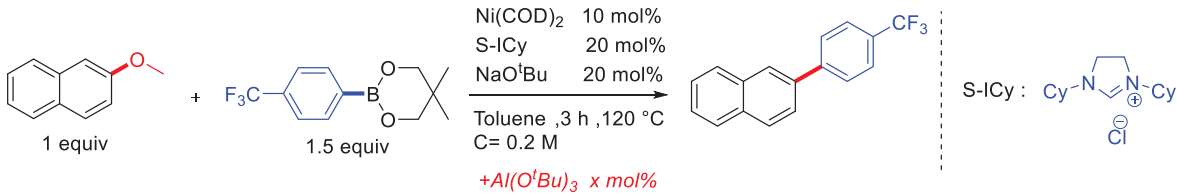


Scheme 56: Possible side reactions between AlMe_3 and Ni/ICy

Besides the desired coordination of Lewis acid to the methoxy group, the addition of excess of the L.A could lead to carboalumination of the double bond in the imidazolium ring, especially in the presence of transition metals, and cause deactivation of the catalyst.^{20,21} Another possibility would involve the direct interaction of the L.A with ICy, and the formation of L.A-L.B donor

acceptor adducts. The rate of the formation of these adducts is related to the strength and the bulkiness of the L.A, which explains the difference of reactivity and loading of $\text{Al}(\text{O}^t\text{Bu})_3$ compared to AlMe_3 . These kind of NHC- AlR_3 donor-acceptor complexes were reported recently and have been fully characterized.²² Of note, the saturated S-ICy ligand has been also evaluated, and very similar results compared to ICy were obtained, suggesting that deactivation by carboalumination is unlikely (Table 8).

Table 8: Testing S-ICy ligand with different L.A loadings.^[a]

			
Entry	$\text{Al}(\text{O}^t\text{Bu})_3$ (mol%)	Time	Yield (%)
1	20	Overnight	100
2	20	3 h	83
3	50	3 h	4

^[a] Reactions performed with $\text{Ni}(\text{COD})_2$ (10 mol%), L (20 mol%), NaO^tBu (20 mol%), methoxynaphthalene (1 equiv), $(p\text{-PhCF}_3)\text{B}(\text{OR})_2$ (1.5 equiv), $\text{Al}(\text{O}^t\text{Bu})_3$ (x mol%). Yields were determined by ^{19}F -NMR spectroscopy using PhCF_3 as internal standard, and GCMS.

3. Evaluation of Lewis acids co-catalysts for the nickel-catalyzed Suzuki-

Miyaura cross-coupling of aryl ethers with PCy_3 ligand

a. Screening of Lewis acids

In the context of cooperative $\text{Ni}^0/\text{L.A}$ cross-couplings we decided to evaluate the effect of the L.A with PCy_3 ligand. In this case, the addition of 4.5 equivalents of CsF has been shown to be mandatory to observe a reactivity by the group of Chatani.¹ In our hands, the cross-coupling reaction carried out using $\text{Ni}(\text{COD})_2$ (10 mol%)/ PCy_3 (20 mol%) in the presence of CsF (4.5 equiv)

afforded the product in 59% yield after 3 h (Entry 0, **Table 9**). In the absence of CsF (4.5 equiv), the reaction did not proceed (Entry 1, **Table 9**). The addition of Al(O^tBu)₃ alone in the absence of CsF (Entry 2, **Table 9**) gave quantitative yields in 3 h, which was isolated in (87% yield), showing that the L.A is also highly effective with PCy₃ ligand. Interestingly, this result indicates that catalytic amounts of Al(O^tBu)₃ provide better results than large excess of CsF in terms of yield and reaction rate.

Table 9: Screening of Lewis acid with PCy₃ ligand. ^[a]

Entry	L.A (mol%)	CsF (equiv)	A(%)	B(%)
0	none	4.5	59	4
1	none	0	0	0
2	Al(O ^t Bu) ₃ (20)	0	100 (87%)*	3
3	Y(O ⁱ Pr) ₃ (20)	0	86	8
4	Zr(O ^t Bu) ₄ (20)	0	95	-

^[a] Reactions performed with Ni(COD)₂ (10 mol%), PCy₃ (40 mol%), CsF (x equiv), methoxynaphthalene (1 equiv), (p-PhCF₃)B(OR)₂ (1.5 equiv), Lewis acid (y mol%). Yields were determined by ¹⁹F NMR spectroscopy using PhCF₃ as internal standard, and by GCMS. * Isolated yield.

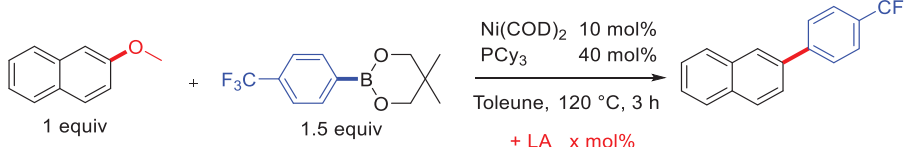
Testing several Lewis acids with this system indicates that some L.A which were not active with Icy, like Y(OⁱPr)₃ and Zr(O^tBu)₄, are actually active with PCy₃ (entries 3-4, **Table 9**). In addition, the extent of homocoupling side-reaction (3%) observed with PCy₃ ligands (entry 2, **Table 9**) is lower compared to that with ICy ligands (up to 15%).

Finally, it was clearly shown that catalytic amounts of Lewis acids significantly enhance the reaction rate and are much more efficient than the large excess of CsF. In addition, the L.A can assist the coupling reaction regardless of the ligand used.

b. Influence of Lewis acid loading with PCy₃ ligand

Then we tried to check the effect of the L.A loading on PCy₃ ligand. In contrast to ICy, PCy₃ is barely affected even by stoichiometric loadings of the L.A (**Table 10**). This suggests that the problem is coming from the carbene itself in ICy ligand.

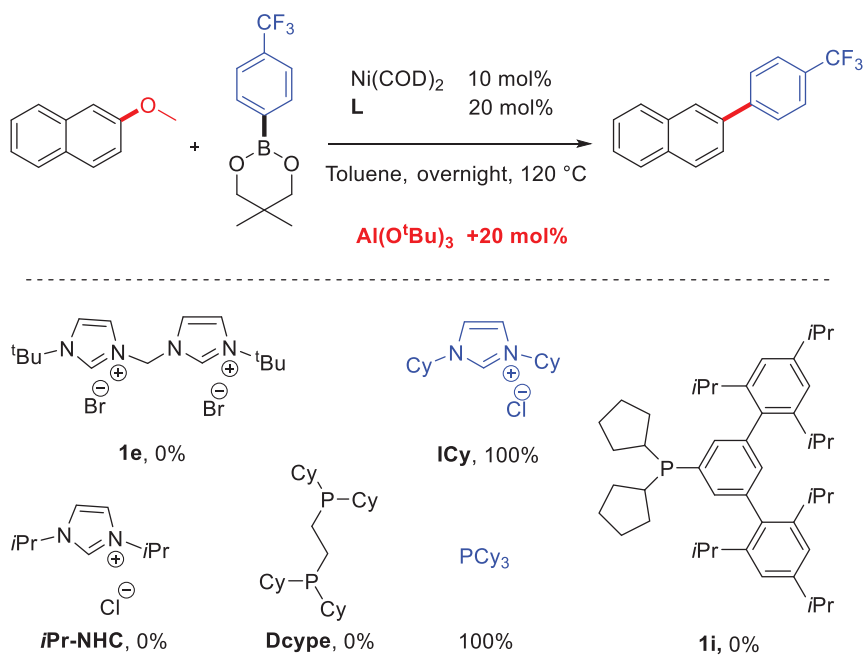
Table 10: Effect of Lewis acid loading with PCy₃ as a ligand.

		
Entry	L.A (mol%)	Yield (%)
1	Al(O ^t Bu) ₃ (20)	100
2	Al(O ^t Bu) ₃ (50)	100
3	Al(O ^t Bu) ₃ (100)	91
4	Y(O ⁱ Pr) ₃ (10)	91
5	Y(O ⁱ Pr) ₃ (20)	86

^[a] Reactions performed with Ni(COD)₂ (10 mol%), PCy₃ (40 mol%), methoxynaphthalene (1 equiv), (p-PhCF₃)B(OR)₂ (1.5 equiv), L.A (x mol%). Yields was determined by ¹⁹F-NMR spectroscopy using PhCF₃ as internal standard, and GCMS.

4. Ligand screening assisted by Al(O^tBu)₃

Considering the progress made in the activation of aryl ethers thanks to the assistance of Lewis acids, and taking into account the fact that only PCy₃ and ICy have been reported to be effective ligands for arylative cross-coupling with PhB(OR)₂, we questioned whether the scope of ligands could be extended by the assistance of Lewis acids. We therefore investigated the impact of a series of LAs on the efficiency of previously reported ineffective ligands (**Scheme 57**).

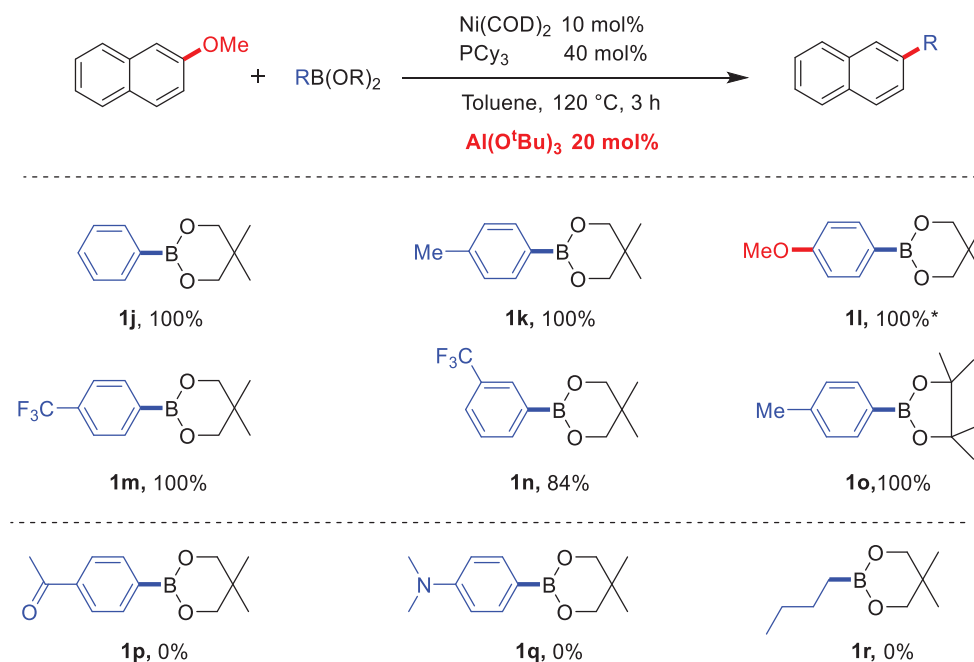


Scheme 57: Ligand screening assisted by $\text{Al}(\text{O}^t\text{Bu})_3$. Reactions performed with $\text{Ni}(\text{COD})_2$ (10 mol%), Bis-NHC^{*t*Bu} (10 mol%), mono-NHC's and Dcype (20 mol%), monophosphines (40 mol%), NaO^tBu (20 mol%), methoxynaphthalene (1 equiv), $(p\text{-PhCF}_3)\text{B}(\text{OR})_2$ (1.5 equiv). Yields were determined by ^{19}F NMR spectroscopy using PhCF_3 as internal standard, and by GCMS.

After testing several ligands, it appeared that the L.A is not able to solve the ligand problem. This shows again how much it is difficult to activate aryl ethers, and emphasizes the key role played by the ligand. It is possible that the problem originates from the catalyst itself, forming dormant species with these ligands.

5. Scope of boronic esters with L.A

Having the best combination of ligand and Lewis acid in hand, we screened different boronate esters. It was clearly shown that in the presence of the cooperative $\text{Ni}^0(\text{PCy}_3)_2/\text{Al}(\text{O}^t\text{Bu})_3$ dual catalyst system, the yield for the cross-couplings of methoxynaphthalene with several organoboron substrates (**1j-1o**) is almost always quantitative, and the reaction is completed in only 3 h, in contrast to the lack of reactivity in the absence of the Lewis acid. (**Scheme 58**).



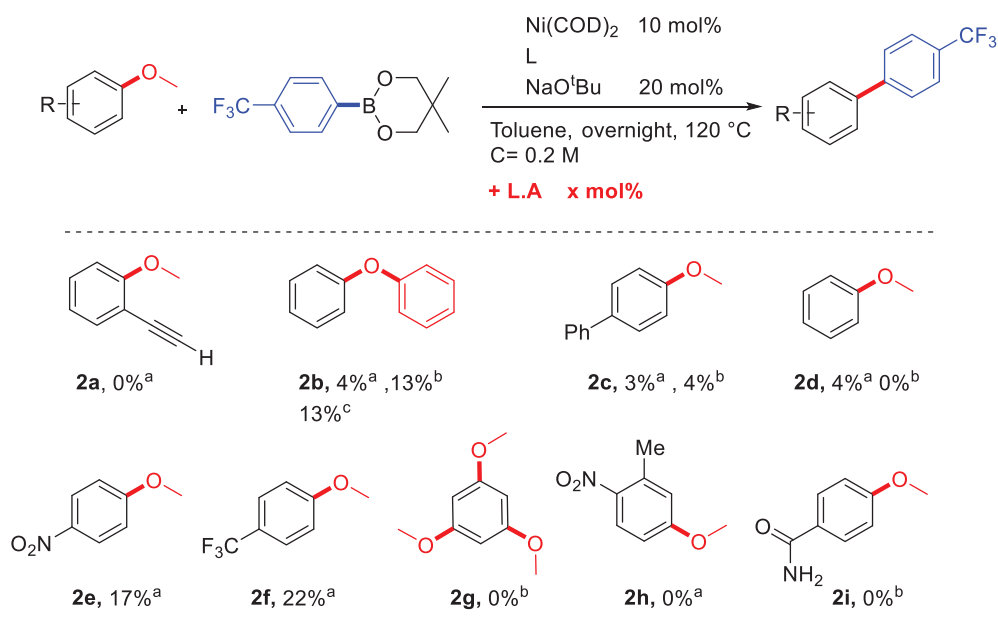
Scheme 58: Scope of boronic esters in the cooperative $\text{Ni}^0/\text{L.A}$ cross-coupling. Reactions performed with Ni(COD)_2 (10 mol%), PCy_3 (40 mol%), methoxynaphthalene (1 equiv), RB(OR)_2 (1.5 equiv), $\text{Al(O}^t\text{Bu)}_3$ (20 mol%). Yields were determined by ^{19}F NMR spectroscopy using PhCF_3 as internal standard, and/or GCMS. *with ICy.

The system also showed unique selectivity with *p*-methoxyboronate ester with ICy ligand, where the C-OMe activation takes place selectively on the methoxynaphthalene and not on the *p*-methoxy group of the boronate ester, also reaching quantitative yields. However, the L.A cannot be effective for substrates containing carbonyl, amine or any L.A coordinating groups (**1p-1q**). In addition, the method proved effective for $\text{Csp}^2\text{-Csp}^2$ bond formation, but did not allow alkylative cross-coupling as illustrated with **1r**.

6. Scope of aryl ethers with L.A

Several anisole derivatives as well as diphenyl ether were screened in the cross-coupling reaction using diverse cooperative Ni/L.A systems. (**Scheme 59**). However, the catalyst systems showed very limited reactivity with them. The best yields achieved with activated anisoles were

in between 17 and 22% (**2e-2f**). Simple anisole gave only 4% yield using the best system ICy/ $\text{Al}(\text{O}^t\text{Bu})_3$ (**2d**). In addition, applying harsh conditions to the coupling of anisole, for instance heating at 160 °C in the presence of 3 equiv of boronate ester, afforded the coupling product in only 7% yield. Besides, PCy_3 was found totally inactive even under these harsh conditions (**Scheme 59**). These observations are in contrast with those made by Chatani in the case of 4-methoxy-1,1'-biphenyl (**2c**) and 1-methoxy-4-(trifluoromethyl)benzene (**2f**), which reactions were reported to reach 76% and 75%, respectively.²



Scheme 59: Evaluation of various electrophiles using several Ni/L.A cooperative systems. ^a ICy / $\text{Al}(\text{O}^t\text{Bu})_3$, ^b PCy_3 / $\text{Al}(\text{O}^t\text{Bu})_3$, ^c ICy / AlMe_3 . Reactions performed with $\text{Ni}(\text{COD})_2$ (10 mol%), ICy (20 mol%), PCy_3 (40 mol%), methoxynaphthalene (1 equiv), $\text{RB}(\text{OR})_2$ (1.5 equiv), $\text{Al}(\text{O}^t\text{Bu})_3$ (20 mol%), AlMe_3 (10 mol%). Yields was determined by ^{19}F NMR spectroscopy using PhCF_3 as internal standard, and/or GCMS.

All other inactivated anisoles were found totally unreactive (**2a, 2g-2i**). In fact, all of them were recovered intact, with not even a trace of the product being detected. Diphenyl ether also afforded low yields (up to 13%) with two cooperative systems (**2b**).

These experiments confirm how extremely challenging remains the activation of aryl ether substrates, especially those lacking π -extended systems.

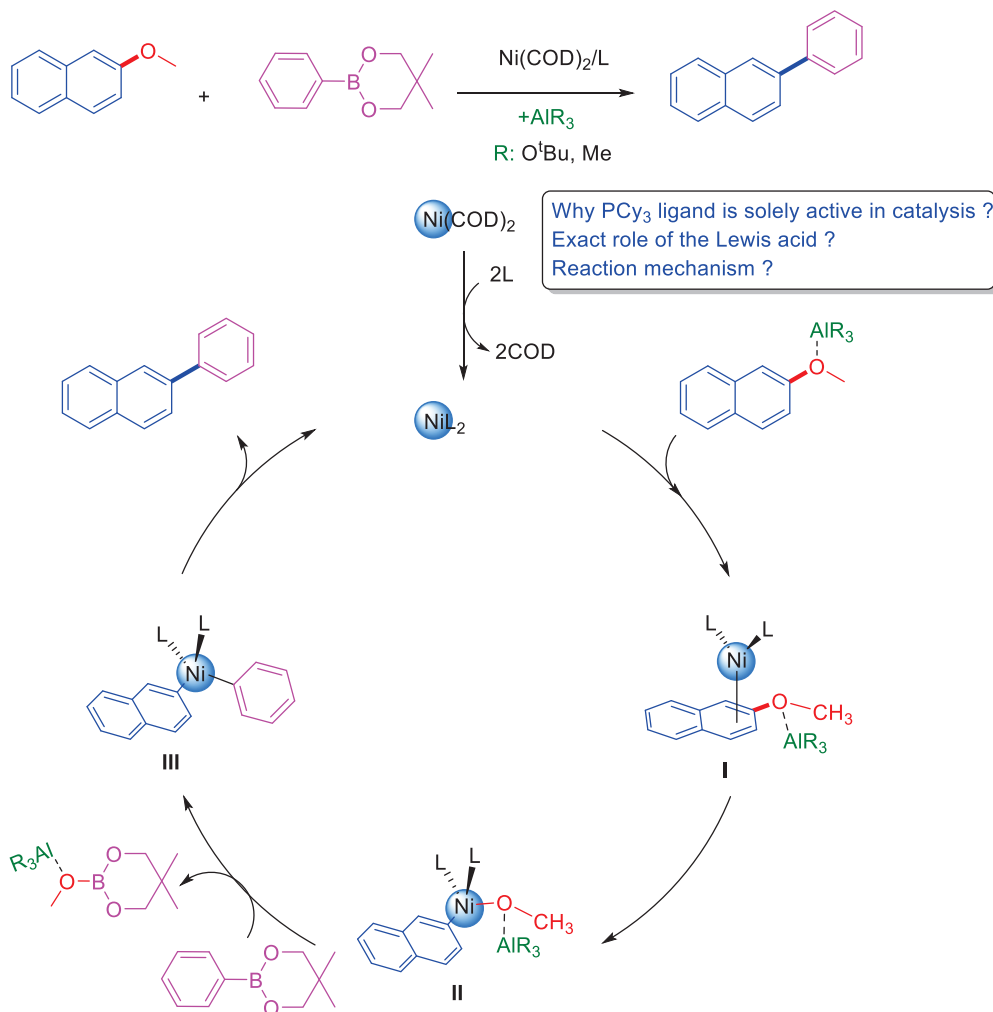
IV. Computational studies

The mechanism of the reaction was examined computationally to gain some understanding into (i) the very peculiar role of the ligand in the reactivity of nickel for the cross-coupling reaction and (ii) the impact of the Lewis acid in the C-O bond activation process.

1. Starting mechanistic hypothesis

In 2017, Tobisu, Chatani and Mori reported that the mechanism of the cross-coupling of aryl ethers with boronate esters proceeds through a $\text{Ni}^0/\text{Ni}^{\text{II}}$ pathway, with oxidative addition of the $\text{C}_{\text{Ar}}\text{-OMe}$ bond to nickel(0) as a starting point.³ The mechanism of the reaction was investigated with the two efficient ligands, *i.e.* PCy_3 and ICy. With PCy_3 ligands, the oxidative addition of $\text{C}_{\text{Ar}}\text{-OMe}$ bond was proposed to occur at the $\text{Ni}(\text{PCy}_3)_2$ species, and to be assisted by the action of CsF and aryl boronic ester, via the formation of a quaternary complex.

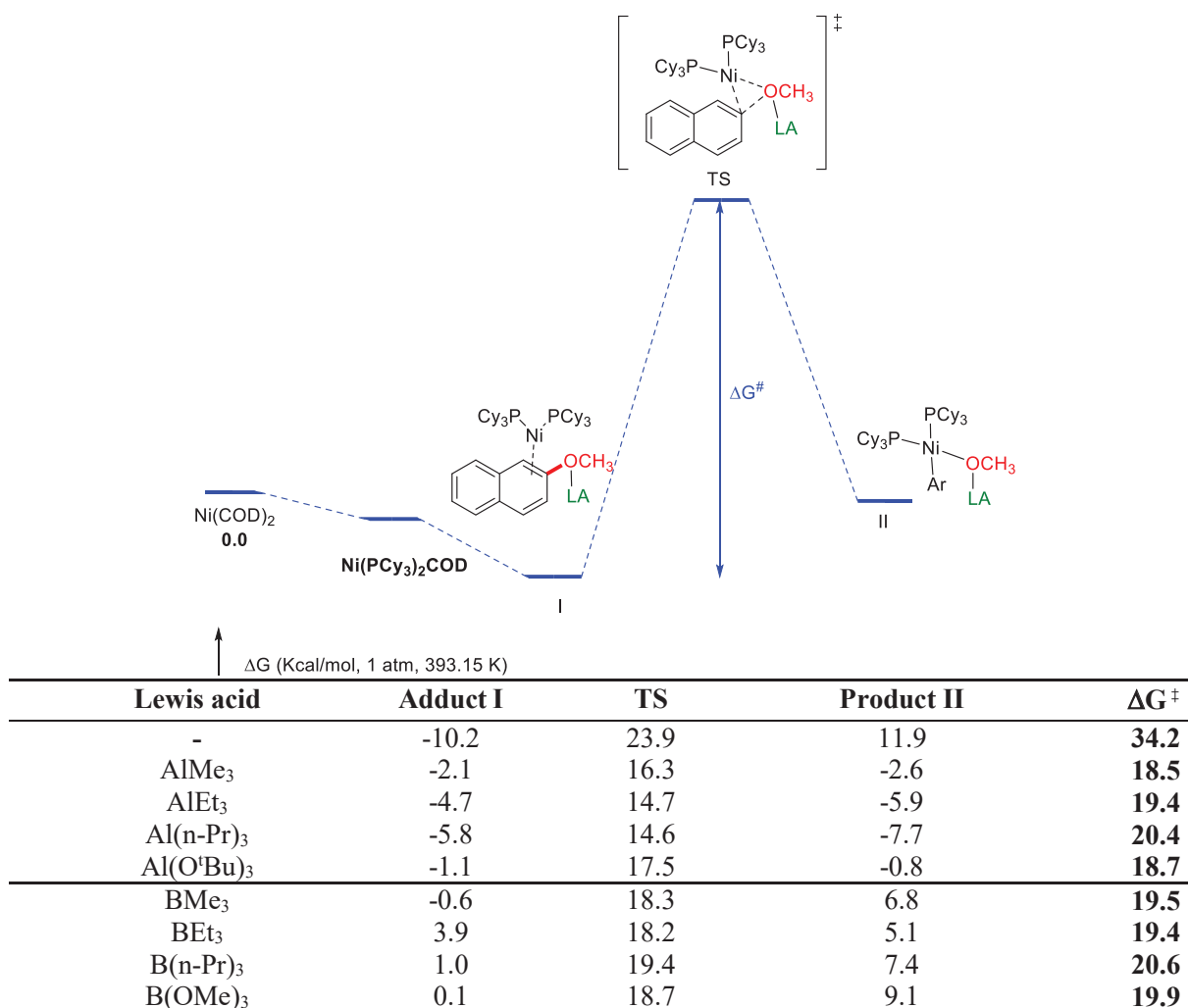
Based on this recent study, we started to explore a mechanistic scenario involving $\text{Ni}^0/\text{Ni}^{\text{II}}$ pathway with phosphine ligands and Lewis acid co-catalysts, with two main questions to address (**Scheme 60**): (i) Why only PCy_3 ligand is active in catalysis? As mentioned earlier, even subtle modification of the substituents leads to complete switch off? The impact of the ligand has not been examined to date; (ii) what is the exact role of the Lewis acid? Is the assistance of the Lewis acid limited to the oxidative addition or does it play a role in other steps (transmetallation, reductive elimination)? With these questions in mind we investigated the individual steps of the putative mechanism.



Scheme 60: Envisioned mechanism for the Ni/LA cooperative cross-coupling.

2. Influence of the Lewis acid co-catalyst

The use of 10 mol% of $\text{Al(O}^t\text{Bu)}_3$ has been shown to significantly enhance the rate of the cross-coupling reaction. Furthermore, we showed that the use of an excess of CsF is not required with PCy_3/Ni catalytic system when aluminum Lewis acid is used as co-catalyst. The exact role of the Lewis acid in the cross-coupling of naphthylether with boronate esters was investigated theoretically. The C-O bond oxidative addition pathway was examined in the presence of a series of Lewis acids to delineate its impact (**Table 11**).

Table 11: The effect of Lewis acids on the oxidative addition of the C-O bond. ^[a]

^[a] Gibbs free energy profile computed with a solvent (PCM model: toluene) at the BP86-D3/def2TZVP-SDD//BP86-D3/6-31G(d)-SDD level of theory and in the presence of Lewis acids for the oxidative addition of naphthylether by $\text{Ni}(\text{PCy}_3)_2(\text{COD})$. Selected energetic values for reactants, intermediates and transition state (in kcal/mol).

In the absence of Lewis acid, the oxidative addition proceeds with a high barrier of 34.2 kcal/mol and the reaction is significantly exergonic. In the presence of aluminum and boron Lewis acids, computed energy barriers of the oxidative addition was found to proceed with a much lower barrier (≤ 20 kcal/mol). The coordination of the Lewis acid to the methoxy group of the substrate also influences the thermodynamics of the formation of the preliminary adduct and of the final oxidative addition product. Significant differences are observed between boron and aluminum-

based Lewis acids, the process becomes thermodynamically favorable (or at least thermoneutral) with aluminum species, while the reaction remains endergonic with boron derivatives.

Thus, in the presence of Lewis acids, the reaction proceeds through its coordination to the methoxy group of naphthylether which destabilizes adduct **I** and weakens the C-O bond strength facilitating the oxidative addition process. In line with the experimental observation, coordination of aluminum based Lewis acids to the substrate decreases the oxidative addition barrier by ~15 kcal/mol and makes the reaction thermodynamically favorable. The weakening of the C-O bond of the substrate is apparent by comparing the C_{Ar}-OMe bond lengths of the intermediates and transition state along the reaction path (**Table 12**). The coordination of Al(O^tBu)₃ was found to induce the highest weakening of the C-O bond (entry 5, **Table 12**). Consistently, this Lewis acid was also found to feature the highest binding affinity with methoxynaphthalene ($\Delta G = -5.6$ kcal/mol).

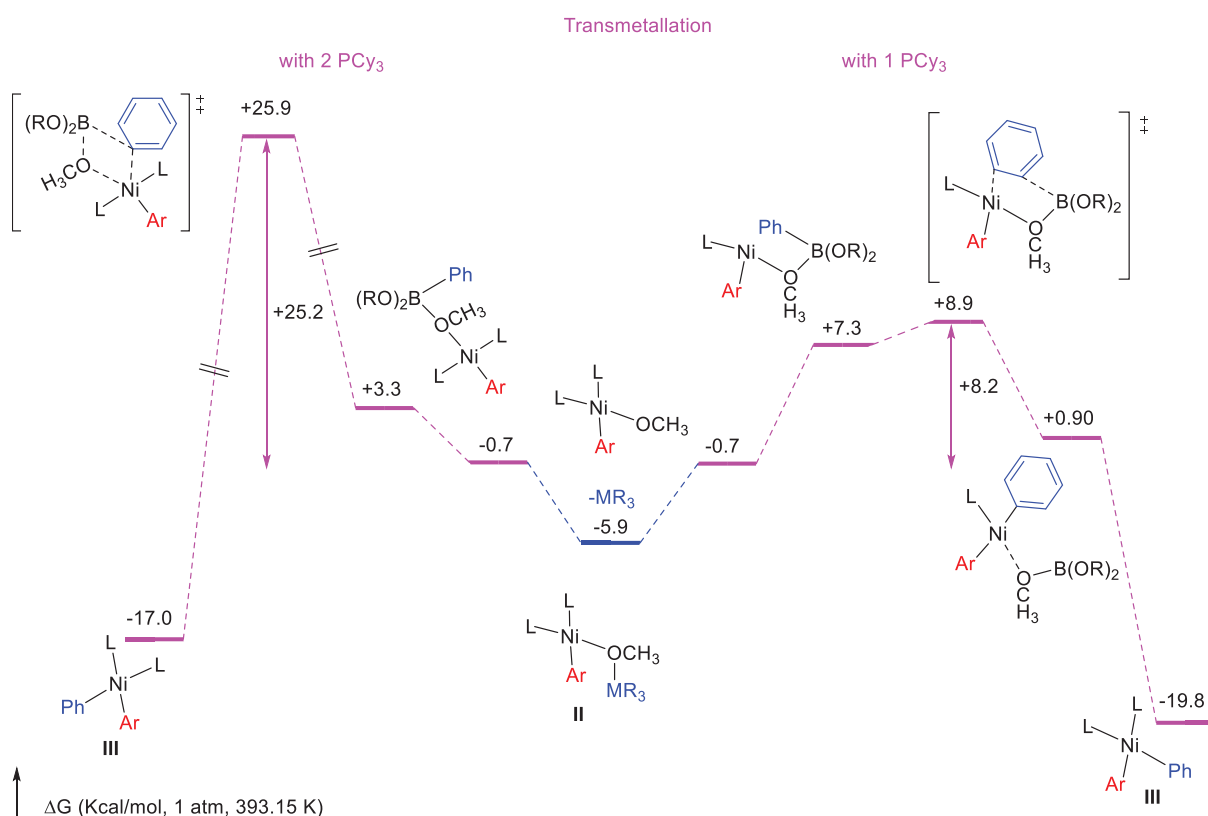
Table 12: Computed C_{Ar}-O bond length values for adducts, transition states and products (in Å).

Entry	Lewis acid	C _{Ar} -O bond length		
		Adduct I	TS	Product II
1	-	1.39	1.77	2.61
2	AlMe ₃	1.45	1.83	2.66
3	AlEt ₃	1.45	1.78	2.65
4	Al(n-Pr) ₃	1.45	1.77	2.64
5	Al(O ^t Bu) ₃	1.46	1.87	2.69
6	BMe ₃	1.43	1.80	2.76
7	BEt ₃	1.42	1.74	2.75
8	B(n-Pr) ₃	1.41	1.75	2.64
9	B(OMe) ₃	1.40	1.79	2.61

3. Transmetallation step

The transmetallation step was also examined computationally to analyze the influence of the Lewis acid for this step. In line with the calculation of Tobisu, Chatani and Mori,³ the

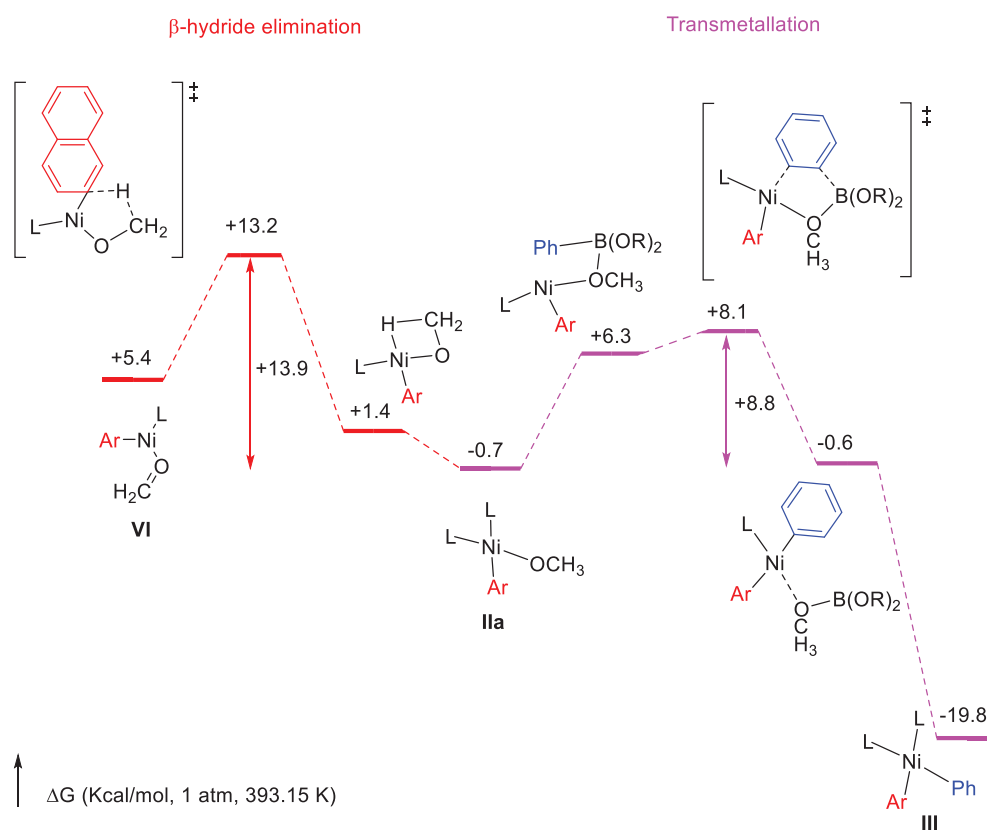
transmetallation involving mono-phosphine nickel intermediate was found to be thermodynamically more favorable than the pathway with two phosphines coordinated to nickel (**Scheme 61**). The transmetallation proceeds via a 4-membered TS involving a boron to oxygen coordination with a very low associated barrier ($\Delta G^\ddagger = 8.9$ kcal/mol). This difference in energy might be due to the steric bulkiness of the second ligand. Thus, after oxidative addition, one of the PCy_3 ligands dissociate while the boronate ester is approaching. The transmetallation proceeds with a slightly higher energy pathway in the presence of Lewis acid (by 1.8 Kcal/mol), suggesting that transmetalation most likely takes place after dissociation of the Lewis acid induced by the interaction with the boronate ester.



Scheme 61: Gibbs free energy profile computed with a solvent (PCM model: toluene) at the BP86-D3/def2TZVP-SDD//BP86-D3/6-31G(d)-SDD level of theory for the transmetalation step.

4. β -hydride elimination vs Transmetallation

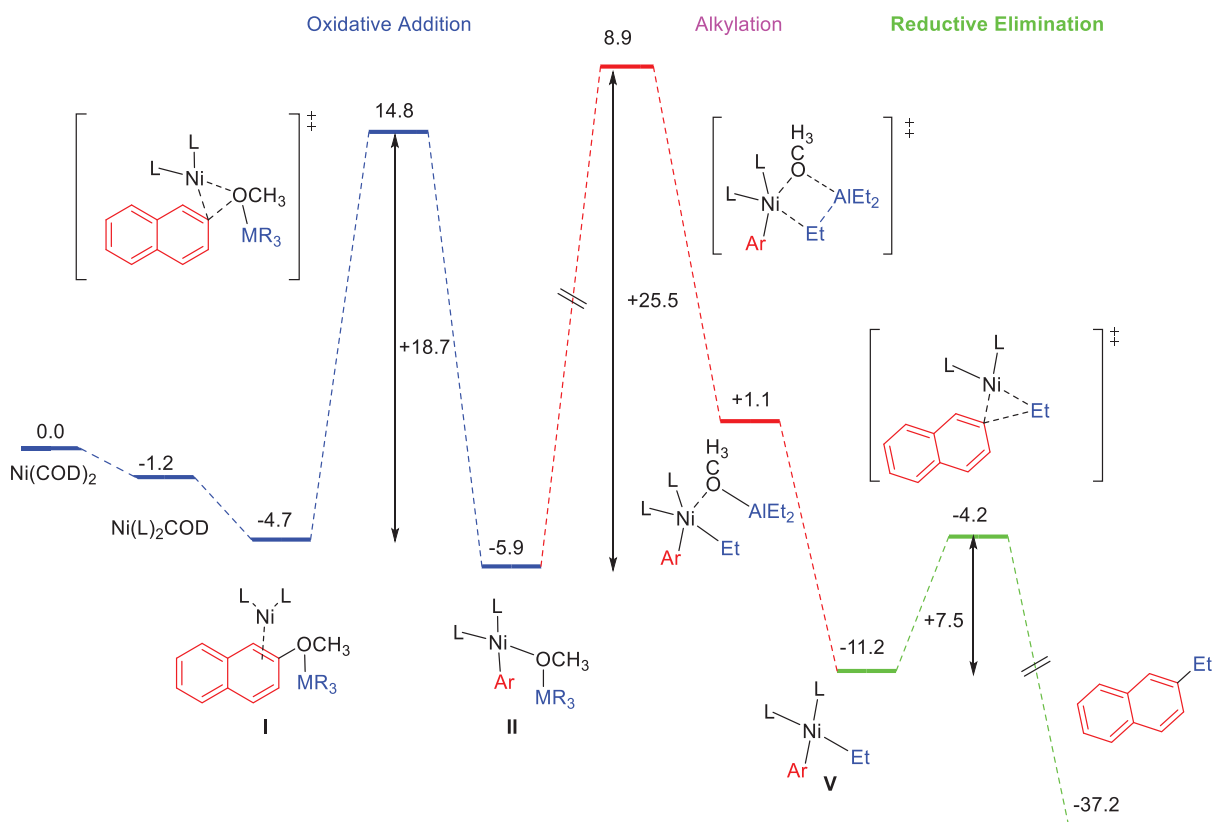
A potential competitive process that has been observed experimentally in the absence of organometallic partner, is the β -hydride elimination of the methoxy group to generate formaldehyde and naphthalene. The energy profile of this competitive reaction was also computed in order to compare its energetic pathway to that of transmetallation. From the oxidative addition intermediate (**IIa**), the β -hydride elimination pathway is thermodynamically less favored than that of transmetallation (**Scheme 62**), which is in good agreement with the experimental observations.



Scheme 62: Gibbs free energy profile computed with a solvent (PCM model: toluene) at the BP86-D3/def2TZVP-SDD//BP86-D3/6-31G(d)-SDD level of theory for the competing β -hydride elimination vs. transmetallation step.

5. Alkylation v.s Transmetallation

The coupling reaction has been shown to proceed well also when alkyl aluminums are used as Lewis acids, which raises the question of possible alkylative cross-coupling via transmetallation between Ni^{II} and AlR_3 .¹³ This pathway remains challenging to exclude and should be computed in comparison to the regular transmetallation with boronate ester (**Scheme 63**).



Scheme 63: Gibbs free energy profile computed with a solvent (PCM model: toluene) at the BP86-D3/def2TZVP-SDD//BP86-D3/6-31G(d)-SDD level of theory for the Alkylative cross-coupling with AlEt_3 , $\text{L}=\text{PCy}_3$.

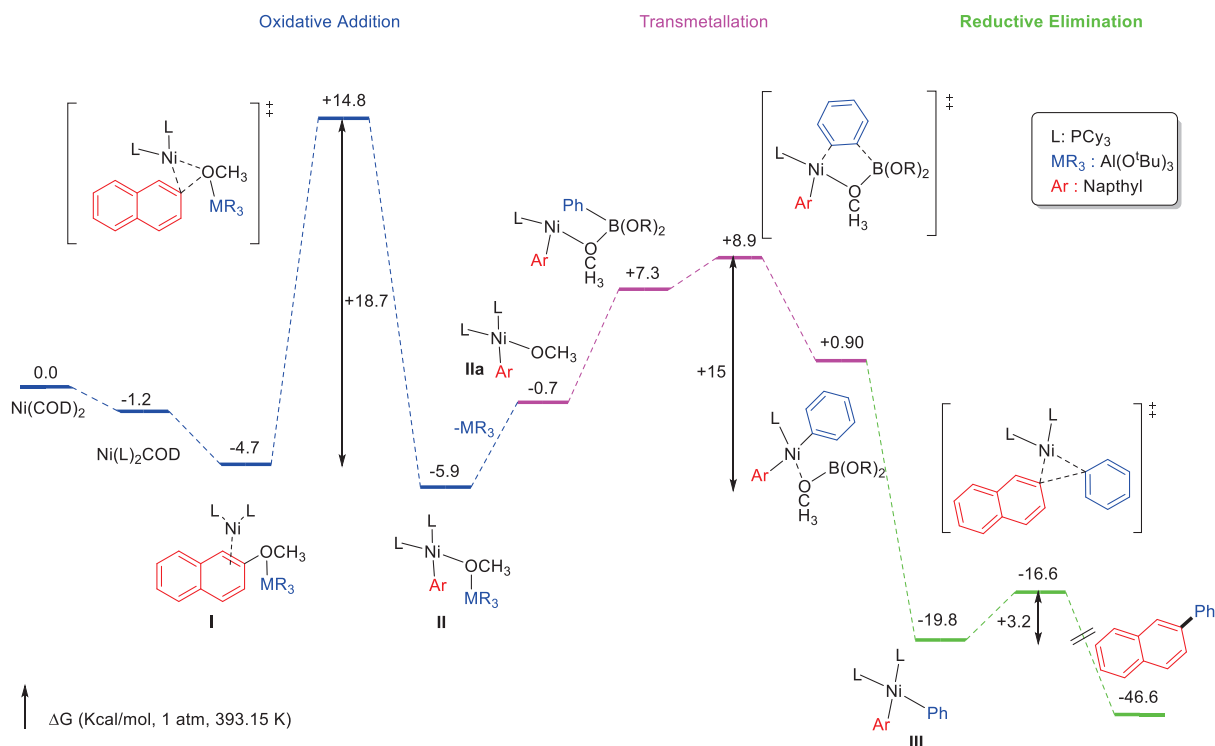
We computed the transmetallation barrier with AlEt_3 that shows the lowest barrier among several alkyl aluminums. It appears that it is kinetically highly unfavorable in comparison to the classical transmetallation. It has even a higher barrier than the oxidative addition itself making it

the rate determining step in the reaction. This clearly explains the experimental observations and direct alkylation can be ruled out of the mechanism.

6. Summary and Proposed mechanism

Based on the above data, we were able to explain why only PCy₃ is the active ligand among all phosphines, due to the thermodynamic sink that only PCy₃ can overcome, thanks to its unique ability to bind to the substrate rather than forming the dimer and being locked at that stage. The effect of Lewis acid in the C-O bond activation process has also been substantiated. Among investigated Lewis acids, Al(O^{*i*}Bu)₃ features the highest affinity to naphthylether resulting in significant lengthening of the C-O_{aryl} bond.

Based on the computational results and experimental observations, a plausible mechanism is presented in (**Scheme 64**), considering that a Ni⁰/Ni^{II} pathway would proceed in the cross coupling reaction. The oxidative addition of naphthylether would occur at the bis-phosphine nickel(0) species and is assisted by Lewis acid coordination to the methoxy moiety. Then, the transmetallation step proceeds more favorably with monoligated Nickel species after decoordination of one phosphine and the Lewis acid. Both, β-hydride elimination and alkylative cross-coupling were excluded due to their high-energy barriers compared to that of transmetallation. Finally, reductive elimination takes place smoothly with a small activation barrier (between 2 to 3 kcal/mol) driven by the high free energy of the formation of C_{Ar}C_{Ar} bond.



Scheme 64: Proposed mechanism. Gibbs free energy profile computed with a solvent (PCM model: toluene) at the BP86-D3/def2TZVP-SDD//BP86-D3/6-31G(d)-SDD level of the theory. PhB(OR)₂ = (5,5-dimethyl-2-phenyl-1,3,2-dioxaborinane).

7. Computational details

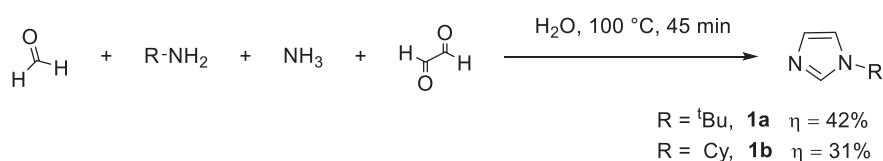
All calculations were performed with Gaussian 09 revision D01.²³ Geometry optimization of the reactants and transition states were carried out at a DFT level of theory using the hybrid functional BP86,^{24,25} without any symmetry restrictions or geometrical constraints. Nickel was represented by a 10 electrons Stuttgart-Koln fully relativistic pseudopotential and its associated basis set of extended valence.^{26,27} During the optimization, all other atoms were represented by polarized all-electron double- ζ 6-31G(d) basis sets.²⁸ The empirical Grimme D3 were used during the optimization.²⁹ Energies were refined by single point calculations using the def2-TZVP basis sets for all atoms except Ni whose basis set remained unchanged.³⁰ Solvation effects by toluene were represented using the PCM implicit solvent model.³¹ The nature of extrema (minimum or

transition state) was verified by analytical frequency calculation. Energy values correspond to Gibbs energy given in kcal/mol estimated at 393 K and 1 atm. Enthalpy and entropy contributions are estimated within the harmonic oscillator approximation. Conformational sampling has been performed by hand. Only the most stable conformers are presented.

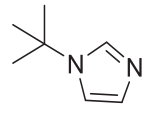
V. Experimental part

1. Synthesis of ligands and Lewis acids

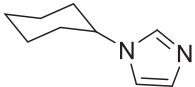
a. Synthesis of bidentate imidazolium ligands



Synthesis of (tert-butyl)-1*H*-imidazole (1a**).** 1-tert-Butylimidazole was prepared according to published procedure.³² In a 50 ml three-necked round bottom flask connected to two dropping funnels and a condenser, water (25 ml) was added. 40% aqueous glyoxal (1 equiv, 0.1 mol, 6.4 ml) and 40% formaldehyde (1 equiv, 0.1 mol, 7.5 ml) were added to the first dropping funnel. Then tert-butylamine (1 equiv, 0.1 mol, 11.5 ml) and 25% aqueous ammonia (1 equiv, 0.1 mol, 10.6 ml) were added to the other one. The mixture was heated to reflux, and both of the solutions were added dropwise simultaneously, while a brown color appears. After completely addition of the reactants, the reaction is kept stirring for an additional 30 min. Water was evaporated at reduced pressure and the crude product was purified by distillation to give the product as pale yellow liquid. Isolated yield (5.2 g, 42%).

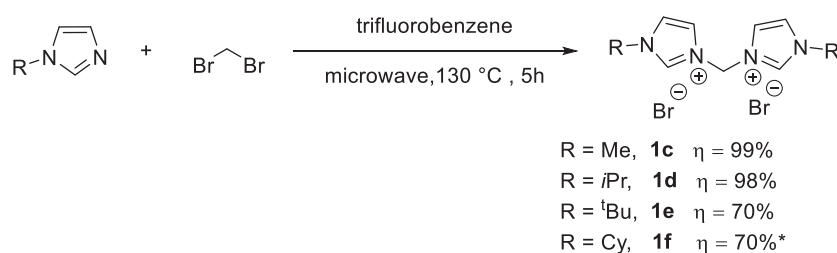

¹H NMR (300 MHz, Chloroform-*d*) δ 7.58 (1H, s, N-CH=N), 7.01 (2H, d, *J* = 6.6 Hz, CH=CH), 1.53 (9H, s, C(CH₃)₃). ¹³C NMR (75 MHz, Chloroform-*d*) δ 134.3 (s, N-CH=N), 129.0 (s, CH=N-CH=CH), 116.3 (s, CH=N-CH=CH), 54.7 (s, C(CH₃)₃), 30.6 (s, C(CH₃)₃). MS (EI) *m/z*: [M]⁺124.

Synthesis of 1-cyclohexyl-1H-imidazole (1b). 1-Cyclohexyl-1H-imidazole was synthesized using the same procedure. Known compound.³³ Isolated as a crystalline white solid after recrystallization from hexanes (4.66 g, 31%).

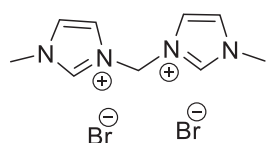
 **¹H NMR** (300 MHz, DMSO-*d*₆) δ 7.67 (1H, s, N-CH=N), 7.21 (1H, s, C₃H₃N₂), 6.86 (1H, s, C₃H₃N₂), 4.00 (1H, m, NCH), 2.51 (2H, m, C₆H₁₁), 1.93 (2H, m, C₆H₁₁) 1.64 (6H, m, C₆H₁₁). **¹³C NMR** (75 MHz, DMSO-*d*₆) δ 142.5 (s, N-CH=N), 135.1 (s, CH=N-CH=CH), 124.4 (s, CH=N-CH=CH), 62.6 (s, NCH), 40.9 (s, C₆H₁₁), 32.1 (s, C₆H₁₁), 31.8 (s, C₆H₁₁). **MS** (EI) *m/z*: [M]⁺150.

***Note:** Isolation of the title compound was complicated by the presence of black viscous polymeric material in the crude product.

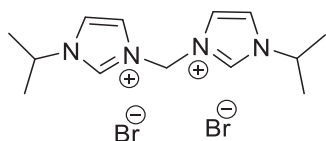
b. Synthesis of Bidentate imidazolium ligands (1c-1f)



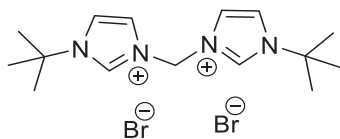
General procedure: Bis-NHC ligands was synthesized according to a modified published procedure⁶. Dibromomethane (1 equiv, 2 mmol, 0.14 ml) and the corresponding imidazole (2 equiv, 4 mmol) were added together to a 5 ml microwave tube. Benzotrifluoride (3 ml) was added and the mixture was sonicated for 5 min. Then it was heated for 5 h at 130 °C by microwave irradiation with 150 W power. The product precipitated, it was isolated by filtration through a pad of silica and washed three times with cold benzotrifluoride (3 x 5 ml). The precipitate was dried under vacuum, giving the corresponding product as white powder in excellent yields.



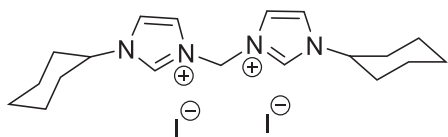
Synthesis of 1,1'-methylene-bis(1-bromo-3-methyl-2,3-dihydro-1H-imidazol-1-ium-2-ide) (1c). Isolated according to the general procedure as white solid (669 mg, 99%). Known compound.³⁴ **¹H NMR** (300 MHz, DMSO-*d*₆) δ 9.52 (2H, s, N-CH=N), 8.06 (2H, s, C₃H₃N₂), 7.81 (2H, s, C₃H₃N₂), 6.74 (2H, s, NCH₂N), 3.91 (6H, s, CH₃). **¹³C NMR** (75 MHz, DMSO-*d*₆) δ 138.5 (s, N-CH=N), 124.8 (s, CH=N-CH=CH), 122.4 (s, CH=N-CH=CH), 79.0 (s, NCH₂N), 36.7 (s, CH₃). **MS** (EI) *m/z*: [M]⁺338.



Synthesis of 1,1'-methylene-bis(1-bromo-3-isopropyl-2,3-dihydro-1H-imidazol-1-ium-2-ide) (1d). Isolated according to the general procedure as white powder (773 mg, 98%). Known compound.³⁴ **¹H NMR** (300 MHz, DMSO-*d*₆) δ 9.75 (2H, s, N-CH=N), 8.16 (2H, s, C₃H₃N₂), 8.06 (2H, s, C₃H₃N₂), 6.71 (2H, s, NCH₂N), 4.71 (2H, sept, *J* = 6.6 Hz, CH(CH₃)₂), 1.51 (12H, d, *J* = 6.7 Hz, CH(CH₃)₂). **MS** (EI) *m/z*: [M]⁺394.



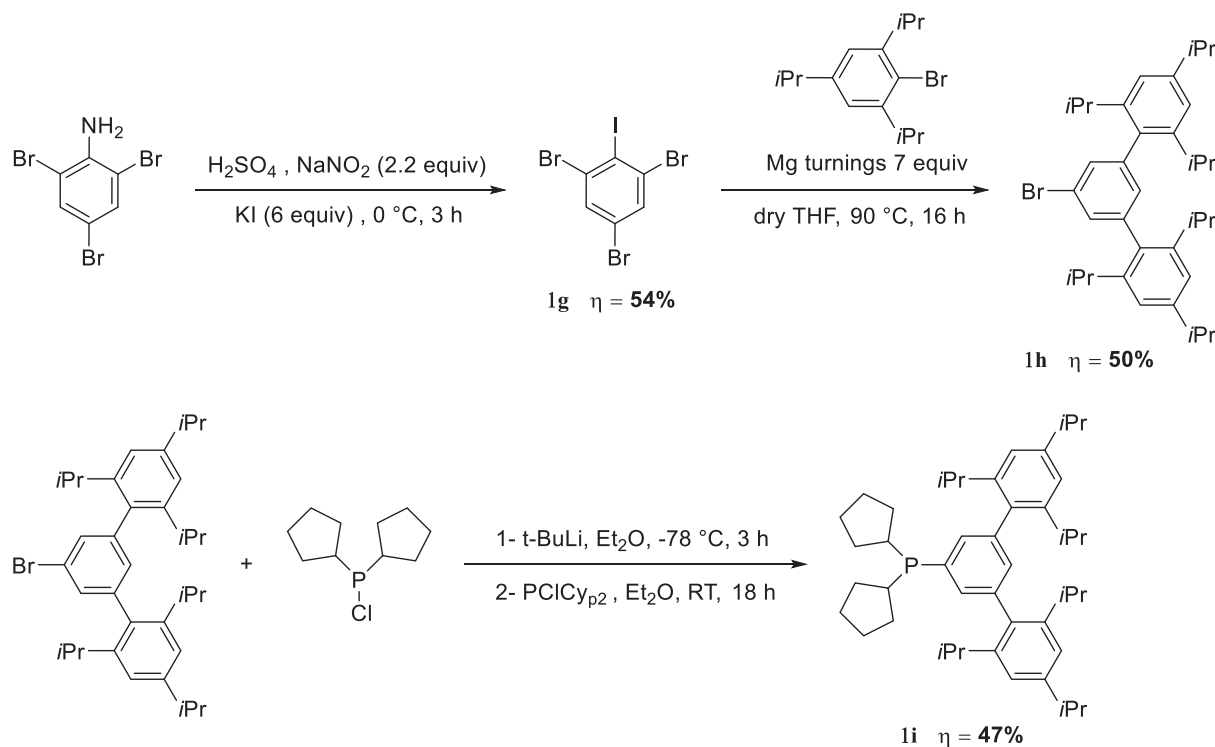
Synthesis of 1,1'-methylene-bis(1-bromo-3-(tert-butyl)-2,3-dihydro-1H-imidazol-1-ium-2-ide) (1e). Isolated according to the general procedure as white powder (625 mg, 74%). Known compound.⁶ **¹H NMR** (300 MHz, DMSO-*d*₆) δ 9.84 (2H, s, N-CH=N), 8.22 (2H, s, C₃H₃N₂), 8.19 (2H, s, C₃H₃N₂), 6.68 (2H, s, NCH₂N), 1.63 (18H, s, C(CH₃)₃). **¹³C NMR** (75 MHz, DMSO-*d*₆) δ 136.8 (s, N-CH=N), 123.0 (s, CH=N-CH=CH), 121.4 (s, CH=N-CH=CH), 60.7 (s, NCH₂N), 58.2 (s, C(CH₃)₃), 29.2 (s, C(CH₃)₃). **MS** (EI) *m/z*: [M]⁺422.



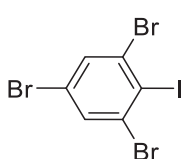
Synthesis of 1,1'-dicyclohexyl-3,3'-diimidazolium diiodide (1f). Prepared with CH₂I₂ (1 equiv, 3.1 mmol, 240 μL) instead of CH₂Br₂ according to the general procedure. Known compound.³⁴ Obtained as colorless solid (796 mg, 70%). **¹H NMR** (300 MHz, DMSO-*d*₆) δ 9.58 (2H, s, N-CH=N), 8.06 (2H, s, C₃H₃N₂), 8.03 (2H, s, C₃H₃N₂), 6.63 (2H, s, NCH₂N), 4.36 (2H, m, NCH), 2.08 (4H, m, C₆H₁₁), 1.82 (4H, m, C₆H₁₁), 1.66 (6H, m, C₆H₁₁), 1.38 (4H, m, C₆H₁₁), 1.23 (2H, m, C₆H₁₁). **¹³C NMR** (75 MHz, DMSO-*d*₆) δ 136.2 (s, N-CH=N), 122.0 (s, CH=N-CH=CH), 121.1 (s, CH=N-CH=CH), 58.7 (s, NCH₂N), 31.9 (s, CH_{Cy}), 24.1 (s, CH_{2,Cy}). **MS** (EI) *m/z*: [M]⁺568.

c. Synthesis of Doyle's ligand

Doyle's ligand was synthesized according to the published procedures (**Scheme 1**).⁸ All the spectrums matched the reported data.

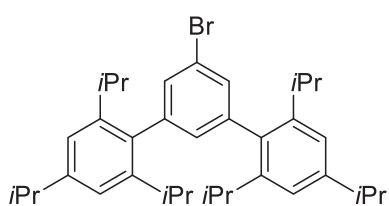


Synthesis of 1,3,5-tribromo-2-iodobenzene (1g). 2,4,6-tribromoaniline (1 equiv, 24.3 mmol, 8.0 g) was dissolved in concentrated H_2SO_4 (20 ml) in an ice cooled bath. A solution of concentrated NaNO_2 (2.2 equiv, 53.4 mmol, 3.68 g) in water (10 ml) was added dropwisely and the reaction is kept running at 0°C for 3 h. A cold solution of KI (6 equiv, 146 mmol, 24.2 g) in water (10 ml) was added to the mixture and the crude product was extracted by EtOAc (3×50 ml). The combined organic layers were washed with a saturated solution of NaHSO_3 and water. Volatiles were removed under vacuum and the product was obtained by recrystallization from hot ethanol as bright orange needle crystals (**5.6 g, 54%**).



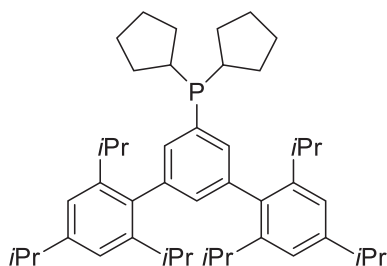
^1H NMR (300 MHz, Chloroform-*d*) δ 7.71 (2H, s, C_6H_2). **^{13}C NMR** (75 MHz, Chloroform-*d*) δ 133.6 (s, C_6H_2), 131.8 (s, C_6H_2), 123.0 (s, C_6H_2), 108.1 (s, C_6H_2). **MS** (EI) m/z : $[\text{M}]^+$ 440.

Synthesis of 5'-bromo-2,2'',4,4'',6,6''-hexaisopropyl-1,1':3',1''-terphenyl (1h). In a dry round bottom flask, a solution of 2-bromo-1,3,5-triisopropylbenzene (3.5 equiv, 15.9 mmol, 4.02 ml) in degassed THF (30 ml) was prepared. Magnesium turnings (7 equiv, 31.8 mmol, 0.772 g) were placed in another round bottom flask equipped with a refluxing condenser under Argon atmosphere and activated by the addition of CH_2Br_2 (0.05 ml) in THF (10 ml) under gentle heating. A portion of the aryl bromide solution (2 ml) was added to initiate the reaction, and the rest of the solution was then added dropwisely. The reaction mixture was refluxed for 14 h. A degassed solution of 1,3,5-tribromo-2-iodobenzene (1 equiv, 4.54 mmol, 2.00 g) in THF (30 ml) was added dropwise to the refluxing organomagnesium solution. The mixture was refluxed for an additional 5 h and poured cautiously into a diluted ice cold aqueous HCl solution (30 ml, 10% wt). The product was extracted by Et_2O (3×60 ml) and washed with water and brine then concentrated under vacuum. The final product was obtained by recrystallization from a saturated solution of hot Et_2O in ethanol as white powder (**1.22 g, 50%**).



^1H NMR (300 MHz, Chloroform-*d*) δ 7.26 (2H, d, $J = 1.4$ Hz, *o*- C_6H_3), 6.96 (4H, s, C_6H_2), 6.88 (1H, t, $J = 1.5$ Hz, *p*- C_6H_3), 2.83 (2H, sept, $J = 6.8$ Hz, *p*- $\text{CH}(\text{CH}_3)_2$), 2.61 (4H, sept, $J = 6.8$ Hz, *o*- $\text{CH}(\text{CH}_3)_2$), 1.21 (12H, d, $J = 7.0$ Hz, $\text{CH}(\text{CH}_3)_2$), 1.08 (12H, d, $J = 6.9$ Hz, $\text{CH}(\text{CH}_3)_2$), 0.97 (12H, d, $J = 6.9$ Hz, $\text{CH}(\text{CH}_3)_2$). **^{13}C NMR** (75 MHz, Chloroform-*d*) δ 148.3 (s, C_{Ar}), 146.3 (s, C_{Ar}), 142.6 (s, C_{Ar}), 135.4 (s, C_{Ar}), 130.7 (s, C_{Ar}), 130.4 (s, C_{Ar}), 121.9 (s, C_{Ar}), 120.6 (s, C_{Ar}), 34.3 (s, $\text{CH}(\text{CH}_3)_2$), 30.4 (s, $\text{CH}(\text{CH}_3)_2$), 24.4 (s, $\text{CH}(\text{CH}_3)_2$), 24.1 (s, $\text{CH}(\text{CH}_3)_2$). **MS** (EI) m/z : $[\text{M}]^+$ 561.

Synthesis of dicyclopentyl(2,2'',4,4'',6,6''-hexaisopropyl-[1,1':3',1''-terphenyl]-5'-yl)phosphane (1i). The title product was prepared using a modified reported procedure.⁸ Three oven dried Schlenk tubes were placed in a dry ice cooled bath at -78° C, and degassed. The first containing 5'-bromo-2,2'',4,4'',6,6''-hexaisopropyl-1,1':3',1''-terphenyl (1 equiv, 0.89 mmol, 0.5 g) in degassed Et₂O (2 ml), the second containing chlorodicyclopentylphosphane (1 equiv, 0.89 mmol, 0.18 g) in Et₂O (1 ml) and the third containing t-BuLi (1.2 equiv, 1.08 mmol, 1.06 ml) in Et₂O (2 ml). The solution of the third Schlenk was transferred using cannula and Argon pressure dropwise to the first Schlenk and stirred for 5 min, followed by transferring the solution of the second Schlenk to the first one using the same method. After complete addition the bath was removed and the reaction was left to stir overnight at RT. After completion of the reaction, as monitored by ³¹P NMR, the reaction mixture was cooled (by ice bath), and a degassed solution of saturated NH₄Cl (15 ml) was added. The product was extracted by Et₂O (3 × 15 ml) and the organic layers were removed using the cannula to a new oven dried Schlenk tube under Argon atmosphere. Volatiles were removed under vacuum and the product was obtained from recrystallization using degassed EtOH under Argon atmosphere, then dried and stored in the glove box as white powder (290 mg, 50%).



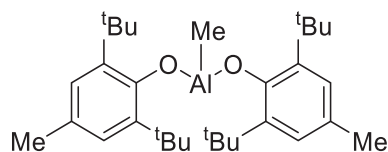
³¹P NMR (122 MHz, Benzene-*d*₆) δ -0.34. ¹H NMR (300 MHz, Benzene-*d*₆) δ 7.50 (2H, dd, *J* = 6.5, 1.6 Hz, *o*-C₆H₃), 7.22 (4H, s, C₆H₂), 7.08 (1H, d, *J* = 1.4 Hz, *p*-C₆H₃), 3.00 (4H, apparent hept, *J* = 7.3 Hz, *o*-CH(CH₃)₂) [split by diastereotopic CH₃ groups], 2.88 (2H, apparent hept, *J* = 6.9 Hz, *p*-CH(CH₃)₂) [split by diastereotopic CH₃ groups], 2.01 – 2.13 (2H, m), 1.79 – 1.91 (2H, m), 1.42 – 1.66 (14H, m), 1.31 (12H, d, *J* = 6.9 Hz) [diastereotopic CH₃ groups], 1.20 – 1.26 (24H, m) [split by diastereotopic CH₃ groups]. ¹³C NMR (76 MHz, Benzene-*d*₆) δ 148.2, 146.5, 140.4 (d, *J* = 6.9 Hz), 138.0, 137.2, 133.4, 131.7, 120.4, 36.3 (d, *J* = 12.4 Hz), 34.6, 30.9,

30.6, 30.1, 26.7 (d, $J = 7.4$ Hz), 26.0 (d, $J = 5.2$ Hz), 24.1 – 24.3 (m), 24.0, 1.1. **MS** (EI) m/z : $[M]^+651$.

d. Synthesis of MAD

Synthesis of bis(2,6-di-tert-butyl-4-methylphenoxy)(methyl)aluminum (MAD) (**1j**).

Bis(2,6-di-tert-butyl-4-methylphenoxy)(methyl)aluminum was synthesized according to a modified published procedure.³⁵ 1,3-Di-tert-butyl-2-methoxy-5-methylbenzene (2 equiv, 5 mmol, 1.17 g) was added to a Schlenk tube cooled in an ice bath and degassed by applying 3 cycles of Argon/vacuum. Degassed DCM (1 ml) was added, followed by dropwise addition of AlMe_3 [2.5 ml of a 1M solution in heptane, 1 equiv, 2.5 mmol] and the reaction mixture was left to stir for 1.5 h at RT. Volatiles were removed under reduced pressure and the crude product was crystallized from pentane giving the product as white powder (1.15 g, 96%).



^1H NMR (300 MHz, Methylene Chloride- d_2) δ 6.93 (s, 4H, C_6H_2), 2.16 (s, 6H, $p\text{-CH}_3$), 1.43 (36H, s, $\text{C}(\text{CH}_3)_3$), -0.44 (3H, s, Al-CH_3)

2. General catalytic procedures

General procedure for ligand screening (Scheme 53): In a glovebox, a 5 mL microwave reaction vial equipped with a magnetic stir bar was charged with a selected ligand [Bis-NHC's (10 mol%, 0.03 mmol) or mono-NHC's or diphosphines (20 mol%, 0.06 mmol) or mono-phosphines (40 mol%, 0.12 mmol), with an additional base NaO^tBu (20 mol%, 0.06 mmol, 5.8 mg) in the case of NHC's] in toluene (0.5 ml), followed by the addition of $\text{Ni}(\text{COD})_2$ (10 mol%, 0.03 mmol, 8.3 mg). After stirring the resulting solution for 5 minutes, methoxynaphthalene (1.0 equiv, 0.3 mmol,

47.5 mg), (*p*-PhCF₃)BOR₂ (1.5 equiv, 0.45 mmol, 116.1 mg) and toluene (1 ml) were sequentially added. In the case of phosphines, CsF (4.5 equiv, 0.6 mmol, 205.1 mg) was additionally added. The tube was sealed, removed from the glovebox and heated overnight at 120 °C (preheated oil bath). Then, the reaction mixture was cooled to room temperature, filtered over Celite®, and all volatiles were removed under reduced pressure. The reaction progress was followed by ¹⁹F-NMR using PhCF₃ as internal standard and GCMS. The products were isolated when necessary by flash chromatography on silica gel using appropriate mixtures of ethyl acetate and cyclohexane.

General procedure for Lewis acids screening (Table 5, Table 9): In a glovebox, a 5 mL microwave reaction vial equipped with a magnetic stir bar was charged with ICy (20 mol%, 0.06 mmol, 16.1 mg) and NaO^tBu (20 mol%, 0.06 mmol, 5.8 mg), or PCy₃ (40 mol%, 0.12 mmol, 33.6 mg) ligand in toluene (0.5 ml), followed by the addition of Ni(COD)₂ (10 mol%, 0.03 mmol, 8.3 mg). After stirring the resulting solution for 5 minutes, a premixed solution of methoxynaphthalene (1.0 equiv, 0.3 mmol, 47.5 mg) with the corresponding Lewis acids (0.05-1 equiv) in toluene (1 ml) was sequentially added followed by the addition of (*p*-PhCF₃)BOR₂ (1.5 equiv, 0.45 mmol, 116.1 mg). The tube was sealed, removed from the glovebox and heated at 120 °C (preheated oil bath) for 3-12 h. The reaction mixture was then cooled to room temperature, filtered over Celite®, and all volatiles were re-moved under reduced pressure. The reaction progress was followed by ¹⁹F-NMR using PhCF₃ as internal standard and GCMS. The products were isolated when necessary by flash chromatography on silica gel using appropriate mixtures of ethyl acetate and cyclohexane.

General procedure for ligands screening with Lewis acids (Scheme 57): In a glovebox, a 5 mL microwave reaction vial equipped with a magnetic stir bar was charged with the corresponding ligand in toluene (0.5 ml), followed by the addition of Ni(COD)₂ (10 mol%, 0.03 mmol,

8.3 mg). After stirring the resulting solution for 5 minutes, a premixed solution of methoxynaphthalene (1.0 equiv, 0.3 mmol, 47.5 mg) with $\text{Al}(\text{O}^t\text{Bu})_3$ (20 mol%, 0.06 mmol, 14.8 mg) in toluene (1 ml) was sequentially added followed by the addition of (*p*-PhCF₃)BOR₂ (1.5 equiv, 0.45 mmol, 116.1 mg). The tube was sealed, removed from the glovebox and heated overnight at 120 °C (preheated oil bath). The reaction mixture was then cooled to room temperature, filtered over Celite®, and all volatiles were re-moved under reduced pressure. The reaction progress was followed by ¹⁹F-NMR using PhCF₃ as internal standard and GCMS. The products was isolated when necessary by flash chromatography on silica gel using appropriate mixtures of ethyl acetate and cyclohexane.

General procedure for boronic esters scope with Lewis acids (Scheme 58): In a glovebox, a 5 mL microwave reaction vial equipped with a magnetic stir bar was charged with PCy₃ (40 mol%, 0.12 mmol, 33.6 mg) ligand in toluene (0.5 ml), followed by the addition of Ni(COD)₂ (10 mol%, 0.03 mmol, 8.3 mg). After stirring the resulting solution for 5 minutes, a premixed solution of methoxynaphthalene (1.0 equiv, 0.3 mmol, 47.5 mg) with $\text{Al}(\text{O}^t\text{Bu})_3$ (20 mol%, 0.06 mmol, 14.8 mg) in toluene (1 ml) was sequentially added followed by the addition of the corresponding boronate ester (1.5 equiv, 0.45 mmol). The tube was sealed, removed from the glovebox and heated at 120 °C (preheated oil bath) for 3 h. The reaction mixture was then cooled to room temperature, filtered over Celite®, and all volatiles were re-moved under reduced pressure. The reaction progress was followed by ¹⁹F-NMR using PhCF₃ as internal standard and GCMS. The products was isolated when necessary by flash chromatography on silica gel using appropriate mixtures of ethyl acetate and cyclohexane.

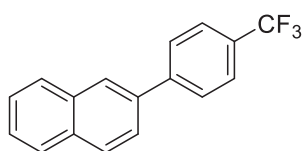
General procedure for aryl ethers scope with Lewis acids (Scheme 59): In a glovebox, a 5 mL microwave reaction vial equipped with a magnetic stir bar was charged with ICy (20 mol%,

0.06 mmol, 16.1 mg) and NaO^tBu (20 mol%, 0.06 mmol, 5.8 mg), or PCy₃ (40 mol%, 0.12 mmol, 33.6 mg) ligand in toluene (0.5 ml), followed by the addition of Ni(COD)₂ (10 mol%, 0.03 mmol, 8.3 mg). After stirring the resulting solution for 5 minutes, a premixed solution of the corresponding aryl ethers (1.0 equiv, 0.3 mmol) with Al(O^tBu)₃ (20 mol%, 0.06 mmol, 14.8 mg) or AlMe₃ [15 µL of a 2M solution in toluene, 10 mol%, 0.03 mmol] in toluene (1 ml) was sequentially added followed by the addition of (*p*-PhCF₃)BOR₂ (1.5 equiv, 0.45 mmol, 116.1 mg). The tube was sealed, removed from the glovebox and heated overnight at 120 °C (preheated oil bath). The reaction mixture was then cooled to room temperature, filtered over Celite®, and all volatiles were removed under reduced pressure. The reaction progress was followed by ¹⁹F-NMR using PhCF₃ as internal standard and GCMS. The products were isolated when necessary by flash chromatography on silica gel using appropriate mixtures of ethyl acetate and cyclohexane.

3. Isolation and characterization of Suzuki cross-coupling products

General procedure: In a glovebox, a 5 mL microwave reaction vial equipped with a magnetic stir bar was charged with a selected ligand [ICy (20 mol%, 0.06 mmol, 16.1 mg) or PCy₃ (40 mol%, 0.12 mmol, 33.6 mg), with an additional base NaO^tBu (20 mol%, 0.06 mmol, 5.8 mg) in the case of ICy] in toluene (0.5 ml), followed by the addition of Ni(COD)₂ (10 mol%, 0.03 mmol, 8.3 mg). After stirring the resulting solution for 5 minutes, methoxynaphthalene (1.0 equiv, 0.3 mmol, 47.5 mg), the corresponding boronate ester (1.5 equiv, 0.45 mmol, 116.1 mg) and toluene (1 ml) were sequentially added. The tube was sealed, removed from the glovebox and heated overnight at 120 °C (preheated oil bath). Then, the reaction mixture was cooled to room temperature, filtered over Celite®, and all volatiles were removed under reduced pressure. The reaction yields was determined by ¹⁹F-NMR using PhCF₃ as internal standard (for products bearing fluorine atoms) and by

integrating the signals of the products by GCMS using n-Dodecane as an internal standard. Only one compound was isolated.



2-(4-(trifluoromethyl)phenyl)naphthalene (A). Known compound.³ Synthesized according to the general procedure with PCy₃ ligand (Entry 2, **Table 9**). Purified by flash chromatography (Ethyl acetate/Cyclohexane, gradient 0 to 70%). Obtained as white powder (71 mg, 87% yield). NMR data matches the reported spectrums. **¹H NMR** (300 MHz, Chloroform-*d*) δ 7.98 (1H, s, CH_{Ar}), 7.91 – 7.78 (3H, m, CH_{Ar}), 7.74 (2H, d, ³*J*_{H-H} = 8.1, CH_{Ar}), 7.70 – 7.60 (3H, m, CH_{Ar}), 7.52 – 7.41 (2H, m, CH_{Ar}). **¹⁹F NMR** (282 MHz, Chloroform-*d*): δ -61.9. **MS** (EI) *m/z*: [M]⁺ 272.

VI. References

- (1) Tobisu, M.; Shimasaki, T.; Chatani, N. Nickel-Catalyzed Cross-Coupling of Aryl Methyl Ethers with Aryl Boronic Esters. *Angew. Chem. Int. Ed.* **2008**, 47 (26), 4866–4869.
- (2) Tobisu, M.; Yasutome, A.; Kinuta, H.; Nakamura, K.; Chatani, N. 1,3-Dicyclohexylimidazol-2-Ylidene As a Superior Ligand for the Nickel-Catalyzed Cross-Couplings of Aryl and Benzyl Methyl Ethers With Organoboron Reagents. *Org. Lett.* **2014**, 16 (21), 5572–5575.
- (3) Schwarzer, M. C.; Konno, R.; Hojo, T.; Ohtsuki, A.; Nakamura, K.; Yasutome, A.; Takahashi, H.; Shimasaki, T.; Tobisu, M.; Chatani, N. Combined Theoretical and Experimental Studies of Nickel-Catalyzed Cross-Coupling of Methoxyarenes with Arylboronic Esters via C-O Bond Cleavage. *J. Am. Chem. Soc.* **2017**, 139 (30), 10347–10358.

- (4) Van Leeuwen, P. W. N. M.; Kamer, P. C. J.; Reek, J. N. H.; Dierkes, P. Ligand Bite Angle Effects in Metal-Catalyzed C-C Bond Formation. *Chem. Rev.* **2000**, *100* (8), 2741–2769.
- (5) Dierkes, P.; Van Leeuwen, P. W. N. M. The Bite Angle Makes the Difference: A Practical Ligand Parameter for Diphosphine Ligands. *J. Chem. Soc. - Dalt. Trans.* **1999**, No. 10, 1519–1529.
- (6) Brendel, M.; Braun, C.; Rominger, F.; Hofmann, P. Bis-NHC Chelate Complexes of Nickel(0) and Platinum(0). *Angew. Chem. Int. Ed.* **2014**, *53* (33), 8741–8745.
- (7) Sauerbrey, S.; Majhi, P. K.; Daniels, J.; Schnakenburg, G.; Bmndle, G. M.; Scherer, K.; Streubel, R. Synthesis, Structure, and Reactions of 1-Fert-Butyl-2-Diphenylphosphino-Imidazole. *Inorg. Chem.* **2011**, *50* (3), 793–799.
- (8) Wu, K.; Doyle, A. G. Parameterization of Phosphine Ligands Demonstrates Enhacement of Nickel Catalysis via Remote Steric Effects. *Nat. Chem.* **2017**, *9* (8), 779–784.
- (9) Wu, K.; Doyle, A. G. Parameterization of Phosphine Ligands Demonstrates Enhacement of Nickel Catalysis via Remote Steric Effects. *Nat. Chem.* **2017**, *9* (8), 779–784.
- (10) Ariki, Z. T.; Maekawa, Y.; Nambo, M.; Crudden, C. M. Preparation of Quaternary Centers via Nickel-Catalyzed Suzuki-Miyaura Cross-Coupling of Tertiary Sulfones. *J. Am. Chem. Soc.* **2018**, *140* (1), 78–81.
- (11) Cornella, J.; Gómez-Bengoa, E.; Martin, R. Combined Experimental and Theoretical Study on the Reductive Cleavage of Inert C-O Bonds with Silanes: Ruling out a Classical Ni(0)/Ni(II) Catalytic Couple and Evidence for Ni(I) Intermediates. *J. Am. Chem. Soc.* **2013**, *135* (5), 1997–2009.
- (12) Ogawa, H.; Minami, H.; Ozaki, T.; Komagawa, S.; Wang, C.; Uchiyama, M. How and Why Does Ni0 Promote Smooth Etheric C-O Bond Cleavage and C-C Bond Formation? A

- Theoretical Study. *Chem. Eur. J.* **2015**, *21* (40), 13904–13908.
- (13) Liu, X.; Hsiao, C. C.; Kalvet, I.; Leiendecker, M.; Guo, L.; Schoenebeck, F.; Rueping, M. Lewis Acid Assisted Nickel-Catalyzed Cross-Coupling of Aryl Methyl Ethers by C-O Bond-Cleaving Alkylation: Prevention of Undesired β -Hydride Elimination. *Angew. Chem. Int. Ed.* **2016**, *55* (20), 6093–6098.
- (14) Kelley, P.; Edouard, G. A.; Lin, S.; Agapie, T. Lewis Acid Accelerated Aryl Ether Bond Cleavage with Nickel: Orders of Magnitude Rate Enhancement Using AlMe₃. *Chem. Eur. J.* **2016**, *22* (48), 17173–17176.
- (15) Alexey G. Sergeev, J. F. H. Selective, Nickel-Catalyzed Hydrogenolysis of Aryl Ethers. *Science*. **2011**, *332* (6028), 439–443.
- (16) Tobisu, M.; Chatani, N. Cross-Couplings Using Aryl Ethers via C-O Bond Activation Enabled by Nickel Catalysts. *Acc. Chem. Res.* **2015**, *48* (6), 1717–1726.
- (17) Nakao, Y.; Yada, A.; Ebata, S.; Hiyama, T. A Dramatic Effect of Lewis-Acid Catalysts on Nickel-Catalyzed Carbocyanation of Alkynes. *J. Am. Chem. Soc.* **2007**, *129* (9), 2428–2429.
- (18) Yada, A.; Yukawa, T.; Idei, H.; Nakao, Y.; Hiyama, T. Nickel/Lewis Acid-Catalyzed Carbocyanation of Alkynes Using Acetonitrile and Substituted Acetonitriles. *Bull. Chem. Soc. Jpn.* **2010**, *83* (6), 619–634.
- (19) Xu, Z.; Mao, J.; Zhang, Y. Pd(OAc)₂-Catalyzed Room Temperature Homocoupling Reaction of Arylboronic Acids under Air without Ligand. *Catal. Commun.* **2008**, *9*, 97–100.
- (20) Bundens, J. W.; Yudenfreund, J.; Franci, M. M. Transition States for the Carboalumination of Alkenes and Alkynes. *Organometallics* **1999**, *18* (19), 3913–3920.
- (21) Zakharov, I. I.; Zakharov, V. A. Quantum-Chemical Study of Ethylene Oligomerization in the Presence of Individual Organoaluminium Compounds. *J. Mol. Catal.* **1982**, *14* (2), 171–

184.

- (22) Wang, X.; Hong, M. Lewis-Pair-Mediated Selective Dimerization and Polymerization of Lignocellulose-Based B-Angelica Lactone into Biofuel and Acrylic Bioplastic. *Angew. Chem. Int. Ed.* **2020**, *59* (7), 2664–2668.
- (23) Frisch, M. J.; Trucks, G. W.; Schlegel, H. B.; Scuseria, G. E.; Robb, M. A.; Cheeseman, J. R.; Scalmani, G.; Barone, V.; Mennucci, B.; Petersson, G. A.; Nakatsuji, H.; Caricato, M.; Li, X.; Hratchian, H. P.; Izmaylov, A. F.; Bloino, J.; Zheng, G. . S. Gaussian 09, Revision D.01, Wallingford CT. **2009**.
- (24) Becke, A. D. Density-Functional Exchange-Energy Approximation with Correct Asymptotic Behavior. *Phys. Rev. A* **1988**, *38* (6), 3098–3100.
- (25) Perdew, J. P. Density-Functional Approximation for the Correlation Energy of the Inhomogeneous Electron Gas. *Phys. Rev. B* **1986**, *33* (12), 8822–8824.
- (26) Dolg, M.; Wedig, U.; Stoll, H.; Preuss, H. Energy-Adjusted Ab Initio Pseudopotentials for the First Row Transition Elements. *J. Chem. Phys.* **1986**, *86* (2), 866–872.
- (27) Martin, J. M. L.; Sundermann, A. Correlation Consistent Valence Basis Sets for Use with the Stuttgart-Dresden-Bonn Relativistic Effective Core Potentials: The Atoms Ga-Kr and In-Xe. *J. Chem. Phys.* **2001**, *114* (8), 3408–3420.
- (28) Hehre, W. J.; Ditchfield, K.; Pople, J. A. Self-Consistent Molecular Orbital Methods. XII. Further Extensions of Gaussian-Type Basis Sets for Use in Molecular Orbital Studies of Organic Molecules. *J. Chem. Phys.* **1972**, *56* (5), 2257–2261.
- (29) Grimme, S.; Antony, J.; Ehrlich, S.; Krieg, H. A Consistent and Accurate Ab Initio Parametrization of Density Functional Dispersion Correction (DFT-D) for the 94 Elements H-Pu. *J. Chem. Phys.* **2010**, *132* (15), 154104.

- (30) Weigend, F.; Ahlrichs, R. Balanced Basis Sets of Split Valence, Triple Zeta Valence and Quadruple Zeta Valence Quality for H to Rn: Design and Assessment of Accuracy. *Phys. Chem. Chem. Phys.* **2005**, 7 (18), 3297–3305.
- (31) Tomasi, J.; Mennucci, B.; Cammi, R. Quantum Mechanical Continuum Solvation Models. *Chem. Rev.* **2005**, 105 (8), 2999–3093.
- (32) Sauerbrey, S.; Majhi, P. K.; Daniels, J.; Schnakenburg, G.; Brändle, G. M.; Scherer, K.; Streubel, R. Synthesis, Structure, and Reactions of 1- *Tert* -Butyl-2-Diphenylphosphino-Imidazole. *Inorg. Chem.* **2011**, 50 (3), 793–799.
- (33) Perry, M. C.; Cui, X.; Powell, M. T.; Hou, D. R.; Reibenspies, J. H.; Burgess, K. Optically Active Iridium Imidazol-2-Ylidene-Oxazoline Complexes: Preparation and Use in Asymmetric Hydrogenation of Arylalkenes. *J. Am. Chem. Soc.* **2003**, 125 (1), 113–123.
- (34) Scherg, T.; Schneider, S. K.; Frey, G. D.; Schwarz, J.; Herdtweck, E.; Herrmann, W. A. Bridged Imidazolium Salts Used as Precursors for Chelating Carbene Complexes of Palladium in the Mizoroki-Heck Reaction. *Synlett* **2006**, 2006 (18), 2894–2907.
- (35) Adachij, T.; Sugimoto, H.; Aida, T.; Inoue, S. Aluminum Thiolate Complexes of Porphyrin as Excellent Initiators for Lewis Acid Assisted High-Speed Living Polymerization of Methyl Methacrylate. *Macromolecules* **1993**, 112, 1238–1243.

Chapter III:

*Investigations on Ni/Lewis acid catalyzed cross-
coupling of aryl ethers with alkenes*

I. Introduction

1. Overview

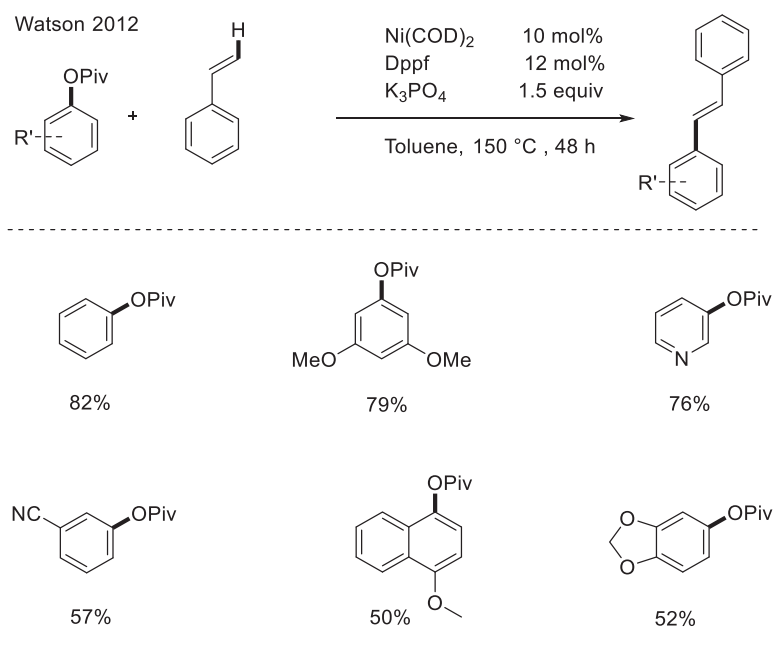
The improvement of greener and less expensive strategies is a progressing challenge within the synthesis of organic compounds. Indeed, in spite of the fact that aryl ethers are amongst the most promising electrophiles in cross-coupling, nickel-catalyzed C-C cross-coupling of aryl ethers are predominantly preformed with organometallic coupling partners (ArB(OR)_2 , ArMgBr , $\text{ArLi}\dots$).¹ On the other hand, direct functionalization with non-organometallic coupling partners are far less explored. Tandem C-O/C-H cross-coupling of mild non-organometallic coupling partners (e.g; arenes, alkenes, alkynes...) is of great interest and represents a perfect shortcut in organic synthesis avoiding the pre-functionalization of starting materials as well as reducing the number of steps and employing an abundant and much less expensive nucleophile. This strategy would essentially contribute to the progress in C-C bond-forming methodologies. In this chapter, we will focus on recent developments disclosing C-O/C-H cross-coupling reactions of phenol derivatives with alkenes, before discussing our investigations in the area of nickel-catalyzed cross-coupling reactions of aryl ethers with alkenes.

II. State of the art

1. Heck-type cross-coupling reactions with phenol derivatives

The first example of nickel-catalyzed Heck-type cross-coupling of phenol derivatives was explored by Watson & al. in 2012.² The transformation involved coupling of aryl pivalates with styrenes catalyzed by Ni(COD)_2 and phosphine ligands. Amongst the several phosphines found

active, bis-phosphines proved more effective than monophosphines, with 1,1'-Bis(diphenylphosphino)ferrocene ligand (Dppf) being the best ligand. Various styrenes reacted well to provide the corresponding coupling products in good yields (**Scheme 65**).

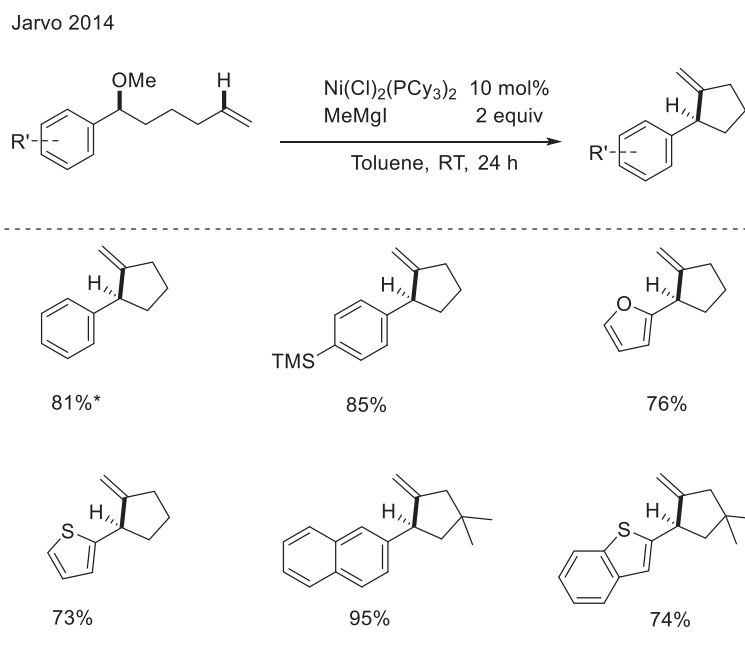


Scheme 65: Scope for Ni-catalyzed Heck cross-coupling of aryl pivalates.

Two mechanisms were hypothesized, either a neutral or a cationic mechanism. In the neutral mechanism, the O.A of aryl pivalates is followed by coordination and migratory insertion of the alkene moiety along with reductive elimination. In the cationic one, the formation of a more reactive cationic Ni^{II} species was proposed, which could be generated by dissociation of pivalate group after O.A.

Later on, Jarvo & al. reported an intramolecular nickel-catalyzed Heck type cross-coupling of benzylic ethers. The best catalytic system was composed of Ni(COD)_2 and tricyclohexyl phosphine ligand. Of note, an excess of MeMgI (2 equiv) was found essential for the reaction to proceed.³ Various ligands were screened, bis-phosphines were found to be much less efficient than

monophosphines. In addition, bis-phosphine ligands were found to shift the selectivity toward methylation of the benzyl ether instead of cyclization. This could be attributed to less favorable coordination of alkene to the 4-coordinate (bis-phosphine)Ni(II) intermediate. Interestingly, the air-stable $\text{Ni}^{\text{II}}(\text{Cl})_2(\text{PCy}_3)_2$ catalyst was found to be effective; the reaction has a broad scope and is generally performed at R.T with retention of stereochemistry (**Scheme 66**). To date, this report stands as the only example of heck-type coupling reaction involving C-OMe bond functionalization.

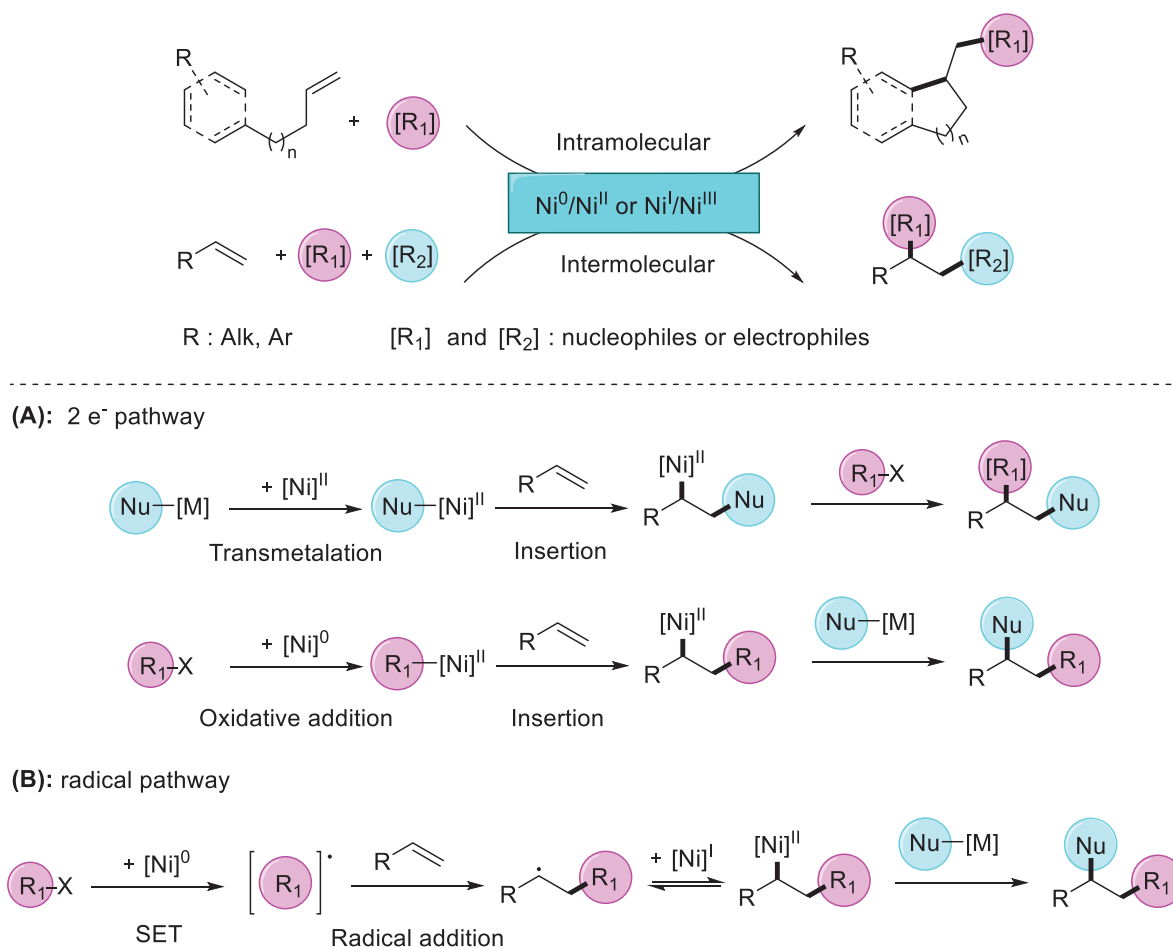


Scheme 66: Scope for the intramolecular Ni-catalyzed Heck cross-coupling of phenol derivatives. *at 60°C

2. Difunctionalization of alkenes

Dicarbofunctionalization of alkenes was developed as an efficient synthetic methodology for preparing substituted molecules from readily accessible alkenes through cross-coupling with various electrophiles and nucleophiles. Nickel complexes were shown to be very effective catalysts

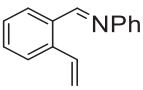
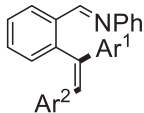
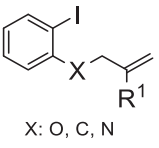
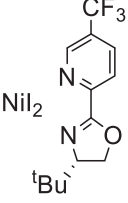
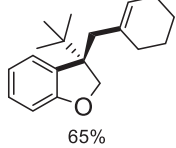
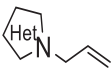
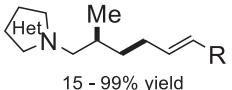
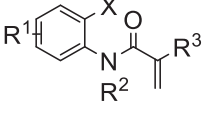
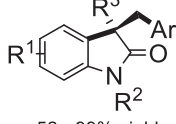
for difunctionalization due to their capability to undergo facile oxidative addition, their low propensity to be deactivated via β -hydride elimination, and their ability to access both two-electron and radical pathways (**Scheme 67**).^{4,5}



Scheme 67: Nickel-catalyzed difunctionalization of alkenes.

Even though a large range of alkene difunctionalizations has been developed, only very few of them used phenolic derivatives (**Table 13**).^{4,6,7,8} The general scope was broad and was extended to biologically active molecules. The proposed mechanisms take place via a two electrons pathway as indicated in (**Scheme 67-A**).

Table 13: Ni-catalyzed difunctionalization of alkenes with phenol derivatives.^[a]

Entry	Alkene	[Nu]	Electrophile	Catalyst/ligand	Product
1		Ar ¹ ZnI	Ar ² OTf	Ni(COD) ₂	
2	 X: O, C, N	-	TfO-CH=CH-R ²		 65%
3		ZnMe ₂	OAc-CH=CH-R	NiBr ₂ (glyme)	 15 - 99% yield
4	 X: I, OTf, OPiv	ArB(OH) ₂	-	Ni(COD) ₂ /PPh ₃	 52 - 99% yield

3. Research objective

Nickel-catalyzed tandem C-O/C-H cross-coupling of aryl ethers with mild non-organometallic coupling partners like arenes, alkenes, or alkynes have never been reported. We were motivated to explore the possibility of developing Heck-type cross-coupling reactions of aryl ethers. As a proof of concept, we thus planned to design a series of model substrates that may be prone to intramolecular Heck transformations, and offer the possibility of isolating and characterizing some key intermediates.

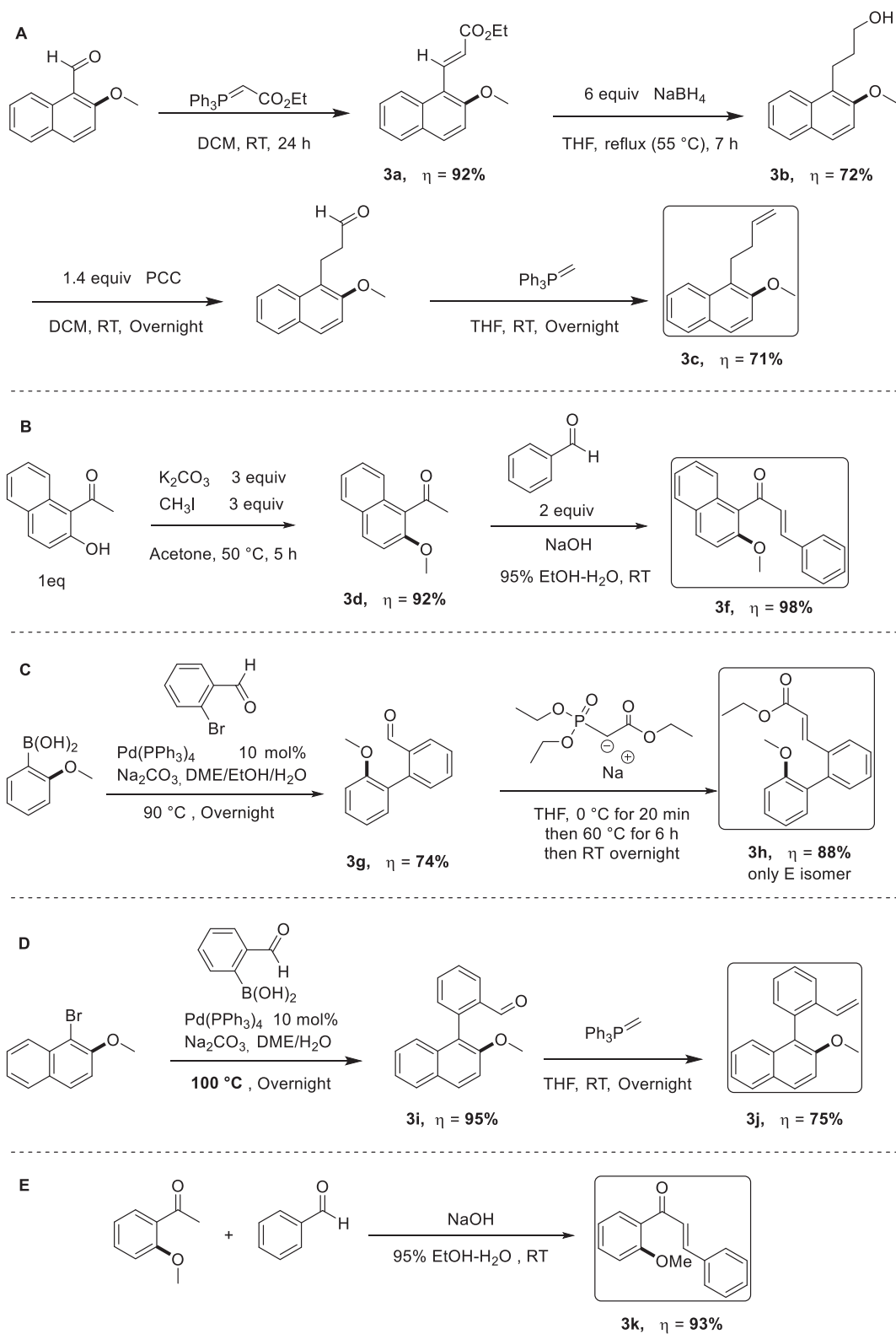
III. Investigations on Heck-type and difunctionalization reactions of aryl ethers

1. Synthesis of model aryl ethers featuring pendant alkene moieties

Inspired by the work of Jarvo on intramolecular Heck transformation of benzylic ethers, and the previous reports on intramolecular Heck-type transformations with halides, we synthesized five model substrates (**3c**, **3f**, **3h**, **3j**, and **3k**), amongst which two of them bear *ortho*-substituted carbonyl groups that can be also tested with ruthenium catalyst (**Scheme 68**).^{3,9,10}

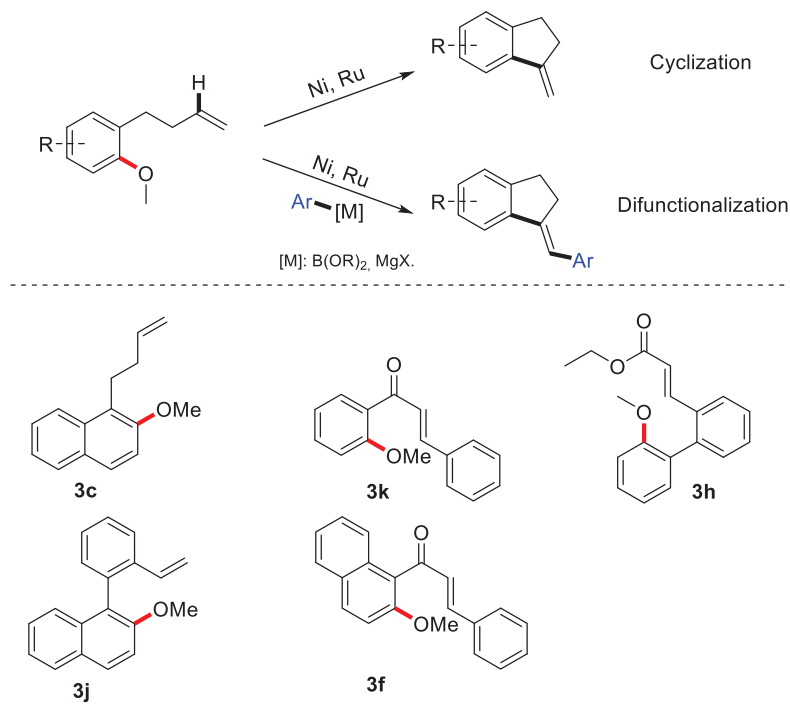
The first substrate, 1-(but-3-en-1-yl)-2-methoxynaphthalene (**3c**), was prepared in four steps from 2-methoxy-1-naphthaldehyde: A first Wittig reaction allowed access to ethyl (*E*)-3-(2-methoxynaphthalen-1-yl)acrylate (**3a**), which was reduced by NaBH₄ to form 3-(2-methoxynaphthalen-1-yl)propan-1-ol (**3b**). Then, oxidation of **3b** was carried out using PCC where the product was purified by simple decantation, extraction and filtration and directly engaged in the next Wittig step to afford the final substrate (**3c**) in 71 % isolated yield (**Scheme 68-A**). The second substrate, (*E*)-1-(2-methoxynaphthalen-1-yl)-3-phenylprop-2-en-1-one (**3f**), was synthesized by methylation of 1-(2-hydroxynaphthalen-1-yl)ethan-1-one with methyl iodide to form 1-(2-methoxynaphthalen-1-yl)ethan-1-one (**3d**), followed by base-assisted condensation, giving **3f** in excellent yield (**Scheme 68-B**).

The two substrates ethyl (*E*)-3-(2'-methoxy-[1,1'-biphenyl]-2-yl)acrylate (**3h**) and (S)-2-methoxy-1-(2-vinylphenyl)naphthalene (**3j**) were synthesized by Pd-catalyzed cross-coupling with the corresponding boronic acids, followed by Wittig reaction affording **3h** and **3j** in very good yields (**Scheme 68-C,D**). The last substrate, (*E*)-1-(2-methoxyphenyl)-3-phenylprop-2-en-1-one (**3k**), was synthesized by condensation reaction in excellent yields (**Scheme 68-E**).



Scheme 68: Synthesis of model substrates for intramolecular Heck reactions.^{11,9,10}

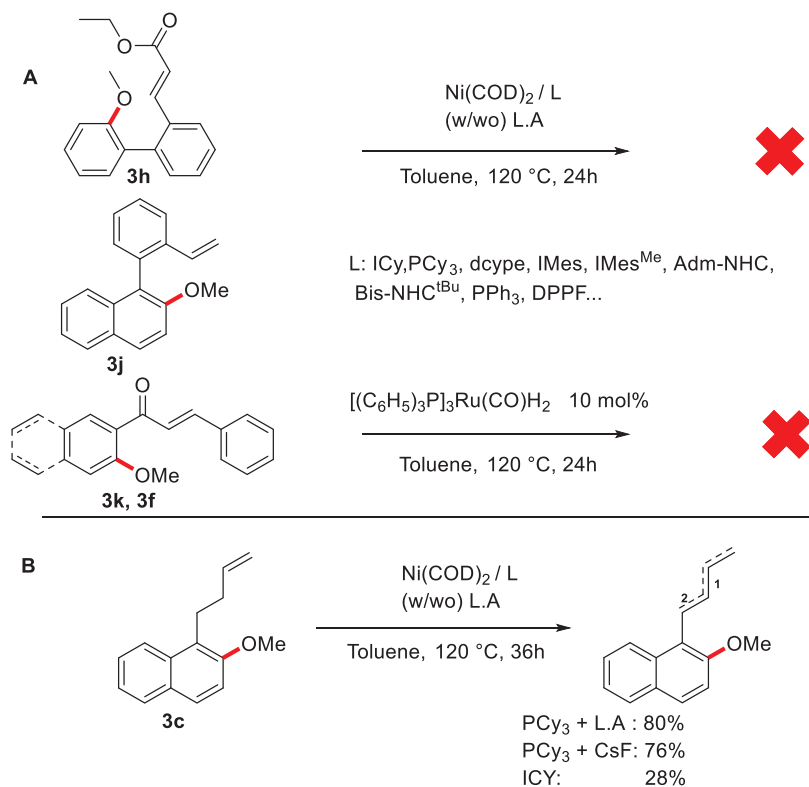
Then, we envisioned to investigate the reactivity of synthesized substrates in Ni and Ru catalyzed Heck cyclization and difunctionalization reactions (**Scheme 69**).



Scheme 69: General concept and the synthesized substrates for intramolecular Heck cross-couplings.

2. Catalytic studies

At the initial stage, we probed the reactivity of substrates **3h**, **3j**, **3k**, and **3f** under Ni catalysis using a series of phosphines and NHC ligands in the presence or absence of Al(O^tBu)₃ as co-catalyst. Unfortunately, none of the expected reactions did take place, and the substrates remained intact, even when PCy₃ or ICy ligands were employed. We further tested the reaction of the two ortho-substituted carbonyl substrates **3k** and **3f** using RuH₂(CO)(PPh₃)₃ as catalyst, which also failed to react, affording only trace amounts of products resulting from hydrogenation of the double bond (**Scheme 70-A**). The hydrogenation process was not totally unexpected since a ruthenium hydride complex is used as catalyst.¹²



Scheme 70: Testing the substrates with several Nickel and Ruthenium systems. L.A = $\text{Al}(\text{O}^i\text{Bu})_3$. Reactions performed with Ni(COD)_2 (10 mol%), $\text{RuH}_2(\text{CO})(\text{PPh}_3)_3$ (10 mol%), Bis-NHC (10 mol%), ICy, dcype, IMes, IMes^{Me}, Adm-NHC, Dppf (20 mol%), PCy₃, PPh₃ (40 mol%), substrate (1 equiv), $\text{Al}(\text{O}^i\text{Bu})_3$ (20 mol%). Yields were determined by GCMS.

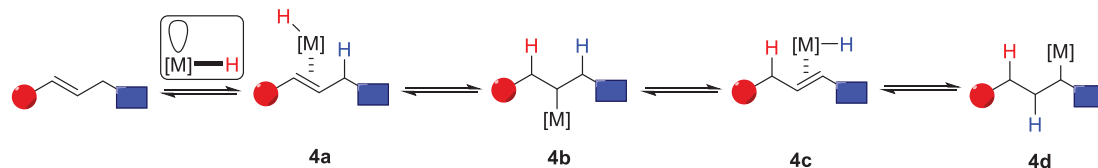
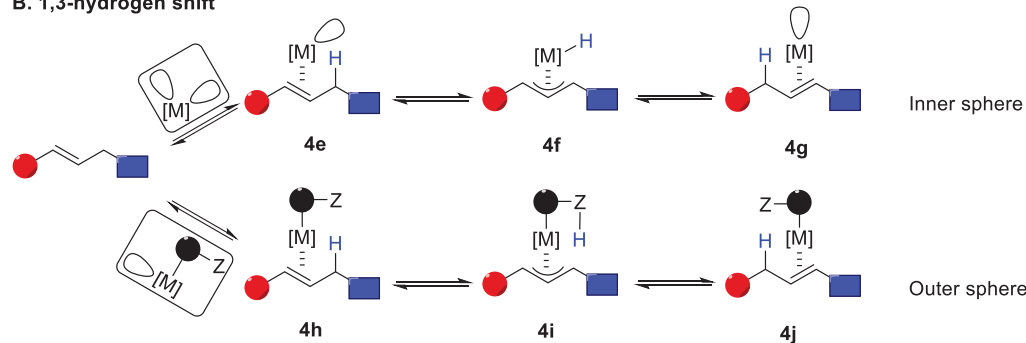
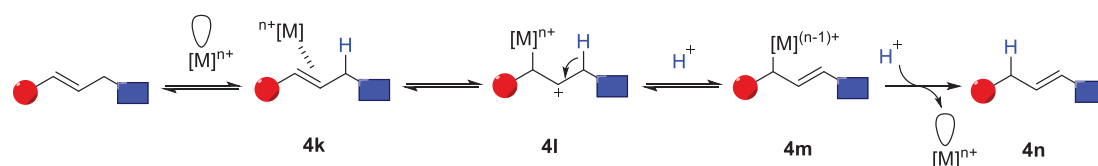
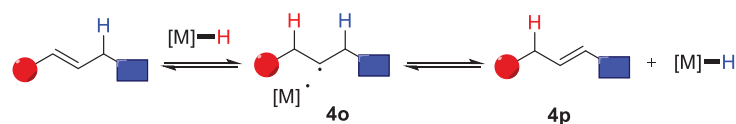
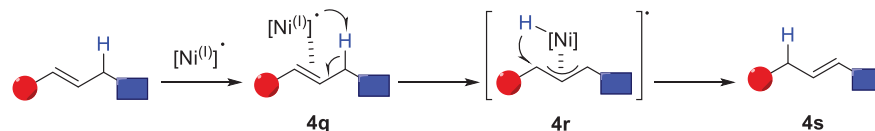
Finally, when substrate **3c** was employed, instead of the cyclization product, alkene migration over the alkyl chain has been observed yielding a mixture of two regioisomers, i.e. allylic isomer (1) and benzylic isomer (2) in a ratio of 3:1 (**Scheme 70-B**). The isomerization ratio was determined by integrating the signals of each isomer on GCMS as well as integrating the characteristic alkene signals of each isomer by ¹H-NMR (Isomer 1: δ 5.62 and 5.39 ppm, Isomer 2: δ 6.20 and 5.91 ppm). The highest yield was achieved using $\text{Ni(COD)}_2/\text{PCy}_3$ in combination with $\text{Al}(\text{O}^i\text{Bu})_3$ (80 % yield).

The alkene migration product was unexpected since it occurs without any source of hydride. The yields were excellent, and the reaction is highly selective toward *E*-isomers (*E/Z*=95%).

In addition, the alkene migration was not limited to one carbon, but chain walking all over the alkyl chain was observed. Generally in literature, alkene migration is achieved by the addition of an hydride source, or via hydrogen scrambling with poor control of the selectivity, along with being predominantly limited only for one carbon.¹³

Several mechanisms were reported for alkene migrations induced by transition metals (**Scheme 71**).^{14,15} The 1,2-alkyl hydride shift mechanism (**Scheme 71-A**) requires a metal-hydride complex with a vacant site. After alkene coordination to the metal hydride complex, hydrometalation takes place forming the alkyl metal species **4b**. Then β -hydride elimination takes place shifting the double bond and generating a new metal-hydride complex **4c**. Subsequent hydrometallations and β -hydride eliminations are repeated to generate the most thermodynamically stable alkene.

The isomerization could also proceed *via* 1,3-allyl hydride mechanism (**Scheme 71-B**) both by inner and outer sphere pathways. The inner sphere pathway requires a 14 e⁻ transition metal complex possessing two vacant sites, the first coordinates to the alkene and the second is responsible for allyl C-H activation that proceeds via O.A forming the η^3 -allyl metal hydride complex **4f**. Rotation over the allyl bond takes place, followed by reductive elimination forming the alkene-shifted species **4g**. The outer sphere mechanism is quite similar where the formation of η^3 -allyl complex **4i** is assisted by ligand deprotonation, followed by rotation and re-protonation to form the more stable species (**4j**).^{16,17}

A. 1,2-hydrogen shift**B. 1,3-hydrogen shift****C. Cationic pathway****D. Diradical pathway****E. Metalloradical pathway****Scheme 71:** Possible Mechanisms for transition metal catalyzed alkene migration.

The activation via cationic pathway (**Scheme 71-C**) requires a highly electrophilic metal complex possessing a vacant site or the use of silver salts like AgOTf.^{18,19} After alkene coordination, an alkyl metal carbonium intermediate **4l** is formed, followed by proton elimination generating the cationic allyl intermediate **4m**. The additional proton generated *in situ* replaces $[M]^{(n-1)+}$ and regenerates the initial catalyst.

The diradical pathway (**Scheme 71-D**) proceeds via hydrometallation of alkene forming the diradical intermediate **4o**,^{20,21} followed by $[M]^{\circ}$ abstraction of hydrogen and the formation of the thermodynamically more stable species **4p**.

The metallo-radical pathway (**Scheme 71-E**), as reported recently by the group of Schoenebeck, requires a metallo-radical Ni^I species that coordinates to the alkene,¹³ followed by allylic hydrogen abstraction forming the η^3 -allyl radical metal hydride intermediate **4r**. Then, rapid hydrogen relocation takes place affording the thermodynamically more stable alkene (**4s**).

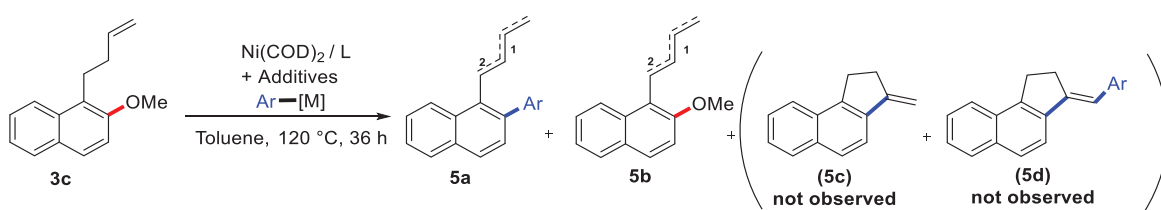
Among all the mechanisms, controlling the *E/Z* selectivity and chain walking are the main issues. The metallo-radical pathway showing excellent *E*-selectivity, along with the ability of relocating to more than one carbon, fits well our experimental observations. However, the metallo-radical pathway involves a Ni^I/Ni^{III} redox process, and in our case the reaction most probably proceeds through a Ni^0/Ni^{II} two electrons redox process. The 1,3-allyl mechanism is very close also, but in contrast to our observations, hydrogen scrambling usually takes place resulting in poor control over the *E/Z* selectivity. The observed reaction in our view may take place via successive β -hydride eliminations and hydrometallations all over the alkyl chain and the excellent selectivity might be induced by the ancillary ligand. These very preliminary results require further investigations to confirm the ability of $Ni(COD)_2/PCy_3$ and $Al(OtBu)_3$ catalytic system to promote isomerization of other alkenes.

3. Investigations on the difunctionalization of ether-tethered alkenes

We then moved to the next stage and investigated the possible difunctionalization of alkenyl substrate **3c** upon addition of an external organometallic coupling partner like $ArB(OR)_2$ or $ArMgX$ to the reaction medium (**Table 14**). Several conditions were evaluated, but neither di-

functionalization nor cyclization compounds **5c** or **5d** were observed with $(p\text{-PhCF}_3)\text{B(OR)}_2$ (Entries 1-4, **Table 14**). The major compound was the product of alkene migration (**5b**), whatever the catalytic system employed. Some trace amounts of arylated compound **5a** were observed with Ni^0/ICy system (Entry 1, **Table 14**). Alkene migration was quantitative with the $\text{Ni}^0/\text{ICy}/\text{Al(O}^t\text{Bu)}_3$ system (Entry 2, **Table 14**), the resulting product being isolated in 81% yield as a mixture of regioisomers, i.e. allylic isomer (1) and benzylic isomer (2). The separation of the isomers was not possible but a ratio of 3:1 in favour of isomer (1) was deduced from analysis of the ^1H NMR spectrum by integrating the diagnostic olefinic resonance signals at 5.62 ppm and 6.20 ppm, attributed to isomer (1) and (2), respectively. In addition, the isomerization ratio was also determined by integrating the signals of each isomer on GCMS.

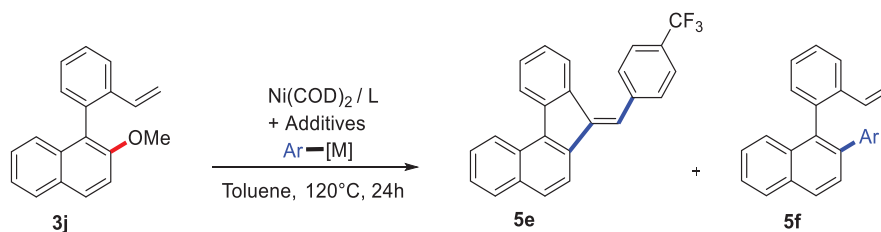
Table 14: Difunctionalization tests with substrate **3c**.^[a]



Entry	L	[M]	Additives	5a (%)	5b (%)
1	ICy	$(p\text{-PhCF}_3)\text{B(OR)}_2$	-	5	95
2	ICy	$(p\text{-PhCF}_3)\text{B(OR)}_2$	$\text{Al(O}^t\text{Bu)}_3$ (10 mol%)	0	100 (81%) ^b
3	PCy ₃	$(p\text{-PhCF}_3)\text{B(OR)}_2$	CsF (4.5 equiv)	0	87
4	PCy ₃	$(p\text{-PhCF}_3)\text{B(OR)}_2$	$\text{Al(O}^t\text{Bu)}_3$ (10 mol%)	0	95
5	PCy ₃	TolMgBr	$\text{Al(O}^t\text{Bu)}_3$ (10 mol%)	87	-
6	PCy ₃	EtMgBr ^c	MgI ₂ (2.4 equiv)	-	100

^[a] Reactions performed with Ni(COD)_2 (10 mol%), ICy (20 mol%), PCy₃ (40 mol%), $(p\text{-PhCF}_3)\text{B(OR)}_2$ (1.5 equiv), TolMgBr (1.5 equiv), EtMgBr (2.4 equiv). Yields of **5a** were determined by ^{19}F -NMR, Yields of **5b** were determined by GCMS. ^[c] At 60°C. ^[b] Isolated yield as a mixture of regioisomers (75% isomer (1), 25% isomer (2)). For RMgX, 14h instead of 24h.

Because of the poor C-OMe bond activation, we used stronger nucleophiles to enhance the reactivity and promote difunctionalization (Entries 5-6, **Table 14**). Even though the C-OMe bond arylation was greatly enhanced with TolMgBr (Entry 5, **Table 14**), bifunctionalization was not observed. The combination of RMgBr with MgI₂ was found successful for C-OMe bond alkylation of aryl ethers.²² In contrast, the similar system gave only alkene migration isomers with **3c** (Entry 6, **Table 14**). These results indicate that alkene migration occurs in all cases whatever the nature of the coupling partner. It is worth of note that alkene migration was improved in the presence of an external organometallic coupling partner. Since alkene migration is expected to be much easier and faster than C-OMe bond activation, the migration isomers would form before arylation takes place. However, as chain walking occurs over the alkyl chain, cyclization with the alkene isomers becomes more and more difficult for geometric problems (formation of highly strained 3 and 4 membered rings). This indicates that alkene migration might be inhibiting the formation of the difunctionalization product. One way to solving this problem is by using a more rigid substrate like **3j** for which alkene migration is not possible (**Table 15**). Nevertheless, this substrate was completely unreactive and remained intact even in the presence of an excess of Grignard reagents. Several phosphines, such as PCy₃, reported for Heck cyclization of benzylic ethers, Dcype, reported for alkylation of aryl ethers, and P(nBu)₃, reported for the activation of *ortho*-bulky aryl ethers,^{11,22,23} were all ineffective (entries 5-6, **Table 15**).

Table 15: Difunctionalization tests with substrate **3j**^[a]

Entry	L	[M]	Additives	5e, 5f (%)
1	ICY	(<i>p</i> -PhCF ₃)B(OR) ₂	-	0
2	ICy	(<i>p</i> -PhCF ₃)B(OR) ₂	Al(O ^t Bu) ₃ (10 mol%)	0
3	PCy ₃	(<i>p</i> -PhCF ₃)B(OR) ₂	CsF (4.5 equiv)	0
4	PCy ₃	(<i>p</i> -PhCF ₃)B(OR) ₂	Al(O ^t Bu) ₃ (10 mol%)	0
5	PCy ₃ /P(nBu) ₃	TolMgBr	Al(O ^t Bu) ₃ (10 mol%)	0
6	PCy ₃ /P(nBu) ₃ /Dcype	EtMgBr ^b	MgI ₂ (2.4 equiv)	0

^[a] Reactions performed with Ni(COD)₂ (10 mol%), ICy (20 mol%), PCy₃ (40 mol%), (*p*-PhCF₃)B(OR)₂ (1.5 equiv), TolMgBr (1.5 equiv), EtMgBr (2.4 equiv). ^b At 100 °C for 18 h. For RMgX, 18h instead of 24h.

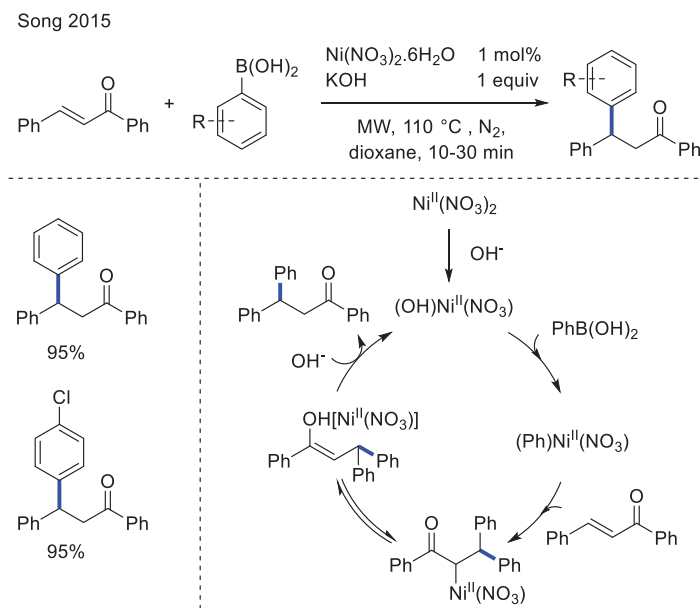
Substrate **3k** is less rigid and bulky than **3j**, without the possibility of alkene migration. In addition, it contains an *ortho*-carbonyl group for which C-OMe bond activation by ruthenium is also feasible (**Table 16**). Unfortunately, none of the Ni- or Ru-based catalytic systems tested afforded the desired difunctionalization product **5g**, and the C-OMe bond remained untouched in all cases (Entries 1-6, **Table 16**). However, a new interesting hydroarylation product **5h** was formed with two Ni systems (Entries 2 and 3, **Table 16**). The Ni/PCy₃/CsF system gave **5h** quantitatively which was determined by integrating the characteristic ¹⁹F NMR signal of **5h** at (-62.3 ppm) using PhCF₃ as an internal standard, **5h** was isolated in 88% yield (Entry 3, **Table 16**).

Table 16: Difunctionalization tests with substrate **3k**^[a]

Entry	Catalytic system	Additives	5g (%)	5h (%)
1	Ni(COD) ₂ /ICy	-	0	0
2	Ni(COD) ₂ /ICy	Al(O ⁱ Bu) ₃ (10 mol%)	0	48
3	Ni(COD) ₂ /PCy ₃	CsF (4.5 equiv)	0	100 (88%) ^b
4	Ni(COD) ₂ /PCy ₃	Al(O ⁱ Bu) ₃ (10 mol%)	0	0
5	Ni(COD) ₂ /PCy ₃	-	0	15
6	RuH ₂ (CO)(PPh ₃) ₃	-	0	0

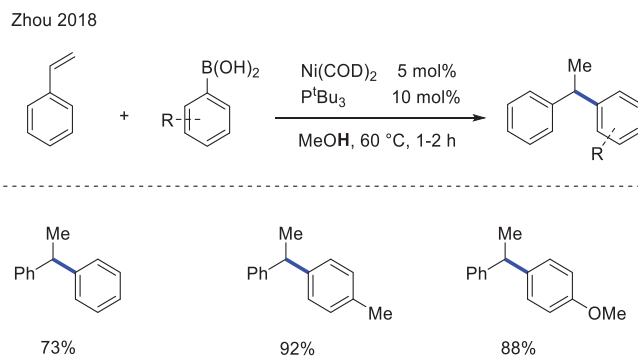
^[a] Reactions performed with Ni(COD)₂ (10 mol%), RuH₂(CO)(PPh₃)₃ (10 mol%), ICy (20 mol%), PCy₃ (40 mol%), (p-PhCF₃)B(OR)₂ (1.5 equiv). Yields were determined by ¹⁹F-NMR spectroscopy using PhCF₃ as internal standard, and GCMS. ^[b] Isolated yield.

The vast majority of hydroarylations were usually achieved using rhodium or other precious transition metals.²⁴ Recently, a few examples have been reported using nickel catalysis. For instance, an interesting nickel-catalyzed hydroarylation of chalcones was discovered by Song in 2015.²⁵ The reaction was superior to our system. It was carried out under ligand-free conditions using the air stable Ni(NO₃)₂·6H₂O complex at a lower catalytic loading (1 mol%) and at room temperature for 10 – 30 min. The scope was broad, enabling hydroarylation of a variety of substrates, and the mechanism was proposed to take place via transmetallation, followed by migratory insertion and reductive elimination (**Scheme 72**).



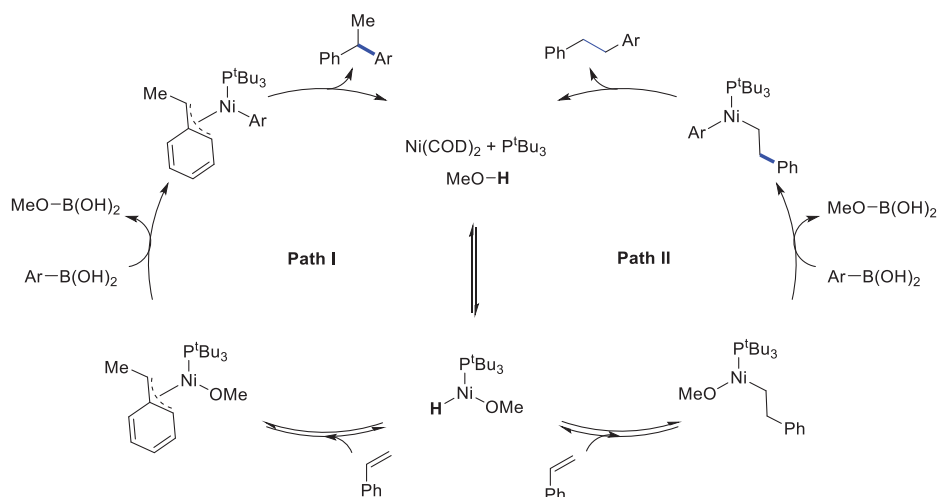
Scheme 72: Nickel-catalyzed hydroarylation of chalcones reported by Song.

Later on, a few examples of hydroarylations of styrenes with boronic acids were reported,²⁶ which are catalyzed by Ni(COD)₂/P^tBu₃ in the presence of methanol. Deuterium labeling experiments with CH₃OD clearly showed that methanol is the source of hydride. It is worth to mention that monophosphines proved to be the only effective ligands. The reaction offers broad substrate scope, good to excellent yields, and high selectivity toward the formation of the branched hydroarylated product (**Scheme 73**). Later on, an enantioselective hydroarylation strategy was developed using a similar catalytic system.²⁷ The enantioselectivity was induced by a chiral bis(oxazoline) ligand.



Scheme 73: Nickel-catalyzed hydroarylation of styrene as reported by Zhou. Branched/linear ratio is 99:1.

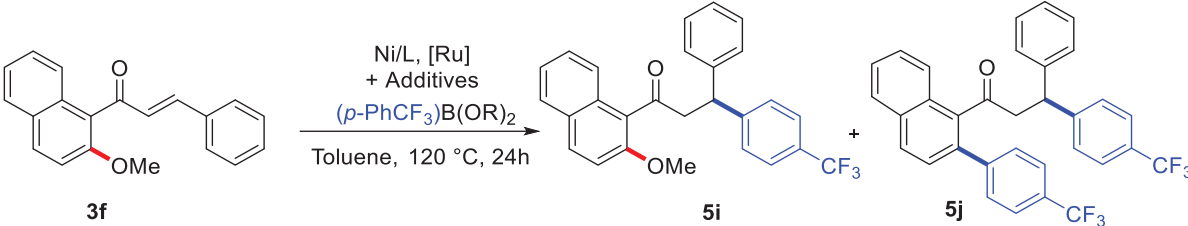
The mechanism of the reaction was proposed to take place via oxidative addition of the $\text{CH}_3\text{O-H}$ bond to Ni^0 forming the Ni^{II} hydride complex $(\text{P}^t\text{Bu}_3)\text{Ni}(\text{OMe})(\text{H})$ (**Scheme 74**). Hydro-metallation of styrene takes then place, generating the benzylic η^3 -nickel intermediate (Path I). This was followed by transmetallation with ArB(OH)_2 and reductive elimination, producing the branched hydroarylated product. The same steps follow with Path II, with the generation of an allyl linear complex that undergoes transmetallation and reductive elimination, forming the linear hydroarylated product. Since Path I involves the formation of a stabilized η^3 -allyl nickel intermediate, the branched product is expected to be the major product as shown experimentally.



Scheme 74: Mechanism for Nickel-catalyzed hydroarylation of styrene.

The use of π -extended aryl ethers is well known to enhance the reactivity of the electrophiles compared to anisoles that are much less reactive. For this reason, we expected substrate **3f** to be more reactive than **3k** (Table 17). Even though the hydroarylation product **5i** is the major product with the Ni/PCy₃/CsF system (Entries 2-3, Table 17), trace amounts of bis-arylated product **5j** resulting from combined C-OMe bond arylation and hydroarylation were also obtained. The use of 3 equiv of (*p*-PhCF₃)B(OR)₂ (Entry 3, Table 17) did not improve further the formation of **5j**. Interestingly, RuH₂(CO)(PPh₃)₃ complex gave **5j** predominantly and in good yield (Entry 4, Table 17).

Table 17: Testing difunctionalization with substrate **3f**.^[a]



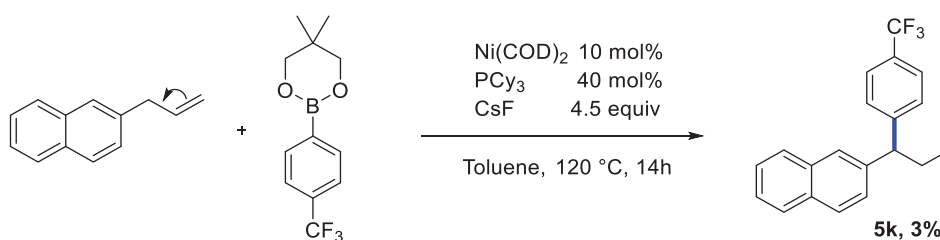
Entry	Catalytic system	Additives	5i (%)	5j (%)
1	Ni(COD) ₂ /ICy	-	0	0
2	Ni(COD) ₂ /PCy ₃	CsF (4.5 equiv)	87	3
3 ^b	Ni(COD) ₂ /PCy ₃	CsF (4.5 equiv)	90	4
4 ^b	RuH ₂ (CO)(PPh ₃) ₃	-	1	54

^[a] Reactions performed with Ni(COD)₂ (10 mol%), RuH₂(CO)(PPh₃)₃ (10 mol%), ICy (20 mol%), PCy₃ (40 mol%), (*p*-PhCF₃)B(OR)₂ (1.5 equiv). Yields was determined by ¹⁹F NMR spectroscopy using PhCF₃ as internal standard, and GCMS.^[b] with (*p*-PhCF₃)B(OR)₂ (3 equiv).

In summary, similarly to what was observed with alkene migration, both Ru and Ni catalysts are reacting with the alkene moiety via hydroarylation, while only Ru promotes the function-

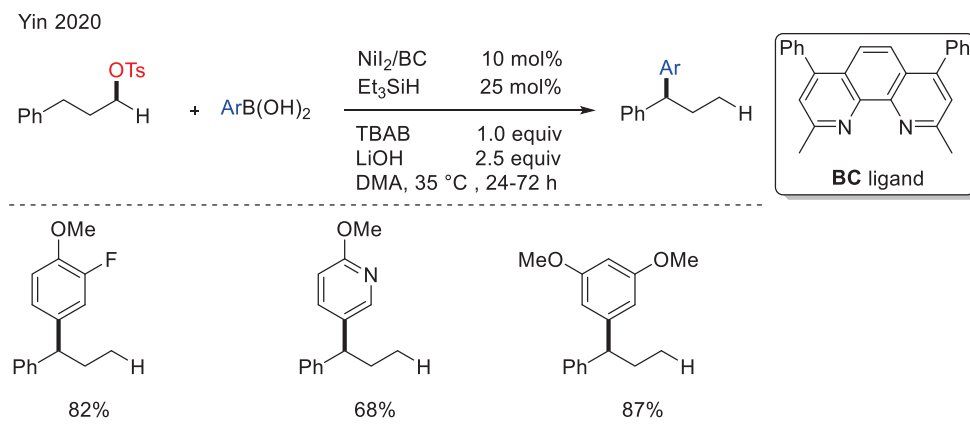
alization of the C-OMe bond via arylation cross-coupling (Entries 2-4). Nevertheless, the bifunctionalization of the alkene is not observed. This could be for kinetic reasons, alkene migration and hydroarylation taking place at a much faster rate than C-OMe bond activation.

We then tested alkene migration and hydroarylation in combination to each other under hydride-free conditions (**Scheme 75**). First, the terminal alkene moiety migrates to the benzylic position and then hydroarylation takes place in a remote functionalization pathway. We thus selected the Ni/PCy₃/CsF system, which was highly effective for both alkene migration and hydroarylation. Despite having full conversion of 2-allylnaphthalene to the migration products (95% *E*-isomer), only traces of remote functionalization product (**5k**) were observed. This is probably because a conjugated carbonyl group is critical for hydroarylation to take place.



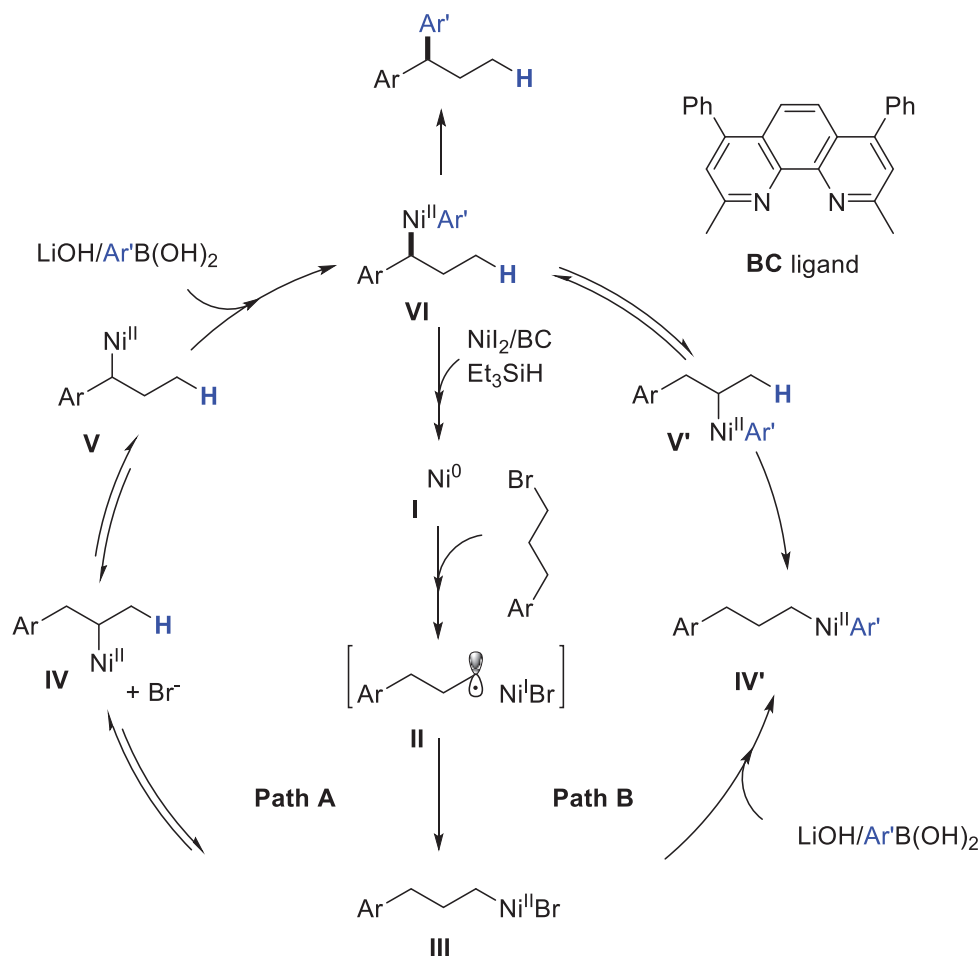
Scheme 75: Remote functionalization. Reactions performed with Ni(COD)₂ (10 mol%), PCy₃ (40 mol%), CsF (4.5 equiv), 2-allylnaphthalene (1 equiv), (*p*-PhCF₃)B(OR)₂ (1.5 equiv). Yields were determined by ¹⁹F NMR spectroscopy using PhCF₃ as internal standard, and GCMS.

Remote functionalization gained a lot of attention recently due to its ability of forming high value molecules.^{14,28} Recently, the group of Yin reported a Ni-catalyzed migratory Suzuki-Miyaura cross-coupling of alkyl tosylates and alkyl halides.²⁹ The reaction was carried out using a combination of NiI₂ and 2,9-dimethyl-4,7-diphenyl-1,10-phenanthroline (BC) ligand, in the presence of Et₃SiH (25 mol%), TBAB (1.0 equiv), and an excess of LiOH (2.5 equiv) that was crucial for the reaction to take place. Several phenanthroline ligands were found effective, with BC being the ligand of choice. Amide-based solvents, notably DMA, afforded the best results (**Scheme 76**).



Scheme 76: Ni-catalyzed Suzuki-Miyaura remote functionalization of alkyl tosylates as reported by Yin.

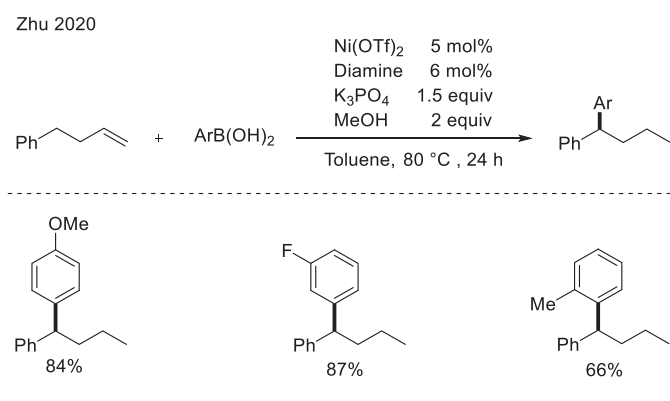
Deuterium labeling experiments starting from a benzylic-labeled substrate, gave D-incorporated products all over the alkyl chain, indicating that nickel chain-walking is a key step in the reaction. Kinetic studies showed a first order dependence on the boronic acid and the base, which suggests that transmetalation is the rate determining step. In addition, the rate was much faster with secondary than primary bromides which suggests a SET pathway for C-Br bond cleavage. Combining these results with the computational studies, it turned out that the mechanism takes place via a $\text{Ni}^0/\text{Ni}^{\text{II}}$ two-electron process involving a SET radical chain pathway (**Scheme 77**). The combination of NiI_2 , Et_3SiH and BC ligand form the Ni^0 species **I** by catalyst reduction and ligand exchange. This is followed by a Ni-assisted homolytic cleavage of C-Br bond by SET, forming the bromonickel^I intermediate and 3-phenylpropyl radical (**II**) that recombine with each other generating the phenylpropylnickel^{II} bromide species (**III**).



Scheme 77: Mechanism for Ni-catalyzed Suzuki-Miyaura remote functionalization of alkyl halides.

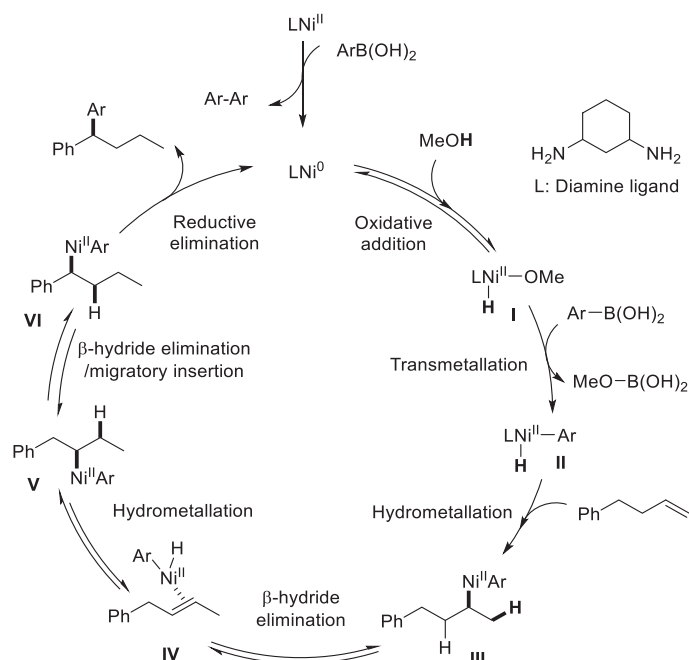
The phenylpropylbromonickel^{II} species **III** can then follow two different pathways that lead to benzylicNi^{II} species **VI**: either by Ni migration all over the alkyl chain by successive migratory insertions and hydrometallation to the benzylicNi^{II} species **V**, which then undergoes transmetalation with the boronic acid (path A); or by direct transmetalation to form species **IV'**, and subsequent migration of arylNi over the alkyl chain (path B). Finally, benzylicNi^{II} species **VI** undergoes reductive elimination that delivers the final product and regenerates the catalyst. Further kinetic and theoretical studies showed that the rate of transmetalation with benzylicNi^{II} is faster, indicating that path A is more reasonable.

A very recent paper has reported interesting experimental results that are very close to our own observations.³⁰ The combination of $\text{Ni}(\text{OTf})_2$ or $\text{Ni}(\text{COD})_2$ with cyclohexane-1,3-diamine ligand was shown to be highly effective for remote functionalization of alkenes with boronic acids and was shown to be highly effective for remote functionalization of alkenes with boronic acids via a synergetic chain walking/hydroarylation pathway. The key to the success of this method, compared to our system, was the use of an external hydride source (MeOH), as well as utilizing diamine ligands instead of phosphines, both being critical for the reaction to proceed (**Scheme 78**).



Scheme 78: Ni-catalyzed remote functionalization of alkenes as reported by Zhu.

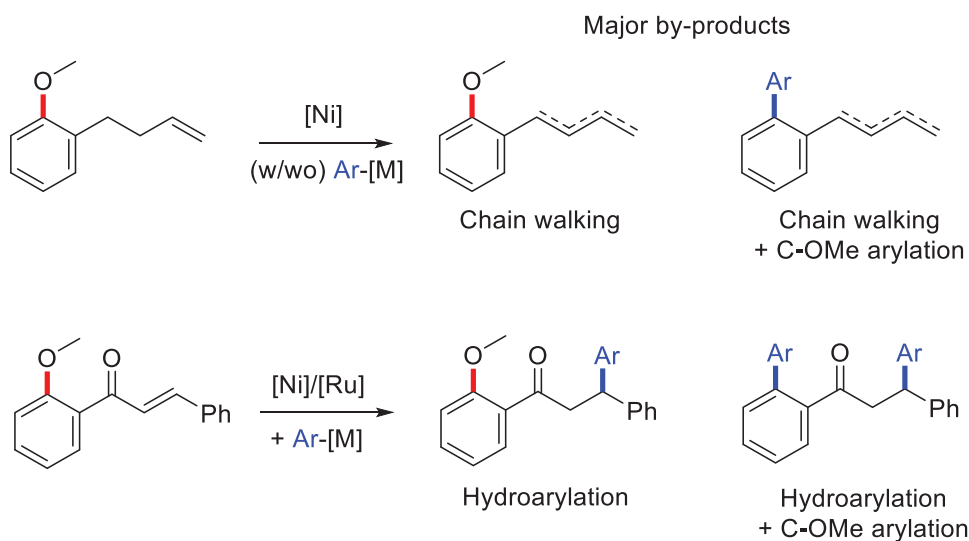
After the formation of LNi^0 from the pre-catalyst (**Scheme 79**), oxidative addition of methanol takes place, generating $(\text{L})\text{Ni}^{\text{II}}(\text{OMe})(\text{H})$ hydride complex (**I**), followed by transmetallation with $\text{ArB}(\text{OH})_2$ to form $(\text{L})\text{Ni}^{\text{II}}(\text{Ar})(\text{H})$ species **II**. Then coordination and hydrometallation of the alkene occurs to give an alkyl-nickel-aryl intermediate (**III**) that undergoes β -hydride elimination, generating $(\text{Ar})\text{Ni}^{\text{II}}(\text{H})$.alkene complex (**IV**) with a shifted double bond. Then successive hydrometallations and β -hydride eliminations take place to generate the more thermodynamically stable benzylic complex **VI** that undergoes reductive elimination, releasing the remote functionalized product and regenerating the initial catalyst.



Scheme 79: Mechanism for Ni-catalyzed remote functionalization of alkenes.

IV. Summary

In conclusion, we synthesized and tested herein five different substrates for Heck cyclization and bi-functionalization with a variety of well-designed catalytic systems based on Nickel or Ruthenium. Cyclization was not observed; besides bi-functionalization, two interesting by-products were encountered (alkene migration and hydroarylation) depending on the substrate used (**Scheme 80**). It appears that alkene migration takes place, with excellent *E/Z* selectivity, whenever an alkyl chain group having a terminal alkene is presented. In the other hand, hydroarylation was only observed with chalcone derivatives having a conjugated carbonyl group. However, both of them inhibit cyclization from taking place, probably for geometric strain and kinetic issues. Trying to combine both of them together in a remote functionalization fashion was unsuccessful since a conjugated carbonyl group was essential for hydroarylation.



Scheme 80: The Major by-products formed in the investigated experimental conditions.

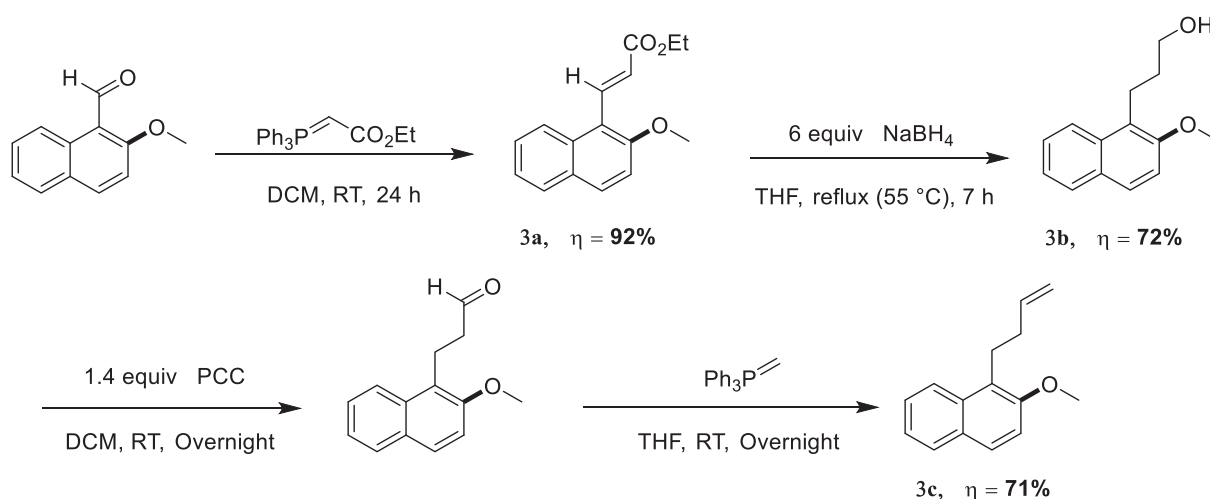
From a mechanistic point of view, we assume that alkene migration is taking place via successive β -hydride eliminations and hydrometallations all over the alkyl chain achieved via a $\text{Ni}^0/\text{Ni}^{\text{II}}$ pathway. In addition, the excellent *E*-selectivity could be induced by the ancillary ligand. However, further mechanistic studies like radical clock experiments and EPR analysis should be carried out in order to confirm a non-radical process. Besides, deuterium labeling experiments could provide a deeper insight about the mechanism and the hydride source.

With respect to hydroarylation, the presence of a conjugated carbonyl group seems to be essential because of its ability to coordinate to Nickel and stabilize the catalytic intermediates. However, it was shown in literature that addition of a hydride source could promote hydroarylation in the absence of a conjugated carbonyl group. This strategy is currently under investigations in our laboratory.²⁶

V. Experimental part

1. Synthesis of model substrates

a. Synthesis of 1-(but-3-en-1-yl)-2-methoxynaphthalene (3c)

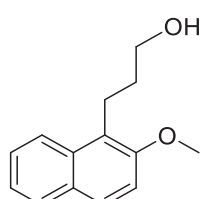


Synthesis of ethyl (E)-3-(2-methoxynaphthalen-1-yl)acrylate (3a). 2-Methoxy-1-naphthaldehyde (1.0 equiv, 10.0 mmol, 1.86 g) and ethyl 2-(triphenyl- λ^5 -phosphaneylidene)acetate (1.4 equiv, 14.0 mmol, 4.87 g) were dissolved in DCM (50 ml) and the resulting solution was stirred for 1 day at RT. The crude was concentrated and purified by flash chromatography (SiO_2 , ethyl acetate in cyclohexane, gradient 0 to 70%), affording the product as a honey oil (2.36 g, 92% yield). NMR data are identical with those previously reported.³¹

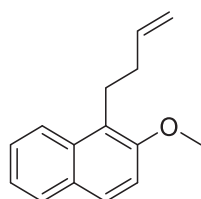
¹H NMR (300 MHz, Chloroform-*d*) δ 8.36 (1H, d, J = 16.2 Hz, C_{10}H_6), 8.20 (1H, d, J = 8.7 Hz, C_{10}H_6), 7.86 (1H, d, J = 9.1 Hz, C_{10}H_6), 7.79 (1H, d, J = 8.2 Hz, C_{10}H_6), 7.49 – 7.57 (1H, m, C_{10}H_6), 7.35 – 7.42 (1H, m, C_{10}H_6), 7.30 (1H, d, J = 9.1 Hz, $\text{CH}=\text{CH}$), 6.76 (1H, d, J = 16.2 Hz, $\text{CH}=\text{CH}$), 4.32 (2H, q, J = 7.2 Hz, OCH_2CH_3), 4.01 (3H, s, OCH_3), 1.38 (3H, t, J = 7.2 Hz, OCH_2CH_3). **MS** (EI) m/z : $[\text{M}]^+$ 256.

Synthesis of 3-(2-methoxynaphthalen-1-yl)propan-1-ol (3b). A suspension of ethyl (E)-3-(2-methoxynaphthalen-1-yl)acrylate (1.0 equiv, 8.0 mmol, 2.05 g) and NaBH_4 (6.0 equiv, 48.0

mmol, 1.81 g) in THF (32 ml) was prepared in a two-necked round bottom flask equipped with a condenser. The solution was heated at 55 °C and methanol (6.2 ml) was added dropwise over 30 min. After complete addition of methanol, the heating was kept further for 6 h. Then the reaction was quenched by ice and aqueous NaOH solution (32 ml, 5 M) followed by extraction with DCM (3 x 16 ml). The combined organic layers were washed with brine and concentrated under reduced pressure. The final product was isolated by flash chromatography (SiO₂, ethyl acetate in cyclohexane, gradient 0 to 70%), affording the product as a colorless oil (1.24 g, 72% yield). NMR data are identical with those previously reported.³²

 **¹H NMR** (300 MHz, Chloroform-*d*) δ 7.98 (1H, dt, *J* = 8.6, 1.0 Hz, C₁₀H₆), 7.80 (1H, d, *J* = 8.2 Hz, C₁₀H₆), 7.75 (1H, d, *J* = 9.0 Hz, C₁₀H₆), 7.49 (1H, ddd, *J* = 8.4, 6.8, 1.4 Hz, C₁₀H₆), 7.36 (1H, ddd, *J* = 8.1, 6.8, 1.2 Hz, C₁₀H₆), 7.29 (1H, d, *J* = 9.0 Hz, C₁₀H₆), 3.98 (3H, s, OCH₃), 3.55 (2H, q, *J* = 6.1 Hz, CH₂-OH), 3.23 (2H, t, *J* = 7.1 Hz, CH₂-CH₂-CH₂-OH), 2.31 (1H, bs, CH₂-OH), 1.94 (2H, tt, *J* = 7.0, 5.9 Hz, CH₂-CH₂-OH). **¹³C NMR** (75 MHz, Chloroform-*d*) δ 154.3 (s, C_{Ar}), 132.9 (s, C_{Ar}), 129.5 (s, C_{Ar}), 128.9 (s, C_{Ar}), 128.6 (s, C_{Ar}), 126.4 (s, C_{Ar}), 123.5 (s, C_{Ar}), 123.2 (s, C_{Ar}), 122.5 (s, C_{Ar}), 113.2 (s, C_{Ar}), 61.5 (s, CH₂-OH), 56.8 (s, OCH₃), 32.2 (s, CH₂-CH₂-CH₂-OH), 20.4 (s, CH₂-CH₂-OH). **MS** (EI) *m/z*: [M]⁺216.

Synthesis of 1-(but-3-en-1-yl)-2-methoxynaphthalene (3c). A solution of 3-(2-methoxynaphthalen-1-yl)propan-1-ol (1.0 equiv, 5.26 mmol, 1.14 g) in DCM (40 ml) was prepared, followed by the addition of pyridinium chlorochromate (1.4 equiv, 7.36 mmol, 1.55 g). The mixture was stirred for 1 h at RT and Et₂O (200 ml) was added. The filtrate was collected via simple decantation or filtration. Volatiles were removed under reduced pressure and the crude product was

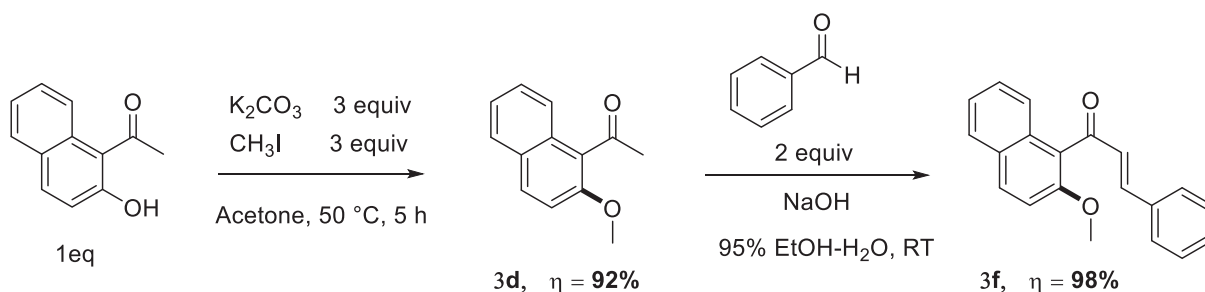


dissolved in THF (16 ml) and then used directly for the next step. In another round bottom flask, the ylide complex was prepared by mixing methyl-triphenylphosphonium bromide (1.0 equiv, 5.26 mmol, 1.87 g) with ⁿBuLi (1.0

equiv, 5.26 mmol, 3.41 ml) in anhydrous THF (16 ml). The reaction was stirred for an hour at RT, followed by a dropwise addition of the aldehyde solution, and the reaction was kept for 6 h at RT. The crude product was isolated by flash chromatography (SiO₂, ethyl acetate in cyclohexane, gradient 0 to 70%), affording a colorless oil (0.8 g, 71% yield).

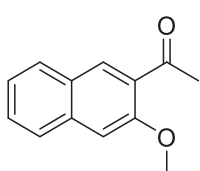
¹H NMR (300 MHz, Chloroform-*d*) δ 7.96 (1H, d, J = 9.0 Hz, C₁₀H₆), 7.80 (1H, d, J = 8.1 Hz, C₁₀H₆), 7.74 (1H, d, J = 9.0 Hz, C₁₀H₆), 7.49 (1H, apparent dt, J = 7.7, 1.7 Hz, C₁₀H₆), 7.34 (1H, apparent dt, J = 7.4, 1.0 Hz, C₁₀H₆), 7.28 (1H, d, J = 9.0 Hz, C₁₀H₆), 5.98 (1H, ddt, J = 6.6, 3.6, 2.8 Hz, CH=CH₂), 5.10 (1H, ddt, J = 17.1, 2.0 Hz, CH=CH₂), 5.00 (1H, ddt, J = 10.1, 2.1, 1.2 Hz, CH=CH₂), 3.96 (3H, s, OCH₃), 3.18 (2H, t, J = 8.1 Hz, CH₂-CH₂-CH), 2.33 – 2.44 (2H, m, CH₂-CH₂-CH). **¹³C NMR** (75 MHz, Chloroform-*d*) δ 154.3 (s, C_{Ar}), 138.9 (s, C_{Ar}), 132.9 (s, C_{Ar}), 129.2 (s, C_{Ar}), 128.5 (s, C_{Ar}), 127.6 (s, C_{Ar}), 126.2 (s, C_{Ar}), 123.3 (s, C_{Ar}), 123.2 (s, C_{Ar}), 123.1 (s, C_{Ar}), 114.4 (s, CH=CH₂), 113.4 (s, CH=CH₂), 56.6 (s, OCH₃), 34.1 (s, CH₂-CH₂-CH), 24.5 (s, CH₂-CH₂-CH). **MS** (EI) m/z : [M]⁺212.

b. Synthesis of (*E*)-1-(2-methoxynaphthalen-1-yl)-3-phenylprop-2-en-1-one (3f)



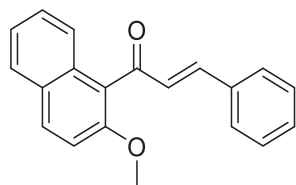
Synthesis of 1-(2-methoxynaphthalen-1-yl)ethan-1-one (3d). A mixture of 1-(2-hydroxynaphthalen-1-yl)ethan-1-one (1.0 equiv, 10.74 mmol, 2.00 g), CH₃I (3.0 equiv, 32.2 mmol, 2.0 ml) and K₂CO₃ (3.0 equiv, 32.2 mmol, 4.45 g) in acetone (30 ml) was prepared and heated for 6 h at 50 °C. The mixture was filtrated through a pad of silica and rinsed with cold acetone and the

filtrate was concentrated under vacuum followed by extraction with DCM (3 x 30 ml). The combined organic layers were concentrated and the crude product was isolated by flash chromatography (SiO₂, ethyl acetate in cyclohexane, gradient 0 to 70%), affording the product as shiny yellow crystals (1.95 g, 92% yield). NMR data are identical with those previously reported.³³



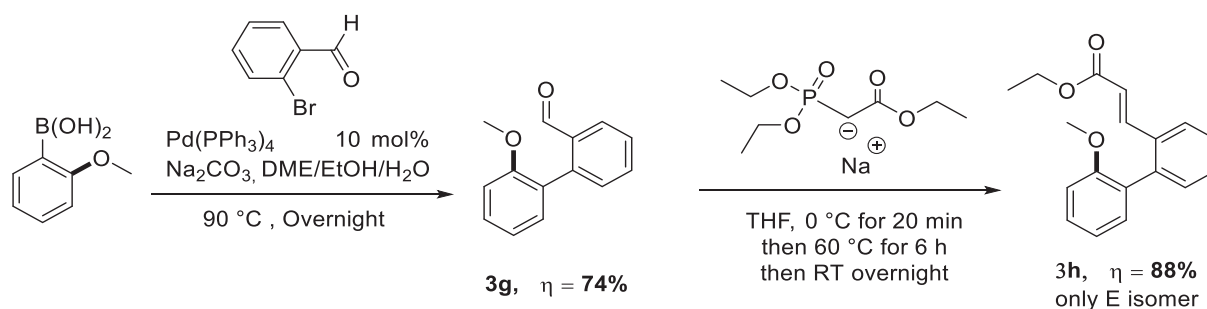
¹H NMR (300 MHz, Chloroform-*d*) δ 7.89 (1H, d, J = 9.1 Hz, C₁₀H₆), 7.78 (2H, t, J = 9.3 Hz, C₁₀H₆), 7.44 – 7.51 (1H, m, C₁₀H₆), 7.33 – 7.40 (1H, m, C₁₀H₆), 7.28 (1H, d, J = 9.1 Hz, C₁₀H₆), 3.98 (3H, s, OCH₃), 2.65 (3H, s, CH₃). **¹³C NMR** (75 MHz, Chloroform-*d*) δ 205.2 (s, C=O), 153.9 (s, C_{Ar}), 131.5 (s, C_{Ar}), 130.3 (s, C_{Ar}), 128.9 (s, C_{Ar}), 128.2 (s, C_{Ar}), 127.7 (s, C_{Ar}), 125.1 (s, C_{Ar}), 124.1 (s, C_{Ar}), 123.6 (s, C_{Ar}), 112.8 (s, C_{Ar}), 56.4 (s, OCH₃), 32.7 (s, CH₃). **MS** (EI) m/z : [M]⁺200.

Synthesis of (E)-1-(3-methoxynaphthalen-2-yl)-3-phenylprop-2-en-1-one (3f). A mixture of 1-(2-methoxynaphthalen-1-yl)ethan-1-one (1.0 equiv, 10.00 mmol, 2.0 g) and benzaldehyde (1.0 equiv, 10.00 mmol, 1.06 g) in ethanol (33 ml) was added to a solution of NaOH (1.16 equiv, 11.60 mmol, 0.46 g) in EtOH-water (16/16 ml). The reaction was stirred for 18 h at room temperature. Volatiles were removed under reduced pressure and the crude product was isolated by flash chromatography (SiO₂, ethyl acetate in cyclohexane, gradient 0 to 70%), affording the product as a white powder (2.8 g, 98% yield). NMR data are identical with those previously reported.³⁴

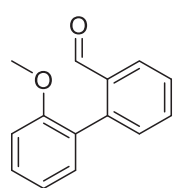


¹H NMR (300 MHz, Chloroform-*d*) δ 7.97 (1H, d, J = 9.0 Hz, Ar-H), 7.86 (1H, d, J = 8.0 Hz, Ar-H), 7.72 (1H, d, J = 8.3 Hz, CH=CH), 7.28 – 7.57 (9H, m, Ar-H), 7.16 (1H, d, J = 16.2 Hz, CH=CH), 3.96 (3H, s, OCH₃). **¹³C NMR** (75 MHz, Chloroform-*d*) δ 197.5 (s, C=O), 154.1 (s, C_{Ar}), 145.8 (s, C_{Ar}), 140.8 (s, C_{Ar}), 134.7 (s, C_{Ar}), 134.6 (s, C_{Ar}), 131.8 (s, C_{Ar}), 131.5 (s, C_{Ar}), 131.3 (s, C_{Ar}), 130.6 (s, C_{Ar}), 128.9 (s, C_{Ar}), 128.8 (s, C_{Ar}), 128.5 (s, C_{Ar}), 128.1 (s, C_{Ar}), 127.5 (s, C_{Ar}), 124.1 (s, CH-CH), 113.1 (s, CH-CH), 56.7 (s, OCH₃). **MS** (EI) m/z : [M]⁺288.

c. Synthesis of ethyl (E)-3-(2'-methoxy-[1,1'-biphenyl]-2-yl)acrylate (3h)

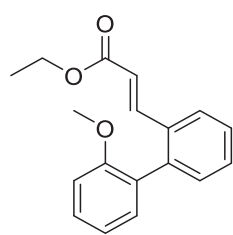


Synthesis of 2'-methoxy-[1,1'-biphenyl]-2-carbaldehyde (3g). Compound **3g** was synthesized according to a modified published procedure.³⁵ In an oven dried Schlenk flask under Argon atmosphere, a solution of (2-methoxyphenyl)boronic acid (1.23 equiv, 18.48 mmol, 2.73 g), 2-bromobenzaldehyde (1.0 equiv, 15.0 mmol, 2.77 g) and Pd(PPh₃)₄ (0.03 equiv, 0.45 mmol, 0.52 g) was prepared in 60 ml of degassed DME. A solution of Na₂CO₃ (2.0 equiv, 30.0 mmol, 3.17 g) was prepared in degassed EtOH/water 14 ml each and added to the first one. The mixture was heated overnight at 90 °C and the reaction was quenched by the addition of water 40 ml and extracted into EtOAc (3 x 40 ml). The combined organic layers was dried by MgSO₄ and concentrated under reduced pressure then purified by flash chromatography (SiO₂, ethyl acetate in cyclohexane, gradient 0 to 70%), affording the product as a white powder (2.35 g, 74% yield) NMR data are identical with those previously reported.



¹H NMR (300 MHz, Chloroform-d) δ 9.79 (1H, d, $J = 0.9$ Hz, $\underline{\text{H-C=O}}$), 8.00 (1H, dd, $J = 7.7, 1.5$ Hz, $\text{C}_{12}\underline{\text{H}}_8$), 7.65 (1H, td, $J = 7.5, 1.5$ Hz, $\text{C}_{12}\underline{\text{H}}_8$), 7.48 (1H, t, $J = 7.4, 1.1$ Hz, $\text{C}_{12}\underline{\text{H}}_8$), 7.42 (1H, dd, $J = 7.5, 1.6$ Hz, $\text{C}_{12}\underline{\text{H}}_8$), 7.36 (1H, dd, $J = 7.7, 1.4$ Hz, $\text{C}_{12}\underline{\text{H}}_8$), 7.29 (1H, dd, $J = 7.5, 1.8$ Hz, $\text{C}_{12}\underline{\text{H}}_8$), 7.09 (1H, td, $J = 7.5, 1.1$ Hz, $\text{C}_{12}\underline{\text{H}}_8$), 6.98 (1H, dd, $J = 8.3, 1.1$ Hz, $\text{C}_{12}\underline{\text{H}}_8$), 3.74 (3H, s, OCH_3). **¹³C NMR** (75 MHz, Chloroform-d) δ 192.7 (s, H-C=O), 141.8 (s, $\underline{\text{C}}_{\text{Ar}}$), 134.0 (s, $\underline{\text{C}}_{\text{Ar}}$), 133.7 (s, $\underline{\text{C}}_{\text{Ar}}$), 131.4 (s, $\underline{\text{C}}_{\text{Ar}}$), 131.2 (s, $\underline{\text{C}}_{\text{Ar}}$), 130.0 (s, $\underline{\text{C}}_{\text{Ar}}$), 127.7 (s, $\underline{\text{C}}_{\text{Ar}}$), 126.8 (s, $\underline{\text{C}}_{\text{Ar}}$), 126.6 (s, $\underline{\text{C}}_{\text{Ar}}$), 121.0 (s, $\underline{\text{C}}_{\text{Ar}}$), 110.6 (s, $\underline{\text{C}}_{\text{Ar}}$), 55.4 (s, $\underline{\text{CH}}_3$). **MS** (EI) m/z : $[\text{M}]^+ 212$.

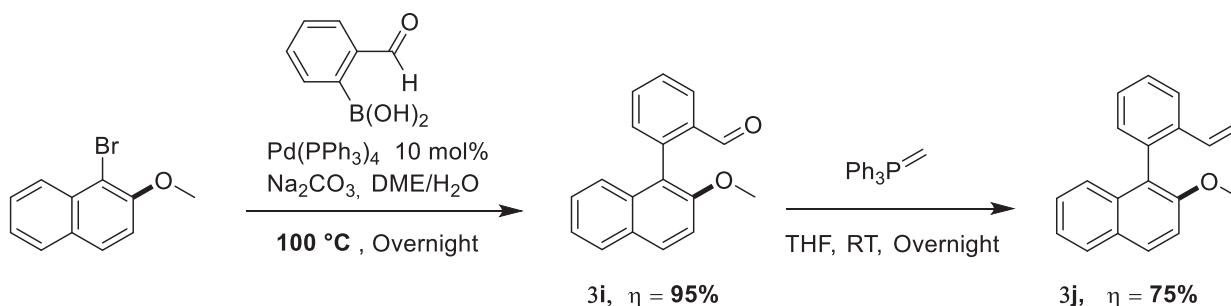
Synthesis of ethyl (*E*)-3-(2'-methoxy-[1,1'-biphenyl]-2-yl)acrylate (3h). In an oven dried Schlenk flask covered with an ice bath a suspension of NaH (1.2 equiv, 0.36 mmol, 14.64 mg) in dry THF (0.2 ml) was prepared. A solution of the phosphonoacetate (1.2 equiv, 0.36 mmol, 72 μ l) in THF (0.4 ml) was prepared and added dropwisely to the sodium hydride solution. The aldehyde (1.0 equiv, 0.3 mmol, 63.67 mg) was dissolved in THF (0.4 ml) and added dropwise to the ylide solution and the mixture was stirred for 30 min at 0 °C. Then, heated for 6 h at 60 °C and left overnight at RT. The reaction progress was monitored by TLC. After full conversion of the aldehyde the volatiles was removed under reduced pressure and the product was purified by flash chromatography (SiO₂, ethyl acetate in cyclohexane, gradient 0 to 70%), affording the product as a yellow oil (74.5 mg, 88% yield). NMR data are identical with those previously reported.³⁶



¹H NMR (300 MHz, Chloroform-*d*) δ 7.83 (1H, d, J = 7.5 Hz, C₁₂H₈), 7.65 (1H, d, J = 16.0 Hz, C₁₂H₈), 7.40 – 7.58 (4H, m, C₁₂H₈), 7.27 (1H, t, J = 7.4 Hz, C₁₂H₈), 7.16 (1H, t, J = 7.3 Hz, C₁₂H₈), 7.10 (1H, d, J = 8.3 Hz, CH=CH-C₁₂H₈), 6.48 (1H, d, J = 16.0 Hz, CH=CH-C₁₂H₈), 4.28 (2H, q, J = 7.3 Hz, OCH₂CH₃), 3.85 (3H, s, OCH₃), 1.38 (3H, t, J = 7.3 Hz, OCH₂CH₃). **MS** (EI)

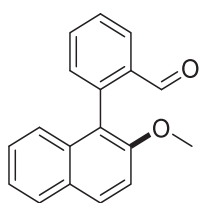
m/z : [M]⁺282.

d. Synthesis of 2-methoxy-1-(2-vinylphenyl)naphthalene (3j)



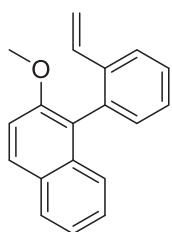
Synthesis of 2-(2-methoxynaphthalen-1-yl)benzaldehyde (3i). In an oven dried Schlenk flask under argon atmosphere a solution of (2-formylphenyl)boronic acid (1.5 equiv, 4.0 mmol,

0.60 g), 1-bromo-2-methoxynaphthalene (1.0 equiv, 2.66 mmol, 0.63 g) and $\text{Pd}(\text{PPh}_3)_4$ (0.1 equiv, 0.26 mmol, 0.3 g) was prepared in 20 ml of degassed DME. A solution of Na_2CO_3 (4.0 equiv, 10.7 mmol, 1.13 g) was prepared in degassed water (5.3 ml) and added to the first one. The mixture was heated overnight at 100 °C and the reaction was quenched by the addition of water 20 ml and extracted into EtOAc (3 x 20 ml). The combined organic layers were dried by MgSO_4 and concentrated under reduced pressure then purified by flash chromatography (SiO_2 , ethyl acetate in cyclohexane, gradient 0 to 70%), affording the product as yellow oil which solidify later under vacuum (0.66 g, 95% yield). NMR data are identical with those previously reported.³⁷



¹H NMR (300 MHz, Chloroform-*d*) δ 9.54 (1H, s, H-C=O), 8.03 (1H, dd, $J = 7.7, 1.5$ Hz, Ar- H), 7.86 (1H, d, $J = 9.1$ Hz, Ar- H), 7.76 (1H, dd, $J = 6.0, 3.3$ Hz, Ar- H), 7.62 (1H, td, $J = 7.5, 1.5$ Hz, Ar- H), 7.47 (1H, t, $J = 7.5$ Hz, Ar- H), 7.17 – 7.32 (5H, m, Ar- H), 3.72 (3H, s, OCH_3). **MS** (EI) m/z : $[\text{M}]^+ 262$.

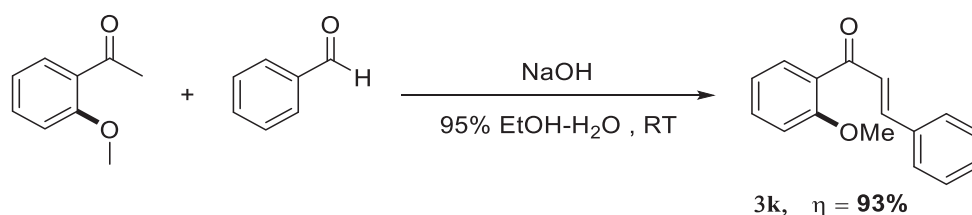
Synthesis of 2-methoxy-1-(2-vinylphenyl)naphthalene (3j). In a round bottom flask, the Ylide complex was prepared by mixing methyl-triphenylphosphonium bromide (1.0 equiv, 4.00 mmol, 1.43 g) with $n\text{BuLi}$ (1.0 equiv, 4.00 mmol, 2.6 ml) in anhydrous THF (12.5 ml). The reaction was stirred for an hour at RT, followed by a drop wise addition of the aldehyde solution (1.0 equiv, 4.00 mmol, 1.05 g) in THF (12.5 ml) and the reaction was kept for 6 h at RT. The crude product was isolated by flash chromatography (SiO_2 , ethyl acetate in cyclohexane, gradient 0 to 70%), affording the product as yellow oil which latter crystalize from pentane at low temperatures giving a white powder (0.77 g, 75% yield).



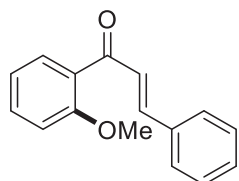
¹H NMR (300 MHz, Chloroform-*d*) δ 7.94 (1H, d, $J = 9.0$ Hz, Ar- H), 7.73 – 7.91 (2H, m, Ar- H), 7.22 – 7.50 (7H, m, Ar- H), 6.33 (1H, dd, $J = 17.6, 11.0$ Hz, CH-CH_2), 5.69 (1H, dd, $J = 17.6, 1.3$ Hz, CH-CH_2), 5.01 (1H, dd, $J = 11.0, 1.3$ Hz, CH-CH_2), 3.85 (3H, s, OCH_3). **¹³C NMR** (75 MHz, Chloroform-*d*) δ 154.1 (s, C_{Ar}),

137.2 (s, $\underline{\text{C}}_{\text{Ar}}$), 135.4 (s, $\underline{\text{C}}_{\text{Ar}}$), 135.1 (s, $\underline{\text{C}}_{\text{Ar}}$), 133.7 (s, $\underline{\text{C}}_{\text{Ar}}$), 131.4 (s, $\underline{\text{C}}_{\text{Ar}}$), 129.3 (s, $\underline{\text{C}}_{\text{Ar}}$), 128.9 (s, $\underline{\text{C}}_{\text{Ar}}$), 127.8 (s, $\underline{\text{C}}_{\text{Ar}}$), 127.7 (s, $\underline{\text{C}}_{\text{Ar}}$), 127.6 (s, $\underline{\text{C}}_{\text{Ar}}$), 126.4 (s, $\underline{\text{C}}_{\text{Ar}}$), 125.3 (s, $\underline{\text{C}}_{\text{Ar}}$), 124.7 (s, $\underline{\text{C}}_{\text{Ar}}$), 123.6 (s, $\underline{\text{C}}_{\text{Ar}}$), 123.6 (s, $\underline{\text{C}}_{\text{Ar}}$), 114.1 (s, CH-CH₂), 113.7 (s, CH-CH₂), 56.8 (s, OCH₃). **MS** (EI) m/z : [M]⁺260.

e. Synthesis of (E)-1-(2-methoxyphenyl)-3-phenylprop-2-en-1-one (3k)



A mixture of 1-(2-methoxyphenyl)ethan-1-one (1.0 equiv, 30.00 mmol, 4.5 g) and benzaldehyde (1.0 equiv, 30.00 mmol, 3.6 g) in ethanol (100 ml) was added to a solution of NaOH (1.16 equiv, 35.0 mmol, 1.4 g) in EtOH-water (50/50 ml). The reaction was stirred for 18 h at room temperature. Volatiles were removed under reduced pressure and the crude product was isolated by flash chromatography (SiO₂, ethyl acetate in cyclohexane, gradient 0 to 70%), affording the product as a white powder (6.64 g, 93% yield). NMR data are identical with those previously reported.³⁸


¹H NMR (300 MHz, Chloroform-*d*) δ 7.45 – 7.60 (4H, m, C₆H₄), 7.24 – 7.45 (5H, m, C₆H₅), 6.88 – 7.02 (2H, m, CH=CH), 3.82 (3H, s, OCH₃). **¹³C NMR** (75 MHz, Chloroform-*d*) δ 193.0 (s, C=O), 158.1 (s, $\underline{\text{C}}_{\text{Ar}}$), 143.3 (s, $\underline{\text{C}}_{\text{Ar}}$), 135.1 (s, $\underline{\text{C}}_{\text{Ar}}$), 132.9 (s, $\underline{\text{C}}_{\text{Ar}}$), 130.4 (s, $\underline{\text{C}}_{\text{Ar}}$), 130.3 (s, $\underline{\text{C}}_{\text{Ar}}$), 129.3 (s, $\underline{\text{C}}_{\text{Ar}}$), 128.9 (s, $\underline{\text{C}}_{\text{Ar}}$), 128.4 (s, $\underline{\text{C}}_{\text{Ar}}$), 127.1 (s, $\underline{\text{C}}_{\text{Ar}}$), 120.8 (s, CH=CH), 111.6 (s, CH=CH), 55.8 (s, OCH₃). **MS** (EI) m/z : [M]⁺238.

2. General catalytic procedures

General procedure for intramolecular cyclization: In a glovebox, a 5 mL microwave reaction vial equipped with a magnetic stir bar was charged with Ni(COD)₂ (10 mol%, 0.03 mmol, 8.3 mg), the ligand [Bis-NHC's (10 mol%, 0.03 mmol) or mono-NHC's and diphosphines (20 mol%, 0.06 mmol) or mono-phosphines (40 mol%, 0.12 mmol)] in toluene (0.5 ml). After stirring the solution for 5 minutes, the selected substrate (1.0 equiv, 0.3 mmol) was sequentially added, w or w/o the addition of the nucleophilic coupling partner generally (1.5 equiv, 0.5 mmol) and an additional base or additive like CsF (2.0 equiv, 0.6 mmol) and MgI₂ (2.4 equiv, 0.72 mmol). The tube was sealed, removed from the glovebox and heated at 120 °C (preheated oil bath) for 3-36 h. The reaction mixture was then cooled to room temperature, filtered over Celite®, and all volatiles were removed under reduced pressure. The reaction progress was followed by ¹⁹F-NMR using PhCF₃ as internal standard (for products bearing fluorine atoms) and GCMS. The products were isolated when necessary by flash chromatography on silica gel using appropriate mixtures of ethyl acetate and cyclohexane.

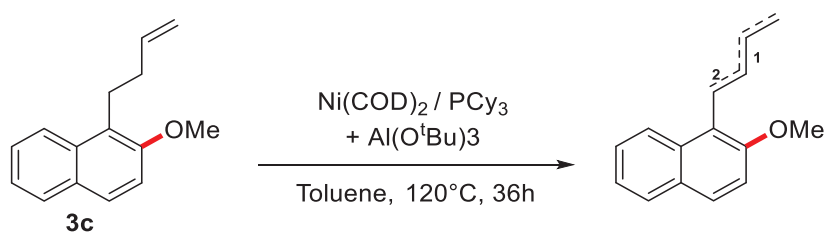
General procedure for intramolecular bifunctionalization: In a glovebox, a 5 mL microwave reaction vial equipped with a magnetic stir bar was charged with Ni(COD)₂ (10 mol%, 0.03 mmol, 8.3 mg), and the ligand [Bis-NHC's (10 mol%, 0.03 mmol) or mono-NHC's or diphosphines (20 mol%, 0.06 mmol) or mono-phosphines (40 mol%, 0.12 mmol)] in toluene (0.5 ml). After stirring the resulting solution for 5 minutes, the selected substrate (1.0 equiv, 0.3 mmol) was sequentially added, w or (w/o) the addition of the coupling partner generally (1.5 equiv, 0.5 mmol) and an additional base or additive like CsF (2.0 equiv, 0.6 mmol) and MgI₂ (2.4 equiv, 0.72 mmol). The tube was sealed, removed from the glovebox and heated at 120 °C (preheated oil bath) for 3-36 h. The reaction mixture was then cooled to room temperature, filtered over Celite®, and all

volatiles were removed under reduced pressure. The reaction progress was followed by ^{19}F -NMR using PhCF_3 as internal standard (for products bearing fluorine atoms) and GCMS. The products was isolated when necessary by flash chromatography on silica gel using appropriate mixtures of ethyl acetate and cyclohexane.

General procedure for difunctionalization of (3f) with Ruthenium : In a glovebox, a 5 mL microwave reaction vial equipped with a magnetic stir bar was charged with $\text{RuH}_2(\text{CO})(\text{PPh}_3)_3$ (10 mol%, 0.03 mmol, 27.6 mg) in toluene (0.5 ml). After stirring the solution for 5 minutes, substrate **3f** (1.0 equiv, 0.3 mmol, 63.3 mg) and $(p\text{-PhCF}_3)\text{B}(\text{OR})_2$ (1.5 equiv, 0.45 mmol, 116.1 mg) were sequentially added. The tube was sealed, removed from the glovebox and heated at 120°C (preheated oil bath) for 24 h. The reaction mixture was then cooled to room temperature, filtered over Celite®, and all volatiles were removed under reduced pressure. The products yields was determined by GCMS.

3. Isolation and characterization of cross-coupling products

a. Isomerization of (3c)

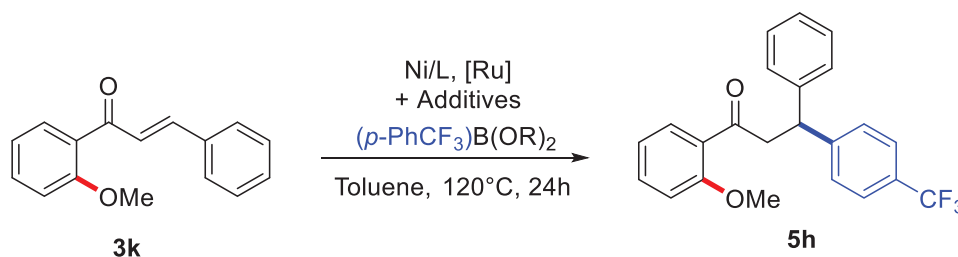


In a glovebox, a 5 mL microwave reaction vial equipped with a magnetic stir bar was charged with $\text{Ni}(\text{COD})_2$ (10 mol%, 0.03 mmol, 8.3 mg), and PCy_3 ligand (40 mol%, 0.12 mmol, 33.6 mg) in toluene (0.5 ml). After stirring the solution for 5 minutes, a solution of premixed **3c** substrate (1.0 equiv, 0.3 mmol, 63.3 mg) with $\text{Al}(\text{O}^t\text{Bu})_3$ (20 mol%, 0.06 mmol, 14.8 mg) in toluene (0.5 ml) was sequentially added. The tube was sealed, removed from the glovebox and heated at

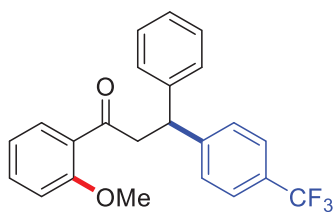
120 °C (preheated oil bath) for 36 h. Then, the reaction mixture was cooled to room temperature, filtered over Celite®, and all volatiles were removed under reduced pressure. The residue was purified by flash chromatography (Ethyl acetate/Cyclohexane, gradient 0 to 70%), affording a mixture of isomeric products (51 mg, 81% yield). The isomerization ratio was determined by integrating the signals of each isomer on GCMS as well as integrating the characteristic alkene signals of each isomer by ¹H-NMR (Isomer 1: δ 5.62 and 5.39 ppm, Isomer 2: δ 6.20 and 5.91 ppm).

***Note:** The isolation of the isomers was not possible and we relied on the characteristic peaks of each to determine the ratios.

b. Synthesis of (5h)



In a glovebox, a 5 mL microwave reaction vial equipped with a magnetic stir bar was charged with Ni(COD)_2 (10 mol%, 0.03 mmol, 8.3 mg), and PCy_3 ligand (40 mol%, 0.12 mmol, 33.6 mg) in toluene (0.5 ml). After stirring the solution for 5 minutes, substrate **3k** (1.0 equiv, 0.3 mmol, 63.3 mg), $(p\text{-PhCF}_3)\text{B(OR)}_2$ (1.5 equiv, 0.45 mmol, 116.1 mg) and CsF (4.5 equiv, 1.35 mmol, 205.1 mg) were sequentially added. The tube was sealed, removed from the glovebox and heated at 120 °C (preheated oil bath) for 24 h. Then, the reaction mixture was cooled to room temperature, filtered over Celite®, and all volatiles were removed under reduced pressure. The crude product was isolated by flash chromatography (Ethyl acetate/Cyclohexane, gradient 0 to 70%), affording **5h** as a white powder (102 mg, 88% yield).



^1H NMR (300 MHz, Chloroform-*d*): δ 7.54 – 7.13 (11H, m, CH_{Ar}), 7.03 – 6.89 (2H, m, CH_{Ar}), 4.82 (1H, t, $J_{\text{H-H}} = 7.5$ Hz, CH), 3.89 (3H, s, OCH_3), 3.77 (2H, dd, $J_{\text{H-H}} = 7.5, 5.6$ Hz, CH_2). **$^{13}\text{C}\{^1\text{H}\}$ NMR** (75 MHz, CDCl_3) δ 200.2 (s, C=O), 158.5 (s, C_{Ar}), 148.7 (s, C_{Ar}), 143.7 (s, C_{Ar}), 133.7 (s, C_{Ar}), 133.0 (s, C_{Ar}), 130.5 (s, C_{Ar}), 129.0 (s, C_{Ar}), 128.8 (s, C_{Ar}), 128.5 (s, C_{Ar}), 128.4 (s, C_{Ar}), 128.4 (s, C_{Ar}), 128.0 (s, C_{Ar}), 126.7 (s, C_{Ar}), 125.5 (s, C_{Ar}), 125.5 (s, C_{Ar}), 125.4 (s, C_{Ar}), 120.9 (s, C_{Ar}), 111.6 (s, C_{Ar}), 55.7 (s, CH), 49.7 (s, OCH_3), 46.2 (s, CH_2). **^{19}F NMR** (282 MHz, CDCl_3) δ -62.3. **MS** (EI) m/z : $[\text{M}]^+$ 384.

VI. References

- (1) Tobisu, M.; Chatani, N. Metal-Catalyzed Aromatic C-O Bond Activation/Transformation. In *Topics in Organometallic Chemistry*; Springer Verlag, 2019; Vol. 63, pp 103–140.
- (2) Ehle, A. R.; Zhou, Q.; Watson, M. P. Nickel(0)-Catalyzed Heck Cross-Coupling via Activation of Aryl C-OPiv Bonds. *Org. Lett.* **2012**, *14* (5), 1202–1205.
- (3) Harris, M. R.; Konev, M. O.; Jarvo, E. R. Enantiospecific Intramolecular Heck Reactions of Secondary Benzylic Ethers. *J. Am. Chem. Soc.* **2014**, *136* (22), 7825–7828.
- (4) Derosa, J.; Apolinar, O.; Kang, T.; Tran, V. T.; Engle, K. M. Recent Developments in Nickel-Catalyzed Intermolecular Dicarbofunctionalization of Alkenes. *Chem. Sci.* **2020**, *11* (17), 4287–4296.
- (5) Qi, X.; Diao, T. Nickel-Catalyzed Dicarbofunctionalization of Alkenes. *ACS Catal.* **2020**, *10* (15), 8542–8556.
- (6) Shrestha, B.; Basnet, P.; Dhungana, R. K.; Kc, S.; Thapa, S.; Sears, J. M.; Giri, R. Ni-Catalyzed Regioselective 1,2-Dicarbofunctionalization of Olefins by Intercepting Heck Intermediates as Imine-Stabilized Transient Metallacycles. *J. Am. Chem. Soc.* **2017**, *139* (31), 10653–10656.
- (7) Tian, Z. X.; Qiao, J. B.; Xu, G. L.; Pang, X.; Qi, L.; Ma, W. Y.; Zhao, Z. Z.; Duan, J.; Du, Y. F.; Su, P.; et al. Highly Enantioselective Cross-Electrophile Aryl-Alkenylation of Unactivated Alkenes. *J. Am. Chem. Soc.* **2019**, *141* (18), 7637–7643.
- (8) Li, Y.; Wang, K.; Ping, Y.; Wang, Y.; Kong, W. Nickel-Catalyzed Domino Heck Cyclization/Suzuki Coupling for the Synthesis of 3,3-Disubstituted Oxindoles. *Org. Lett.* **2018**, *20* (4), 921–924.
- (9) Jutand, A. *Mechanisms of the Mizoroki–Heck Reaction*, Martin Oes.; 2009.

- (10) Márquez, I. R.; Miguel, D.; Millán, A.; Marcos, M. L.; De Cienfuegos, L. Á.; Campaña, A. G.; Cuerva, J. M. Ti/Ni-Mediated Inter- and Intramolecular Conjugate Addition of Aryl and Alkenyl Halides and Triflates. *J. Org. Chem.* **2014**, *79* (4), 1529–1541.
- (11) Harris, M. R.; Konev, M. O.; Jarvo, E. R. Enantiospecific Intramolecular Heck Reactions of Secondary Benzylic Ethers. *J. Am. Chem. Soc.* **2014**, *136* (22), 7825–7828.
- (12) Lee, H. M.; Smith, D. C.; He, Z.; Stevens, E. D.; Yi, C. S.; Nolan, S. P. Catalytic Hydrogenation of Alkenes by the Ruthenium-Carbene Complex HRu(CO)Cl(PCy₃)(IMes) IMes = Bis(1,3-(2,4,6-Trimethylphenyl)Imidazol-2-Ylidene). *Organometallics* **2001**, *20* (4), 794–797.
- (13) Kapat, A.; Sperger, T.; Guven, S.; Schoenebeck, F. E-Olefins through Intramolecular Radical Relocation. *Science*. **2019**, *363* (6425), 391–396.
- (14) Vasseur, A.; Bruffaerts, J.; Marek, I. Remote Functionalization through Alkene Isomerization. *Nat. Chem.* **2016**, *8* (3), 209–219.
- (15) Hassam, M.; Taher, A.; Arnott, G. E.; Green, I. R.; Van Otterlo, W. A. L. Isomerization of Allylbenzenes. *Chem. Rev.* **2015**, *115* (11), 5462–5569.
- (16) *Applied Homogeneous Catalysis with Organometallic Compounds*; Cornils, B., Herrmann, W. A., Eds.; Wiley, 2002.
- (17) *The Organometallic Chemistry of the Transition Metals: Sixth Edition*; Crabtree, R. H., Ed.; Wiley Blackwell: Hoboken, NJ, USA, 2014; Vol. 9781118138.
- (18) Sen, A.; Lai, T. W. Catalytic Isomerization of Alkenes by Palladium(II) Compounds. An Alternative Mechanistic View. *Inorg. Chem.* **1981**, *20* (11), 4036–4038.
- (19) Gooßen, L. J.; Ohlmann, D. M.; Dierker, M. Silver Triflate-Catalysed Synthesis of γ -Lactones from Fatty Acids. *Green Chem.* **2010**, *12* (2), 197–20.

- (20) Crossley, S. W. M.; Barabé, F.; Shenvi, R. A. Simple, Chemoselective, Catalytic Olefin Isomerization. *J. Am. Chem. Soc.* **2014**, *136* (48), 16788–16791.
- (21) Li, G.; Kuo, J. L.; Han, A.; Abuyuan, J. M.; Young, L. C.; Norton, J. R.; Palmer, J. H. Radical Isomerization and Cycloisomerization Initiated by H• Transfer. *J. Am. Chem. Soc.* **2016**, *138* (24), 7698–7704.
- (22) Tobisu, M.; Takahira, T.; Morioka, T.; Chatani, N. Nickel-Catalyzed Alkylative Cross-Coupling of Anisoles with Grignard Reagents via C-O Bond Activation. *J. Am. Chem. Soc.* **2016**, *138* (21), 6711–6714.
- (23) Harkness, G. J.; Clarke, M. L. Less Hindered Ligands Give Improved Catalysts for the Nickel Catalysed Grignard Cross-Coupling of Aromatic Ethers. *Catal. Sci. Technol.* **2018**, *8* (1), 328–334.
- (24) Gunnoe, T. B.; Habgood, L. G. *Catalytic Hydroarylation of Carbon-Carbon Multiple Bonds*; Ackermann, L., Ed.
- (25) Chen, W.; Sun, L.; Huang, X.; Wang, J.; Peng, Y.; Song, G. Ligand-Free Nickel-Catalysed 1,4-Addition of Arylboronic Acids to α,β -Unsaturated Carbonyl Compounds. *Adv. Synth. Catal.* **2015**, *357* (7), 1474–1482.
- (26) Xiao, L. J.; Cheng, L.; Feng, W. M.; Li, M. L.; Xie, J. H.; Zhou, Q. L. Nickel(0)-Catalyzed Hydroarylation of Styrenes and 1,3-Dienes with Organoboron Compounds. *Angew. Chem. Int. Ed.* **2018**, *57* (2), 461–464.
- (27) Chen, Y. G.; Shuai, B.; Xu, X. T.; Li, Y. Q.; Yang, Q. L.; Qiu, H.; Zhang, K.; Fang, P.; Mei, T. S. Nickel-Catalyzed Enantioselective Hydroarylation and Hydroalkenylation of Styrenes. *J. Am. Chem. Soc.* **2019**, *141* (8), 3395–3399.
- (28) Lee, W. C.; Wang, C. H.; Lin, Y. H.; Shih, W. C.; Ong, T. G. Tandem Isomerization and C-

- H Activation: Regioselective Hydroheteroarylation of Allylarenes. *Org. Lett.* **2013**, *15* (20), 5358–5361.
- (29) Li, Y.; Luo, Y.; Peng, L.; Li, Y.; Zhao, B.; Wang, W.; Pang, H.; Deng, Y.; Bai, R.; Lan, Y.; et al. Reaction Scope and Mechanistic Insights of Nickel-Catalyzed Migratory Suzuki–Miyaura Cross-Coupling. *Nat. Commun.* **2020**, *11* (1), 1–13.
- (30) He, Y.; Liu, C.; Yu, L.; Zhu, S. Ligand-Enabled Nickel-Catalyzed Redox-Relay Migratory Hydroarylation of Alkenes with Arylborons. *Angew. Chem. Int. Ed.* **2020**, *59* (23), 9186–9191.
- (31) Voelker, T.; Xia, H.; Fandrick, K.; Johnson, R.; Janowsky, A.; Cashman, J. R. 2,5-Disubstituted Tetrahydrofurans as Selective Serotonin Re-Uptake Inhibitors. *Bioorganic Med. Chem.* **2009**, *17* (5), 2047–2068.
- (32) Zarate, C.; Nakajima, M.; Martin, R. A Mild and Ligand-Free Ni-Catalyzed Silylation via C-OMe Cleavage. *J. Am. Chem. Soc.* **2017**, *139* (3), 1191–1197.
- (33) Kišić, A.; Stephan, M.; Mohar, B. Asymmetric Transfer Hydrogenation of 1-Naphthyl Ketones by an Ansa-Ru(II) Complex of a DPEN-SO₂N(Me)-(CH₂)₂(η 6-p-Tol) Combined Ligand. *Org. Lett.* **2013**, *15* (7), 1614–1617.
- (34) Franz, K. D.; Haddon, R. C. Improved Syntheses of 9-Hydroxy and 9-Butoxy-1-Phenalenone. *Org. Prep. Proced. Int.* **1980**, *12* (3–4), 238–242.
- (35) Pradeep, P.; Ngwira, K. J.; Reynolds, C.; Rousseau, A. L.; Lemmerer, A.; Fernandes, M. A.; Johnson, M. M.; de Koning, C. B. Novel Methodology for the Synthesis of the Benzo[b]Phenanthridine and 6H-Dibenzo[c,h]Chromen-6-One Skeletons. Reactions of 2-Naphthylbenzylamines and 2-Naphthylbenzyl Alcohols. *Tetrahedron* **2016**, *72* (51), 8417–8427.

- (36) Zhang, X. S.; Zhang, Y. F.; Chen, K.; Shi, Z. J. Controllable Mono-/Di-Alkenylation of Aryl Alkyl Thioethers Tuned by Oxidants via Pd-Catalysis. *Org. Chem. Front.* **2014**, *1* (9), 1096–1100.
- (37) Jumde, V. R.; Iuliano, A. Deoxycholic Acid Derived Monophosphites as Chiral Ligands in the Asymmetric Suzuki-Miyaura Cross-Coupling. *Tetrahedron Asymmetry* **2011**, *22* (24), 2151–2155.
- (38) Müller, C.; López, L. G.; Kooijman, H.; Spek, A. L.; Vogt, D. Chiral Bidentate Phosphabenzene-Based Ligands: Synthesis, Coordination Chemistry, and Application in Rh-Catalyzed Asymmetric Hydrogenations. *Tetrahedron Lett.* **2006**, *47* (12), 2017–2020.

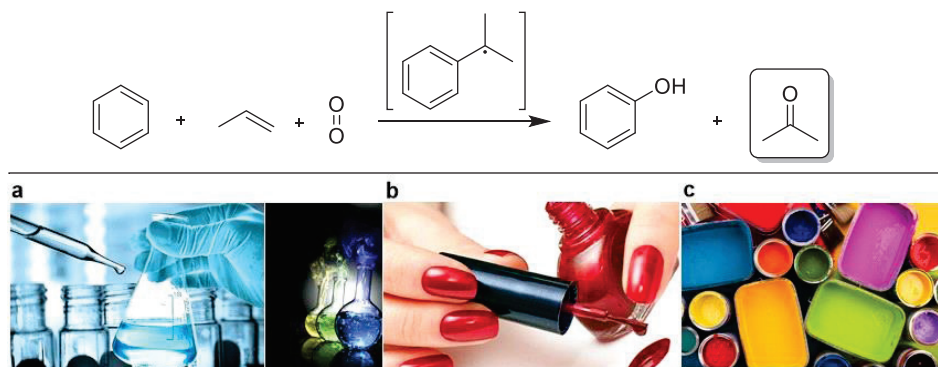
Part II:

***Nickel-Catalyzed Mono-Selective α -Ary-
lation of Acetone with Aryl Chlorides
and Phenol Derivatives***

Introduction

Acetone: production and applications

Acetone is one of the most widely produced and employed bulk chemicals, which is produced from propylene, predominantly via cumene process in a fraction of 7 million tons annually. In the cumene process, the combination of benzene with propylene produces cumene, which gets oxidized in air to produce phenol and acetone. The reaction proceeds via a radical mechanism (**Scheme 1**).¹ In addition, acetone is naturally produced in the human body through normal metabolic processes. It is primarily used as solvent in organic chemistry and for the synthesis of methyl methacrylate (via the acetone cyanohydrin route),² as well as for familiar household uses like nail polish remover and paint thinner.



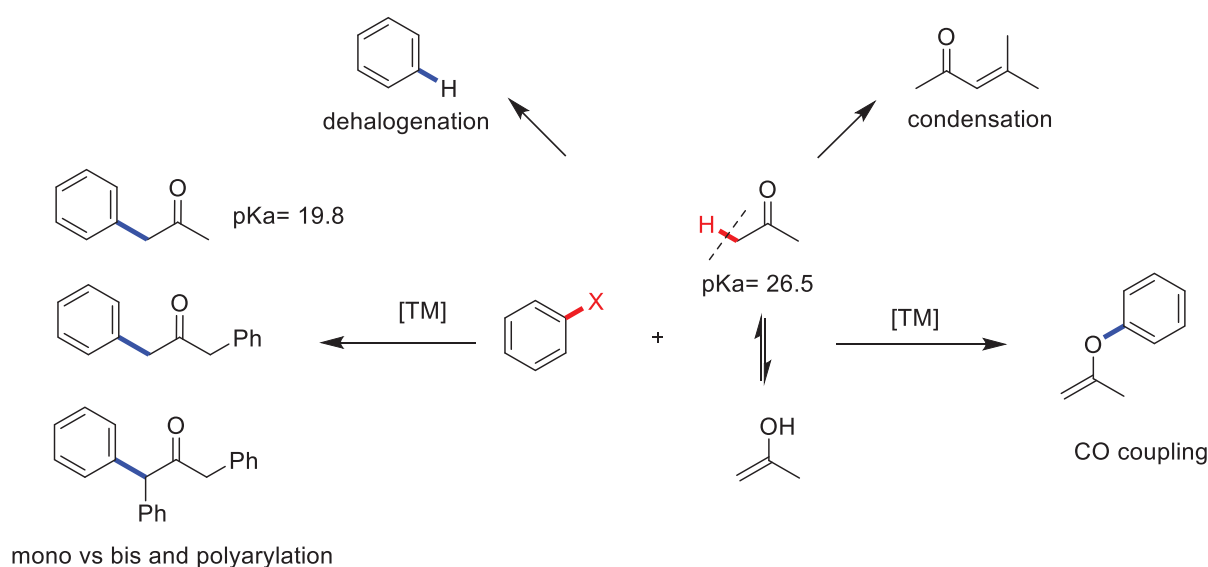
Scheme 1: Production and general uses of acetone. ^aorganic solvent, ^bnail polish remover, ^cpaint thinner.

Arylation of acetone

Substituted α -aryl ketones represent important building blocks for many biologically active molecules and pharmaceutical compounds.^{3,4} Their preparation initially relied on arylation of enolizable ketones under metal free conditions via radical processes, but this strategy is uncontrollable, non-selective, and has a limited substrate-scope.^{5,6} More recently, transition metal-catalyzed α -arylation of carbonyl compounds has emerged as a very powerful and direct methodology to

forge $\text{Csp}^3\text{-Csp}^2$ bonds. Significant progress has been achieved in the field with substituted ketones.⁷ However, the selective monoarylation of acetone is much less developed and represents an important goal in synthetic chemistry.⁸

In fact, achieving selective mono-arylation of acetone is very challenging for many reasons. First, the formed phenyl acetone product features more acidic benzylic protons that are prone to further arylation.⁹ Second, due to the equilibrium formed between ketone and enol in the presence of base, C-O instead of C-C product could be formed.¹⁰ Third, aldol condensation and dehalogenation by-products might be formed (**Scheme 2**).



Scheme 2: Selectivity challenges for transition metal-catalyzed α -arylation of acetone.

In this part of the manuscript, we will present in the first chapter the state of the art for the development of transition metal-catalyzed α -arylation of substituted carbonyl compounds, *via* the formation of enolate intermediates, with a focus on palladium catalysts. The few examples of

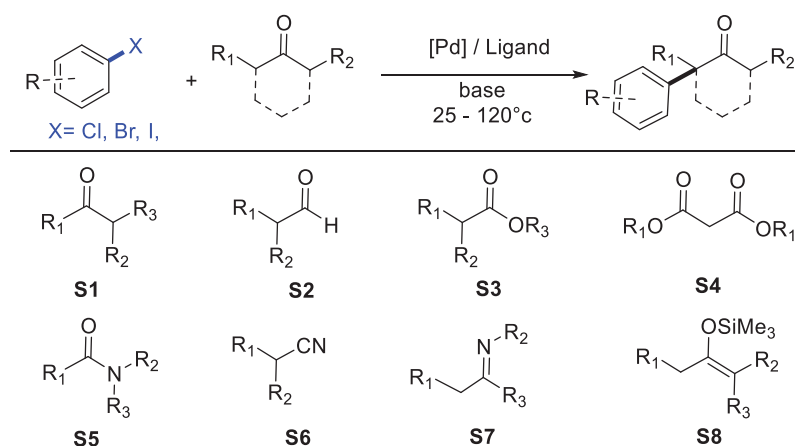
nickel-catalyzed α -arylation of substituted ketones will be discussed, and finally the very few efficient catalytic systems, all based on noble palladium catalysts, reported for the selective mono-arylation of acetone will be presented. The second chapter will be dedicated to the description of our results in the development and understanding of the first efficient nickel-catalyzed α -arylation of acetone.

Chapter I:

Bibliographic survey on transition metal catalyzed α -arylation of ketones

I. Palladium-catalyzed α -arylation of substituted ketones

Over the last decades, several methodologies were reported for Pd-catalyzed α -arylation of carbonyl compounds.^{11,12,13} Interestingly, various substituted carbonyl derivatives bearing an α -acidic proton were shown to be excellent candidates for this transformation (**Scheme 3**).³ The major studies focused on ketone derivatives (S1).^{14,15,16} However, aldehydes (S2),¹⁷ esters (S3),^{18,19} malonates (S4),²⁰ amides (S5),^{21,22} nitriles (S6),²³ ketimines²⁴ (S7), as well as silyl enol ethers²⁵ (S8) were shown to be also effective.



Scheme 3: General scope of carbonyl derivatives used for Pd-catalyzed α -arylation. $R(1, 2, 3) = \text{Ar, Alkyl}$.

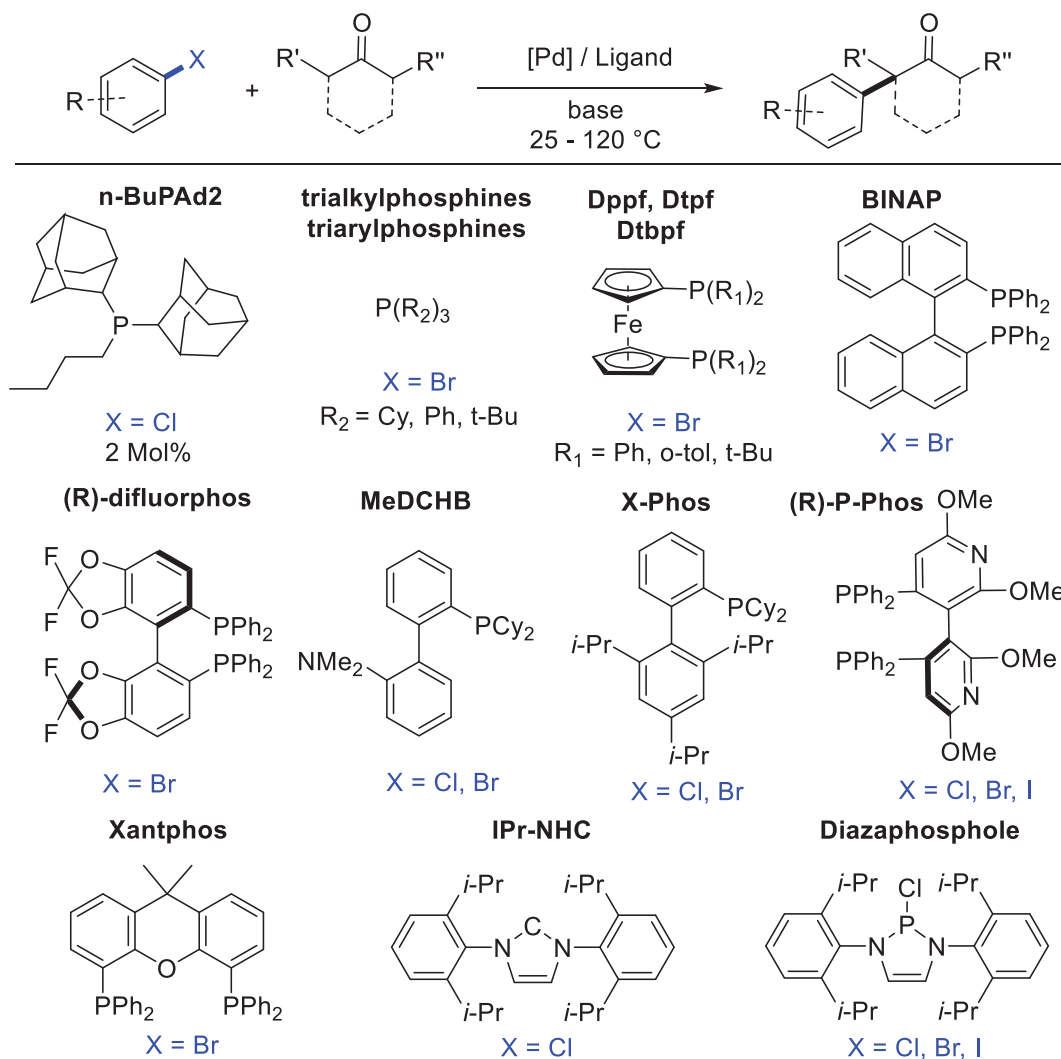
Even though different research groups tested these carbonyl nucleophiles, they actually had several reaction conditions in common. First of all, simple Pd^{II} pre-catalysts like $\text{Pd}(\text{OAc})_2$ were often used, Pd^0 catalysts like $\text{Pd}(\text{PPh}_3)_4$ were being used only in very few transformations.

The generally accepted mechanism involves a $\text{Pd}^0/\text{Pd}^{\text{II}}$ pathway²⁶ and proceeds in three main steps: oxidative addition of the aryl halide, transmetalation with the deprotonated ketone, and C-C bond reductive elimination. Generally, strong bases like LiHMDS, NaO^tBu or NaH are added in order to deprotonate the acidic proton and form the enolate. The main difference that

controls the selectivity and reactivity is the nature of the ancillary ligand. The mostly used ligands are strongly donating bulky phosphines (**Scheme 4**).

Taking a closer look on the ligand design, it appears that using bulky ligands is essential to stabilize the *in situ* generated Pd⁰ intermediate, along with minimizing the possibility of di-arylation. Diphosphines or monophosphines with chelating groups (like -NMe₂ in **MeDCHB**) are particularly employed to saturate the Pd complex and reduce its propensity for β-hydride elimination. Furthermore, alkyl rather than aryl phosphines (such as -P(^tBu)₂ in **DTBPF** instead of -PPh₂ in **DPPF**) have been shown to increase the lifetime and TON number of the active catalyst. Moreover, a variety of chiral ligands was used to induce stereoselective arylations.

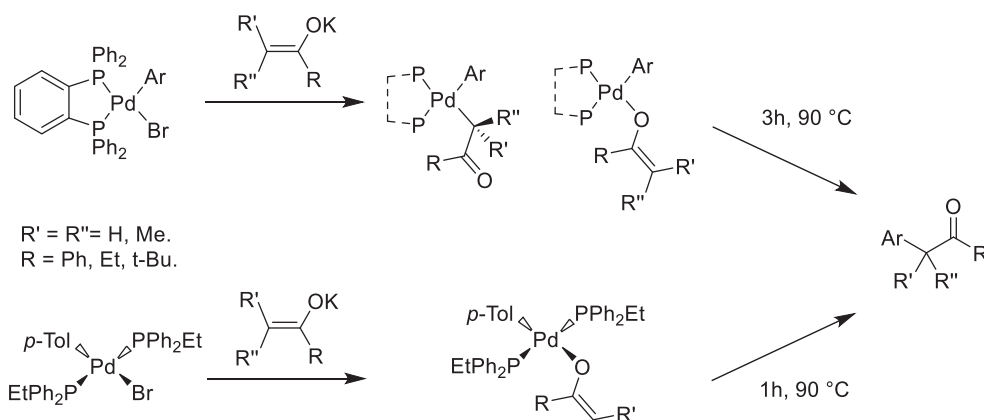
The primary catalytic framework utilizes Dppf ligand.²⁷ Afterwards, the bulkier DTBPF ligand gave a more effective catalytic system.²⁸ Mechanistic studies carried out with DTBPF ligands indicate that only one phosphine is coordinated to palladium in the transmetallation step with enolate. This indicates that bulky monophosphines could be also used, opening the field to monophosphines integration in catalysis.²⁹ In the other hand, at the initial stage, Buchwald & al. used sterically hindered chelating *o*-biphenyl ligands to inhibit β-hydride elimination and stabilize the complex.³⁰ However, it appears afterward that non-chelating ligands are generally more efficient where Pd complexes are stabilized by forming palladacyclic intermediates.³¹



Scheme 4: Main ligands used for Pd-catalyzed α -arylation of substituted and cyclic ketones.

Further mechanistic information on the reaction of the Pd(II)-aryl intermediate with enolate has been gained by the group of Hartwig. Several intermediates were isolated thanks to the use of chelating ligands having small bite angles, and modest electron donation like 1,2-bis(diphenylphosphino)benzene (**DPPBz**) and diphenylethylphosphine. The transmetalating complexes can be formed with a simple addition of enolate to the oxidative addition complexes (**Scheme 5**). After

evaluating the mode of coordination, it appears that generally the C-bound isomer is more electronically favored if the enolate is located *trans* to a phosphine (with **DPPBz** ligand), and the O-bound isomer is favored if the enolate is located *trans* to an aryl group (with **PPh₂Et** ligand).³²

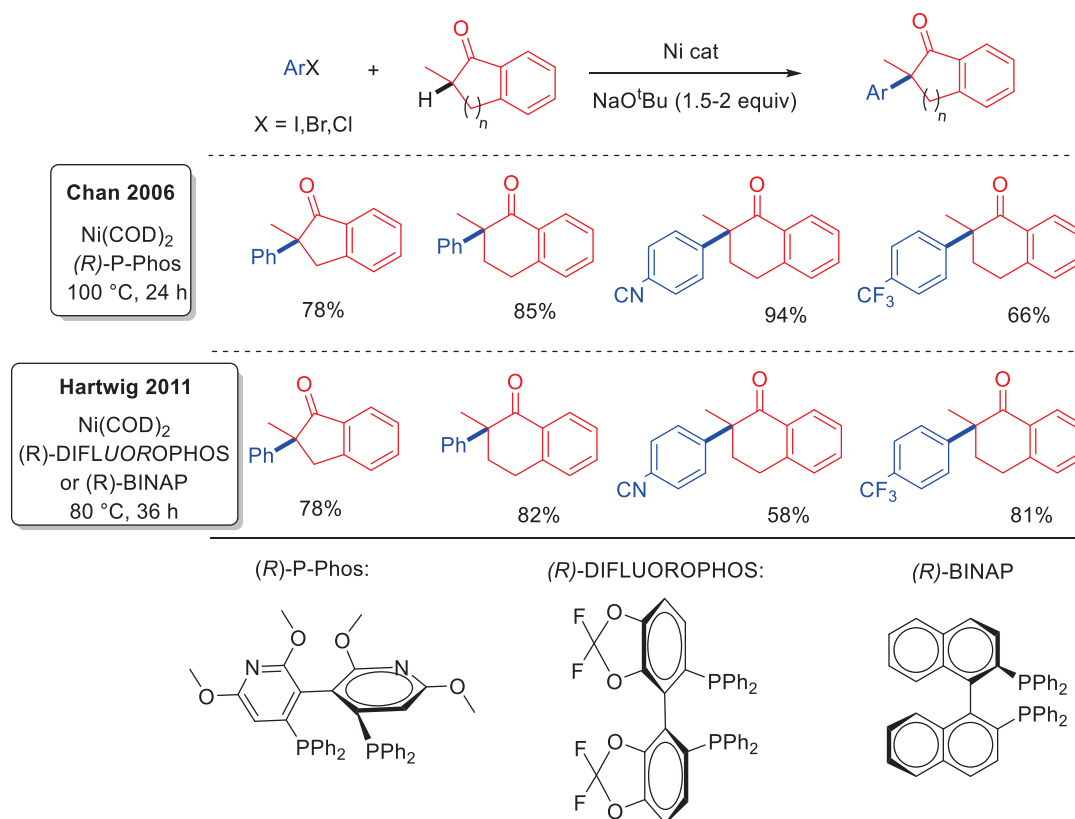


Scheme 5: Transmetalation and reductive elimination of the isolated aryl palladium enolate complexes.

Both isolated C- and O-bound palladium enolates undergo reductive elimination upon heating at 90 °C giving the α -arylated product in excellent yields, which supports the expected $\text{Pd}^0/\text{Pd}^{\text{II}}$ catalytic cycle.¹¹

II. Nickel-catalyzed α -arylation of substituted ketones

Researchers are always inspired to develop more reactive, cheaper and greener catalytic systems. The replacement of Pd with Ni is of great interest for these reasons. In addition, nickel is capable of activating more challenging electrophiles, thanks to its higher nucleophilic nature. In this context, Chan and Hartwig's groups reported the cross-coupling of aryl halides with several cyclic and penta-substituted ketones, catalyzed by diphosphine complexes of nickel (**Scheme 6**).^{33,34}

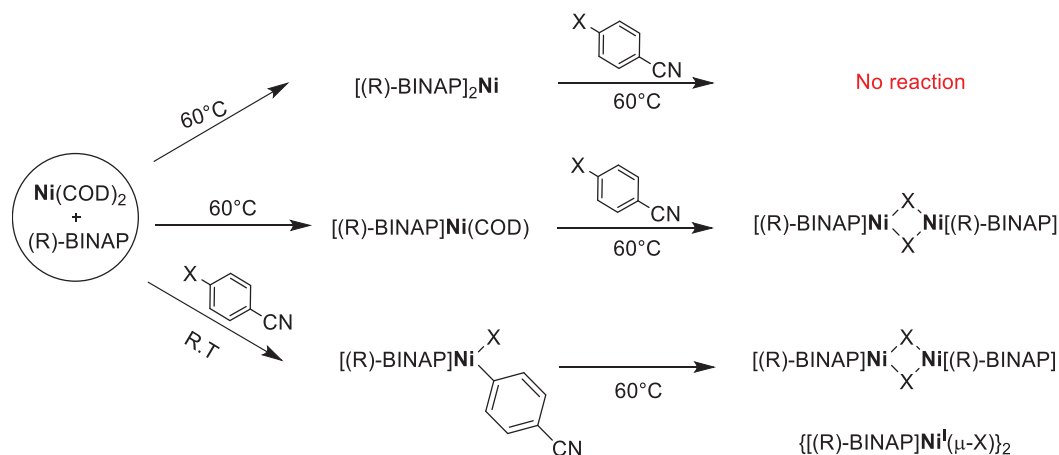


Scheme 6: Ni-catalyzed α -arylation of cyclic penta-substituted ketones as reported by the groups of Chan and Hartwig.

Screening of ligands showed that several diphosphines were active, with (R)-P-Phos, (R)-DIFLUOROPHOS and (R)-BINAP being the most active and selective ligands. The scope of the α -arylation is broader under the conditions developed by Hartwig & al., encompassing several heterocycles at lower temperatures. In contrast to Pd-catalyzed arylations, the enantioselectivity in the arylation of para-substituted indanones was excellently controlled with nickel. Interestingly, the arylation proceeds also well with unactivated aryl chlorides. It is worth noting that aryl chlorides are even more reactive than aryl bromides under nickel catalysis.

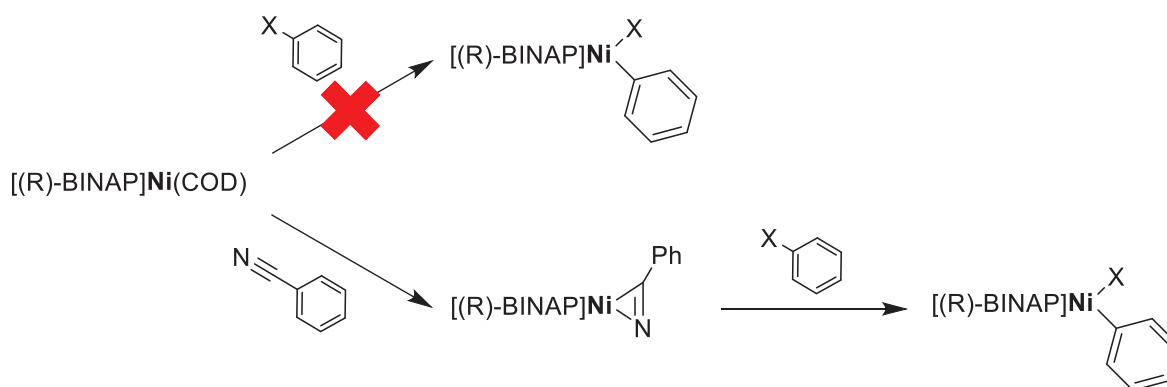
Thorough mechanistic studies were carried out by the group of Hartwig, indicating a classical $\text{Ni}^0/\text{Ni}^{\text{II}}$ catalytic cycle similar to that observed under Pd-catalysis.³⁴ The combination of $\text{Ni}(\text{COD})_2$ with (R)-BINAP at 60 °C led to the formation of two species, $[(\text{R})\text{-BINAP}]_2\text{Ni}$ and

$[(R)\text{-BINAP}]\text{Ni}(\text{COD})$ (**Scheme 7**). The addition of 4-cyanophenyl halide to $[(R)\text{-BINAP}]_2\text{Ni}$ failed to produce the oxidative addition complex since it is coordinatively saturated. On the other hand, the reaction of 4-cyanophenyl halide to $[(R)\text{-BINAP}]\text{Ni}^0(\text{COD})$ at 60 °C led to full conversion to Ni^{I} species ($\{[(R)\text{-BINAP}]\text{Ni}^{\text{I}}(\mu\text{-X})\}_2$).



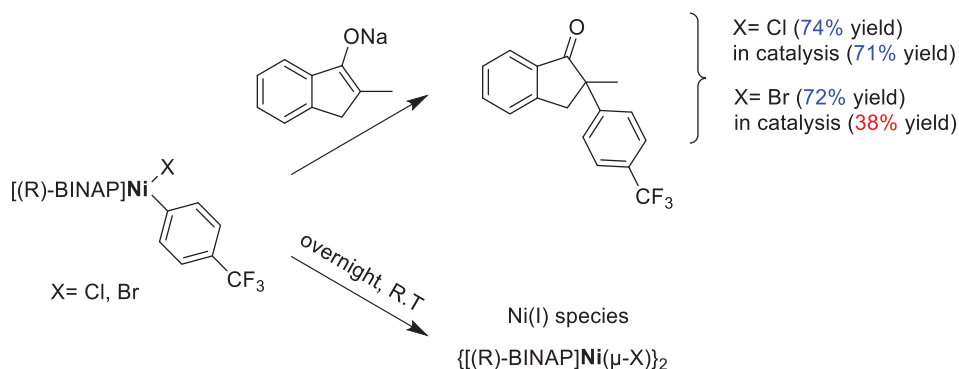
Scheme 7: Evaluation of several reaction intermediates.

The oxidative addition complex $[(R)\text{-BINAP}]\text{Ni}^{\text{II}}(\text{PhCN})\text{Cl}$ was formed by adding 4-cyanophenyl chloride to the combination of $\text{Ni}(\text{COD})_2$ and $(R)\text{-BINAP}$, or to $[(R)\text{-BINAP}]\text{Ni}^0(\text{COD})$ complex at room temperature (**Scheme 7**). However, this is not the case with all the other substrates like chlorobenzene where COD group is not easily exchanged, and direct formation of the O.A complex is not possible (**Scheme 8**). One way to solve this problem is by adding benzonitrile (PhCN) to $[(R)\text{-BINAP}]\text{Ni}^0(\text{COD})$ complex, which leads to the formation of $[(R)\text{-BINAP}]\text{Ni}(\eta^2\text{-NC-Ph})$ complex by the replacement of COD with the cyano group. This complex is stable and was isolated. The cyano group can be easily removed, the addition of chlorobenzene to $[(R)\text{-BINAP}]\text{Ni}(\eta^2\text{-NC-Ph})$ lead to the formation of the corresponding oxidative addition complex. The O.A complexes are unstable and decompose overnight at RT forming $\{[(R)\text{-BINAP}]\text{Ni}^{\text{I}}(\mu\text{-X})\}_2$ species.



Scheme 8: The formation of O.A complexes from $[(R)\text{-BINAP}]\text{Ni}(\text{COD})$ in the presence of PhCN .

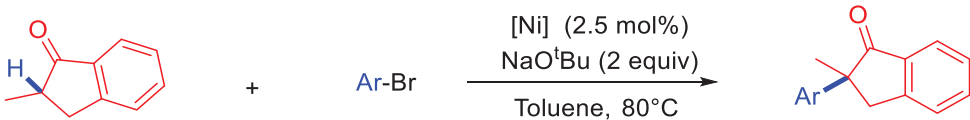
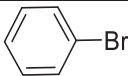
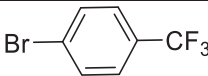
After having isolated several oxidative addition complexes, their reaction with the sodium enolate of 2-methyl-1-indanone was evaluated in stoichiometric conditions (**Scheme 9**). The two complexes $[(R)\text{-BINAP}]\text{Ni}(\text{PhCF}_3)\text{Cl}$ and $[(R)\text{-BINAP}]\text{Ni}(\text{PhCF}_3)\text{Br}$ gave the α -arylated product in very good yields. In contrast, a much lower yield for $[(R)\text{-BINAP}]\text{Ni}(\text{PhCF}_3)\text{Br}$ complex was obtained in catalytic conditions. This indicates that $[(R)\text{-BINAP}]\text{Ni}(\text{PhCF}_3)\text{Br}$ complex undergoes decomposition to a less reactive species. Indeed, both complexes were found to decompose overnight at room temperature forming the Ni^{I} species $\{[(R)\text{-BINAP}]\text{Ni}^{\text{I}}(\mu\text{-X})\}_2$ in high yields (71%). The rate of decomposition of the bromo complex is faster than that of the chloro derivative, which explains the obtained results in catalysis.³⁴



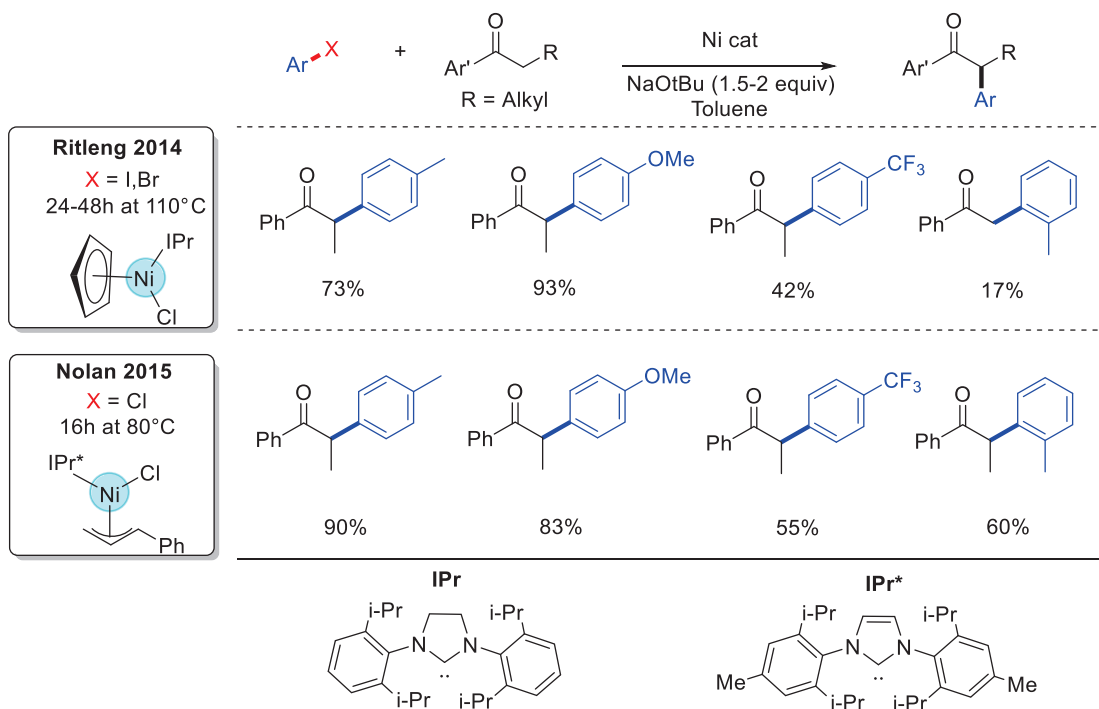
Scheme 9: Stability and reactivity of the oxidative addition complexes.

The Ni^{I} complexes $\{[(\text{R})\text{-BINAP}]\text{Ni}(\mu\text{-X})\}_2$ have a comparable reactivity as Ni^0 and Ni^{II} analogs (**Table 1**). However, the enantioselectivity was highly reduced with Ni^{I} species, and additionally, formation of the homocoupling by-product prevents Ni^{I} species from being used in catalysis.

Table 1: Reactivity of $\text{Ni}(0, \text{I}$ and $\text{II})$ species in catalysis.

		
		
$\text{Ni}^0(\text{COD})_2 / (\text{R})\text{-BINAP}$	61%	38%
$[(\text{R})\text{-BINAP}]\text{Ni}^{\text{II}}(\text{PhCF}_3)\text{Br}$	-	38%
$\{[(\text{R})\text{-BINAP}]\text{Ni}^{\text{I}}(\mu\text{-X})\}_2$	49%	32%

Later on, Ritleng and Nolan groups have shown that NHC's are also potent ligands for Ni-catalyzed α -arylation of substituted ketones. They reported interesting catalytic performances with Ni^{II} -NHC $[\text{Ni}(\text{IPr})\text{CpCl}]^{35}$ and $[\text{Ni}(\text{IPr}^*)(\text{cin})\text{Cl}]^{36}$ complexes, respectively (**Scheme 10**). The catalytic system developed by Ritleng & al. works well for the coupling of propiophenone derivatives with aryl bromide or iodide substrates, but proved unreactive for chloride derivatives. The catalytic system developed by Nolan & al. was shown to be reactive for the α -arylation of a series of propiophenones with aryl chloride substrates. The reaction proceeds with various aryl halides, with electron-rich substrates being more reactive than electron-poor and bulky aryl halides.

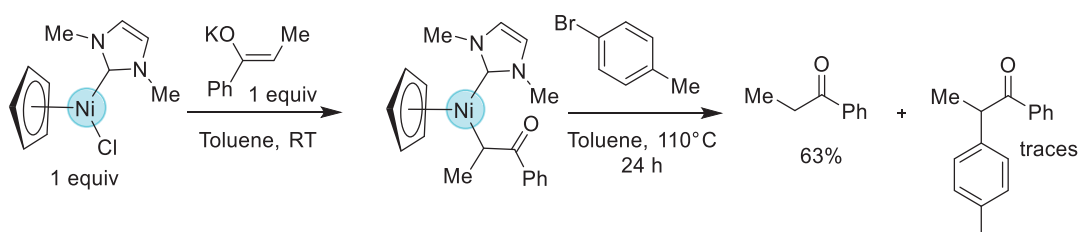


Scheme 10: Ritleng-Nolan scope for Ni-catalyzed α -arylation of substituted ketones.

Concerning the mechanism, Ritleng & al proposed the occurrence of a radical pathway on the basis of a series of stoichiometric experiments. The addition of 1 equiv. of propiophenone enolate to $[\text{Ni}(\text{IMes})\text{CpCl}]$ complex led to the formation of the α -carbonyl nickel complex $[\text{Ni}(\text{IMes})\{\text{CH}(\text{CH}_3)\text{C}(\text{O})\text{Ph}\}\text{Cp}]$ (**Scheme 11**). The addition of *p*-bromotoluene to this intermediate gave mainly propiophenone. With catalytic amount of the α -carbonyl nickel complex, the coupling product was obtained in low yields. The occurrence of a radical pathway was proposed based on the fact that addition of radical scavengers like TEMPO and galvinoxyl led to reaction inhibition.

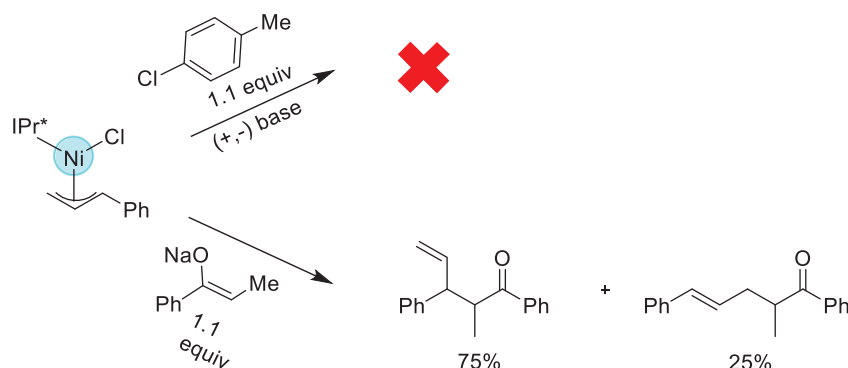
Of note, having O.A of *p*-bromotoluene to the transmetallating complex is not straightforward due to the presence of highly coordinating Cp and NHC ligands, as well as to the fact that Ni-Cp complexes usually have a tri-coordinated trigonal planar structure, and forming a 4-coordi-

nate Ni-Cp is geometrically unfavorable. In addition, expecting α -arylation and reductive elimination from a non-arylated Ni^{II} complex, as shown previously with Pd (see **section I**), is highly forbidden. Furthermore, TEMPO and galvinoxyl are compounds possessing a stable radical in their structure that can interact with the catalyst and form unreactive species, which means that the inhibition of the reaction in their presence does not always mean that the reaction is via a radical pathway. Based on this, the experiments carried out by Ritleng are not sufficient to prove the proposed radical mechanism, and a Ni⁰/Ni^{II} pathway can therefore not be completely excluded.



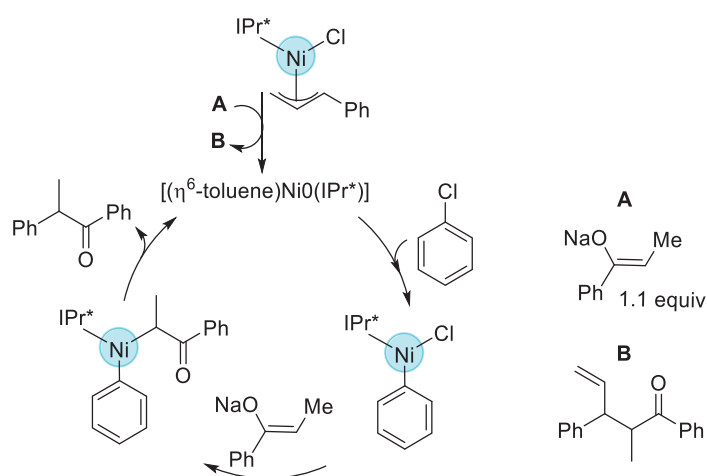
Scheme 11: Synthesis and reactivity of the transmetallating complex $[\text{Ni}(\text{IMes})\{\text{CH}(\text{CH}_3)\text{C}(\text{O})\text{Ph}\}\text{Cp}]$.

Mechanistic studies were also carried out by Nolan's group. The addition of 4-chlorotoluene to $[\text{Ni}(\text{IPr}^*)(\text{cin})\text{Cl}]$ complex does not lead to the formation of the oxidative addition complex (**Scheme 12**). Furthermore, adding the propiophenone sodium enolate to $[\text{Ni}(\text{IPr}^*)(\text{cin})\text{Cl}]$ formed the corresponding allylic substitution products.



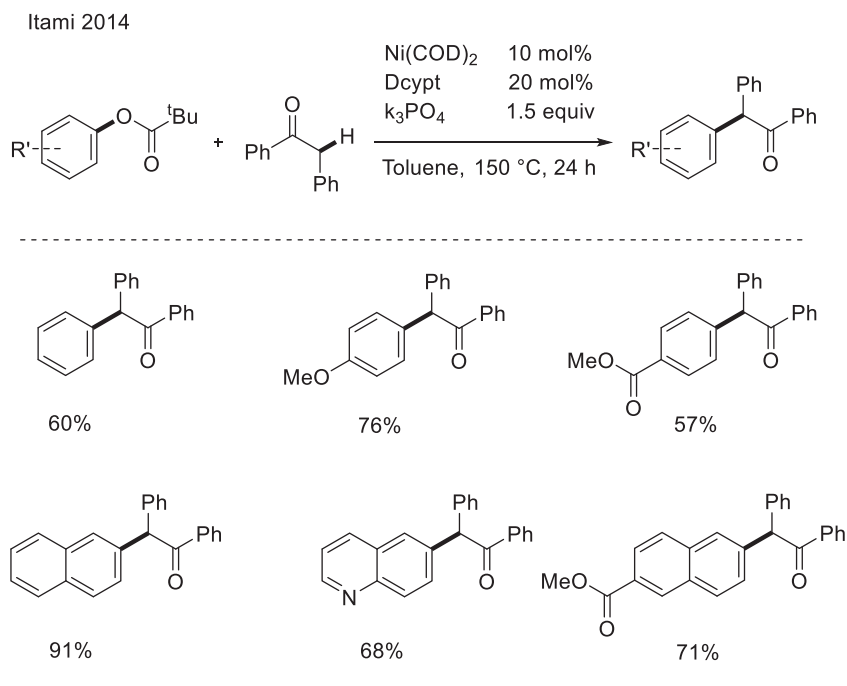
Scheme 12: Stoichiometric reactivity of $[\text{Ni}(\text{IPr}^*)(\text{cin})\text{Cl}]$ complex.

Based on these observations, it was proposed that $[\text{Ni}(\text{IPr}^*)(\text{cin})\text{Cl}]$ works as a pre-catalyst and reacts directly with the enolate, forming $[(\eta^6\text{-toluene})\text{Ni}^0(\text{IPr}^*)]$ complex and releasing isomeric α -allyl-ketones **B** and **B'**. The reaction of 4-chlorotoluene with $[(\eta^6\text{-toluene})\text{Ni}^0(\text{IPr}^*)]$ complex generates the oxidative addition complex $[\text{Ni}^{\text{II}}(\text{IPr}^*)(\text{Ph})\text{Cl}]$, which undergoes transmetalation with the enolate and finally reductive elimination, releasing the α -arylated product and regenerating the $[(\eta^6\text{-toluene})\text{Ni}^0(\text{IPr}^*)]$ complex (**Scheme 13**).



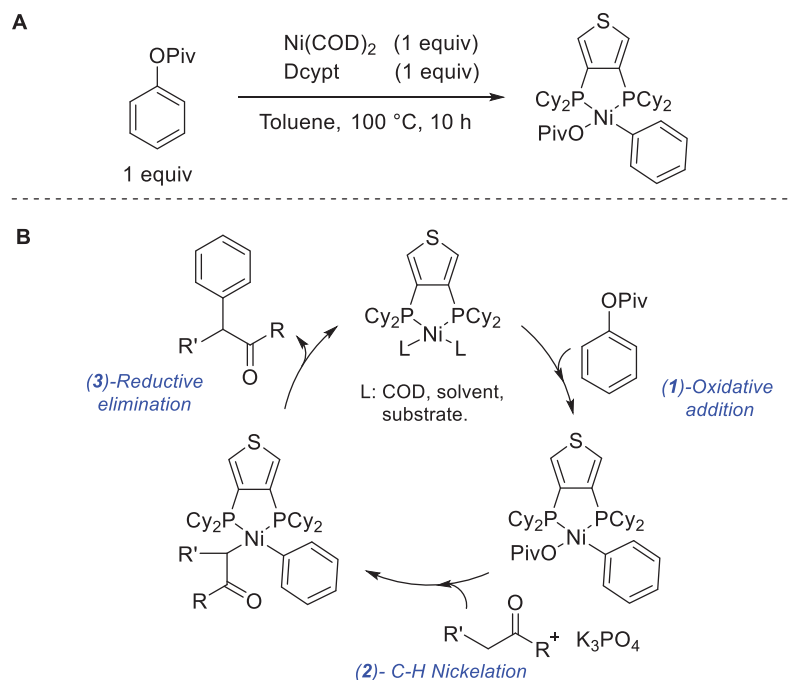
Scheme 13 : Proposed mechanism for the α -arylation with $[\text{Ni}(\text{IPr}^*)(\text{cin})\text{Cl}]$ catalyst.

The first nickel-catalyzed α -arylation of ketones with phenol derivatives was reported by Itami in 2014.³⁷ The transformation was catalyzed by $\text{Ni}(\text{COD})_2$ and 3,4-bis(dicyclohexylphosphino)thiophene ligand. Screening of various ligands showed that bidentate phosphines are the most efficient for the transformation, while very low reactivities were observed with monophosphines and NHC's. The catalytic system showed good activity with various aryl pivalates (**Scheme 14**).



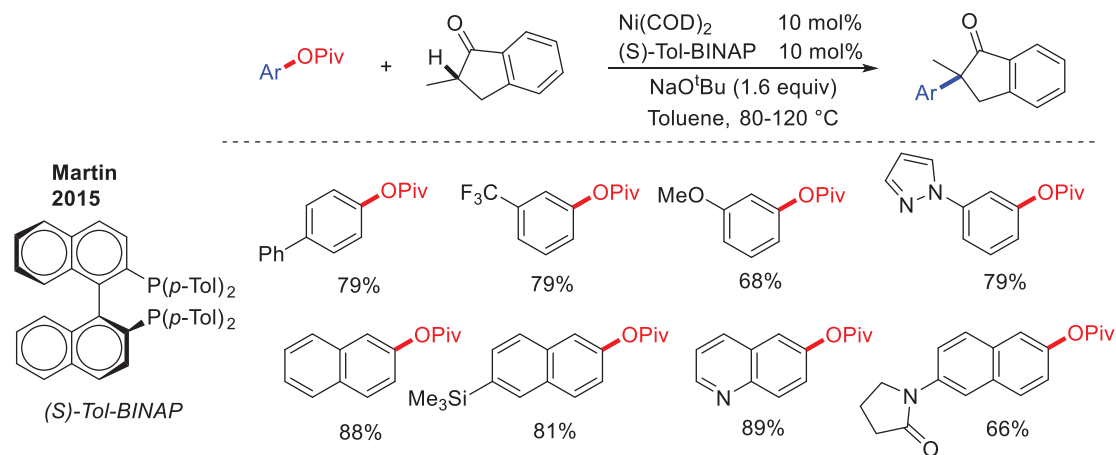
Scheme 14: Scope for nickel-catalyzed α -arylation of ketones with phenol derivatives.

The oxidative addition complex $(\text{Dcyp})\text{Ni}^{\text{II}}(\text{Ph})(\text{OPiv})$ was isolated and fully characterized (**Scheme 15-A**). It was found to be effective in catalysis. This indicates the involvement of a $\text{Ni}^0/\text{Ni}^{\text{II}}$ catalytic cycle (**Scheme 15-B**). After oxidative addition of ArOPiv to $(\text{Dcyp})\text{Ni}^0(\text{L})_2$ complex (step 1), the generated $(\text{Dcyp})\text{Ni}^{\text{II}}(\text{Ar})(\text{OPiv})$ undergoes C-H Nickelation assisted by the base (step 2), followed by reductive elimination and release of the α -arylated product (step 3).



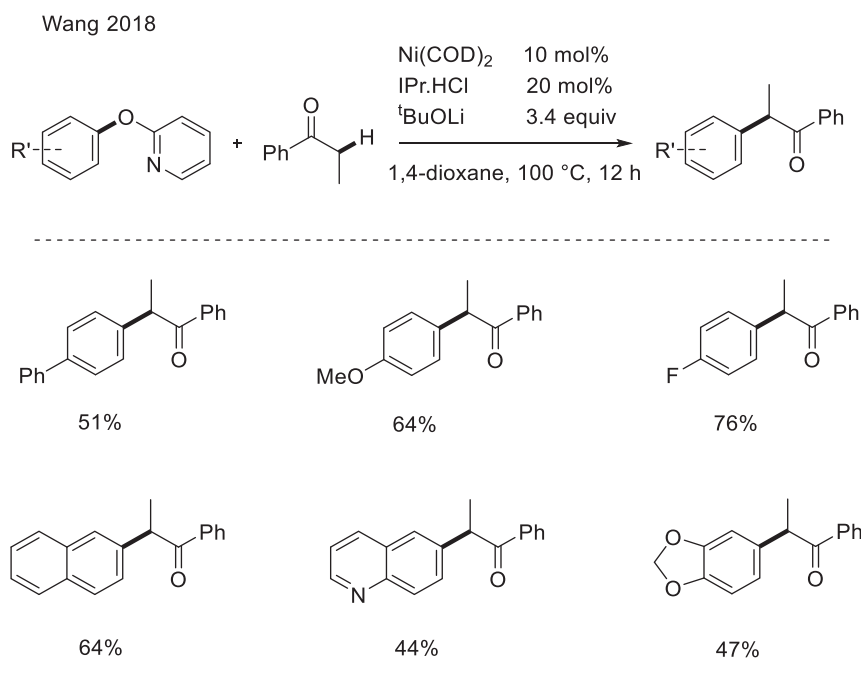
Scheme 15: Plausible mechanism for Nickel-catalyzed α -arylation of ketones with phenol derivatives.

Subsequently, the group of Martin developed an enantioselective Ni-catalyzed cross-coupling of cyclic penta-substituted ketones with aryl pivalates (**Scheme 16**). The reaction proceeds with a combination of Ni(COD)_2 and BINAP ligands in the presence of 1.6 equiv of NaO^tBu as base. Several chiral biphosphines were reactive, with (S)-Tol-BINAP being the most efficient both in terms of activity and stereoselectivity. The scope was broad with very good yields. Electron-deficient substrates were more reactive than electron-rich ones, and the scope was extended to heterocycles. No mechanistic studies were done and the mechanism was thought to involve either oxidative addition or the formation of Ni "ate" species.³⁸



Scheme 16: Scope for Ni-catalyzed α -arylation of substituted ketones with aryl pivalates.

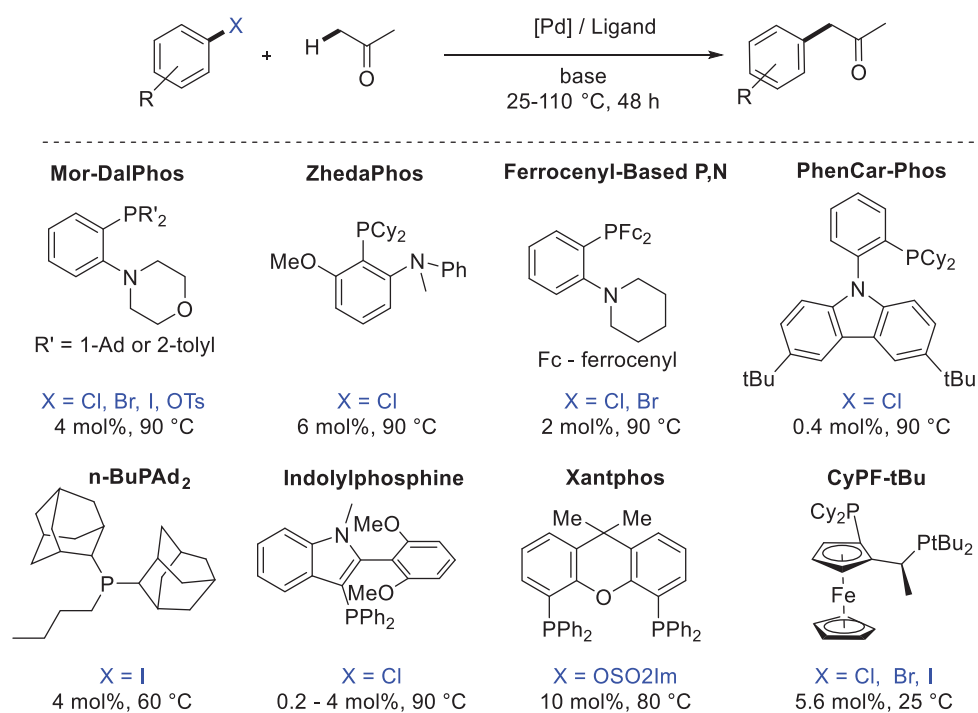
The Ni-catalyzed α -arylation of substituted ketones with activated 2-pyridyl ethers was achieved by Wang in 2018,³⁹ and was catalyzed by the combination of $\text{Ni}(\text{COD})_2$ and $\text{IPr}\cdot\text{HCl}$ ligand. Among several phosphines and NHC's, the use of $\text{IPr}\cdot\text{HCl}$ was critical for the transformation. A series of substrates could be coupled successfully with good yields (**Scheme 17**).



Scheme 17: Scope for Ni-catalyzed α -arylation of substituted ketones with 2-pyridyl ethers.

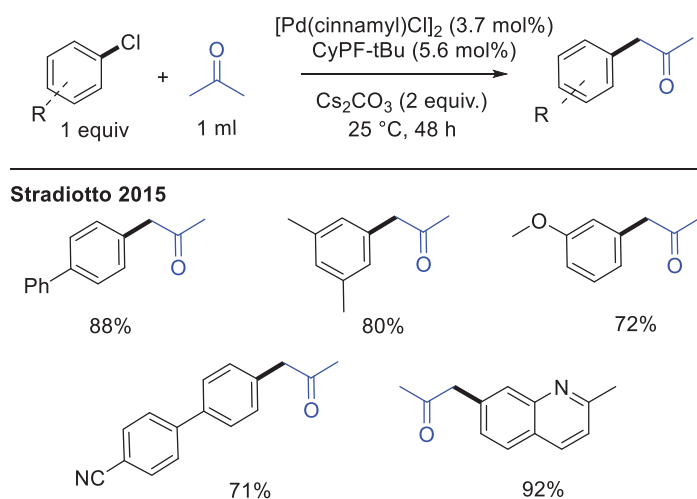
III. Palladium-catalyzed α -arylation of acetone

As mentioned before, the catalytic α -arylation of acetone has been reported in few cases only with palladium catalysts. The first Pd-catalyzed mono- α -arylation of acetone was reported by Stradiotto's group, with $[\text{Pd}(\text{cinnamyl})\text{Cl}]_2$ and Mor-DalPhos ligand.⁹ Inspired by Stradiotto's success, several superior catalytic systems were then developed using a variation of P,N-type ligands like ZhedaPhos,⁴⁰ ferrocenyl-based P,N-ligands⁴¹ and PhenCar-Phos⁴² (**Scheme 18**). Indol-phosphine ligands enable the activation of some unactivated aryl chlorides at lower catalytic loading.⁴³ Diphosphine ligands have also been shown to be interesting ligands, the use of Xantphos ligand was shown to enable the α -arylation of acetone with aryl imidazolylsulfonates.⁴⁴ Moreover, among all the reported ligands, Josiphos ligand CyPF-tBu was the most efficient for Pd catalysis in terms of scope and reaction conditions. Notably, it is the only reported α -arylation catalyst system that could perform at room temperature (**Scheme 18**).^{45,46} Of note, alkyl phosphine ligands like n-BuPAD₂ have been used for carbonylative α -arylation of acetophenones and acetone to form the corresponding valuable 1,3-diketones.⁴⁷ Among the reported catalytic systems, three palladium precursors are routinely used ($[\text{Pd}(\text{cinnamyl})\text{Cl}]_2$, $\text{Pd}(\text{OAc})_2$ and $\text{Pd}(\text{dba})_2$). Cs_2CO_3 is commonly used as base, the use of strong bases like NaO^tBu having a negative impact on the yield.



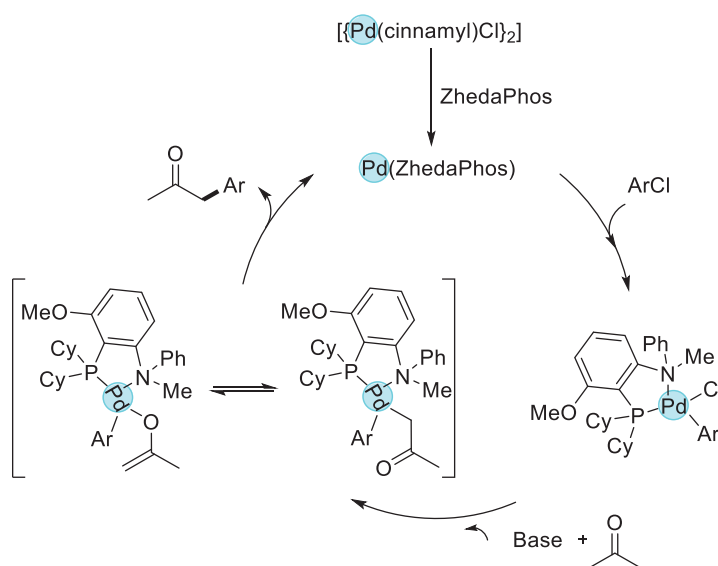
Scheme 18: General scope of ligands used for Pd-catalyzed α -arylation of acetone. [Pd] = [Pd(cinnamyl)Cl]₂, Pd(OAc)₂, Pd(dba)₂. Base = Cs₂CO₃, K₃PO₄.

The scope was broad, including various aryllic and heterocyclic substrates (**Scheme 19**).



Scheme 19: Selected substrates for Pd-catalyzed α -arylation of acetone at R.T.

The reactions were generally proposed to proceed via a $\text{Pd}^0/\text{Pd}^{\text{II}}$ 2e^- redox process. For example, the group of Ma proposed the mechanism displayed in (**Scheme 20**). After the formation of $(\text{ZhedaPhos})\text{Pd}^0$, oxidative addition of the aryl chloride takes place generating complex $(\text{ZhedaPhos})\text{Pd}^0(\text{Ar})(\text{Cl})$. This was followed by transmetallation with the acetone enolate to form two C- and O-bound palladium species that are in equilibrium. Finally, reductive elimination takes place giving the α -arylated product and regenerating the catalyst. In contrast to previous reports, kinetic studies showed a first order dependence on the aryl chloride species indicating that oxidative addition and not transmetallation is the rate-determining step.⁴⁰



Scheme 20: Proposed mechanism for Pd-catalyzed α -arylation of acetone.

IV. Conclusion

The state of the art indicates that, while several palladium and more recently nickel catalysts have been shown to promote efficient arylation of substituted ketones, very few examples of α -arylation of acetone were reported using palladium catalysts.⁸ In contrast, abundant and less

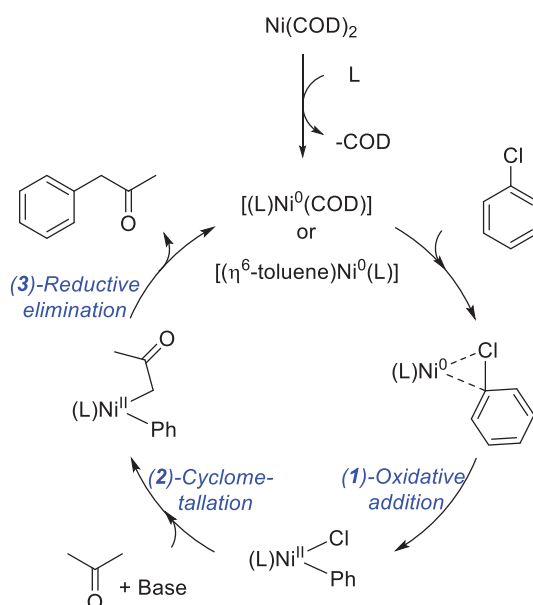
expensive nickel catalysts have never been reported. They were only used with cyclic and penta-substituted ketones where arylation is limited to only one position. Mechanistic studies carried out with nickel catalysts indicate that the main operative pathway involves $\text{Ni}^0/\text{Ni}^{\text{II}}$ redox cycles. The facile reduction of Ni^{II} intermediates into Ni^{I} species has been shown to be deleterious for catalytic efficiency, and the importance of the ancillary ligand to prevent side reactions has been also highlighted.

Chapter II:

*Development of a nickel-catalyzed mono-selective
 α -arylation of acetone*

I. Objective and envisioned methodology with nickel

In this context, we planned to develop a nickel-catalyzed mono-selective α -arylation of acetone, with aryl chlorides but also phenol derivatives. We envisioned that using a large excess of acetone would minimize the chance of multi-arylation. In addition, the use of a mild base could avoid O-arylation and aldol condensation. Based on the commonly used bases with palladium, Cs_2CO_3 appeared as a judicious choice to start with. Since dehalogenation is reduced by saturating the metallic center and preventing β -hydride elimination from taking place, bulky bidentate ligands were our primary choice. In analogy with reports on Pd catalysis, we envisioned a $\text{Ni}^0/\text{Ni}^{\text{II}}$ 2e^- redox process (**Scheme 21**). The simplified mechanism involves three main steps (i) oxidative addition of chlorobenzene to $[\text{Ni}^0]$ complex. (ii) cyclometallation of acetone assisted by the base. (iii) Reductive elimination combined with catalyst regeneration.



Scheme 21: Simplified catalytic cycle via oxidative addition.

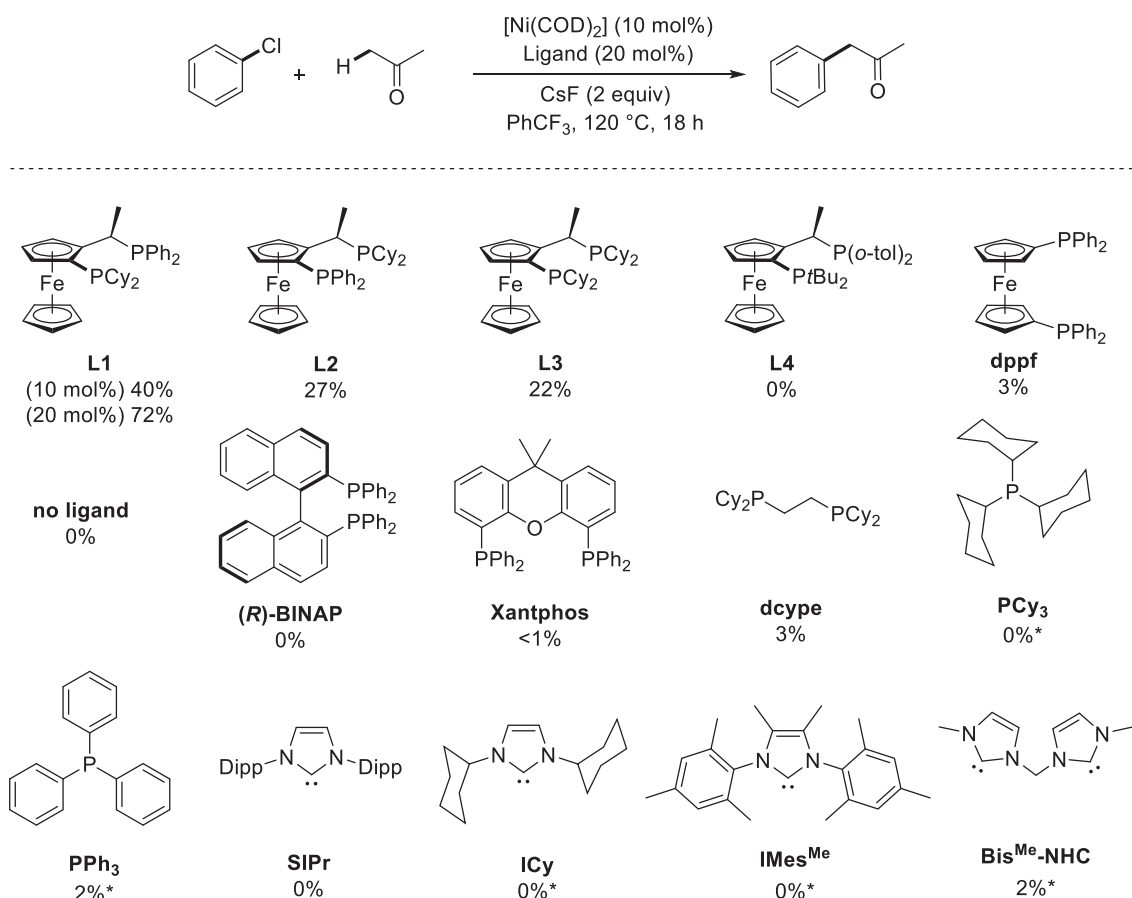
Toluene was widely used for this type of transformation and it was expected to be one of the most suitable solvents being able to form $[(\eta^6\text{-toluene})\text{Ni}^0(\text{L})]$ species and stabilize the complex.³⁶ The stability of the nickel intermediates is crucial and decomposition to Ni^{I} species which have been shown to be, at least, less reactive is one of the main deactivation pathways.⁴⁸ In addition, the selectivity of nickel complexes to form C-C instead of C-O coupling is very important, the use of a mild base will help minimize the C-O coupling. However, keto-enol tautomerization could also take place following transmetallation and lead to loss of selectivity. The reactivity and selectivity of the complexes could be controlled by choosing the correct ligand. Based on that, designing the ancillary ligand is therefore the key parameter to enable an efficient catalytic system.

II. Catalytic studies

1. Screening of ligands

Inspired by the unique reactivity observed previously with Josiphos ligands with palladium, we selected, to start with, a series of Josiphos ligands that were generously offered by Solvias AG Company. Very pleasingly, preliminary survey of $\text{Ni}(\text{COD})_2/\text{JosiPhos}$ ligands for the catalytic arylation of acetone with chlorobenzene gave selectively the mono- α -arylated product in good yields (72%) using the following set of condition: $\text{Ni}(\text{COD})_2$ (10 mol%), Josiphos (**L1**) (20 mol%), chlorobenzene (1.0 equiv), acetone (30 equiv) and CsF (2.0 equiv) in trifluorotoluene (1 mL). Comparatively, under otherwise identical conditions, the combination of Cs_2CO_3 as base and toluene as solvent exhibited inferior performance (*vide infra*). The reaction was then examined using a selection of chelating phosphine ligands reported to favor $\text{Ni}^0/\text{Ni}^{\text{II}}$ catalysis.³⁴ Among the screened ligands, Josiphos family showed the highest reactivity, with (R)-1-[(S)-2-(Dicyclohex-

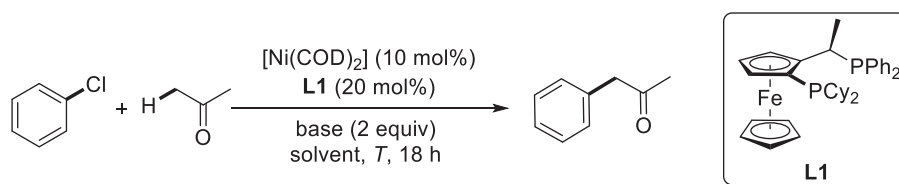
ylphosphino)ferrocenyl]ethyldiphenylphosphine (**L1**) affording the best results (**Scheme 22**). Unfortunately, very low reactivity was observed using similar ferrocene-based diphosphine ligands (**L2**, **L3**, **L4** and **dppf**). This type of ligands have been recently shown to be efficient for Ni-catalyzed cross-coupling of small molecules including ammonia,^{49,45,50} but they have not been used for nickel catalyzed arylation of carbonyl derivatives. The yield of the reaction is significantly reduced when an equimolar amount instead of two equivalents of ligand **L1** is used with respect to nickel (40 % vs. 72 %). A control experiment carried out in the absence of the ligand resulted in no product formation. More strikingly, all the other evaluated ligands, including diphosphine type ligands such as (*R*)-**BINAP**, **dppf**, **Xantphos** and **dcype** as well as monophosphines (**PCy₃**, **PPh₃**), monodentate and bidentate NHC's (**SIPr**, **ICy**, **IMes^{Me}**, **Bis^{Me}-NHC**) proved ineffective under these reaction conditions.



Scheme 22: Evaluation of ligands for the α -arylation of acetone with chlorobenzene. ^[a] Yields determined by ¹H NMR spectroscopy using 1,3,5-trimethoxybenzene as internal standard. Dipp = 2,6-diisopropylphenyl. *with 4-chloroanisole in toluene.

2. Optimization experiments

Different bases, solvents and reaction conditions were also surveyed with the nickel/Josi-phos (**L1**) catalytic system using the α -arylation of acetone with chlorobenzene as model reaction (**Table 2**). The best reaction conditions remained those previously established where the reaction was carried out in trifluorotoluene using CsF as a base, Ni(COD)₂ (10 mol%) and JosiPhos (**L1**) (20 mol%), giving the desired α -arylated acetone in 72% isolated yield (entry 6, **Table 2**). Remarkably, the mono α -arylation product was obtained selectively without any traces of bis-arylation product. Decreasing the temperature to 100 °C led to significant diminution of the yield (entry 11, **Table 2**).

Table 2: Base, solvent and temperature screening for the α -arylation of acetone with chlorobenzene^[a]

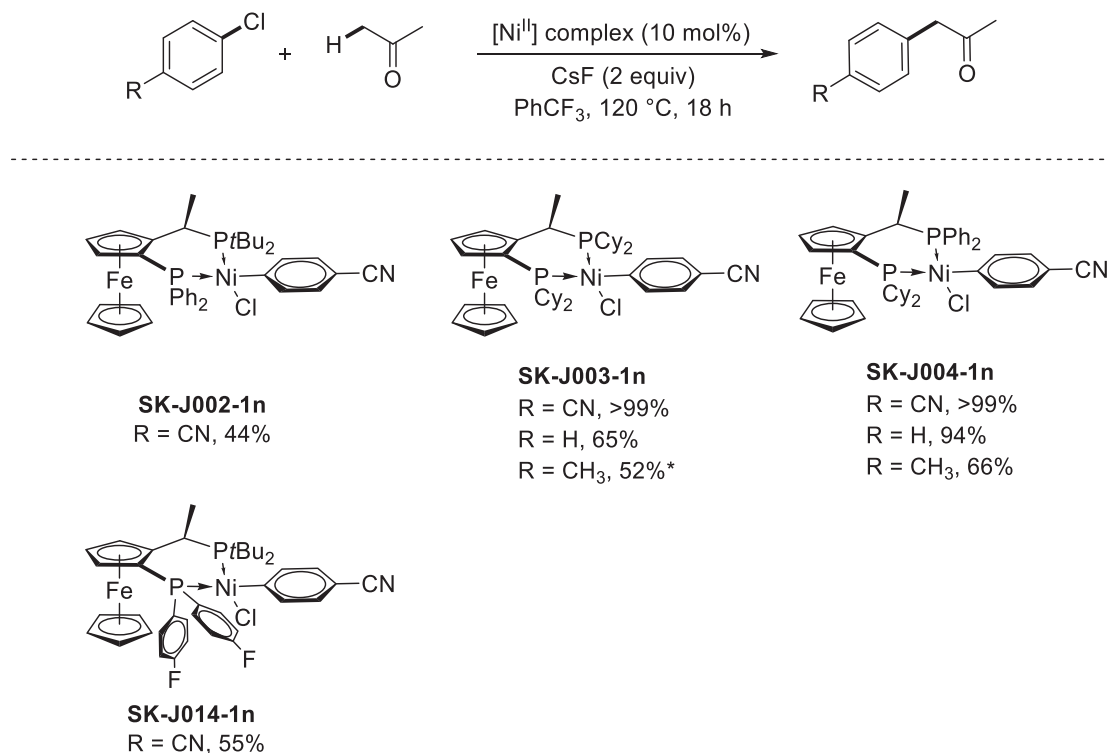
Entry	Solvent	Base	T , °C	Yield, %
1	toluene	CsF	120	62
2	toluene	Cs ₂ CO ₃	120	55
3	toluene	K ₃ PO ₄	120	48
4	toluene	NaO ^t Bu	120	33
5	toluene	NEt ₃	120	0
6	PhCF ₃	CsF	120	72
7	toluene/PhCF ₃ = 1:1	Cs ₂ CO ₃	120	54
8	diglyme	CsF	120	36
9	dioxane	CsF	120	43
10	DME	CsF	120	59
11	PhCF ₃	CsF	100	41
12	PhCF ₃	CsF	25	0

^[a] Reactions performed under the standard conditions on 0.3 mmol scale using 1 equiv of chlorobenzene and 30 equiv acetone. Yields determined by ¹H NMR spectroscopy using 1,3,5-trimethoxybenzene as internal standard.

Finally, non-polar solvents like PhCF₃ and toluene are the best for the transformation. Aprotic coordinating solvents like dioxane, diglyme and DME gave a less efficient catalytic system probably due to their interaction with the metallic center. Mild bases like CsF and Cs₂CO₃ perform very well. In contrast to what was observed previously,³⁴ strong bases like NaO^tBu give lower yields, indicating that the transmetallation via enolate is a forbidden transition.

3. Screening of Ni^{II} air stable complexes

We evaluated four commercially available Ni^{II} catalysts for the selective α -arylation of acetone (**Scheme 23**). The complexes were active, **SK-J003-1n** and **SK-J004-1n** showing exceptional reactivity being more effective than the $\text{Ni}(\text{COD})_2/\text{J004}$ catalytic system. We screened these complexes with several substrates, **SK-J004-1n** showed superior reactivity and unique selectivity affording solely the desired product in excellent yields.



Scheme 23: Evaluation of commercially available Ni^{II} precursors for the α -arylation of acetone. ^[a] Reactions were performed with ArCl (0.3 mmol, 1 equiv.), acetone (9 mmol, 30 equiv.), CsF (0.6 mmol, 2 equiv.), $[\text{Ni}]$ (10 mol%) and PhCF_3 (1 mL). The reaction mixture was stirred for 18 hours at 120°C . Yields determined by ^1H NMR spectroscopy using 1,3,5-trimethoxybenzene as internal standard. *with 50/50 ratio of C-C and C-O coupling.

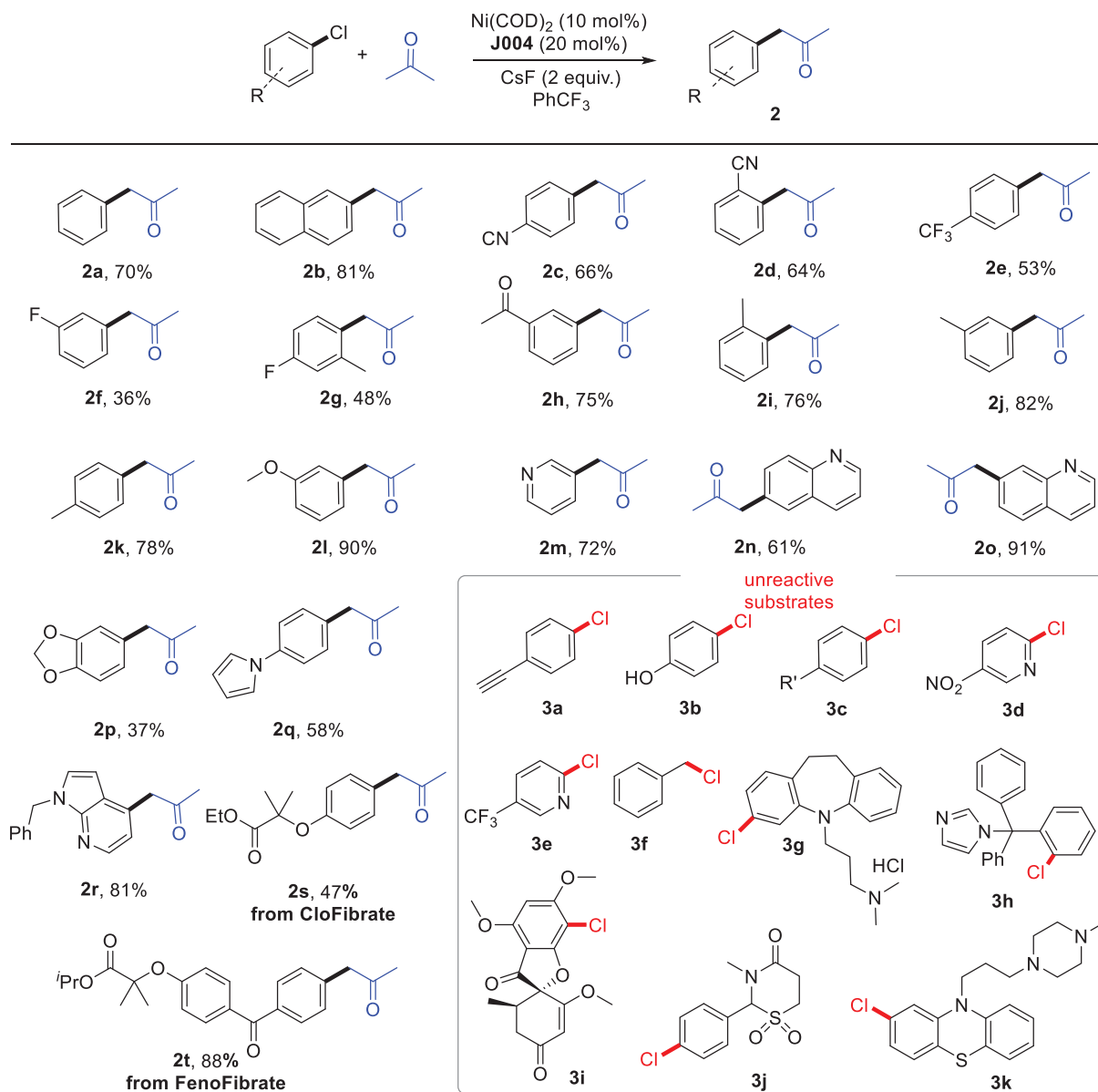
III. *Scope of the reaction*

1. General scope with aryl chlorides

With optimal conditions in hand, the scope of the reaction was examined with a wide range of aryl chlorides, including extended π -electron 2-chloronaphthalene, chloroarenes bearing electron-withdrawing or electron-donating substituents, and heteroarenes. In all cases examined, mono-arylated products were obtained selectively as the sole product of the reaction (**Scheme 24**). The arylation of acetone with electron-poor aryl chlorides could be achieved in moderate to good yields. Para- and ortho-substituted cyano aryl chlorides were converted selectively with good yields (**2c**, **2d**). Fluorinated compounds were also obtained in 30 % yield (**2e–2g**). Full selectivity toward the arylation of acetone was achieved with 3-chloroacetophenone affording compound (**2h**) in very good isolated yield. Interestingly, employment of electron-rich aryl chlorides delivered the corresponding products in excellent yields (**2j**, **2l**). The cross-coupling could tolerate pyridines, quinolinones (**2m–2o**), benzodioxoles (**2q**), pyrroles (**2q**), and azaindoles (**2q**) in good to excellent yields. Furthermore, the developed methodology was also amenable to the functionalization of biologically relevant aryl chlorides. Indeed, Clofibrate (**Atromid-S®**) as well as Fenofibrate (**Tri-Cor®**), both used for treatment of abnormal blood lipid levels, were successfully converted to the corresponding mono α -arylated product with moderate to excellent yields (**2s** and **2t**).

In the other hand, a substrate bearing an acetylenic group (**3a**) was unreactive probably due to coordination of the alkyne to the metallic center. In addition, reactions with substrates having unprotected acidic protons did not proceed (**3b**, **3c**). In contrast of having pyridines active, 2-chloropyridine derivatives (**3d**, **3e**) were unreactive, probably due to the interaction of the nitrogen

atom at ortho position with the metallic center generating a dormant catalytic system. More strikingly, benzyl chloride (**3f**) and few other chlorinated drugs (**3g-3k**) were unreactive under these conditions.

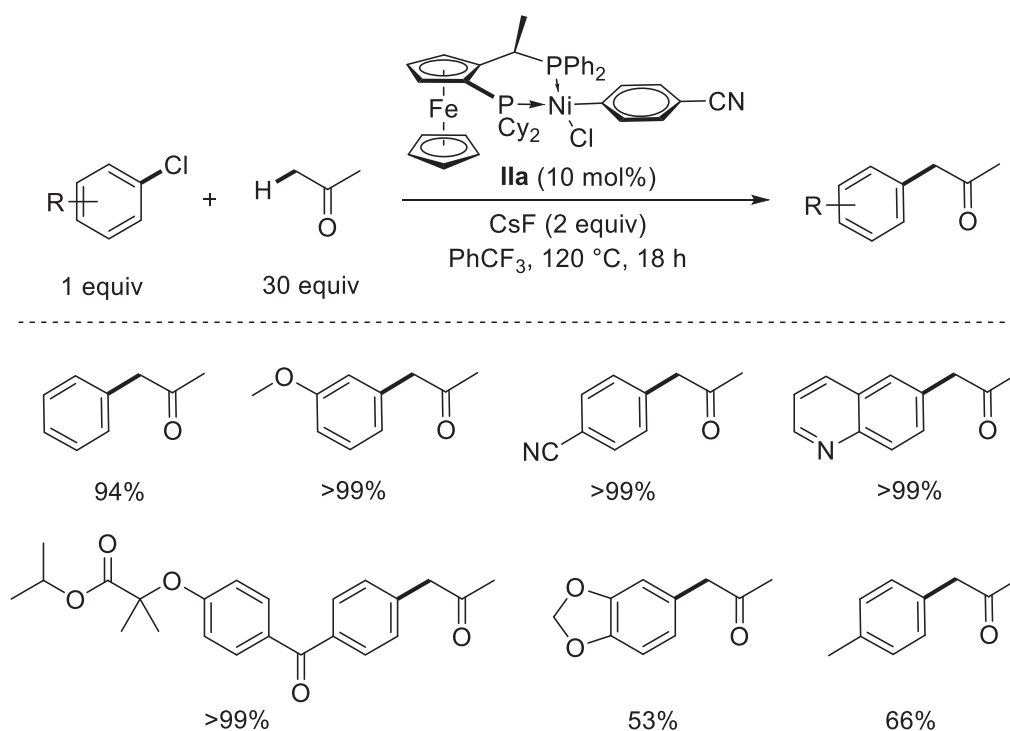


Scheme 24: Aryl chlorides scope. Reactions were performed with PhCl (0.3 mmol, 1 equiv.), acetone (9 mmol, 30 equiv.), CsF (0.6 mmol, 2 equiv.), Ni(COD)₂ (10 mol%), ligand (20 mol%) and PhCF₃ (1 mL). The reaction mixture was stirred for 18 hours at 120 °C. Yields shown are those of isolated products.^b Yields determined by ¹H NMR spectroscopy using 1,3,5-trimethoxybenzene as internal standard.^c Cs₂CO₃ instead of CsF. R': piperazine.

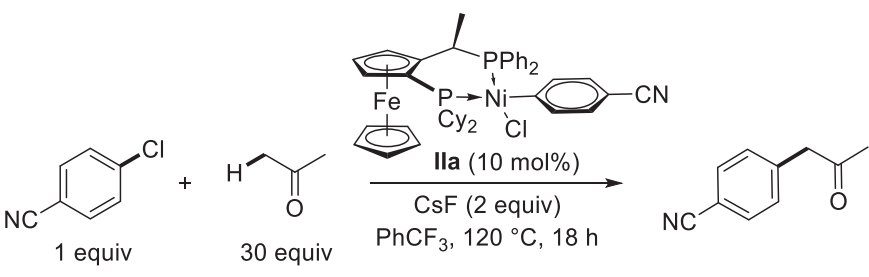
2. Scope with Ni^{II} pre-catalysts

Interestingly, compared to Ni^0 species, the aryl Ni^{II} complex **SK-J004-1n (IIa)** showed enhanced catalytic activity. Based on these observations, the catalytic cross-coupling of a set of aryl chlorides was re-evaluated using complex **IIa** as pre-catalyst (**Table 3**). From a practical point of view, Ni^{II} complex **IIa** offers several advantages: it is air stable, commercially available, and features enhanced catalytic efficiency. Furthermore, the reaction can proceed at lower temperature (95% yield at 80 °C), at shorter reaction time (65% yield after 1h) and the catalyst loading could be reduced down to 1 mol% while maintaining substantial activity (**Table 4**).

Table 3: Substrate scope using nickel(II) complex **IIa** as a catalyst^[a]



^[a] Reactions performed under the standard conditions on 0.3 mmol scale. Yields determined by 1H NMR spectroscopy using 1,3,5-trimethoxybenzene as internal standard.

Table 4: Optimization of the reaction conditions of the α -arylation of acetone using **IIa** as a catalyst^[a]


Entry	Variation from standard conditions	Yield (%)
1	none	>99
2	5 mol% of IIa instead of 10 mol%	>99
3	1 mol% of IIa instead of 10 mol%	47
4	1h instead of 18h	65
5	80 °C instead of 120 °C	95

^[a] Reactions performed under the standard conditions on 0.3 mmol scale. Yields determined by ¹H NMR spectroscopy using 1,3,5-trimethoxybenzene as internal standard.

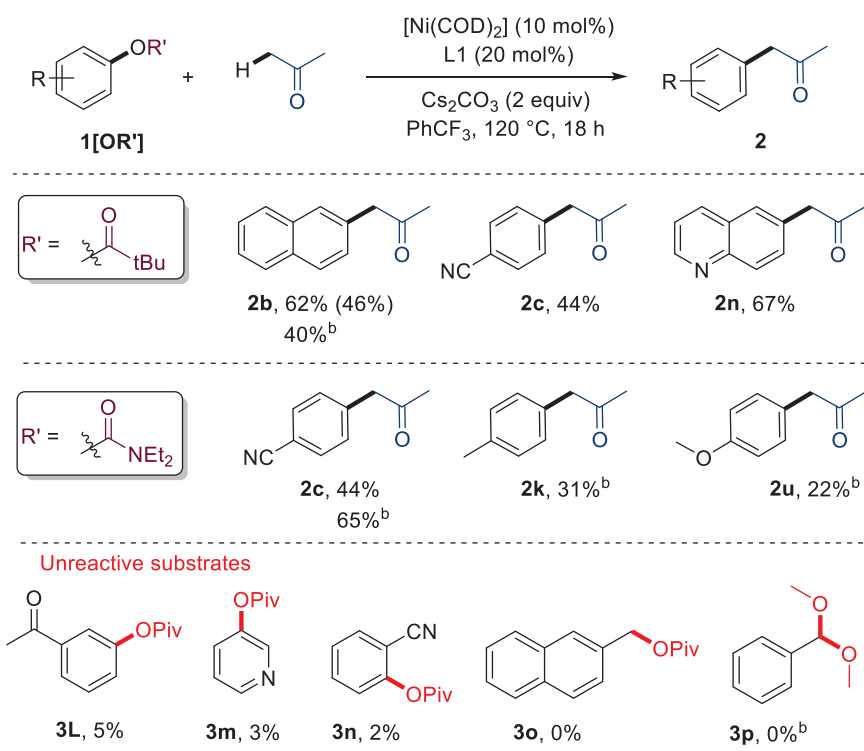
Even though two equivalents of **L1** was essential for Ni⁰ system, an equimolar loading was sufficient with **complex IIa**. This could be attributed to the release of 4-(2-oxopropyl)benzonitrile (**2c**) product (10 mol%) that could protect and stabilize the Ni⁰ catalyst by η^2 -coordination of the cyano group.³⁴

3. Reaction with phenol derivatives

In order to further emphasize the complementarity of this nickel-catalyzed process with the precedent methods using palladium catalysts (**section III**), some phenol derivatives were evaluated as electrophiles (**Table 5**). Very satisfyingly, a primary selection of aryl pivalates as well as aryl carbamates were found to be suitable substrates for arylation providing the corresponding products in moderate to good yields (**2b-2u**). Although the conditions have not been optimized with phenol

derivatives, it is worth noting that the coupling reaction is not limited to π -extended aryl substrates.⁵¹ In addition, Cs_2CO_3 was more reactive with aryl pivalates while CsF was more effective with aryl carbamates.

Table 5: α -Arylation of acetone with phenol derivatives^[a]



^[a] Reactions were performed with ArOR' (0.3 mmol, 1 equiv.), acetone (9 mmol, 30 equiv.), base (0.6 mmol, 2 equiv.), $\text{Ni}(\text{COD})_2$ (10 mol%), L1 (20 mol%) and PhCF_3 (1 mL). The reaction mixture was stirred for 18 hours at 120 °C. Yields determined by ^1H NMR spectroscopy using 1,3,5-trimethoxybenzene as internal standard. Yield in parentheses refers to isolated yield. ^[b] CsF instead of Cs_2CO_3 .

On the other hand, few (hetero)aryl substrates that were active as chloride derivatives (**3l-3n**) are poorly active as pivalates. More strikingly, in contrast of having high reactivity with naphthalene pivalate derivatives (**2b**, **2n**), naphthalene-methyl pivalate was completely unreactive (**3o**). The more challenging dimethoxymethyl acetal (**3p**) did not succeed limiting the reactivity of this system to carbamates and pivalates. In contrast with aryl pivalates and carbamates, aryl ethers were completely unreactive under these catalytic conditions.

4. Scope of ketones

We explored the efficiency of our methodology towards a series of cyclic and substituted ketones (**Table 6**). Among the examined ketones, the reaction proceeded only with less sterically hindered alkyl ketones (pentanone and butanone). The experimental trend clearly shows that the catalytic system is sensitive to steric parameters. Furthermore, direct cross-coupling of toluacetone (**3d**) which is the product generated from the coupling of acetone with 4-chlorotoluene, was completely unreactive even when used in large excess, (Entries 5-6, **Table 6**) indicating that the system is highly selective towards single monoarylation. The high steric hindrance of the Josiphos ligand (**L1**) most likely inhibits coordination of bulky ketones.

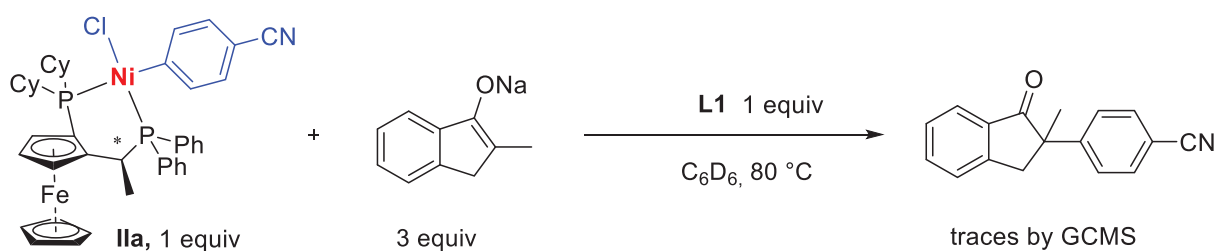
Since we are using a chiral diphosphine ligand (**L1**) in catalysis, we tried to explore it for stereoselective arylations with pentanone (**Table 6**). Unfortunately, in addition to obtaining very low yields, no stereoselectivity was observed. The Ni^0 system (Entries 10 and 11, **Table 6**) was more reactive but also induced very low enantioselectivity (Entry 9, **Table 6**). We hypothesized that the formed product could tautomerize at high temperatures, although decreasing the temperature to 80 °C did not improve the enantioselectivity (entry 11, **Table 6**).

Table 6: Evaluating several Ni^0 and Ni^{II} catalytic systems for Nickel-catalyzed α -arylation of ketones.^[a]

Ketones					
	3a	3b	3c	3d	
	3e	3f	3g	3h	
Entry	Ketone	[Ni]	T, °C	Yield (%)	E.r.
1	3a	IIa	120	0	-
2	3b	IIa	120	0	-
3	3c	IIa	120	0	-
4	3c	$\text{Ni}(\text{COD})_2/\text{L1}$	120	0	-
5	3d	IIa	120	0	-
6 ^[b]	3d	IIa	120	0	-
7	3e	IIa	120	0	-
8 ^[c]	3e	IIa	120	traces	-
9 ^[d]	3f	IIa	120	18	50:50
10 ^[d]	3f	$\text{Ni}(\text{COD})_2/\text{L1}$	120	26	60:40
11 ^[d]	3f	$\text{Ni}(\text{COD})_2/\text{L1}$	80	21	60:40
12	3g	IIa	120	19	-
13	3g	$\text{Ni}(\text{COD})_2/\text{L1}$	120	22	-
14	3h	IIa	120	0	-

^[a] Reactions performed under the standard conditions on 0.3 mmol scale with the corresponding ketones (20 equiv; 6.0 mmol). Yields determined by ^1H NMR spectroscopy using 1,3,5-trimethoxybenzene as internal standard. ^[b] 1 equiv of tolylacetone was used. ^[c] NaOtBu (0.6 mmol, 2 equiv) in toluene instead of CsF and PhCF_3 . ^[d] Products were isolated by column chromatography. Enantiomeric ratios were determined by chiral HPLC.

In contrast with that observed by the group of Hartwig,³⁴ the reaction of **IIa** with the sodium enolate of 2-methyl-1-indanone conducted at 80 °C in the presence of 1 equiv of **L1** did not afford the corresponding arylated product (**Scheme 25**). These results indicate that due to the high bulkiness and buried volume of the ligand **L1**, this catalytic system is selective towards small nucleophiles.⁴⁶

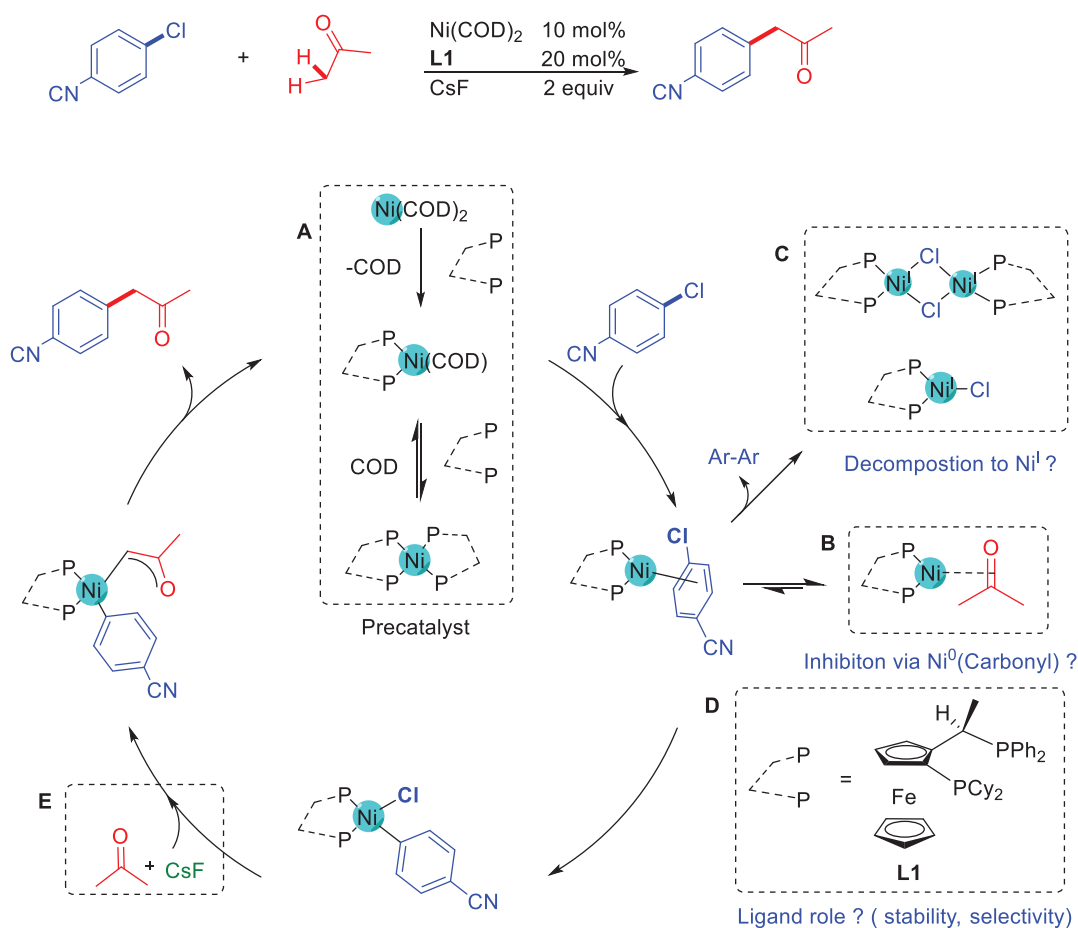


Scheme 25: Direct addition of sodium enolate to **IIa**.

IV. Mechanistic studies

1. Proposed mechanism and key questions

Having examined the scope and the complementarity of the nickel-catalyzed α -arylation of acetone methodology, we turned our attention to the reaction mechanism. Based on previous mechanistic work on nickel-catalyzed cross-coupling reactions with diphosphine ligands,^{34,52} it is reasonable to envision a $\text{Ni}^0/\text{Ni}^{\text{II}}$ pathway (**Scheme 26**).



Scheme 26: Proposed catalytic cycle with potential side reactions.

After the formation of the active pre-catalyst, coordination and oxidative addition of the substrate takes place forming the aryl Ni^{II} complex **IIa**, followed by cyclometallation and reductive elimination that regenerates the active pre-catalyst and releases the desired α -arylated ketone.

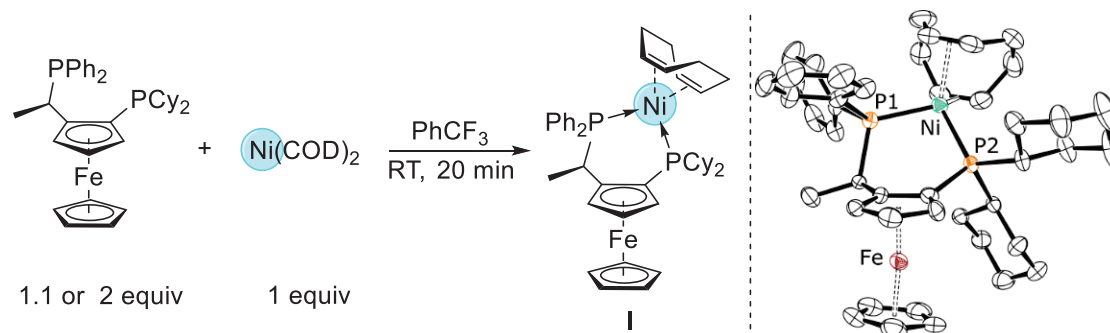
However, the feasibility of such a mechanism for the challenging α -arylation of acetone under the developed catalytic conditions raises some questions about: (i) the structure of the active Ni⁰ species, (ii) the possible inhibition via acetone coordination to Ni⁰, (iii) The stability of Ni^{II} intermediates at high temperatures (decomposition to Ni^I), and (iv) the key influence of the ancillary ligand. Thus we decided to carry out a series of stoichiometric and catalytic reactions to address these questions.

2. *Nature and reactivity of Ni⁰ active species*

The reaction of Ni(COD)₂ with two equivalents of chelating Josiphos ligands, as carried out in our catalytic protocol, may result in the competitive formation of 4-coordinate Ni⁰ species ligated by two Josiphos ligands,⁵³ raising the question of its reactivity in catalysis. Indeed, many Ni(bis-phosphine)₂ species are unreactive in catalysis, but a recent comprehensive study has shown that depending on the steric and electronic properties of the bis-phosphine ligands, the corresponding Ni(bis-phosphine)₂ complex may be susceptible to ligand exchange.⁵³ On the other hand, the generation of the desired (Josiphos)Ni(COD) species by dissociation of COD has been shown to be a difficult process that is generally favored upon addition of benzonitrile to generate a catalytically active benzonitrile ligated Ni⁰ species.⁴⁹

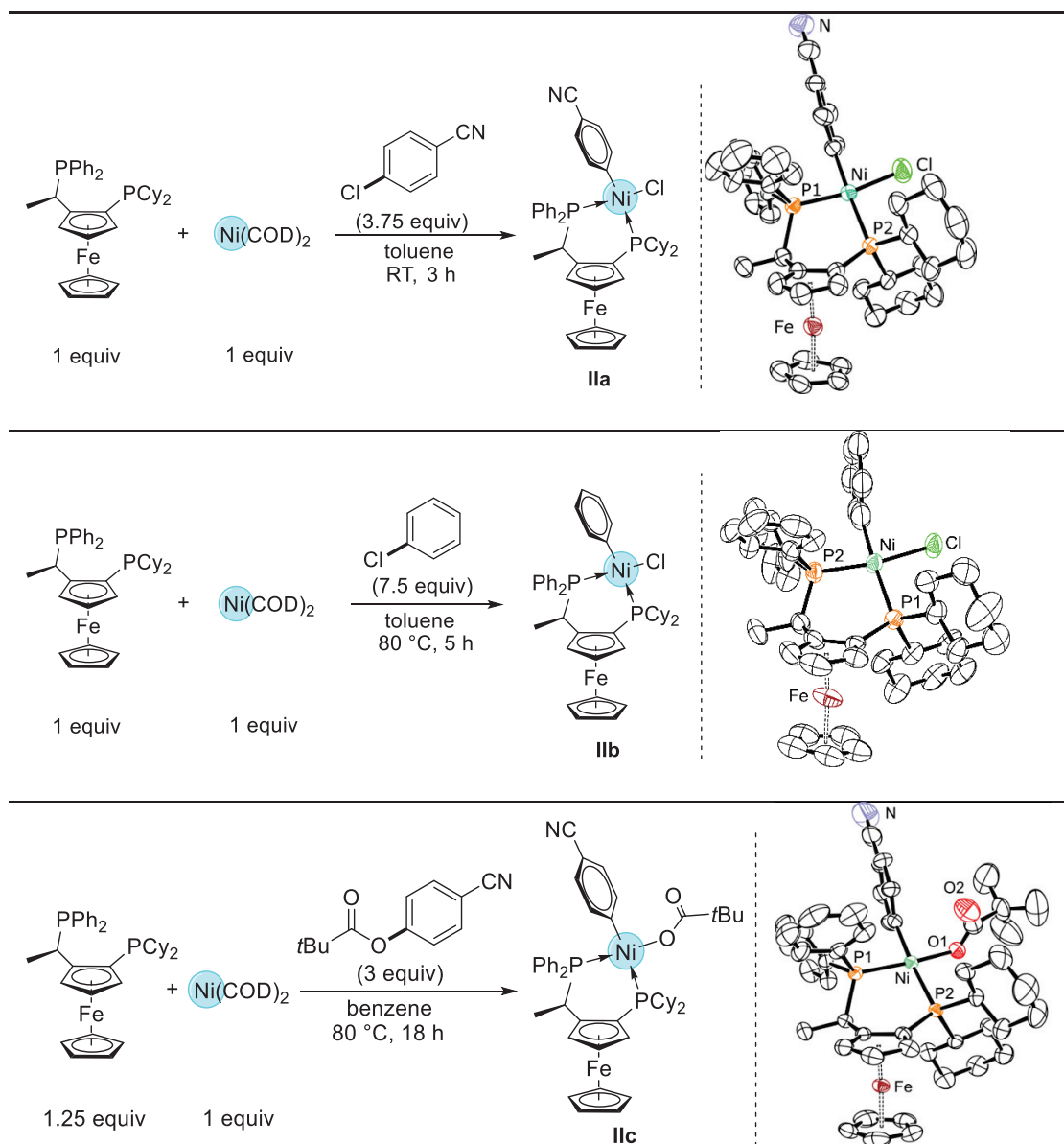
Following the same conditions as the catalytic protocol, we performed the reaction between Ni(COD)₂ and 2 equivalents of the ligand **L1** in trifluorotoluene. Under these conditions, the reaction occurred at room temperature and resulted in the rapid precipitation of complex **I**

[(L1)Ni(COD)]. Consistently, treatment of Ni(COD)₂ with 1.1 equivalent of the ligand also afforded rapid precipitation of complex **I** from trifluorotoluene, which was isolated in 88% yield. The complex was fully characterized in solution and in the solid state. Both NMR spectroscopic data and X-Ray diffraction analysis revealed the exclusive formation of a 4-coordinate nickel(0) species surrounded by the bidentate Josiphos ligand and the COD ligand featuring η^4 coordination (**Scheme 27**). The excess of the ligand remained free in the solution, as indicated by ³¹P{¹H} NMR analysis of the reaction mixture at room temperature. However, heating the solution of Ni(COD)₂ and 2 equivalents of **L1** in trifluorotoluene at 90°C for several hours resulted in the formation of complex **I** and a new species corresponding to (Josiphos)₂Ni, as indicated by ³¹P{¹H} NMR spectroscopy and HRMS analysis, in a 1:1 ratio.



Scheme 27: Synthesis of complex **I** (left) and molecular structure of **I** (right; hydrogen atoms are omitted for clarity).

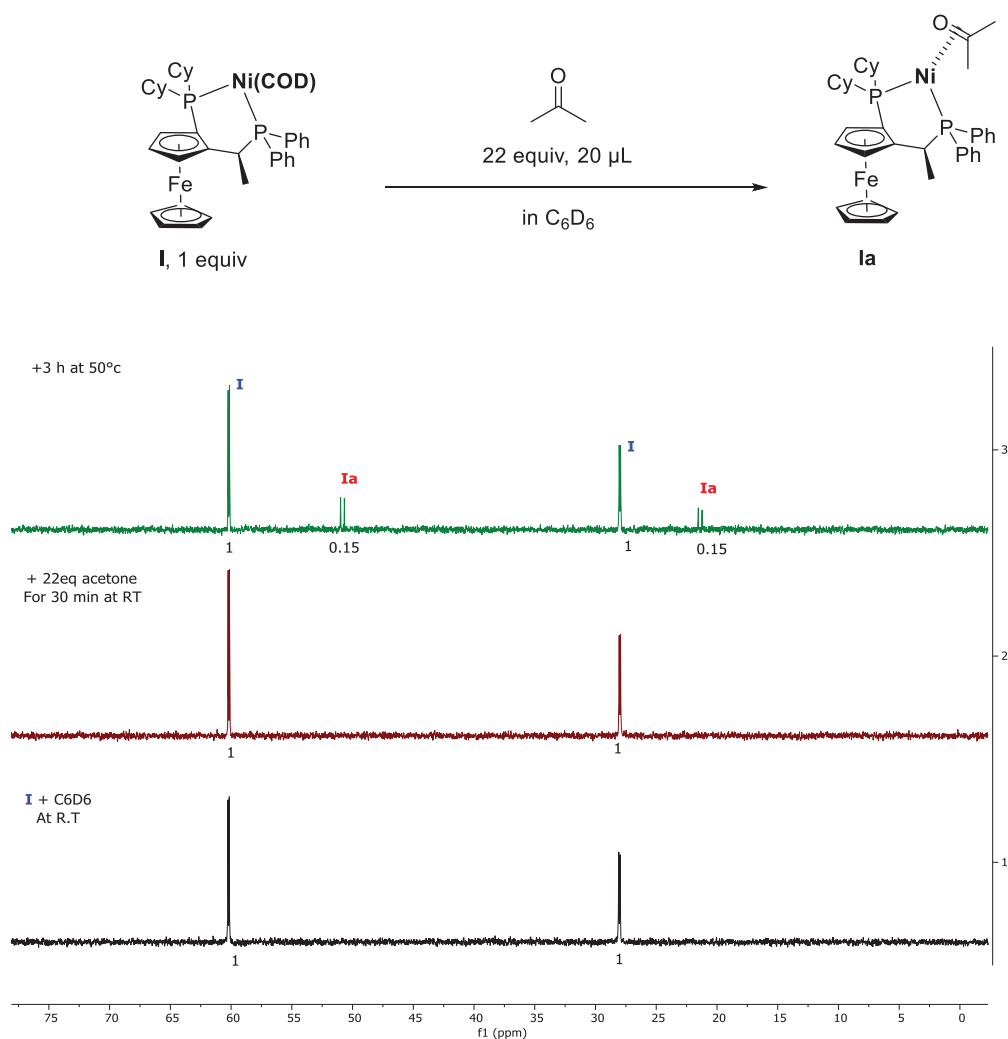
Then, we evaluated the reactivity of complex **I** with 4-chlorobenzonitrile, chlorobenzene and 4-cyanophenyl pivalate. These smoothly and quantitatively converted to the desired oxidative addition complexes **IIa**, **IIb** and **IIc**, which have been isolated in 98%, 65% and 62% yields, respectively. All complexes have been isolated and structurally characterized (**Scheme 28**). As expected, the less active unsubstituted chlorobenzene required heating at 80 °C to obtain similar yields.



Scheme 28: Oxidative addition of 4-chlorobenzonitrile, chlorobenzene and 4-cyanophenyl pivalate to $\text{Ni}(\text{COD})_2/\mathbf{1}$ (left) and molecular structures of **IIa**, **IIb** and **IIc** (right; hydrogen atoms and Et_2O solvent molecule are omitted for clarity).

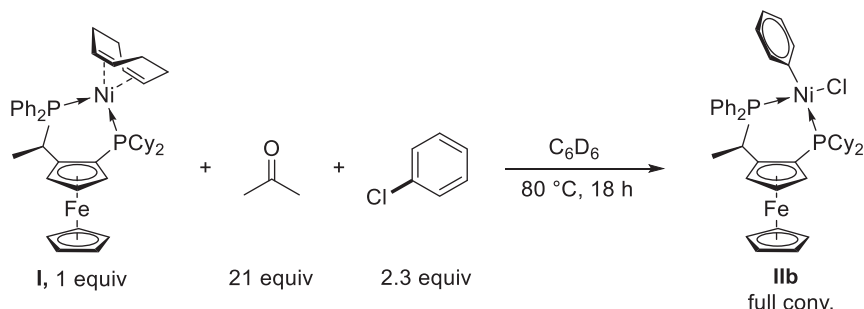
The presence of excess of carbonyl moiety has been shown to possibly inhibit the oxidative addition of aryl halides to Ni^0 species by leading to thermodynamically stable carbonyl ligated nickel(0) species.⁵⁴ Thus, we were interested in exploring the reactivity of Ni^0 species towards oxidative addition in the presence of an excess of coordinating and non-sterically hindered acetone.

The direct addition of an excess of acetone to (**I**) was monitored by ^{31}P -NMR spectroscopy (**Scheme 29**). The addition of acetone does not have any influence on the complex at RT. However, heating the reaction mixture for 3 h at 50 °C resulted in the formation of a new species in 15% ^{31}P -NMR spectroscopic yield that has been assigned to the acetone adduct (**Ia**). Further heating from 80 to 120 °C led to complete decomposition to unidentified species. These results suggests the formation of an equilibrium between the two coordinating species COD and acetone. The formation of the acetone adduct is not favored even in the presence of huge excess of acetone (22 equiv).



Scheme 29: Probing the effect of direct addition of acetone to **I** by ^{31}P -NMR.

In addition, the reaction of complex **I** with chlorobenzene was carried out in the presence of high excess of acetone, the oxidative addition complex (**IIb**) is formed in quantitative manner upon heating for 18h at 80 °C (**Scheme 30**).



Scheme 30: Oxidative addition of chlorobenzene in the presence of acetone.

Finally, addition of chlorobenzene to a 1:1 mixture of complex **I** and (**L1**)₂Ni(0) led to quantitative formation of the oxidative addition product **IIb**, indicating that (**L1**)₂Ni(0) is a reactive species. We hypothesized that the steric bulk of the Josiphos ligand, combined with the specific stereoelectronic properties imparted by the ferrocene backbone could be destabilizing for (Josiphos)₂Ni and induces facile displacement of one Josiphos ligand by chlorobenzene.

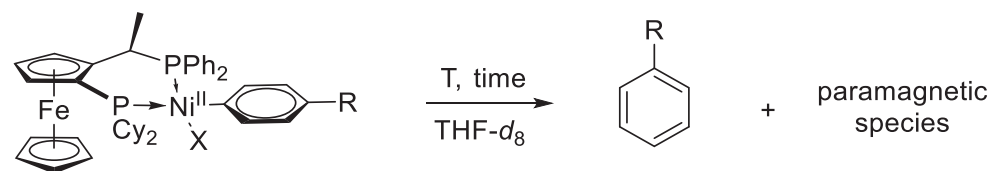
3. Thermal stability and reactivity of Ni^{II}–aryl intermediates

After oxidative addition and the formation of Ni^{II} complexes, decomposition to Ni^I species can take place smoothly via disproportionation especially at high temperatures. The formed Ni^I species are known to be less reactive than Ni^{II} species for α -arylation of indanones.³⁴ In our case, all the ensuing Ni^{II} aryl complexes were found to be stable in both the solid state and in solution. Remarkably, in contrast with those previously reported with Ni^{II} aryl complexes featuring BINAP,⁵⁵ DPPF,⁵² or Xantphos⁵⁶ ligands, complexes **IIa,b,c** are stable in solution even upon heating at 80 °C for several hours) (**Table 7**). Of note, bisphosphine ligated Ni^{II} aryl intermediates

generally require ortho-substituted aryl moieties to feature enhanced stability,⁵⁷ and very rapid decomposition to Ni^I species is observed with non-substituted phenyl moieties.^{52,55,56}

These results emphasize that chelating Josiphos ligand **L1** plays a key role in the stabilization of the Ni^{II} aryl intermediates towards decomposition to Ni^I species. Therefore, the higher propensity of Josiphos ligand to stabilize Ni^{II} intermediates compared to other diphosphines such as dppf or BINAP, is likely to be the key difference to achieve the challenging coupling reaction of aryl halides and pivalates with acetone.

Table 7: Decomposition study of **IIa**, **IIb** and **IIc**^[a]



IIa : X = Cl, R = CN

IIb : X = Cl, R = H

IIc : X = OPiv, R = CN

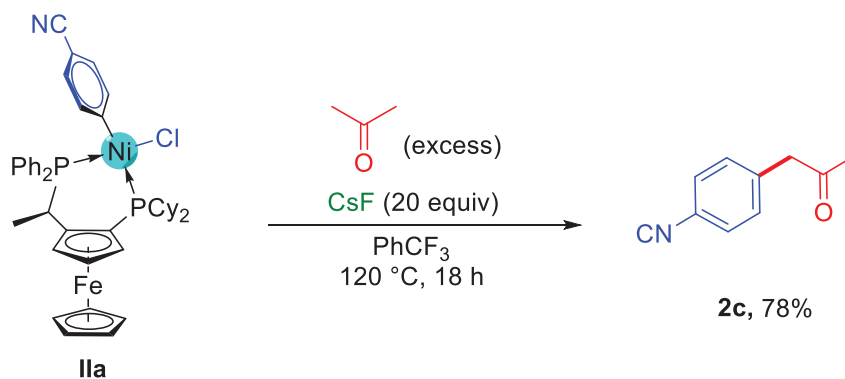
detected by GC-MS

complex	Entry	T, °C	Time	Decomposition (%)
IIa	1	80	2h	0
	2	100	+ 16h	55
	3	120	+ 1h40	60
	4	120	+ 1h45	62
	5	120	+ 22h	77
IIb ^[b]	1	80	18h	2
	2	120	+ 2h	50
	3	120	+ 3h15	>99
IIc ^[b]	1	100	3h	8
	2	120	+ 18h	55
	3	120	+ 18h	>99

^[a] The study was performed with the corresponding catalyst (0.03 mmol) in THF-*d*₈ (0.5 mL). R = H or CN. X = Cl or OPiv. ^[b] In C₆D₆ instead of THF-*d*₈. The percentage of decomposition was determined by integrating the characteristic ¹H NMR peaks of **IIa,b,c** with respect to the deuterated solvent residue.

In order to prove our proposition of a Ni⁰/ Ni^{II} catalytic cycle, the activity of the isolated oxidative addition complex **IIa** was tested directly with acetone (**Scheme 31**). Very satisfyingly,

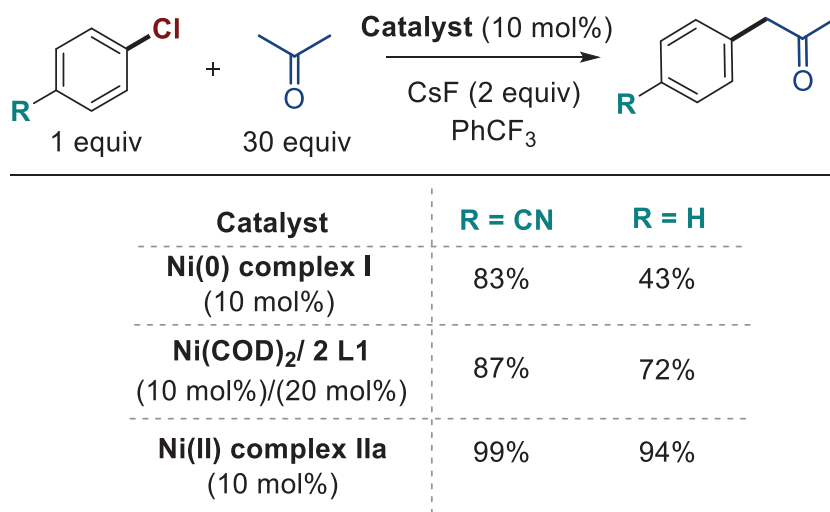
Nickel(II) complex **IIa** proved to be a reactive intermediate for the coupling with acetone affording the corresponding product **2c** in high yield (78%).



Scheme 31: Direct coupling of **IIa** with acetone.

4. Evaluation of catalytic competence of Ni⁰ and Ni^{II} intermediates

Finally, we evaluated the catalytic behavior of Ni⁰ and Ni^{II} species for the coupling of acetone with 4-chlorobenzonitrile and chlorobenzene (**Scheme 32**). In both cases, monitoring of the reactions by ³¹P{¹H} NMR spectroscopy indicated the presence of L1Ni(II)-Aryl species as the catalysts resting state. Overall, mechanistic studies support the occurrence of Ni⁰/Ni^{II} catalytic cycle as the main pathway. The influence of the second equivalent of ligand *vs.* Ni was analyzed by comparing the catalytic activity of complex **I** and Ni(COD)₂/2Josiphos (**Scheme 32**). While very similar results were obtained with 4-chlorobenzonitrile, the reaction yield is higher with electron neutral chlorobenzene with Ni(COD)₂/2Josiphos (72% yield *vs* 43% with **I**). These results indicate that (L1)₂Ni(0) intermediate, generated *in situ* during catalysis with an excess of ligand, is catalytically active and suggest that the second equivalent of ligand may enhance the stability of Ni⁰ species. In the case of 4-chlorobenzonitrile, the stability and activity of the Ni⁰ species can be improved by the η²-coordination of the cyano group of the substrate.



Scheme 32: Comparative catalytic activities of nickel species for the α -arylation of acetone with 4-chlorobenzonitrile and chlorobenzene. Reactions performed under the standard conditions on 0.3 mmol scale. Yields determined by ^1H NMR spectroscopy using 1,3,5-trimethoxybenzene as internal standard. Yields were calculated considering that 10% of product can be produced from the catalyst.

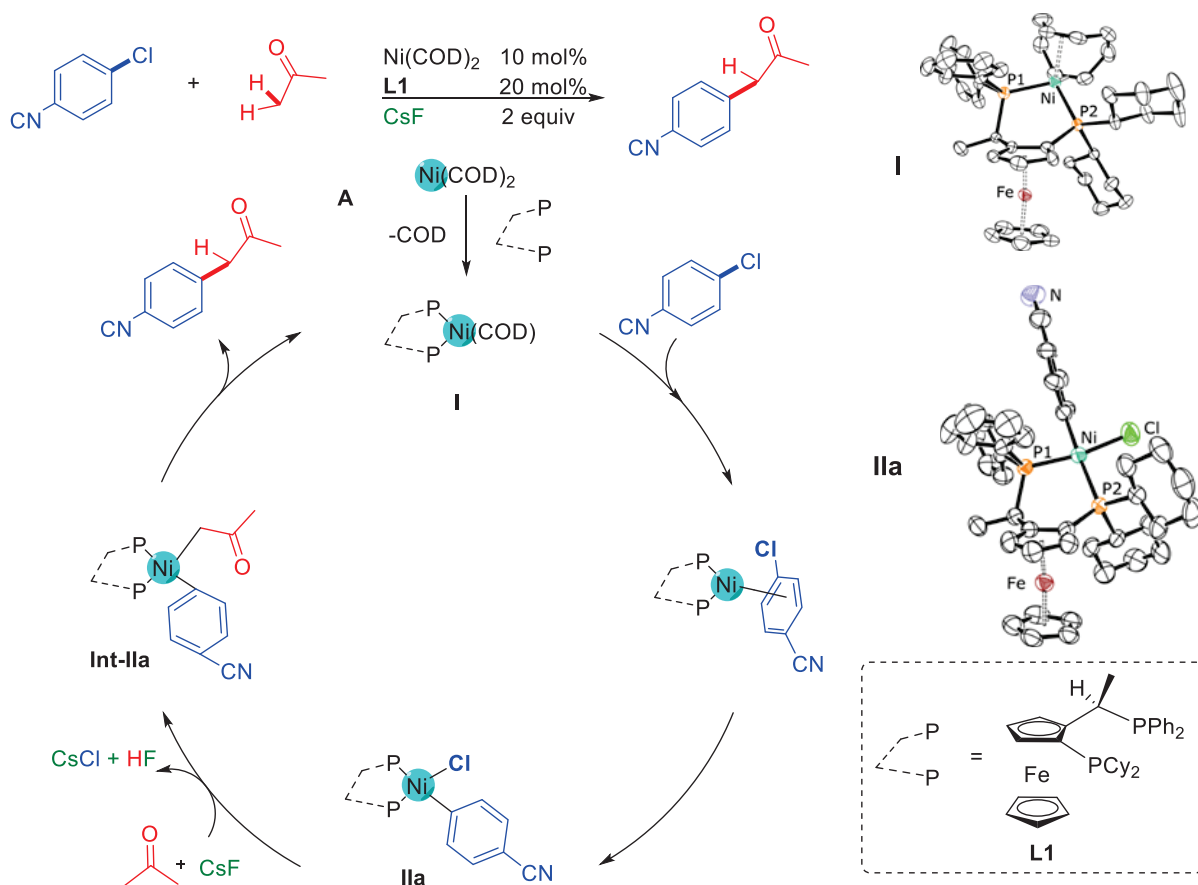
These results corroborate the occurrence of $\text{Ni}^0/\text{Ni}^{\text{II}}$ mechanism and emphasize that chelating Josiphos ligand **L1** plays a key role in the stabilization of the Ni^{II} aryl intermediates towards decomposition to Ni^{I} species. Therefore, the higher propensity of Josiphos ligand to stabilize Ni^{II} intermediates compared to other diphosphines such as Dppf or BINAP, is likely to be the key difference to achieve the challenging coupling reaction of aryl halides and pivalates with acetone.

V. Summary

In conclusion, we developed a new methodology for the selective mono- α -arylation of acetone with aryl chlorides and phenolic derivatives using earth abundant and cost effective nickel as efficient catalysts. Key to implementing this methodology was the privileged structure of Josiphos ligand **L1**. The catalytic system demonstrated a high compatibility with several functional

groups and the desired products are usually obtained in good to excellent yield. Interestingly, complex structures could also be encompassed in the substrate scope. Furthermore, the methodology has been extended to the unprecedented coupling of acetone with phenol derivatives.

Mechanistic studies allowed the isolation and characterization of key Ni^0 and Ni^{II} catalytic intermediates (**I**, **IIa**, **IIb**, **IIc**). The difference in reactivity between Ni/Josiphos systems and other Ni/diphosphine catalyst systems likely results from enhanced stabilization of Ni^{II} -aryl intermediates with Josiphos ligands. Finally, we demonstrate that air and thermally stable Ni^{II} aryl complexes display enhanced catalytic activity providing a very practical protocol. Based on these results, we propose the $\text{Ni}^0/\text{Ni}^{\text{II}}$ mechanism described in (**Scheme 33**).



Scheme 33: Proposed mechanism for Nickel-catalyzed α -arylation of acetone.

VI. Experimental part

1. General remarks

All catalytic reactions were set up inside an inert atmosphere (Ar) glovebox, and worked up outside of the glovebox under air. Manipulations of air-sensitive compounds were performed using standard Schlenk-line and glovebox techniques. Oven-dried microwave reaction vial (Biotage® Microwave Reaction Kit-351521, 2-5 mL) were generally used. Anhydrous acetone was purchased from Sigma-Aldrich at the highest grade and degassed three times using freeze-pump-thaw technique prior to use. All other anhydrous solvents (DME, diglyme, benzotrifluoride, 1,4-dioxane, diethyl ether, dichloromethane, toluene) were purchased at the highest grade, degassed and stored over activated 4 Å molecular sieves. Deuterated solvents (C_6D_6 , toluene- d_8 , $CDCl_3$, CD_2Cl_2 and methanol- d_4) were degassed and stored over activated 4 Å molecular sieves. 1H , ^{13}C , ^{31}P and ^{19}F NMR spectra were recorded on Bruker Avance 300, 400 or 500 spectrometers at 298K unless otherwise stated. Chemical shifts (δ) are expressed in parts per million. 1H and $^{13}C\{^1H\}$ NMR spectra were recorded with reference to the solvent resonances (for $CDCl_3$, δ_H at 7.26 ppm, δ_C at 77.16 ppm; for C_6D_6 , δ_H at 7.16 ppm, δ_C at 128.06 ppm; for CD_2Cl_2 , δ_H at 5.32 ppm, δ_C at 53.84 ppm). The following abbreviations and their combinations are used: br, broad; s, singlet; d, doublet; t, triplet; q, quartet; sept, septet; m, multiplet. The 1H and ^{13}C NMR signals were attributed by means of 2D HSQC and HMBC experiments. Crude reaction products were identified using GC-MS analysis. NMR yields were determined by adding 1,3,5-trimethoxybenzene (δ_H ($CDCl_3$) = 6.08 (s, 3H), 3.75 (s, 9H) ppm) as an internal standard to the crude reaction mixtures and by integration of crude 1H NMR spectra. Flash chromatographies were performed using silica gel (40-63 μm). TLC analyses were carried out on pre-coated TLC-sheets ALUGRAM Xtra SIL G/UV₂₅₄. The plates were visualized using a 254 nm ultraviolet lamp. GC-MS analyses were performed

using Shimadzu GC-2010 Gas Chromatograph coupled to a GCMS-QP2010S mass spectrometer using helium as the carrier gas at a flow rate of 1.19 mL/min and an initial oven temperature of 60 °C. The column used was a Zebron 5ms (30 m length, 0.25 mm diameter and 0.25 μ m thickness) lined with a mass (EI 0.7 kV) detection system. The injector temperature was 250 °C. The detector temperature was 250 °C. HPLC analyses were done using a Shimadzu Prominence system equipped with a chiral polysaccharide-based columns from Phenomenex (Lux series). The high-resolution mass spectra (HRMS) were recorded by direct introduction in a positive and negative ion mode on a hybrid quadrupole time-of-flight mass spectrometer (MicroTOFQ-II, Bruker Daltonics, Bremen) with an Electrospray Ionization (ESI) ion source. The solutions were infused at 180 μ L/h. The mass range of the analysis was 50-1000 m/z and the calibration was done with sodium formate.

All reagents were purchased from commercial resources and used without further purification. Josiphos ligands were generously provided by Solvias. 1-benzyl-4-chloro-7-azaindole (**1r[Cl]**) was prepared according to a modified literature procedure.⁵⁸ Aryl pivalates 2-naphthyl pivalate (**1b[OPiv]**),⁵⁹ 4-cyanophenyl pivalate (**1c[OPiv]**),⁶⁰ 6-quinoliny pivalate (**1n[OPiv]**)⁶¹ and aryl carbamates 4-cyanophenyl *N,N*-diethyl *O*-carbamate (**1c[OC(O)NEt₂]**),⁶² 4-tolyl *N,N*-diethyl *O*-carbamate (**1k[OC(O)NEt₂]**),⁶³ 4-methoxyphenyl *N,N*-diethyl *O*-carbamate (**1u[OC(O)NEt₂]**)⁶⁴ were synthesized according to literature procedures.

2. Optimization experiments

a. General procedure (for ligand screening)

In a glovebox, a 5 mL microwave reaction vial equipped with a magnetic stir bar was charged with Ni(COD)₂ (10 mol%; 0.03 mmol, 8.3 mg), the appropriate ligand (20 mol%; 0.06 mmol) and benzotrifluoride (1 mL). After stirring the resulting solution for 5 minutes, chlorobenzene (1.0 equiv; 0.3 mmol; 30 μ L), acetone (30 equiv; 9.0 mmol; 0.66 mL) and CsF (2.0 equiv; 0.6 mmol; 91.5 mg) were sequentially added. The tube was sealed, removed from the glovebox and heated at 120 °C (preheated oil bath) for 18 h. Then the reaction mixture was cooled to room temperature, filtered over Celite®, and 1,3,5-trimethoxybenzene (0.33 equiv; 0.1 mmol; 16.8 mg) was added as an internal standard for ¹H NMR spectroscopy analysis. All volatiles were removed under reduced pressure and the crude product (in CDCl₃) was analyzed by ¹H NMR spectroscopy to determine the yield of the reaction.

b. General procedure for base, solvent and temperature screening

In a glovebox, a 5 mL microwave reaction vial equipped with a magnetic stir bar was charged with Ni(COD)₂ (10 mol%; 0.03 mmol, 8.3 mg), **L1** (20 mol%; 0.06 mmol; 35.6 mg) and the appropriate solvent (1 mL). After stirring the resulting solution for 5 minutes, chlorobenzene (1.0 equiv; 0.3 mmol; 30 μ L), acetone (30 equiv; 9.0 mmol; 0.66 mL) and the appropriate base (2.0 equiv; 0.6 mmol) were sequentially added. The tube was sealed, removed from the glovebox and heated at the appropriate temperature (preheated oil bath) for 18 h. Then the reaction mixture was cooled to room temperature, filtered over Celite®, and 1,3,5-trimethoxybenzene (0.33 equiv; 0.1 mmol; 16.8 mg) was added as an internal standard for ¹H NMR spectroscopic analysis. All volatiles were removed under reduced pressure and the crude product was analyzed by ¹H NMR spectroscopy in CDCl₃ to determine the yield of the reaction.

Note: Due to the poor solubility of CsF and other inorganic bases used, the intense stirring (750 rpm) is very important in this catalytic reaction.

c. General procedure (for screening of Ni^{II} air stable complexes)

In a glovebox, a 5 mL microwave reaction vial equipped with a magnetic stir bar was charged with the selected catalyst (10 mol%; 0.03 mmol) and benzotrifluoride (1 mL). After stirring the resulting solution for 5 minutes, the selected aryl chloride (1.0 equiv; 0.3 mmol), acetone (30 equiv; 9.0 mmol; 0.66 ml) and CsF (2.0 equiv; 0.6 mmol; 91.5 mg) were sequentially added. The tube was sealed, removed from the glovebox and heated at 120 °C (preheated oil bath) for 18 h. Then the reaction mixture was cooled to room temperature, filtered over Celite®, and 1,3,5-trimethoxybenzene (0.33 equiv; 0.1 mmol; 16.8 mg) was added as an internal standard for ¹H NMR spectroscopy. All volatiles were removed under reduced pressure and the crude product was analyzed by ¹H NMR spectroscopy in CDCl₃ to determine the yield of the reaction.

3. Scope

a. General procedure for aryl chlorides scope

In a glovebox, a 5 mL microwave reaction vial equipped with a magnetic stir bar was charged with Ni(COD)₂ (10 mol%; 0.03 mmol, 8.3 mg), **L1** (20 mol%; 0.06 mmol; 35.6 mg) and benzotrifluoride (1 mL). After stirring the resulting solution for 5 minutes and formation of an orange precipitate, the selected aryl chloride (1.0 equiv; 0.3 mmol), acetone (30 equiv; 9.0 mmol; 0.66 ml) and CsF (2.0 equiv; 0.6 mmol; 91.5 mg) were sequentially added. The tube was sealed, removed from the glovebox and heated at 120 °C (preheated oil bath) for 18 h. Then, the reaction mixture was cooled to room temperature, filtered over Celite®, and all volatiles were removed

under reduced pressure. The crude product was purified by flash chromatography on silica gel using appropriate mixtures of ethyl acetate and cyclohexane to give the desired α -aryl ketone.

b. General procedure for scope with air-stable Ni^{II} system

In a glovebox, a 5 mL microwave reaction vial equipped with a magnetic stir bar was charged with **IIa** (10 mol%; 0.03 mmol, 24 mg) and benzotrifluoride (1 mL). After stirring the resulting solution for 5 minutes, the selected aryl chloride (1.0 equiv; 0.3 mmol), acetone (30 equiv; 9.0 mmol; 0.66 mL) and CsF (2.0 equiv; 0.6 mmol; 91.5 mg) were sequentially added. The tube was sealed, removed from the glovebox and heated at 120 °C (preheated oil bath) for 18 h. Then the reaction mixture was cooled to room temperature, filtered over Celite®, and 1,3,5-trimethoxybenzene (0.33 equiv; 0.1 mmol; 16.8 mg) was added as an internal standard for ¹H NMR spectroscopy. All volatiles were removed under reduced pressure and the crude product was analyzed by ¹H NMR spectroscopy in CDCl₃ to determine the yield of the reaction.

c. General procedure for the scope of ketones

In a glovebox, a 5 mL microwave reaction vial equipped with a magnetic stir bar was charged with the selected catalyst system (**IIa** (10 mol%; 0.03 mmol, 24 mg) or the combination of Ni(COD)₂ (10 mol%; 0.03 mmol, 8.3 mg) with **L1** (20 mol%; 0.06 mmol; 35.6 mg)) and PhCF₃ (1 mL). After stirring the resulting solution for 5 minutes, 4-chlorobenzonitrile (1.0 equiv; 0.3 mmol; 41.2 mg), the corresponding ketone (20 equiv; 6.0 mmol) and CsF (2.0 equiv; 0.6 mmol, 91.1 mg) were sequentially added. The tube was sealed, removed from the glovebox and heated at 120 °C in a preheated oil bath for 18 h. Then the reaction mixture was cooled to room temperature, filtered over Celite®, and 1,3,5-trimethoxybenzene (0.33 equiv; 0.1 mmol; 16.8 mg) was added as an internal standard for ¹H NMR spectroscopic analysis. All volatiles were removed under reduced

pressure and the crude product was either isolated by flash chromatography (Ethyl acetate/Cyclohexane, gradient 0 to 70%) or analyzed by ^1H NMR spectroscopy in CDCl_3 to determine the yield of the reaction. The enantiomeric ratios were determined using chiral HPLC.

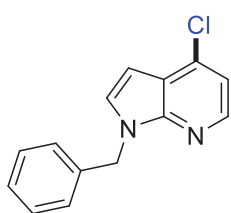
d. General procedure for scope of phenol derivatives

In a glovebox, a 5 mL microwave reaction vial equipped with a magnetic stir bar was charged with $\text{Ni}(\text{COD})_2$ (10 mol%; 0.03 mmol, 8.3 mg), **L1** (20 mol%; 0.06 mmol; 35.6 mg) and benzotrifluoride (1 mL). After stirring the resulting solution for 5 minutes and formation of orange precipitation, the selected phenol derivative (1.0 equiv, 0.3 mmol), acetone (30 equiv; 9.0 mmol; 0.66 mL) and CsF (2.0 equiv; 0.6 mmol; 91.2 mg) or Cs_2CO_3 (2.0 equiv; 0.6 mmol; 195.5 mg) were sequentially added. The tube was sealed, removed from the glovebox and heated at 120 °C (pre-heated oil bath) for 18 h. Then the reaction mixture was cooled to room temperature, filtered over Celite®, and 1,3,5-trimethoxybenzene (0.33 equiv; 0.1 mmol; 16.8 mg) was added as an internal standard for ^1H NMR spectroscopy analysis. All volatiles were removed under reduced pressure and the crude product (in CDCl_3) was analyzed by ^1H NMR spectroscopy to determine the yield of the reaction. In the case of 1-(naphthalen-2-yl)propan-2-one, the crude product was purified by flash chromatography (Ethyl acetate/Cyclohexane, gradient 0 to 10%).

4. Synthesis and characterizations

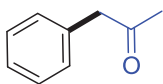
a. Preparation of 1-benzyl-4-chloro-7-azaindole (1r[Cl])

To an ice cooled solution of 4-chloro-7-azaindole (1.0 equiv; 2.00 mmol; 305 mg) in dry DMF (3 mL), NaH (60% dispersion in mineral oil, 1.1 equiv; 2.20 mmol, 88.0 mg) was added as a solid. After stirring the resulting solution at 0 °C for 1 hour, benzyl bromide (1.1 equiv, 2.20 mmol, 262 μ L) was added. The reaction mixture was allowed to stir at room temperature for 18 h, at which time it was quenched with ice-cold water (30 mL) and the product was extracted with ethyl acetate (3 x 30 mL). The combined organic layers were dried over Na₂SO₄, concentrated under reduced pressure, and purified by flash chromatography (SiO₂, ethyl acetate in cyclohexane, gradient 0 to 70%), affording the product as a colorless oil (370 mg, 76% yield).

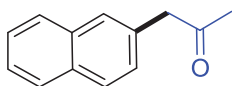


¹H NMR (300 MHz, CDCl₃): δ 8.11 (1H, d, J = 5.1 Hz), 7.20–7.06 (6H, m), 6.98 (1H, d, J = 5.1 Hz), 6.46 (1H, d, J = 3.6 Hz), 5.35 (2H, s, PhCH₂); **¹³C{¹H} NMR** (75 MHz, CDCl₃): δ 148.3 (s), 143.3 (s), 137.3 (s), 135.9 (s), 128.7 (s), 128.4 (s), 127.7 (s), 127.4 (s), 119.7 (s), 116.0 (s), 98.7 (s), 48.2 (s, PhCH₂). **HRMS** (ESI) m/z : [M+H]⁺ calcd. for C₁₄H₁₂ClN₂: 243.0684; Found:

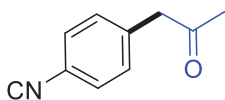
243.0679.

b. Isolation and characterization of α -aryl ketones

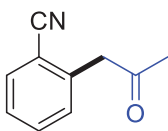
1-phenylpropan-2-one (2a). Known compound.⁶⁵ Purified by flash chromatography (Ethyl acetate/Cyclohexane, gradient 0 to 70%). Obtained as a colorless oil (0.029 g, 72% yield). $^1\text{H NMR}$ (300 MHz, CDCl_3): δ 7.31–7.06 (5H, m, C_6H_5), 3.62 (2H, s, CH_2), 2.08 (s, 3H, CH_3); $^{13}\text{C}\{^1\text{H}\}$ NMR (101 MHz, CDCl_3): δ 206.6 (s, C=O), 134.4 (s, *ipso*- C_6H_5), 129.5 (s, C_6H_5), 128.9 (s, C_6H_5), 127.2 (s, C_6H_5), 51.2 (s, CH_2), 29.4 (s, CH_3). **MS** (EI) m/z : $[\text{M}]^+$ 134.



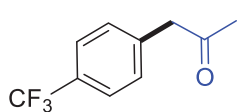
1-(naphthalen-2-yl)propan-2-one (2b). Known compound.⁵⁹ Purified by flash chromatography (Ethyl acetate/Cyclohexane, gradient 0 to 10%). Obtained as a colorless oil (0.045 g, 81% yield). $^1\text{H NMR}$ (300 MHz, CDCl_3): δ 7.88–7.78 (3H, m), 7.68 (1H, s), 7.53–7.43 (2H, m), 7.33 (1H, dd, $J = 8.4, 1.8$ Hz), 3.86 (2H, s, CH_2), 2.19 (3H, s, CH_3); ^{13}C NMR (75 MHz, CDCl_3): δ 206.5 (s, C=O), 133.7 (s), 132.6 (s), 131.9 (s), 128.6 (s), 128.2 (s), 127.8 (s), 127.7 (s), 127.5 (s), 126.4 (s), 126.0 (s), 51.3 (s, CH_2), 29.5 (s, CH_3). **MS** (EI) m/z : $[\text{M}]^+$ 184.



1-(4-isocyanophenyl)propan-2-one (2c). Known compound.⁶⁰ Purified by flash chromatography (Ethyl acetate/Cyclohexane, gradient 0 to 70%). Obtained as a white powder (0.033 g, 70% yield). $^1\text{H NMR}$ (300 MHz, CDCl_3): δ 7.63 (2H, d, $^3J_{\text{H-H}} = 8.3$ Hz), 7.30 (2H, d, $^3J_{\text{H-H}} = 8.3$ Hz), 3.79 (2H, s, CH_2), 2.22 (s, 3H, CH_3); $^{13}\text{C}\{^1\text{H}\}$ NMR (101 MHz, CDCl_3): δ 204.5 (s, C=O), 139.5 (s), 132.5 (s, C_6H_4), 130.5 (s, C_6H_4), 118.8 (s), 111.2 (s), 50.5 (s, CH_2), 29.9 (s, CH_3). **MS** (EI) m/z : $[\text{M}]^+$ 159.



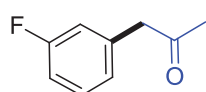
2-(2-oxopropyl)benzonitrile (2d). Known compound.⁶⁶ Purified by flash chromatography (Ethyl acetate/Cyclohexane, gradient 0 to 70%). Obtained as a colorless oil (0.031 g, 64% yield). $^1\text{H NMR}$ (300 MHz, CDCl_3): δ 7.67 (1H, dd, $J = 7.7, 1.2$ Hz), 7.57 (1H, td, $J = 7.7, 1.4$ Hz), 7.38 (1H, td, $J = 7.7, 1.1$ Hz), 7.31 (1H, d, $J = 7.8$ Hz), 3.99 (2H, s, CH_2), 2.30 (3H, s, CH_3); $^{13}\text{C}\{^1\text{H}\}$ NMR (126 MHz, CDCl_3): δ 203.7 (s, C=O), 138.3 (s), 133.1 (s, C_6H_4), 133.0 (s, C_6H_4), 131.0 (s, C_6H_4), 127.8 (s, C_6H_4), 117.9 (s, CN), 113.5 (s), 48.8 (s, CH_2), 30.3 (s, CH_3). **MS** (EI) m/z : $[\text{M}]^+$ 159.



1-(4-(trifluoromethyl)phenyl)propan-2-one (2e). Known compound.⁶⁰

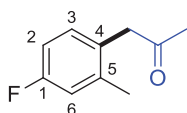
Purified by flash chromatography (Ethyl acetate/Cyclohexane, gradient 0 to 70%). Obtained as a white solid (0.032 g, 53% yield).

$^1\text{H NMR}$ (300 MHz, CDCl_3) δ 7.59 (2H, d, $^3J_{\text{H-H}} = 8.0$ Hz, C_6H_4), 7.31 (2H, d, $^3J_{\text{H-H}} = 8.0$ Hz, C_6H_4), 3.78 (2H, s, CH_2), 2.20 (3H, s, CH_3); $^{13}\text{C}\{^1\text{H}\}$ NMR (101 MHz, CDCl_3): δ 205.2 (s, C=O), 138.2 (s), 130.0 (s, C_6H_4), 129.5 (q, $^2J_{\text{C-F}} = 32.4$ Hz, CF_3), 125.7 (q, $^3J_{\text{C-F}} = 3.7$ Hz, C_6H_4), 124.3 (q, $^1J_{\text{C-F}} = 272.2$ Hz, CF_3), 50.5 (s, CH_2), 29.7 (s, CH_3); $^{19}\text{F NMR}$ (376 MHz, CDCl_3): δ -62.6. **MS** (EI) m/z : $[\text{M}]^+$ 202.



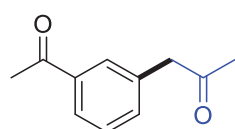
1-(3-fluorophenyl)propan-2-one (2f). Known compound.⁶⁰ Purified by flash chromatography (Ethyl acetate/Cyclohexane, gradient 0 to 70%). Obtained as a

colorless oil (0.025 g, 54% yield). $^1\text{H NMR}$ (300 MHz, CDCl_3): δ 7.34–7.26 (1H, m, C_6H_4), 7.01–6.90 (3H, m, C_6H_4), 3.70 (2H, s, CH_2), 2.18 (3H, s, CH_3); $^{13}\text{C}\{^1\text{H}\}$ NMR (101 MHz, CDCl_3): δ 205.6 (s, C=O), 163.0 (d, $^1J_{\text{C-F}} = 246.3$ Hz, FC), 136.6 (d, $^3J_{\text{C-F}} = 7.6$ Hz, CH_2), 130.3 (d, $^3J_{\text{C-F}} = 8.4$ Hz, C_6H_4), 125.3 (d, $^4J_{\text{C-F}} = 2.7$ Hz, C_6H_4), 116.6 (d, $^2J_{\text{C-F}} = 21.4$ Hz, C_6H_4), 114.2 (d, $^2J_{\text{C-F}} = 21.1$ Hz, C_6H_4), 50.6 (d, $^4J_{\text{C-F}} = 1.6$ Hz, CH_2), 29.6 (s, CH_3); $^{19}\text{F NMR}$ (282 MHz, CDCl_3): δ -112.9 (m). **MS** (EI) m/z : $[\text{M}]^+$ 152.



1-(4-fluoro-2-methylphenyl)propan-2-one (2g). Purified by flash chromatography (Ethyl acetate/Cyclohexane, gradient 0 to 70%). Obtained as a colorless oil (0.036 g, 73% yield).

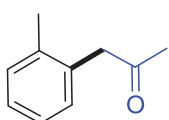
$^1\text{H NMR}$ (400 MHz, CDCl_3): δ 7.07 (1H, dd, $^3J_{\text{H-H}} = 8.0$ Hz, $^4J_{\text{H-F}} = 6.1$ Hz, H^3), 6.92–6.83 (2H, m, H^6 and H^2), 3.68 (2H, s, CH_2), 2.22 (s, 3H, C^5CH_3), 2.15 (s, 3H, C(O)CH_3); $^{13}\text{C}\{^1\text{H}\}$ NMR (101 MHz, CDCl_3): δ 206.1 (d, $^6J_{\text{C-F}} = 1.0$ Hz, C=O), 162.0 (d, $^1J_{\text{C-F}} = 245.0$ Hz, C^1F), 139.3 (d, $^3J_{\text{C-F}} = 7.9$ Hz, C^5CH_3), 131.8 (d, $^3J_{\text{C-F}} = 8.5$ Hz, C^3H), 129.0 (d, $^4J_{\text{C-F}} = 3.2$ Hz, C^4), 117.3 (d, $^2J_{\text{C-F}} = 21.2$ Hz, C^6H), 113.0 (d, $^2J_{\text{C-F}} = 21.1$ Hz, C^2H), 48.3 (s, CH_2), 29.4 (s, C(O)CH_3), 19.9 (d, $^4J_{\text{C-F}} = 1.1$ Hz, C^5CH_3); $^{19}\text{F}\{^1\text{H}\}$ NMR (376 MHz, CDCl_3): δ -116.1. **HRMS** (EI) m/z : $[\text{M}]^+$ calcd. for $\text{C}_{10}\text{H}_{11}\text{FO}$: 166.0788; Found: 166.0783.



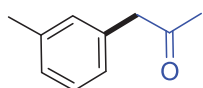
1-(3-acetylphenyl)propan-2-one (2h). Known compound.⁶⁷ Purified by flash chromatography (Ethyl acetate/Cyclohexane, gradient 0 to 70%).

Obtained as a colorless oil (0.039 g, 75% yield). $^1\text{H NMR}$ (400 MHz, CDCl_3): δ 7.86 (1H, dt, $^3J_{\text{H-H}} = 7.4$ Hz, $^4J_{\text{H-H}} = 1.6$ Hz, C_6H_4), 7.79 (1H, s, C_6H_4), 7.44 (1H, t, $^3J_{\text{H-H}}$

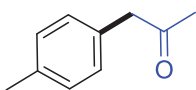
$_{\text{H}} = 7.5 \text{ Hz}$, C_6H_4), 7.40 (1H, dt, $^3J_{\text{H-H}} = 7.6 \text{ Hz}$, $^4J_{\text{H-H}} = 1.5 \text{ Hz}$, C_6H_4), 3.78 (2H, s, CH_2), 2.60 (3H, s, $\text{CH}_3\text{C}(\text{O})\text{Ar}$), 2.20 (3H, s, $\text{CH}_2\text{C}(\text{O})\text{CH}_3$); $^{13}\text{C}\{^1\text{H}\}$ NMR (101 MHz, CDCl_3): δ 205.6 (s, CH_2CO), 198.1 (s, ArCO), 137.6 (s, $\text{C}(\text{O})\text{C}$), 134.8 (s, CH_2C), 134.3 (s, C_6H_4), 129.3 (s, C_6H_4), 129.0 (s, C_6H_4), 127.3 (s, C_6H_4), 50.6 (s, CH_2), 29.7 (s, $\text{CH}_2\text{C}(\text{O})\text{CH}_3$), 26.8 (s, $\text{CH}_3\text{C}(\text{O})\text{Ar}$). HRMS (ESI) m/z : $[\text{M}+\text{H}]^+$ calcd. for $\text{C}_{11}\text{H}_{13}\text{O}_2$: 177.0910; Found: 177.0910.



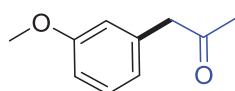
1-(*o*-tolyl)propan-2-one (2i). Known compound.⁶⁸ Purified by flash chromatography (Ethyl acetate/Cyclohexane, gradient 0 to 70%). Obtained as a colorless oil (0.034g, 76% yield). ^1H NMR (300 MHz, CDCl_3): δ 7.21–7.10 (4H, m), 3.71 (2H, s, CH_2), 2.25 (s, 3H, CH_3), 2.14 (s, 3H, COCH_3); $^{13}\text{C}\{^1\text{H}\}$ NMR (101 MHz, CDCl_3): δ 206.5 (s, CO), 137.0 (s), 133.3 (s), 130.6 (s, C_6H_4), 130.5 (s, C_6H_4), 127.5 (s, C_6H_4), 126.4 (s, C_6H_4), 49.3 (s, CH_2), 29.4 (s, CH_3), 19.7 (s, CH_3). MS (EI) m/z : $[\text{M}]^+$ 148.



1-(*m*-tolyl)propan-2-one (2j). Known compound.⁵⁹ Purified by flash chromatography (Ethyl acetate/Cyclohexane, gradient 0 to 30%). Obtained as a colorless oil (0.037 g, 82% yield). ^1H NMR (300 MHz, CDCl_3): δ 7.23 (1H, t, $^3J_{\text{H-H}} = 7.60 \text{ Hz}$), 7.09 (1H, d, $^3J_{\text{H-H}} = 7.8 \text{ Hz}$), 7.02 (1H, s), 7.01 (1H, d, $^3J_{\text{H-H}} = 7.8 \text{ Hz}$), 3.66 (1H, s, CH_2), 2.35 (1H, s, CH_3), 2.15 (1H, s, COCH_3); $^{13}\text{C}\{^1\text{H}\}$ NMR (101 MHz, CDCl_3): δ 206.7 (s, CO), 138.5 (s), 134.2 (s), 130.2 (s, C_6H_4), 128.7 (s, C_6H_4), 127.9 (s, C_6H_4), 126.5 (s, C_6H_4), 51.1 (s, CH_2), 29.3 (s, CH_3), 21.4 (s, CH_3). MS (EI) m/z : $[\text{M}]^+$ 148.

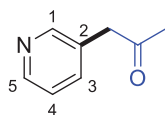


1-(*p*-tolyl)propan-2-one (2k). Known compound.⁵⁹ Purified by flash chromatography (Ethyl acetate/Cyclohexane, gradient 0 to 30%). Obtained as a colorless oil (0.035 g, 78% yield). ^1H NMR (300 MHz, CDCl_3): δ 7.15 (2H, d, $^3J_{\text{H-H}} = 8.0 \text{ Hz}$), 7.09 (2H, d, $^3J_{\text{H-H}} = 8.1 \text{ Hz}$), 3.65 (s, 2H, CH_2), 2.34 (s, 3H, CH_3), 2.14 (s, 3H, COCH_3); $^{13}\text{C}\{^1\text{H}\}$ NMR (101 MHz, CDCl_3): δ 206.8 (s, CO), 136.7 (s), 131.2 (s), 129.5 (s, C_6H_4), 129.3 (s, C_6H_4), 50.7 (s, CH_2), 29.2 (s, CH_3), 21.1 (s, CH_3). MS (EI) m/z : $[\text{M}]^+$ 148.

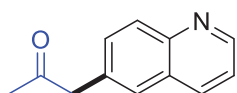


1-(3-methoxyphenyl)propan-2-one (2l). Known compound.⁶⁹ Purified by flash chromatography (Ethyl acetate/Cyclohexane, gradient 0 to 70%). Obtained as a yellow oil (0.045mg, 90% yield). ^1H NMR (300 MHz, CDCl_3):

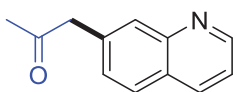
δ 7.25 (1H, t, $^3J_{\text{H-H}}=7.9$ Hz), 6.83–6.77 (2H, m), 6.75 (1H, t, $^4J_{\text{H-H}}=1.9$ Hz), 3.80 (3H, s, OCH_3), 3.66 (2H, s, CH_2), 2.15 (3H, s, CH_3); $^{13}\text{C}\{^1\text{H}\}$ NMR (101 MHz, CDCl_3): δ 206.5 (s, CO), 160.0 (s), 135.8 (s), 129.9 (s), 121.9 (s), 115.1 (s), 112.6 (s), 55.3 (s, OCH_3), 51.2 (s, CH_2), 29.3 (s, CH_3). MS (EI) m/z : $[\text{M}]^+$ 164.



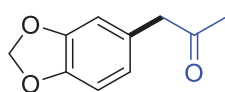
1-(pyridin-3-yl)propan-2-one (2m). Purified by flash chromatography (Ethyl acetate/Cyclohexane, gradient 0 to 70%). Obtained as a colorless oil (0.029 g, 72% yield). ^1H NMR (300 MHz, CDCl_3): δ 8.51 (1H, d, $^3J_{\text{H-H}}=4.1$ Hz, H^5), 8.44 (1H, s, H^1), 7.52 (1H, dt, $^3J_{\text{H-H}}=7.8$ Hz, $^4J_{\text{H-H}}=1.4$ Hz, H^3), 7.26 (1H, dd, $^3J_{\text{H-H}}=4.8$ Hz, $^3J_{\text{H-H}}=7.8$ Hz, H^4), 3.71 (2H, s, CH_2), 2.21 (3H, s, CH_3); $^{13}\text{C}\{^1\text{H}\}$ NMR (101 MHz, CDCl_3): δ 204.9 (s, CO), 150.6 (s, C^1), 148.6 (s, C^5), 137.1 (s, C^3), 129.9 (s, C^2), 123.6 (s, C^4), 47.7 (s, CH_2), 29.8 (s, CH_3). HRMS (ESI) m/z : $[\text{M}+\text{H}]^+$ calcd. for $\text{C}_8\text{H}_{10}\text{NO}$: 136.0757; Found: 136.0758.



1-(quinolin-6-yl)propan-2-one (2n). Purified by flash chromatography (Ethyl acetate/Cyclohexane, gradient 0 to 70%). Obtained as a colorless oil (0.034 g, 61% yield). ^1H NMR (300 MHz, CDCl_3): δ 8.88 (1H, d, $J=3.0$ Hz), 8.09 (2H, t, $J=8.3$ Hz), 7.63 (1H, d, $J=1.5$ Hz), 7.54 (1H, dd, $J=8.6, 1.9$ Hz), 7.38 (1H, dd, $J=8.3, 4.2$ Hz, 1H), 3.89 (2H, s, CH_2), 2.21 (3H, s, CH_3); $^{13}\text{C}\{^1\text{H}\}$ NMR (75 MHz, CDCl_3): δ 205.9 (s, CO), 150.5 (s, CH), 147.5 (s), 135.9 (s, CH), 132.7 (s), 131.3 (s, CH), 130.0 (s, CH), 128.4 (s), 128.1 (s, CH), 121.5 (s, CH), 50.8 (s, CH_2), 29.7 (s, CH_3). HRMS (ESI) m/z : $[\text{M}+\text{H}]^+$ calcd. for $\text{C}_{12}\text{H}_{12}\text{NO}$: 186.0913; Found: 186.0912.

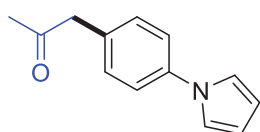


1-(quinolin-7-yl)propan-2-one (2o). Purified by flash chromatography (Ethyl acetate/Cyclohexane, gradient 0 to 70%). Obtained as a colorless oil (0.05 g, 91% yield). ^1H NMR (300 MHz, CDCl_3): δ 8.85 (1H, s), 8.09 (1H, d, $J=7.9$ Hz), 7.90 (1H, s), 7.74 (1H, d, $J=8.2$ Hz), 7.34 (2H, d, $J=7.5$ Hz), 3.87 (2H, s, CH_2), 2.17 (3H, s, CH_3); $^{13}\text{C}\{^1\text{H}\}$ NMR (76 MHz, CDCl_3): δ 205.8 (s, CO), 150.6 (s, CH), 148.1 (s), 136.0 (s, CH), 135.9 (s), 129.5 (s, CH), 128.3 (s, CH), 128.1 (s, CH), 127.2 (s), 121.1 (s, CH), 51.0 (s, CH_2), 29.6 (s, CH_3). HRMS (ESI) m/z : $[\text{M}+\text{H}]^+$ calcd. for $\text{C}_{12}\text{H}_{12}\text{NO}$: 186.0913; Found: 186.0910.



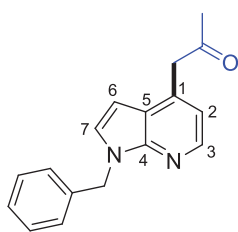
1-(benzo[d][1,3]dioxol-5-yl)propan-2-one (2p). Known compound.⁶⁰

Purified by flash chromatography (Ethyl acetate/Cyclohexane, gradient 0 to 70%). Obtained as a colorless oil (0.020 g, 37% yield). ¹H NMR (300 MHz, CDCl₃): δ 6.77 (1H, d, ³J_{H-H} = 7.8 Hz), 6.68 (1H, d, ⁴J_{H-H} = 1.6 Hz), 6.64 (1H, dd, ³J_{H-H} = 7.9 Hz, ³J_{H-H} = 1.4 Hz), 5.95 (2H, s, OCH₂O), 3.60 (2H, s, CH₂C=O), 2.15 (3H, s, C=O(CH₃)); ¹³C NMR (75 MHz, CDCl₃): δ 206.6 (s, C=O), 148.1 (s), 146.8 (s), 128.0 (s), 122.6 (s), 109.9 (s), 108.6 (s), 101.2 (s), 50.7 (s, CH₂C=O), 29.3 (s, C=O(CH₃)). MS (EI) *m/z*: [M]⁺ 178.



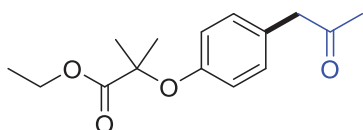
1-(4-(1H-pyrrol-1-yl)phenyl)propan-2-one (2q). Known compound.⁶⁰

Purified by flash chromatography (Ethyl acetate/Cyclohexane, gradient 0 to 70%). Obtained as a white solid (0.035 g, 58% yield). ¹H NMR (300 MHz, CDCl₃): δ 7.28 (2H, apparent d, *J* = 8.6 Hz, C₆H₄), 7.16 (2H, apparent d, *J* = 8.6 Hz, C₆H₄), 6.99 (2H, t, *J* = 2.2 Hz, C₄H₄N), 6.26 (2H, t, *J* = 2.2 Hz, C₄H₄N), 3.64 (2H, s, CH₂C=O), 2.11 (3H, s, C=O(CH₃)); ¹³C NMR (75 MHz, CDCl₃): δ 206.1 (s, C=O), 139.9 (s, C_{Ph}-N), 131.6 (s, C_{Ph}-CH₂), 130.7 (s, C₆H₄), 120.9 (s, C₆N₄), 119.4 (s, C₄H₄N), 110.6 (s, C₄H₄N), 50.2 (s, CH₂C=O), 29.5 (s, C=O(CH₃)). MS (EI) *m/z*: [M]⁺ 199.



1-(1-benzyl-1H-pyrrolo[2,3-b]pyridin-4-yl)propan-2-one (2r). Purified

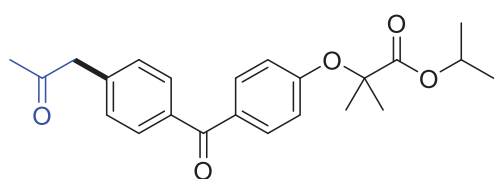
by flash chromatography (Ethyl acetate/Cyclohexane, gradient 0 to 70%). Obtained as a colorless oil (0.065 g, 81% yield). ¹H NMR (300 MHz, CDCl₃): δ 8.23 (1H, d, ³J_{H-H} = 4.8 Hz, H³), 7.24–7.11 (5H, m, C₆H₅), 7.10 (1H, d, ³J_{H-H} = 3.7 Hz, H⁷), 6.86 (1H, d, ³J_{H-H} = 4.8 Hz, H²), 6.39 (1H, d, ³J_{H-H} = 3.6 Hz, H⁶), 5.40 (2H, s, Ph-CH₂), 3.86 (2H, s, CH₂C=O), 2.07 (3H, s, C=O(CH₃)); ¹³C NMR (75 MHz, CDCl₃): δ 205.0 (s, C=O), 147.9 (s, C⁴), 143.4 (s, C³), 137.7 (s, *ipso*-C₆H₅), 135.5 (s, C¹), 128.8 (s, *m*-C₆H₅), 128.1 (s, C⁷), 127.7 (s, *p*-C₆H₅), 127.6 (s, *o*-C₆H₅), 120.5 (s, C⁵), 117.0 (s, C²), 98.5 (s, C⁶), 48.5 (s, CH₂C=O), 48.1 (s, PhCH₂), 29.5 (s, C=O(CH₃)). HRMS (ESI) *m/z*: [M+H]⁺ calcd. for C₁₇H₁₇N₂O: 265.1335; Found: 265.1335.



Ethyl-2-methyl-2-(4-(2-oxopropyl)phenoxy)propanoate (2s).

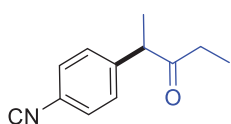
Purified by flash chromatography (Ethyl acetate/Cyclohexane, gradient 0 to 70%). Obtained as a colorless oil (0.037g, 47%

yield). **¹H NMR**(300 MHz, CDCl₃): δ 7.06 (2H, d, *J* = 8.7 Hz, C₆H₄), 6.80 (2H, d, *J* = 8.7 Hz, C₆H₄), 4.22 (2H, q, *J* = 7.1 Hz, CH₃CH₂O), 3.61 (2H, s, CH₂C=O), 2.12 (3H, s, C=O(CH₃)), 1.58 (6H, s, C(CH₃)₂), 1.24 (3H, t, *J* = 7.1 Hz, CH₃CH₂O); **¹³C NMR** (75 MHz, CDCl₃): δ 206.8 (s, (CH₂)C=O(CH₃)), 174.4 (s, C=O(OEt)), 154.7 (s, O-C_{Ar}), 130.2 (s, C₆H₄), 127.9 (s, CH₂-C_{Ar}), 119.5 (s, C₆H₄), 79.3 (s, OC(CH₃)₂), 61.5 (s, CH₃CH₂O), 50.3 (s, CH₂C=O), 29.3 (s, C=O(CH₃)), 25.5 (s, OC(CH₃)₂), 14.2 (s, CH₃CH₂O). **HRMS** (ESI) *m/z*: [M+Na]⁺ calcd. for C₁₅H₂₀NaO₄: 287.1254; Found: 287.1252.



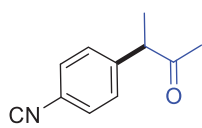
Isopropyl-2-methyl-2-(4-(4-(2-oxopropyl)benzoyl)phenoxy)propanoate (2t).

Purified by flash chromatography (Ethyl acetate/Cyclohexane, gradient 0 to 70%). Obtained as a yellow oil (0.101 g, 88% yield). **¹H NMR** (300 MHz, CDCl₃): δ 7.74 (4H, t, *J* = 8.9 Hz, C₆H₄), 7.30 (2H, d, *J* = 7.8 Hz, C₆H₄), 6.86 (2H, d, *J* = 8.4 Hz, C₆H₄), 5.08 (1H, sept, *J* = 6.3 Hz, CH(CH₃)₂), 3.79 (2H, s, CH₂C=O), 2.19 (3H, s, C=O(CH₃)), 1.65 (6H, s, OC(CH₃)₂), 1.20 (6H, d, *J* = 6.3 Hz, OCH(CH₃)₂); **¹³C NMR** (75 MHz, CDCl₃): δ 205.3 (s, (CH₂)C=O(CH₃)), 195.0 (s, (C₆H₄)C=O(C₆H₄)), 173.1 (s, C=O(OiPr)), 159.6 (s, C_{Ar}), 138.4 (s, C_{Ar}), 136.9 (s, C_{Ar}), 132.0 (s, CH_{Ar}), 130.5 (s, C_{Ar}), 130.2 (s, CH_{Ar}), 129.4 (s, CH_{Ar}), 117.2 (s, CH_{Ar}), 79.4 (s, OC(CH₃)₂), 69.3 (s, OCH(CH₃)₂), 50.7 (s, CH₂C=O), 29.6 (s, C=O(CH₃)), 25.4 (s, OC(CH₃)₂), 21.5 (s, OCH(CH₃)₂). **HRMS** (ESI) *m/z*: [M+H]⁺ calcd. for C₂₃H₂₇O₅: 383.1853; Found: 383.1851.



2-(4-isocyanophenyl)pentan-3-one (4f). Purified by flash chromatography (Ethyl acetate/Cyclohexane, gradient 0 to 70%). Obtained as a yellow oil

(0.015 g, 26% yield). **¹H NMR** (300 MHz, CDCl₃): δ 7.62 (2H, d, ³*J*_{H-H} = 8.0 Hz, C₆H₄), 7.34 (2H, d, ³*J*_{H-H} = 8.2 Hz, C₆H₄), 3.84 (1H, q, ³*J*_{H-H} = 7.0 Hz, -CH-CH₃), 2.40 (2H, q, ³*J*_{H-H} = 7.2 Hz, -CH₂-CH₃), 1.41 (3H, d, ³*J*_{H-H} = 7.5 Hz, -CH-CH₃), 0.98 (3H, t, ³*J*_{H-H} = 7.5 Hz, -CH₂-CH₃); **¹³C{¹H} NMR** (75 MHz, CDCl₃): δ 210.1 (s, CO), 146.2 (s, C₆H₄), 132.8 (s, C₆H₄), 128.8 (s, C₆H₄), 118.7 (s, CN), 111.2 (s, C₆H₄), 52.7 (s, CH), 34.9 (s, CH₂), 17.7 (s, -CH-CH₃), 8.0 (s, -CH₂-CH₃). **HRMS** (EI) *m/z*: [M+H]⁺ calcd. for C₁₂H₁₄NO: 188.1070; Found: 188.1063.

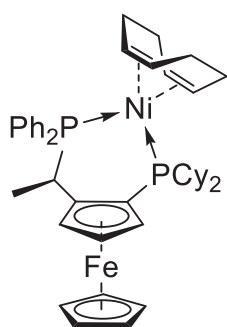


3-(4-isocyanophenyl)butan-2-one (4g). Obtained in 22% yield as determined by ^1H NMR spectroscopy using 1,3,5-trimethoxybenzene as internal standard (not isolated). Known compound.⁷⁰

5. Mechanistic studies

Synthesis of NiL1(COD) precatalyst (**I**)

In a glovebox, a 20 mL vial was charged with Ni(COD)₂ (1.0 equiv ; 0.076 mmol; 21.0 mg), L1 [(1.1 equiv; 0.084 mmol ; 50.0 mg) or L1 (2.0 equiv; 0.152 mmol ; 91.0 mg)] and benzo-*trifluoride* (2.5 mL). The resulting mixture was stirred at RT for 20 min at which time an orange precipitate was formed. Pentane (2.5 mL) was added to aid precipitation of the compound, which was collected on a glass frit, washed with pentane (3 x 1 mL), and dried under reduced pressure to give complex **I** as an orange powder (51.3 mg, 88% yield). Crystals suitable for X-ray crystallography were grown from a saturated Et₂O solution of **I** at 20 °C.



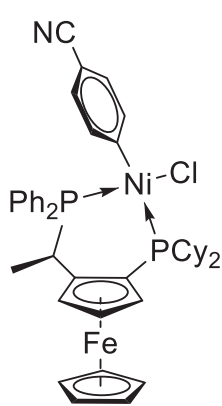
¹H NMR (400 MHz, C₆D₆): δ 7.50 (2H, dd, ³J_{H-H} = ³J_{H-P} = 7.2 Hz, *o*-C₆H₅), 7.36 (2H, ddd, ³J_{H-H} = ³J_{H-P} = 7.8 Hz, ⁴J_{H-H} = 1.5 Hz, *o*-C₆H₅), 7.20 (2H, t, ³J_{H-H} = 7.5 Hz, *m*-C₆H₅), 7.12 (1H, t, ³J_{H-H} = 7.3 Hz, *p*-C₆H₅), 7.05–7.03 (3H, m, *m*-C₆H₅+*p*-C₆H₅), 4.96 (1H, br. s, CH_{COD}), 4.27 (1H, br. s, CH_{COD}), 4.14 (1H, s, CH_{Cp}), 4.09 (1H, br. s, CH_{COD}), 4.05 (5H, s, C₅H₅), 3.99 (1H, br. s, CH_{COD}), 3.72 (1H, t, *J* = 2.2 Hz, CH_{Cp}), 3.30 (1H, s, CH_{Cp}), 3.18 (1H, q, ³J_{H-H} = 6.8 Hz, CH(CH₃)), 2.71–2.58 (2H, m, H_{Cy}), 2.41–1.71 (21H, m, H_{Cy}+COD), 1.59–1.10 (10H, m, H_{Cy} + CH₃) ; **¹³C{¹H} NMR** (100.6 MHz, C₆D₆): δ 138.8 (dd, ¹J_{C-P} = 17.2 Hz, ³J_{C-P} = 7.9 Hz, *ipso*-C₆H₅), 136.0 (d, ²J_{C-P} = 12.7 Hz, *o*-C₆H₅), 132.2 (d, ¹J_{C-P} = 20.6 Hz, *ipso*-C₆H₅), 131.6 (d, ²J_{C-P} = 8.3 Hz, *o*-C₆H₅), 128.9 (d, ⁴J_{C-P} = 1.4 Hz, *p*-C₆H₅), 128.2 (d, ³J_{C-P} = 6.1 Hz, *m*-C₆H₅), 127.1 (s, *p*-C₆H₅), 127.0 (d, ³J_{C-P} = 4.8 Hz, *m*-C₆H₅), 92.3 (dd, *J*_{C-P} = 17.8 Hz, *J*_{C-P} = 7.5 Hz, C_{Cp}), 85.8 (dd, ²J_{C-P} = 9.5 Hz, ²J_{C-P} = 2.8 Hz, CH_{COD}), 84.9 (dd, ²J_{C-P} = 7.5 Hz, ²J_{C-P} = 3.1 Hz, CH_{COD}), 84.4 (dd, ²J_{C-P} = 10.1 Hz, ²J_{C-P} = 4.0 Hz, CH_{COD}), 78.6 (dd, ²J_{C-P} = 9.1 Hz, ²J_{C-P} = 3.2 Hz, CH_{COD}), 76.1 (t, *J*_{C-P} = 9.2 Hz, C_{Cp}), 73.7 (s, CH_{Cp}), 70.0 (s, C₅H₅), 68.3 (d, *J*_{C-P} = 6.5 Hz, CH_{Cp}), 66.5 (d, *J*_{C-P} = 4.1 Hz, CH_{Cp}), 36.9 (dd, ¹J_{C-P} = 13.7 Hz, ³J_{C-P} = 6.3 Hz, CH_{Cy}), 36.0 (d, ¹J_{C-P} = 14.9 Hz, CH_{Cy}), 35.2 (dd, *J*_{C-P} = 9.2 Hz, *J*_{C-P} = 5.2 Hz, CH(CH₃)), 33.6 (d, *J*_{C-P} = 5.2 Hz, CH₂), 31.2 (d, *J*_{C-P} = 4.3 Hz, CH₂), 31.0 (d, *J*_{C-P} = 5.9 Hz, CH₂), 29.4 (d, *J*_{C-P} = 3.5 Hz, CH₂), 29.1 (d, *J*_{C-P} = 5.0 Hz, CH₂), 28.5 (d, *J*_{C-P} = 5.8 Hz, CH₂), 28.1 (d, *J*_{C-P} = 13.7 Hz, CH₂), 27.9 (d, *J*_{C-P}

= 8.6 Hz, $\underline{\text{CH}_2}$), 27.8 (s, $\underline{\text{CH}_2}$), 27.7 (s, $\underline{\text{CH}_2}$), 27.3 (s, $\underline{\text{CH}_2}$), 27.2 (d, $J_{\text{C-P}} = 5.6$ Hz, $\underline{\text{CH}_2}$), 26.5 (s, $\underline{\text{CH}_2}$), 25.4 (d, $J_{\text{C-P}} = 5.5$ Hz, $\underline{\text{CH}_2}$), 14.4 (d, $^2J_{\text{C-P}} = 5.9$ Hz, $\underline{\text{CH}_3}$); $^{31}\text{P}\{^1\text{H}\}$ NMR (162 MHz, C_6D_6): δ 60.2 (1P, d, $^2J_{\text{P-P}} = 13.1$ Hz, $\underline{\text{PPh}_2}$), 28.0 (1P, d, $^2J_{\text{P-P}} = 13.3$ Hz, $\underline{\text{PCy}_2}$). HRMS (ESI) m/z : $[\text{M}+\text{H}]^+$ calcd. for $\text{C}_{44}\text{H}_{57}\text{FeNiP}_2$: 761.2633; Found: 761.2631.

6. Synthesis of Nickel(II) complexes

a. Synthesis of $\text{NiCl}(p\text{-C}_6\text{H}_4\text{-CN})\text{L1}$ (**IIa**)

In a glovebox, a 20 mL vial was charged with $\text{Ni}(\text{COD})_2$ (1.0 equiv; 0.160 mmol; 44.0 mg), L1 (1.25 equiv; 0.200 mmol; 119 mg) and toluene (1 mL). 4-Chlorobenzonitrile (3.75 equiv; 0.600 mmol; 82.5 mg) was added, and the mixture was stirred at RT for 3 hours at which time an orange precipitate was formed. Pentane (1 mL) was added to aid precipitation of the compound, which was collected on a glass frit, washed with pentane (3 x 1 mL), and dried under reduced pressure to give **IIa** as an orange powder (124 mg, 98% yield). Crystals suitable for X-ray crystallography were grown by vapor diffusion of pentane into a concentrated solution of **IIa** in DCM at 20 °C.

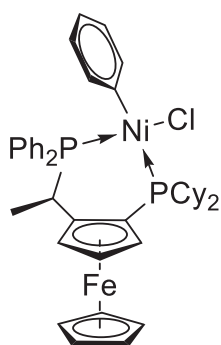


^1H NMR (500 MHz, CD_2Cl_2): δ 7.51 (2H, dd, $^3J_{\text{H-H}} = 6.9$ Hz, $^3J_{\text{H-P}} = 8.7$ Hz, $o\text{-C}_6\text{H}_5$), 7.43 (1H, t, $^3J_{\text{H-H}} = 7.4$ Hz, $p\text{-C}_6\text{H}_5$), 7.39 (1H, t, $^3J_{\text{H-H}} = 7.4$ Hz, $p\text{-C}_6\text{H}_5$), 7.31–7.23 (4H, m, $m\text{-C}_6\text{H}_5$), 7.19–7.12 (2H, m, $o\text{-C}_6\text{H}_5$), 6.79 (2H, br. s, C_6H_4), 6.58 (2H, d, $^3J_{\text{H-H}} = 6.7$ Hz, C_6H_4), 4.71 (1H, s, $\underline{\text{CH}}_{\text{Cp}}$), 4.23 (5H, s, C_5H_5), 4.19 (1H, s, $\underline{\text{CH}}_{\text{Cp}}$), 3.83 (1H, s, $\underline{\text{CH}}_{\text{Cp}}$), 3.32 (1H, dq, $^2J_{\text{H-P}} = 5.8$ Hz, $^3J_{\text{H-H}} = 6.9$ Hz, $\underline{\text{CH}}(\text{CH}_3)$), 2.89 (1H, br. s, $\underline{\text{H}}_{\text{Cy}}$), 2.55–2.39 (3H, m, $\underline{\text{H}}_{\text{Cy}}$), 2.21–1.77 (12H, m, $\underline{\text{H}}_{\text{Cy}}$), 1.63–1.37 (6H, m, $\underline{\text{H}}_{\text{Cy}}$), 1.24 (3H, dd, $^3J_{\text{H-P}} = 11.7$ Hz, $^3J_{\text{H-H}} = 6.9$ Hz, $\underline{\text{CH}_3}$); $^{13}\text{C}\{^1\text{H}\}$ NMR (126 MHz, CD_2Cl_2): δ 174 (dd, $^2J_{\text{C-P}} = 79.6$ Hz, $^2J_{\text{C-P}} = 40.2$ Hz, NiC), 135.2 (d, $^2J_{\text{C-P}} = 10.0$ Hz, $o\text{-C}_6\text{H}_5$), 131.9 (d, $^2J_{\text{C-P}} = 7.8$ Hz, $o\text{-C}_6\text{H}_5$), 131.4 (d, $^4J_{\text{C-P}} = 2.0$ Hz, $p\text{-C}_6\text{H}_5$), 131.1 (dd, $^1J_{\text{C-P}} = 51.1$ Hz, $^3J_{\text{C-P}} = 2.0$ Hz, $ipso\text{-C}_6\text{H}_5$), 129.9 (d, $^4J_{\text{C-P}} = 2.1$ Hz, $p\text{-C}_6\text{H}_5$), 128.7 (d, $^3J_{\text{C-P}} = 9.7$ Hz, $m\text{-C}_6\text{H}_5$), 128.2 (d, $^3J_{\text{C-P}} = 10.3$ Hz, $m\text{-C}_6\text{H}_5$), 127.4 (br. s, C_6H_4), 124.5 (d, $^1J_{\text{C-P}} = 44.3$ Hz, $ipso\text{-C}_6\text{H}_5$), 120.9 (s, $\underline{\text{CN}}$), 104.1 (s, $\underline{\text{C-CN}}$), 90.9 (dd, $J_{\text{C-P}} = 16.0$ Hz, $J_{\text{C-P}} = 6.0$ Hz, $\underline{\text{C}}_{\text{Cp}}$), 73.4 (s, $\underline{\text{CH}}_{\text{Cp}}$), 69.9 (s, C_5H_5), 69.7 (dd, $J_{\text{C-P}}$

= 20.9 Hz, J_{C-P} = 6.3 Hz, \underline{C}_{Cp}), 69.0 (d, J_{C-P} = 4.8 Hz, \underline{CH}_{Cp}), 68.9 (d, J_{C-P} = 6.9 Hz, \underline{CH}_{Cp}), 36.8 (d, $^1J_{C-P}$ = 17.8 Hz, \underline{CH}_{Cy}), 34.5 (dd, $^1J_{C-P}$ = 15.8 Hz, $^3J_{C-P}$ = 7.7 Hz, $\underline{CH}(\underline{CH}_3)$), 33.5 (d, $^1J_{C-P}$ = 25.0 Hz, \underline{CH}_{Cy}), 30.5 (s, \underline{CH}_2), 29.2 (d, J = 2.9 Hz, \underline{CH}_2), 29.1 (d, J = 1.4 Hz, \underline{CH}_2), 28.3 (d, J = 3.8 Hz, \underline{CH}_2), 27.9 (d, J = 20.4 Hz, \underline{CH}_2), 28.0 (s, \underline{CH}_2), 27.6 (d, J = 11.8 Hz, \underline{CH}_2), 27.4 (d, J = 11.0 Hz, \underline{CH}_2), 26.8 (s, \underline{CH}_2), 26.4 (s, \underline{CH}_2), 14.5 (d, $^2J_{C-P}$ = 7.2 Hz, $\underline{CH}(\underline{CH}_3)$); $^{31}P\{^1H\}$ NMR (202 MHz, CD_2Cl_2): δ 52.5 (1P, d, $^2J_{P-P}$ = 44.7 Hz, \underline{PPh}_2), 12.6 (1P, d, $^2J_{P-P}$ = 44.7 Hz, \underline{PCy}_2). HRMS (ESI) m/z : $[M-Cl]^+$ calcd. for $C_{43}H_{48}FeNNiP_2$: 754.1959; Found: 754.1939.

b. Synthesis of $NiCl(Ph)L1$ (**IIb**)

In a glovebox, a 5 mL microwave reaction vial was charged with $Ni(COD)_2$ (1.0 equiv; 0.160 mmol; 44.0 mg), L1 (1.25 equiv; 0.200 mmol; 119 mg) and toluene (1 mL). Chlorobenzene (7.5 equiv; 1.20 mmol; 122 μ L) was added, and the tube was sealed, removed from the glovebox and heated at 80 °C for 5 hours. Cooling to room temperature caused formation of an orange precipitate. Pentane (1 mL) was added to aid precipitation of the compound, which was collected on a glass frit, washed with pentane (3 x 1 mL), and dried under reduced pressure to give **IIb** as an orange powder (83 mg, 65% yield). Crystals suitable for X-ray crystallography were grown by vapor diffusion of pentane into a concentrated solution of **IIb** in DCM at 20 °C.

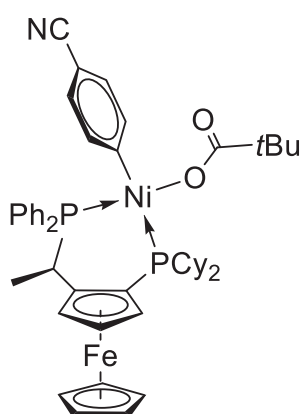


1H NMR (300 MHz, CD_2Cl_2): δ 7.43–7.18 (10H, m, \underline{PPh}_2), 6.55 (2H, br. s, NiC_6H_5), 6.42–6.31 (3H, m, NiC_6H_5), 4.68 (1H, d, J = 1.3 Hz, \underline{CH}_{Cp}), 4.22 (5H, s, C_5H_5), 4.20 (1H, d, J = 2.6 Hz, \underline{CH}_{Cp}), 3.87 (1H, s, \underline{CH}_{Cp}), 3.25 (1H, dq, $^2J_{H-P}$ = 5.6 Hz, $^3J_{H-H}$ = 6.6 Hz, $\underline{CH}(\underline{CH}_3)$), 2.81 (1H, dtt, $^2J_{H-P}$ = 9.3 Hz, $^3J_{H-H}$ = 12.0 Hz, J_{H-H} = 3.2 Hz, \underline{CH}_{Cy}), 2.51–2.34 (3H, m, \underline{CH}_{Cy} , \underline{CH}_2), 2.23–1.79 (12H, m, \underline{CH}_2), 1.63–1.34 (6H, m, \underline{CH}_2), 1.21 (3H, dd, $^3J_{H-P}$ = 11.3, $^3J_{H-H}$ = 6.9 Hz, \underline{CH}_3); $^{13}C\{^1H\}$ NMR (101 MHz, CD_2Cl_2): δ 158.9 (dd, $^2J_{C-P}$ = 78.3 Hz, $^2J_{C-P}$ = 42.0 Hz, $Ni\underline{C}$), 135.0 (d, $^2J_{C-P}$ = 9.7 Hz, $P(o-\underline{C}_6H_5)$), 132.3 (d, $^2J_{C-P}$ = 7.9 Hz, $P(o-\underline{C}_6H_5)$), 132.1 (d, $^1J_{C-P}$ = 52.0 Hz, $P(ipso-\underline{C}_6H_5)$), 130.8 (d, $^4J_{C-P}$ = 2.2 Hz, $P(p-\underline{C}_6H_5)$), 129.5 (d, $^4J_{C-P}$ = 2.2 Hz, $P(p-\underline{C}_6H_5)$), 128.3 (d, $^3J_{C-P}$ = 9.7 Hz, $P(m-\underline{C}_6H_5)$), 127.5 (d, $^3J_{C-P}$ = 9.9 Hz,

$P(m\text{-}\underline{C}_6H_5)$), 125.6 (br. s, $Ni\underline{C}_6H_5$), 125.5 (d, $^1J_{C-P} = 46.0$ Hz, $P(ipso\text{-}\underline{C}_6H_5)$), 121.1 (s, $Ni(p\text{-}\underline{C}_6H_5)$), 91.6 (dd, $J_{C-P} = 16.2$ Hz, $J_{C-P} = 6.3$ Hz, \underline{C}_{Cp}), 73.3 (s, \underline{CH}_{Cp}), 70.3 (dd, $J_{C-P} = 18.3$ Hz, $J_{C-P} = 5.9$ Hz, \underline{C}_{Cp}), 69.8 (s, \underline{C}_5H_5), 68.9 (d, $J_{C-P} = 6.6$ Hz, \underline{CH}_{Cp}), 68.8 (d, $J_{C-P} = 4.4$ Hz, \underline{CH}_{Cp}), 36.0 (d, $^1J_{C-P} = 17.3$ Hz, \underline{CH}_{Cy}), 34.9 (dd, $^1J_{C-P} = 14.3$ Hz, $^3J_{C-P} = 9.1$ Hz, $\underline{CH}(\underline{CH}_3)$), 33.9 (d, $^1J_{C-P} = 24.2$ Hz, \underline{CH}_{Cy}), 30.0 (s, \underline{CH}_2), 29.13 (s, \underline{CH}_2), 29.11 (s, \underline{CH}_2), 28.6 (d, $J_{C-P} = 3.4$ Hz, \underline{CH}_2), 28.1–27.9 (m, $2\underline{CH}_2$), 27.7 (d, $J_{C-P} = 12.1$ Hz, \underline{CH}_2), 27.4 (d, $J = 10.8$ Hz, \underline{CH}_2), 26.9 (s, \underline{CH}_2), 26.4 (s, \underline{CH}_2), 14.6 (d, $^2J_{C-P} = 7.0$ Hz, $\underline{CH}(\underline{CH}_3)$); $^{31}P\{^1H\}$ NMR (162 MHz, CD_2Cl_2): δ 50.7 (1P, d, $^2J_{P-P} = 39.4$ Hz, PPh_2), 12.5 (1P, d, $^2J_{P-P} = 39.4$ Hz, PCy_2). HRMS (ESI) m/z : $[M-Cl]^+$ calcd. for $C_{42}H_{49}FeNiP_2$: 729.2007; Found: 729.2021.

c. Synthesis of $Ni(OPiv)(p-C_6H_4-CN)L1$ (IIc**)**

In a glovebox, a 5 mL microwave reaction vial was charged with $Ni(COD)_2$ (1.0 equiv; 0.09 mmol; 24.8 mg), L1 (1.25 equiv; 0.112 mmol; 66.8 mg) and C_6H_6 (1 mL). 4-cyanophenyl pivalate (3 equiv; 0.27 mmol; 54.8 mg) was added, and the tube was sealed, removed from the glovebox and heated at 80 °C for 18 hours. Volatiles were removed under reduced pressure and the minimum of DCM was added to solubilize the product followed by the addition of pentane (1 mL) to precipitate the compound, which was collected on a glass frit, washed with pentane (3 x 1 mL), and dried under reduced pressure to give **IIc** as an orange powder (48 mg, 62% yield). Crystals suitable for X-ray crystallography were grown from a saturated Et_2O solution of **IIc** at 20 °C.



1H NMR (500 MHz, C_6D_6): δ 8.07 (2H, br. s, $o-C_6H_5$), 7.29 (2H, dd, $^3J_{H-H} = 7.9$ Hz, $^4J_{H-P} = 5.5$ Hz, C_6H_4), 7.20 (2H, dd, $^3J_{H-H} = 8.7$ Hz, $^3J_{H-P} = 9.6$ Hz, $o-C_6H_5$), 7.14 (2H, t, $^3J_{H-H} = 7.6$ Hz, $m-C_6H_5$), 7.04 (1H, t, $^3J_{H-H} = 7.2$ Hz, $p-C_6H_5$), 6.94 (1H, t, $^3J_{H-H} = 7.3$ Hz, $p-C_6H_5$), 6.86 (2H, t, $^3J_{H-H} = 7.3$ Hz, $m-C_6H_5$), 6.64 (2H, d, $^3J_{H-H} = 7.3$ Hz, C_6H_4), 4.31 (1H, s, CH_{Cp}), 3.89 (5H, s, C_5H_5), 3.88 (1H, s, CH_{Cp}), 3.76 (1H, s, CH_{Cp}), 2.97 (1H, dq, $^3J_{H-H} = ^2J_{H-P} = 6.6$ Hz, $CH(CH_3)$), 2.69 (1H, br. s, H_{Cy}), 2.54 (1H, br. s, H_{Cy}), 2.38 (1H, td, $^3J_{H-H} = 12.3$ Hz, $^2J_{H-P} = 10.3$ Hz, CH_{Cy}), 2.28–1.91 (7H, m, H_{Cy}), 1.93–1.68 (6H, m, H_{Cy}), 1.58–1.40 (3H, m, H_{Cy}), 1.36–1.28 (3H, m, H_{Cy}), 1.16 (9H, s, $C(CH_3)_3$), 1.07 (3H, dd, $^3J_{H-P} = 11.3$, $^3J_{H-H} = 7.0$ Hz, $CH(CH_3)$); **$^{13}C\{^1H\}$ NMR** (126 MHz, C_6D_6): δ 183.0 (s, $C=O$), 173.4 (dd, $^2J_{C-P} = 78.0$ Hz, $^2J_{C-P} = 42.1$ Hz, NiC), 137.1 (br. s, C_6H_4), 134.0 (d, $^2J_{C-P} = 8.7$ Hz, $o-C_6H_5$), 133.7 (d, $^2J_{C-P} = 9.2$ Hz, $o-C_6H_5$), 131.1 (dd, $^1J_{C-P} = 51.0$ Hz, $^3J_{C-P} = 1.9$ Hz, $ipso-C_6H_5$), 130.5 (d, $^4J_{C-P} = 2.5$ Hz, $p-C_6H_5$), 130.3 (d, $^4J_{C-P} = 2.4$ Hz, $p-C_6H_5$), 128.6 (d, $^3J_{C-P} = 10.1$ Hz, $m-C_6H_5$), 127.9 (d, $^3J_{C-P} = 9.8$ Hz, $m-C_6H_5$), 127.3 (d, $J_{C-P} = 5.9$ Hz, C_6H_4), 126.3 (d, $^1J_{C-P} = 43.0$ Hz, $ipso-C_6H_5$), 120.6 (s, CN), 105.6 (s, $C-CN$), 92.6 (dd, $J_{C-P} = 16.8$ Hz, $J_{C-P} = 6.0$ Hz, C_{Cp}), 73.1 (s, CH_{Cp}), 70.0 (s, C_5H_5), 69.9 (d, $J_{C-P} = 20.6$ Hz, $J_{C-P} = 5.8$ Hz, C_{Cp}), 69.2 (d, $J_{C-P} = 6.9$ Hz, CH_{Cp}), 68.8 (d, $J_{C-P} = 4.6$ Hz, CH_{Cp}), 39.8 (d, $^4J_{C-P} = 2.9$ Hz, $C(CH_3)_3$), 35.4 (d, $^1J_{C-P} = 15.5$ Hz, CH_{Cy}), 35.3 (d, $^1J_{C-P} = 16.0$ Hz, $CH(CH_3)$), 33.9 (d,

$^1J_{C-P} = 22.5$ Hz, \underline{CH}_{Cy}), 29.2 (br. s, CH_2), 28.6 (s, $C(\underline{CH}_3)_3$), 28.3 (d, $J = 4.7$ Hz, \underline{CH}_2), 28.2 (d, $J = 9.4$ Hz, \underline{CH}_2), 28.0 (d, $J = 12.2$ Hz, \underline{CH}_2), 27.6 (d, $J = 12.8$ Hz, \underline{CH}_2), 27.5 (d, $J = 10.4$ Hz, \underline{CH}_2), 27.0 (s, \underline{CH}_2), 26.4 (s, \underline{CH}_2), 14.3 (br. s, $CH(\underline{CH}_3)$); $^{31}P\{^1H\}$ NMR (202 MHz, C_6D_6): δ 49.4 (1P, d, $^2J_{P-P} = 40.9$ Hz, \underline{PPh}_2), 13.2 (1P, d, $^2J_{P-P} = 40.9$ Hz, \underline{PCy}_2). HRMS (ESI) m/z : $[M-OCOtBu]^+$ calcd. for $C_{43}H_{48}FeNNiP_2$: 754.1959; Found: 754.1936.

7. Oxidative addition in the presence of acetone

General procedure: In a glovebox, a 4 mL vial equipped with a magnetic stir bar was charged with **I** (1 equiv; 0.013 mmol; 10 mg), chlorobenzene (2.3 equiv; 0.030 mmol; 3 μ L), acetone (21 equiv; 0.272 mmol; 20 μ L), and C_6D_6 (0.5 mL) (**Scheme 30**). After stirring the resulting solution for 5 minutes, it was transferred to a J. Young NMR tube. The tube was sealed and removed from the glovebox. The reaction mixture was directly analyzed by $^{31}P\{^1H\}$ NMR spectroscopy, indicating no reaction and presence of only starting material **I**. Then the tube was heated at 80 °C (preheated oil bath) for 18 h and analyzed again by $^{31}P\{^1H\}$ and 1H NMR spectroscopy, showing complete consumption of the starting material and exclusive formation of the oxidative addition complex **Iib** ($\delta^{31}P$ (C_6D_6): 49.8 (d, $^2J_{P-P} = 38.6$ Hz), 13.8 (d, $^2J_{P-P} = 38.7$ Hz)).

8. Decomposition studies

a. Decomposition study of $NiCl(p-C_6H_4-CN)L1$ (**IIa**)

In a glovebox, a 4 mL vial was charged with **IIa** (0.03 mmol; 24 mg). THF- d_8 (0.5 mL) was subsequently added to completely dissolve the complex. The resulting clear solution was placed in a J. Young NMR tube. The tube was sealed and removed from the glovebox. The contents were directly analyzed by 1H and $^{31}P\{^1H\}$ NMR spectroscopy, indicating the starting point of the kinetic experiment. THF- d_8 was used as an internal standard for calculation of 1H NMR conversion

of **IIa**. Then, the solution was heated to the desired temperature. In suitable time intervals the **IIa** to THF-*d*₈ ratio was determined from ¹H NMR spectra by signal integration. The ³¹P{¹H} NMR spectra showed slow disappearance of **IIa** signals with no new signal formation. No 4,4'-dicyanobiphenyl was detected by GC-MS, instead traces of 4-chlorobenzonitrile and benzonitrile were observed. **Note:** the solution remains clear, no precipitation formation over temperature change.

b. Decomposition study of NiCl(Ph)L1 (IIb)

In a glovebox, a 4 mL vial was charged with **IIb** (1 equiv, 0.03 mmol; 24 mg) and L1 (1 equiv, 0.03 mmol; 18 mg) which was added as an internal standard for ³¹P{¹H} NMR spectroscopic analysis. C₆D₆ (0.5 mL) was subsequently added to completely dissolve the solids. The resulting clear solution was placed in a J. Young NMR tube. The tube was sealed and removed from the glovebox. The contents were directly analyzed by ¹H and ³¹P{¹H} NMR spectroscopy, indicating the starting point of the kinetic experiment. Then, the solution was heated to the desired temperature. In suitable time intervals the **IIb** to L1 ratio was determined from ³¹P{¹H} NMR spectra by signal integration. The ³¹P{¹H} NMR spectra showed slow disappearance of **IIb** signals with no new signal formation. No biphenyl was detected by GC-MS. **Note:** the solution becomes brown over the temperature change.

c. Decomposition study of Ni(OPiv)(p-C₆H₄-CN)L1 (IIc)

In a glovebox, a 4 mL vial was charged with **IIc** (0.03 mmol; 25 mg). C₆D₆ (0.5 mL) was subsequently added to completely dissolve the complex. The resulting clear solution was placed in a J. Young NMR tube. The tube was sealed and removed from the glovebox. The contents were directly analyzed by ¹H and ³¹P{¹H} NMR spectroscopy, indicating the starting point of the kinetic experiment. Then, the solution was heated to the desired temperature. In suitable time intervals,

the **IIc** to C₆D₆ ratio was determined from ¹H NMR spectra by signal integration. The ³¹P{¹H} NMR spectra showed slow disappearance of **IIc** signals with no new signal formation.

9. *Reactivity of IIa with acetone*

General procedure: In a glovebox, a 5 mL microwave reaction vial equipped with a magnetic stir bar was charged with **IIa** (1 equiv; 0.03 mmol; 23.7 mg) and benzotrifluoride (1 mL). After stirring the resulting solution for 5 minutes, acetone (9 mmol; 0.66 ml) and CsF (20.0 equiv; 0.60 mmol; 91.2 mg) were sequentially added. The tube was sealed, removed from the glovebox and heated at 120 °C (preheated oil bath) for 18 h. Then the reaction mixture was cooled to room temperature, filtered over Celite®, and 1,3,5-trimethoxybenzene (3.3 equiv; 0.1 mmol; 16.8 mg) was added as an internal standard for ¹H NMR spectroscopy. All volatiles were removed under reduced pressure and the crude product was analyzed by ¹H NMR spectroscopy in CDCl₃, indicating formation of the desired product in **78%** yield.

10. *Evaluation of Nickel precursors in catalytic conditions*

General procedure: In a glovebox, a 5 mL microwave reaction vial equipped with a magnetic stir bar was charged with the selected catalyst system and benzotrifluoride (1 mL). After stirring the resulting solution for 5 minutes, the selected aryl chloride (1.0 equiv; 0.3 mmol), acetone (30 equiv; 9.0 mmol; 0.66 ml) and CsF (2.0 equiv; 0.6 mmol; 91.5 mg) were sequentially added. The tube was sealed, removed from the glovebox and heated at 120 °C (preheated oil bath) for 18 h. Then the reaction mixture was cooled to room temperature, filtered over Celite®, and 1,3,5-trimethoxybenzene (0.33 equiv; 0.1 mmol; 16.8 mg) was added as an internal standard for ¹H NMR spectroscopy. All volatiles were removed under reduced pressure and the crude product

was analyzed by ^1H NMR spectroscopy in CDCl_3 to determine the yield of the reaction (**Scheme 32**).

11. X-ray crystal structure determination

Experimental. Single-crystal X-ray diffraction studies of complexes **I**, **IIa**, **IIb** and **IIc** were carried out with a Gemini diffractometer and the related analysis software.⁷¹ Samples were mounted in inert oil and directly transferred on the diffractometer and crystallographic data were obtained at room temperature. An absorption correction based on the crystal faces was applied to the data sets (analytical).^{72,73} The structures were solved by direct methods using the SIR97 program,⁷⁴ combined with Fourier difference syntheses and refined against F using reflections with $[I/\sigma(I) > 3]$ by using the CRYSTALS program.⁷⁵ All atomic displacement parameters for non-hydrogen atoms were refined with anisotropic terms. The hydrogen atoms were theoretically located on the basis of the conformation of the supporting atom and were refined by using the riding model. X-ray diffraction crystallographic data and refinement details for both complexes are summarized in (**Table 9**) and selected bond lengths are collated in (**Table 10**).

For each structure, the obtained Flack parameter value has been refined in order to show that the obtained value is close to 0, considering associated error value and not fixed to 0.

In the case of complex **IIa**, the electron density within the structure free space has been checked and doesn't correspond to any solvent molecules even considering statistical disorder.

CCDC 1993566, 1993564, 1993573, 19993569 contain the supplementary crystallographic data for **I**, **IIa**, **IIb** and **IIc** crystal structures, respectively. These data can be obtained free of charge from The Cambridge Crystallographic Data Centre via www.ccdc.cam.ac.uk/data_request/cif.

Table 8. Single-crystal X-ray diffraction data and crystal structure refinement results for complexes **I**, **IIa**, **IIb** and **IIc**.

	I	IIa	IIb	IIc
Formula	C ₄₄ H ₅₆ Fe ₁ Ni ₁ P ₂	C ₄₃ H ₄₈ Cl ₁ Fe ₁ N ₁ Ni ₁ P ₂	C ₄₂ H ₄₉ Cl ₁ Fe ₁ Ni ₁ P ₂	C ₅₂ H ₆₇ Fe ₁ N ₁ Ni ₁ O ₃ P ₂
Mw (g.mol ⁻¹)	761.43	790.8	765.8	930.6
T (K)	293	293	293	293
Crystal system	Orthorhombic	Orthorhombic	Trigonal	Orthorhombic
Space group	P2 ₁ 2 ₁ 2 ₁	P2 ₁ 2 ₁ 2 ₁	P3 ₂ 21	P2 ₁ 2 ₁ 2 ₁
Crystal shape	Block	Needle	Block	Needle
Crystal color	Orange	Orange	Red	Orange
Crystal size (mm ³)	0.10×0.13×0.94	0.13×0.16×0.99	0.14×0.17×0.35	0.16×0.18×0.72
Density	1.336	1.156	1.345	1.267
μ (mm ⁻¹)	0.996	0.889	1.065	0.790
a (Å)	11.4853(5)	11.1833(8)	10.4524(2)	10.2158(3)
b (Å)	11.6964(5)	19.607(2)	10.4524(2)	20.1462(6)
c (Å)	28.1724(9)	20.719(2)	59.952(1)	23.7097(7)
α (°)	90	90	90	90
β (°)	90	90	90	90
γ (°)	90	90	120	90
V (Å ³)	3784.6(2)	4542.9(5)	5672.4(2)	4879.7(2)
Z	4	4	6	4
Unique refl. / R_{int}	8669 / 0.050	10363 / 0.030	9719 / 0.093	12373 / 0.033
R(F) / R_w(F)	0.0367 / 0.0445	0.0459 / 0.0631	0.0879 / 0.1043	0.0349 / 0.0448
S	1.09	1.30	1.39	1.30
No. refl. Used	6052	6290	5867	9823
No. refined param.	434	443	425	542
Elec. residue (e⁻.Å⁻³)	-0.31 / +0.35	-0.30 / +0.74	-1.58 / +0.78	-0.31 / +0.54
Flack parameter	-0.020(9)	-0.017(7)	0.075(9)	-0.017(3)
Abs. correction	Analytical	Analytical	Analytical	Analytical

Table 9. Important bond lengths (\AA) for complexes **I**, **IIa**, **IIb** and **IIc**.

	I	IIa	IIb	IIc
Ni-Cl	-	2.195(2)	2.189(2)	-
Ni-P	2.211(1)	2.266(1)	2.265(2)	2.2670(9)
	2.166(2)	2.148(2)	2.135(2)	2.1281(8)
Ni-C	2.103(5)	1.911(5)	1.90(1)	1.929(3)
	2.108(5)			
	2.119(5)			
	2.134(5)			
Ni-O	-	-	-	1.895(2)
P-C	1.886(4)	1.843(5)	1.818(7)	1.819(3)
	1.838(4)	1.823(5)	1.842(8)	1.851(3)
	1.829(4)	1.852(6)	1.856(8)	1.854(3)
	1.851(5)	1.869(5)	1.823(8)	1.862(3)
	1.874(4)	1.821(5)	1.814(7)	1.817(3)
	1.870(4)	1.824(5)	1.851(9)	1.819(3)
Fe-C	2.055(4)	2.065(5)	2.033(7)	2.064(2)
	2.101(4)	2.056(5)	2.043(8)	2.047(3)
	2.047(4)	2.046(6)	2.037(9)	2.043(3)
	2.028(5)	2.048(6)	2.01(1)	2.038(3)
	2.028(4)	2.047(6)	2.053(8)	2.030(3)
	2.023(5)	2.070(6)	2.03(1)	2.040(3)
	2.030(5)	2.060(6)	2.02(1)	2.035(3)
	2.054(5)	2.040(6)	2.01(1)	2.035(3)
	2.068(5)	2.040(6)	2.036(9)	2.041(3)
	2.053(5)	2.065(5)	2.07(1)	2.053(3)

VII. References

- (1) Luyben, W. L. Design and Control of the Cumene Process. *Ind. Eng. Chem. Res.* **2010**, *49* (2), 719–734.
- (2) Nagai, K. New Developments in the Production of Methyl Methacrylate. *Appl. Catal. A Gen.* **2001**, *221* (1–2), 367–377.
- (3) Hao, Y. J.; Hu, X. S.; Zhou, Y.; Zhou, J.; Yu, J. S. Catalytic Enantioselective α -Arylation of Carbonyl Enolates and Related Compounds. *ACS Catal.* **2020**, *10* (2), 955–993.
- (4) Singh, F. V.; Vatsyayan, R.; Goel, A. Arylanthranilodinitriles : A New Biaryl Class of Antileishmanial Agents Q. *Bioorg. Med. Chem. Lett.* **2006**, *16* (10), 2734–2737.
- (5) Rossi, R. A.; Pierini, A. B.; Peñeñory, A. B. Nucleophilic Substitution Reactions by Electron Transfer. *Chem. Rev.* **2003**, *103* (1), 71–167.
- (6) Pichette Drapeau, M.; Fabre, I.; Grimaud, L.; Ciofini, I.; Ollevier, T.; Taillefer, M. Transition-Metal-Free α -Arylation of Enolizable Aryl Ketones and Mechanistic Evidence for a Radical Process. *Angew. Chem. Int. Ed.* **2015**, *54* (36), 10587–10591.
- (7) Culkin, D. A.; Hartwig, J. F. Palladium-Catalyzed α -Arylation of Carbonyl Compounds and Nitriles. *Acc. Chem. Res.* **2003**, *36* (4), 234–245.
- (8) Schranck, J.; Rotzler, J. Valorization of the Primary Building Blocks Ammonia and Acetone Featuring Pd- and Ni-Catalyzed Monoarylations. *Org. Process Res. Dev.* **2015**, *19* (12), 1936–1943.
- (9) Hesp, K. D.; Lundgren, R. J.; Stradiotto, M. Palladium-Catalyzed Mono- α -Arylation of Acetone with Aryl Halides and Tosylates. *J. Am. Chem. Soc.* **2011**, *133* (14), 5194–5197.
- (10) Willis, M. C.; Taylor, D.; Gillmore, A. T. Palladium-Catalyzed Intramolecular O-Arylation of Enolates: Application to Benzofuran Synthesis. *Org. Lett.* **2004**, *6* (25), 4755–4757.

- (11) Culkin, D. A.; Hartwig, J. F. Palladium-Catalyzed α -Arylation of Carbonyl Compounds and Nitriles. *Acc. Chem. Res.* **2003**, *36* (4), 234–245.
- (12) Bellina, F.; Rossi, R. Transition Metal-Catalyzed Direct Arylation of Substrates with Activated Sp³-Hybridized C-H Bonds and Some of Their Synthetic Equivalents with Aryl Halides and Pseudohalides. *Chem. Rev.* **2010**, *110* (2), 1082–1146.
- (13) Johansson, C. C. C.; Colacot, T. J. Metal-Catalyzed α -Arylation of Carbonyl and Related Molecules: Novel Trends in C-C Bond Formation by C-H Bond Functionalization. *Angew. Chem. Int. Ed.* **2010**, *49* (4), 676–707.
- (14) Ehrentraut, A.; Zapf, A.; Beller, M. Progress in the Palladium-Catalyzed α -Arylation of Ketones with Chloroarenes. *Adv. Synth. Catal.* **2002**, *344* (2), 209–217.
- (15) Gøgsig, T. M.; Taaning, R. H.; Lindhardt, A. T.; Skrydstrup, T. Palladium-Catalyzed Carbonylative α -Arylation for Accessing 1,3-Diketones. *Angew. Chem. Int. Ed.* **2012**, *51* (3), 798–801.
- (16) Hu, X. Q.; Lichte, D.; Rodstein, I.; Weber, P.; Seitz, A. K.; Scherpf, T.; Gessner, V. H.; Gooßen, L. J. Ylide-Functionalized Phosphine (YPhos)-Palladium Catalysts: Selective Monoarylation of Alkyl Ketones with Aryl Chlorides. *Org. Lett.* **2019**, *21* (18), 7558–7562.
- (17) Terao, Y.; Fukuoka, Y.; Satoh, T.; Miura, M.; Nomura, M. Palladium-Catalyzed α -Arylation of Aldehydes with Aryl Bromides. *Tetrahedron Lett.* **2002**, *43* (1), 101–104.
- (18) Lee, S.; Beare, N. A.; Hartwig, J. F. Palladium-Catalyzed α -Arylation of Esters and Protected Amino Acids. *J. Am. Chem. Soc.* **2001**, *123* (34), 8410–8411.
- (19) Stauffer, S. R.; Beare, N. A.; Stambuli, J. P.; Hartwig, J. F. Palladium-Catalyzed Arylation of Ethyl Cyanoacetate. Fluorescence Resonance Energy Transfer as a Tool for Reaction Discovery. *J. Am. Chem. Soc.* **2001**, *123* (19), 4641–4642.

- (20) Beare, N. A.; Hartwig, J. F. Palladium-Catalyzed Arylation of Malonates and Cyanoesters Using Sterically Hindered Trialkyl- and Ferrocenyldialkylphosphine Ligands. *J. Org. Chem.* **2002**, *67* (2), 541–555.
- (21) Shaughnessy, K. H.; Hamann, B. C.; Hartwig, J. F. Palladium-Catalyzed Inter- and Intramolecular α -Arylation of Amides. Application of Intramolecular Amide Arylation to the Synthesis of Oxindoles. *J. Org. Chem.* **1998**, *63* (19), 6546–6553.
- (22) Jette, C. I.; Geibel, I.; Bachman, S.; Hayashi, M.; Sakurai, S.; Shimizu, H.; Morgan, J. B.; Stoltz, B. M. Palladium-Catalyzed Construction of Quaternary Stereocenters by Enantioselective Arylation of Γ -Lactams with Aryl Chlorides and Bromides. *Angew. Chem. Int. Ed.* **2019**, *58* (13), 4297–4301.
- (23) Culkin, D. A.; Hartwig, J. F. Synthesis, Characterization, and Reactivity of Arylpalladium Cyanoalkyl Complexes: Selection of Catalysts for the α -Arylation of Nitriles. *J. Am. Chem. Soc.* **2002**, *124* (32), 9330–9331.
- (24) Barluenga, J.; Jiménez-Aquino, A.; Valdés, C.; Aznar, F. The Azaallylic Anion as a Synthon for Pd-Catalyzed Synthesis of Heterocycles: Domino Two- and Three-Component Synthesis of Indoles. *Angew. Chem. Int. Ed.* **2007**, *46* (9), 1529–1532.
- (25) Su, W.; Raders, S.; Verkade, J. G.; Liao, X.; Hartwig, J. F. Pd-Catalyzed α -Arylation of Trimethylsilyl Enol Ethers with Aryl Bromides and Chlorides: A Synergistic Effect of Two Metal Fluorides as Additives. *Angew. Chem. Int. Ed.* **2006**, *45* (35), 5852–5855.
- (26) Takayuki Hamada; André Chieffi; Jens Åhman, A.; Buchwald, S. L. An Improved Catalyst for the Asymmetric Arylation of Ketone Enolates. *J. Am. Chem. Soc.* **2002**, *124* (7), 1261–1268.
- (27) Whitesides, G. M.; Gaasch, J. F.; Stedronsky, E. R. Mechanism of Thermal Decomposition

- of Di-n-Butylbis (Triphenylphosphine) Platinum (II). *J. Am. Chem. Soc.* **1972**, *94* (15), 5258–5270.
- (28) Hamann, B. C.; Hartwig, J. F. Palladium-Catalyzed Direct α -Arylation of Ketones. Rate Acceleration by Sterically Hindered Chelating Ligands and Reductive Elimination from a Transition Metal Enolate Complex. *J. Am. Chem. Soc.* **1997**, *119* (50), 12382–12383.
- (29) Kawatsura, M.; Hartwig, J. F. Simple, Highly Active Palladium Catalysts for Ketone and Malonate Arylation: Dissecting the Importance of Chelation and Steric Hindrance. *J. Am. Chem. Soc.* **1999**, *121* (7), 1473–1478.
- (30) Fox, J. M.; Huang, X.; Chieffi, A.; Buchwald, S. L. Highly Active and Selective Catalysts for the Formation of α -Aryl Ketones. *J. Am. Chem. Soc.* **2000**, *122* (7), 1360–1370.
- (31) Johansson, C. C. C.; Colacot, T. J. Metal-Catalyzed α -Arylation of Carbonyl and Related Molecules: Novel Trends in C-C Bond Formation by C-H Bond Functionalization. *Angew. Chem. Int. Ed.* **2010**, *49* (4), 676–707.
- (32) Culkin, D. A.; Hartwig, J. F. C-C Bond-Forming Reductive Elimination of Ketones, Esters, and Amides from Isolated Arylpalladium (II) Enolates. *J. Am. Chem. Soc.* **2001**, *123* (24), 5816–5817.
- (33) Chen, G.; Kwong, Y.; Chan, O.; Yu, W.; Chan, A. S. C. Nickel-Catalyzed Asymmetric α -Arylation of Ketone Enolates. *Chem. Commun.*, **2006**, 1413–1415.
- (34) Ge, S.; Hartwig, J. F. Nickel-Catalyzed Asymmetric α -Arylation and Heteroarylation of Ketones with Chloroarenes: Effect of Halide on Selectivity, Oxidation State, and Room-Temperature Reactions. *J. Am. Chem. Soc.* **2011**, *133*, 16330–16333.
- (35) Henrion, M.; Chetcuti, M. J.; Ritleng, V. From Acetone Metalation to the Catalytic α -Arylation of Acyclic Ketones with NHC-Nickel(II) Complexes. *Chem. Commun.* **2014**, 50

- (35), 4624–4627.
- (36) Fernández-Salas, J. A.; Marelli, E.; Cordes, D. B.; Slawin, A. M. Z.; Nolan, S. P. General and Mild Ni⁰-Catalyzed α -Arylation of Ketones Using Aryl Chlorides. *Chem. Eur. J.* **2015**, *21* (10), 3906–3909.
- (37) Takise, R.; Muto, K.; Yamaguchi, J.; Itami, K. Nickel-Catalyzed α -Arylation of Ketones with Phenol Derivatives. *Angew. Chem. Int. Ed.* **2014**, *4*, 6791–6794.
- (38) Cornella, J.; Jackson, E. P.; Martin, R. Nickel-Catalyzed Enantioselective C-C Bond Formation Through. *Angew. Chem. Int. Ed.* **2015**, 4075–4078.
- (39) Li, J.; Wang, Z. Nickel-Catalyzed Transformation of Aryl 2-Pyridyl Ethers via Cleavage of the Carbon – Oxygen Bond : Synthesis of Mono- α - Arylated Ketones. *Synthesis (Stuttg.)*. **2018**, 3217–3223.
- (40) Li, P.; Lü, B.; Fu, C.; Ma, S. Zheda-Phos for General α -Monoarylation of Acetone with Aryl Chlorides. *Adv. Synth. Catal.* **2013**, *355* (7), 1255–1259.
- (41) Gäbler, C.; Korb, M.; Schaarschmidt, D.; Hildebrandt, A.; Lang, H. Ferrocenyl-Based *P,N* Catalysts for the Mono- α -Arylation of Acetone. *Adv. Synth. Catal.* **2014**, *356* (14–15), 2979–2983.
- (42) Fu, W. C.; Zhou, Z.; Kwong, F. Y. Preparation of a Highly Congested Carbazoyl-Derived *P,N*-Type Phosphine Ligand for Acetone Monoarylations. *Organometallics* **2016**, *35*, 1553–1558.
- (43) Fu, W. C.; So, C. M.; Chow, W. K.; Yuen, O. Y.; Kwong, F. Y. Design of an Indolylphosphine Ligand for Reductive Elimination-Demanding Monoarylation of Acetone Using Aryl Chlorides. *Org. Lett.* **2015**, *17* (18), 4612–4615.
- (44) Ackermann, L.; Mehta, V. P. Palladium-Catalyzed Mono- α -Arylation of Acetone with Aryl

- Imidazolylsulfonates. *Chem. Eur. J.* **2012**, *18* (33), 10230–10233.
- (45) MacQueen, P. M.; Chisholm, A. J.; Hargreaves, B. K. V.; Stradiotto, M. Palladium-Catalyzed Mono- α -Arylation of Acetone at Room Temperature. *Chem. Eur. J.* **2015**, *21* (31), 11006–11009.
- (46) Schranck, J.; Rotzler, J. Valorization of the Primary Building Blocks Ammonia and Acetone Featuring Pd- and Ni-Catalyzed Monoarylations. *Org. Process Res. Dev.* **2015**, *19* (12), 1936–1943.
- (47) Schranck, J.; Tlili, A.; Alsabeh, P. G.; Neumann, H.; Stradiotto, M.; Beller, M. Palladium-Catalysed Carbonylative α -Arylation of Acetone and Acetophenones to 1,3-Diketones. *Chem. Eur. J.* **2013**, *19* (38), 12624–12628.
- (48) Ge, S.; Hartwig, J. F. Nickel-Catalyzed Asymmetric α -Arylation and Heteroarylation of Ketones with Chloroarenes: Effect of Halide on Selectivity, Oxidation State, and Room-Temperature Reactions. *J. Am. Chem. Soc.* **2011**, *133* (41), 16330–16333.
- (49) Green, R. A.; Hartwig, J. F. Nickel-Catalyzed Amination of Aryl Chlorides with Ammonia or Ammonium Salts. *Angew. Chem. Int. Ed.* **2015**, *54* (12), 3768–3772.
- (50) Schranck, J.; Furer, P.; Hartmann, V.; Tlili, A. Nickel-Catalyzed Amination of Aryl Carbamates with Ammonia. *Eur. J. Org. Chem.* **2017**, *2017* (24), 3496–3500.
- (51) Tobisu, M.; Chatani, N. Cross-Couplings Using Aryl Ethers via C-O Bond Activation Enabled by Nickel Catalysts. *Acc. Chem. Res.* **2015**, *48* (6), 1717–1726.
- (52) Yin, G.; Kalvet, I.; Englert, U.; Schoenebeck, F. Fundamental Studies and Development of Nickel-Catalyzed Trifluoromethylthiolation of Aryl Chlorides: Active Catalytic Species and Key Roles of Ligand and Traceless MeCN Additive Revealed. *J. Am. Chem. Soc.* **2015**, *137* (12), 4164–4172.

- (53) Clevenger, A. L.; Stolley, R. M.; Staudaher, N. D.; Al, N.; Rheingold, A. L.; Vanderlinden, R. T.; Louie, J. Comprehensive Study of the Reactions between Chelating Phosphines and Ni(COD)_2 . *Organometallics* **2018**, *37* (19), 3259–3268.
- (54) Cooper, A. K.; Leonard, D. K.; Bajo, S.; Burton, P. M.; Nelson, D. J. Aldehydes and Ketones Influence Reactivity and Selectivity in Nickel-Catalysed Suzuki-Miyaura Reactions. *Chem. Sci.* **2020**, *11* (7), 1905–1911.
- (55) Ge, S.; Green, R. A.; Hartwig, J. F. Controlling First-Row Catalysts: Amination of Aryl and Heteroaryl Chlorides and Bromides with Primary Aliphatic Amines Catalyzed by a BINAP-Ligated Single-Component Ni(0) Complex. *J. Am. Chem. Soc.* **2014**, *136* (4), 1617–1627.
- (56) Diccianni, J. B.; Katigbak, J.; Hu, C.; Diao, T. Mechanistic Characterization of (Xantphos) Ni(I) -Mediated Alkyl Bromide Activation: Oxidative Addition, Electron Transfer, or Halogen-Atom Abstraction. *J. Am. Chem. Soc.* **2019**, *141* (4), 1788–1796.
- (57) Chatt, J.; Shaw, B. L. Alkyls and Aryls of Transition Metals. Part III. Nickel(II) Derivatives. *J. Chem. Soc.* **1960**, No. 0, 1718.
- (58) Khoje, A. D.; Charnock, C.; Wan, B.; Franzblau, S.; Gundersen, L. L. Synthesis and Antimycobacterial Activities of Non-Purine Analogs of 6-Aryl-9-Benzylpurines: Imidazopyridines, Pyrrolopyridines, Benzimidazoles, and Indoles. *Bioorganic Med. Chem.* **2011**, *19* (11), 3483–3491.
- (59) Quasdorf, K. W.; Tian, X.; Garg, N. K. Cross-Coupling Reactions of Aryl Pivalates with Boronic Acids. *J. Am. Chem. Soc.* **2008**, *130* (44), 14422–14423.
- (60) Yue, H.; Guo, L.; Liu, X.; Rueping, M. Nickel-Catalyzed Synthesis of Primary Aryl and Heteroaryl Amines via C-O Bond Cleavage. *Org. Lett.* **2017**, *19* (7), 1788–1791.
- (61) Muto, K.; Yamaguchi, J.; Itami, K. Nickel-Catalyzed C-H/C-O Coupling of Azoles with

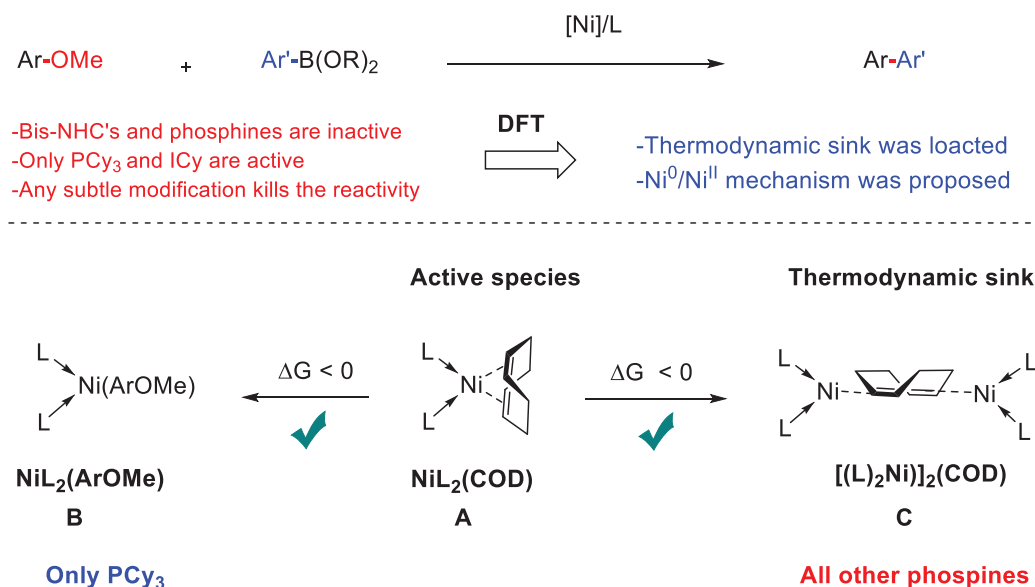
- Phenol Derivatives. *J. Am. Chem. Soc.* **2012**, *134* (1), 169–172.
- (62) Antoft-Finch, A.; Blackburn, T.; Snieckus, V. N,N-Diethyl O-Carbamate: Directed Metalation Group and Orthogonal Suzuki-Miyaura Cross-Coupling Partner. *J. Am. Chem. Soc.* **2009**, *131* (49), 17750–17752.
- (63) Miah, M. A. J.; Sibi, M. P.; Chattopadhyay, S.; Familoni, O. B.; Snieckus, V. Directed Ortho-Metalation of O-Aryl N, N-Dialkylcarbamates: Methodology, Anionic Ortho-Fries Rearrangement, and Lateral Metalation. *Eur. J. Org. Chem.* **2018**, *2018* (4), 440–446.
- (64) Miah, M. A. J.; Sibi, M. P.; Chattopadhyay, S.; Familoni, O. B.; Snieckus, V. Directed Ortho-Metalation of Aryl Amides, O-Carbamates, and Methoxymethoxy Systems: Directed Metalation Group Competition and Cooperation. *Eur. J. Org. Chem.* **2018**, *2018* (4), 447–454.
- (65) He, C.; Guo, S.; Huang, L.; Lei, A. Copper Catalyzed Arylation / C - C Bond Activation : An Approach toward α -Aryl Ketones. *J. Am. Chem. Soc.* **2010**, *132*, 8273–8275.
- (66) Schubert, T.; Kula, M. R.; Müller, M. Chemoenzymatic Synthesis of (S)-8-O-Methylmellein by *Candida Parapsilosis* Carbonyl Reductase. *Synthesis (Stuttg.)*. **1999**, *1999* (12), 2045–2048.
- (67) Fu, W. C.; Zhou, Z.; Kwong, F. Y. Preparation of a Highly Congested Carbazoyl-Derived p,n-Type Phosphine Ligand for Acetone Monoarylations. *Organometallics* **2016**, *35* (10), 1553–1558.
- (68) Duong, H. A.; Gilligan, R. E.; Cooke, M. L.; Phipps, R. J.; Gaunt, M. J. Copper (II)-Catalyzed Meta- Selective Direct Arylation of α -Aryl Carbonyl Compounds. *Angew. Chem. Int. Ed.* **2011**, *50* (2), 463–466.
- (69) Hesp, K. D.; Lundgren, R. J.; Stradiotto, M. Palladium-Catalyzed Mono- α -Arylation of

- Acetone with Aryl Halides and Tosylates. *J. Am. Chem. Soc.* **2011**, 5194–5197.
- (70) Durandetti, M.; Nédélec, J. Y.; Périchon, J. Nickel-Catalyzed Direct Electrochemical Cross-Coupling between Aryl Halides and Activated Alkyl Halides. *J. Org. Chem.* **1996**, 61 (5), 1748–1755.
- (71) CrysAlisPro, v. 1.171.33.46 (Rel. 27-08-2009 CrysAlis171.NET), Oxford Diffraction Ltd. **2009**.
- (72) de Meulenaer, J.; Tompa, H. The Absorption Correction in Crystal Structure Analysis. *Acta Crystallogr.* **1965**, 19 (6), 1014–1018.
- (73) Blessing, R. H. An Empirical Correction for Absorption Anisotropy. *Acta Crystallogr. Sect. A* **1995**, 51 (1), 33–38.
- (74) Altomare, A.; Burla, M. C.; Camalli, M.; Cascarano, G. L.; Giacovazzo, C.; Guagliardi, A.; Moliterni, A. G. G.; Polidori, G.; Spagna, R. SIR97: A New Tool for Crystal Structure Determination and Refinement. *J. Appl. Crystallogr.* **1999**, 32 (1), 115–119.
- (75) Schröder, L.; Watkin, D. J.; Cousson, A.; Cooper, R. I.; Paulus, W. CRYSTALS Enhancements: Refinement of Atoms Continuously Disordered along a Line, on a Ring or on the Surface of a Sphere. *J. Appl. Crystallogr.* **2004**, 37 (4), 545–550.

General conclusion and outlook

The main objectives of this research project were focused on the development and understanding of two types of nickel catalyzed cross-coupling reactions. We carried out experimental investigations on the impact of the ancillary ligands on the reactivity and selectivity of nickel complexes for (i) the cross-coupling of aryl ethers and (ii) the α -arylation of acetone with aryl chlorides and phenol derivatives.

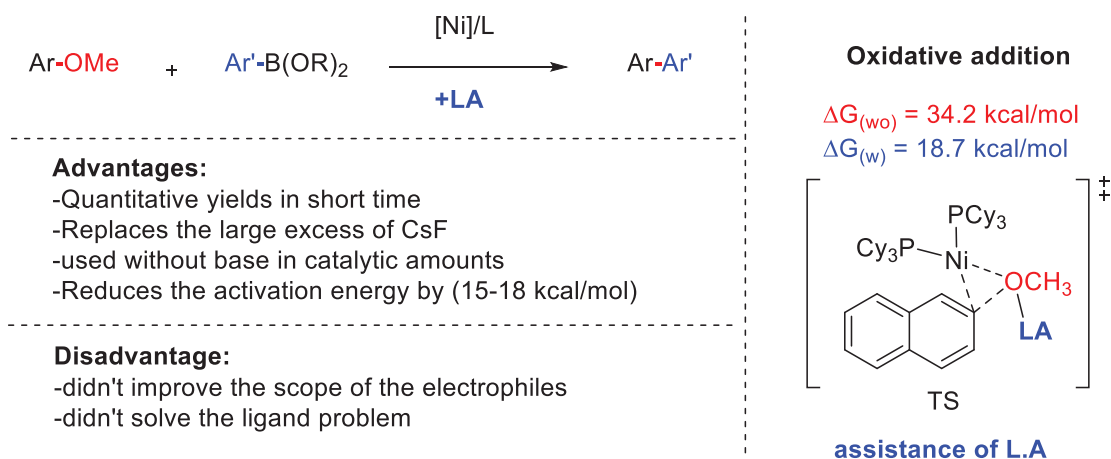
In the first part of the PhD work, the main objectives were to understand the very peculiar role of the ligand in nickel catalyzed cross-couplings of aryl ethers and to explore the influence of Lewis acid co-catalysts in the reactivity of nickel species for the activation of $C_{Ar}-O$ bonds. With these objectives in mind, we investigated the cross-coupling of aryl ethers with organoboron species ($ArB(OR)_2$). The impact of the ligand was first examined by screening a series of mono and bis-NHC ligands as well as several phosphines with various steric and electronic properties. All the screened ligands were completely ineffective, with the exception of previously reported ICy and PCy_3 ligands; S-ICy and Adm-NHC ligands also showed some reactivity. DFT calculations were carried out to gain some insights into the very unique reactivity of PCy_3 among phosphine ligand family. While no significant differences were observed with the other phosphine ligands for the $C_{Ar}-O$ bond oxidative addition pathway, DFT calculations indicated that the key difference occurs during the formation of the active species upon mixing $Ni(COD)_2$ with two equivalent of phosphine in toluene (**Scheme 1**). A thermodynamic sink was found and was shown to inhibit the reactivity of other ligands by forming a dormant species that only PCy_3 ligand can overcome, which provide some explanation on the unique reactivity of PCy_3 as ligand among phosphines.



Scheme 1: Singular reactivity of PCy₃ as ligand may originate from its ability to generate the key L₂Ni(COD) species.

Then we investigated a cooperative Ni/Lewis acid catalytic system, in which the Lewis acid was envisioned to act as a co-catalyst facilitating the activation of the C_{Ar}-O bond. Several Lewis acids were screened as co-catalysts in combination with PCy₃/Ni(COD)₂. Interestingly, we found that the use of catalytic amount of Al(O^tBu)₃ significantly improved the catalytic efficiency for the cross-coupling of aryl ethers with boronate esters. Indeed, this dual catalytic system accelerated the reaction rate and allowed the reaction to be carried out without the requirement of an excess of CsF base (4.5 equiv) used in a previous system. However, the Lewis acid assistance strategy did not allow for an improvement of the scope of the electrophiles used and it could not solve the ligand problem. DFT calculations indicated a significant role of the Lewis acid co-catalyst by decreasing the activation barrier by 18 kcal/mol (**Scheme 2**). Also, the theoretical calculations showed why Al(O^tBu)₃ is the most promising Lewis acid having the strongest Al-O interactions and the best affinity to the substrate. Furthermore, it shows that oxidative addition is achieved using a bis-ligated nickel complex, while reductive elimination takes place through a mono-ligated

one. The calculations were carried out assuming that the reaction proceeds through a $\text{Ni}^0/\text{Ni}^{\text{II}}$ two electrons redox mechanism, but several parameters are not clearly understood yet. Based on DFT calculations, the C-O bond oxidative addition should be a very feasible process in the presence of Lewis acid, but the experimental conditions required are still harsh and the scope of nucleophilic partners very limited. These observations suggest that other mechanisms may take place and further mechanistic studies are still requested in order to discriminate between the different possible scenarios that are proposed in literature.



Scheme 2: The significant role of the L.A in accelerating the reaction and improving the yields.

Despite important synthetic efforts, this part of the PhD work pointed out at the challenges associated with the functionalization of inert C-OMe bonds. Although several cross-coupling reactions have been developed over the last few years with aryl ether electrophiles, as described in the state of the art, the synthetic potential of aryl ethers as electrophiles in cross-coupling reactions still appears as very limited compared to other C-O or C-N based coupling partners. This is mainly due to the lack of precise information on the parameters governing the C-O bond cleavage step. Even if we have confirmed that assistance of Lewis acid is an interesting strategy, the role of Lewis acid in the C-O bond cleavage event remains unclear. The oxidative addition of the C-OMe bond

has not been evidenced yet, despite intense experimental efforts. This raises the question of the occurrence of such step in the recently reported nickel-catalyzed cross-coupling reactions. Our investigations on cross-coupling of aryl ethers with alkenes also corroborate that the oxidative addition of C-O bond does not occur under these conditions. The C-O bond remained intact even in the presence of Lewis acid, some reactivity being observed only in the presence of strong nucleophilic partners, accompanied with the formation of alkene migration and hydroarylation by-products. Intense mechanistic efforts are clearly required before envisioning further synthetic opportunities with aryl ethers as electrophiles.

In the second part, we developed the first nickel-catalyzed mono-selective α -arylation of acetone with aryl chlorides. The combination of $\text{Ni}(\text{COD})_2$ with a Josiphos biphosphine ligand (**L1**) was key to achieve high selectivity and activity for the mono-arylation of acetone. Interestingly, the system was extended effectively to phenol derivatives and we managed to make a direct successful cross-coupling of aryl carbamates and pivalates with acetone via a tandem CO/CH activation strategy. Furthermore, our catalytic system was highly selective for the desired product and was effective with a variety of substrates including complex structures (drugs). Through mechanistic studies, we found a superior 2nd generation air-stable and commercially available Ni^{II} complex that can be easily used and employed by synthetic chemists (**Figure 1**).

Having examined the scope and the complementarity of the nickel-catalyzed α -arylation of acetone methodology, we turned our attention to the reaction mechanism. A $\text{Ni}^0/\text{Ni}^{\text{II}}$ pathway was validated by the isolation and characterization of several key intermediates that were found to be effective in catalysis.

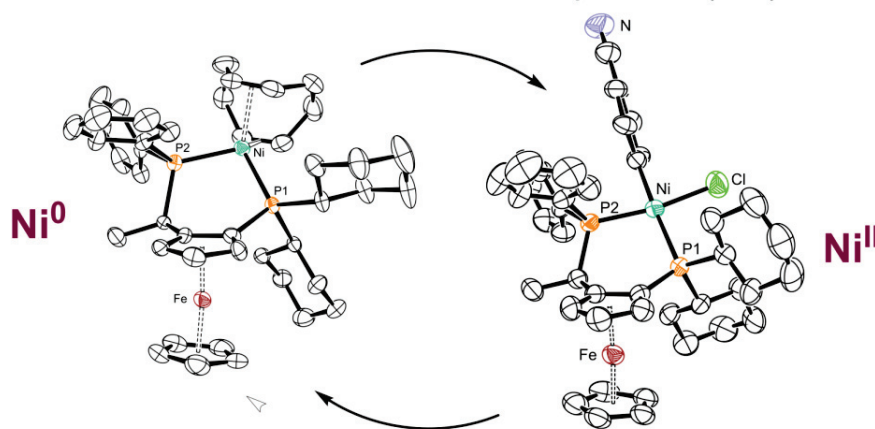


$\text{X} = \text{Hal} \text{ \& \; OR}$

■ No α,α -diarylated products

■ Air-stable $\text{Ni}(\text{II})$ precatalysts

■ Abundant and inexpensive $(\text{Het})\text{Ar}-\text{X}$



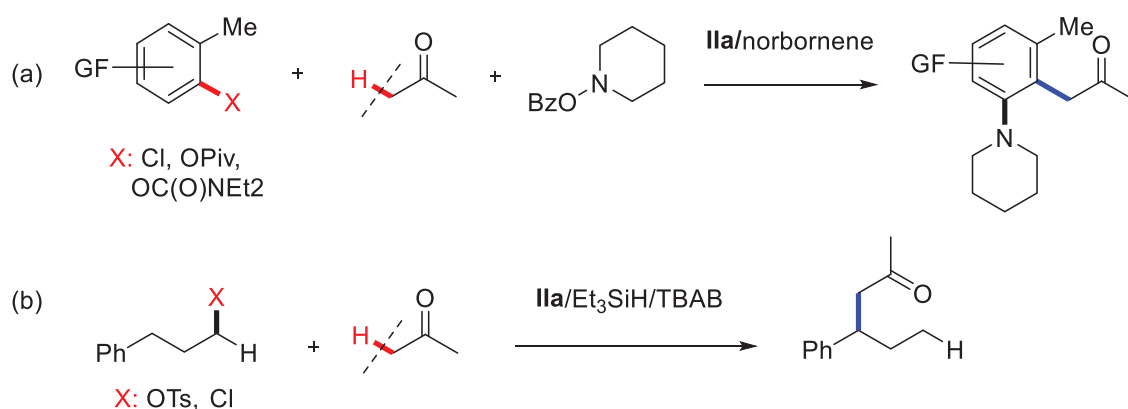
Thermally stable Ni^{II} /Josiphos complexes ensure $\text{Ni}^0/\text{Ni}^{\text{II}}$ cycle

Figure 2: Nickel-catalyzed α -arylation of acetone with aryl chlorides and phenol derivatives.

In the course of our mechanistic investigations, we were able to gain some information on the potential side reactions and deactivation pathways concerning the active pre-catalyst: inhibition of oxidative addition by acetone coordination, decomposition to Ni^{I} species, as well as a better understanding on the role of the ligand and the base.¹ Importantly, these studies also highlighted the synthetic interest of Josiphos-type ligands for nickel catalysis. The high thermal stability of the ensuing Ni^{II} species provides interesting opportunities for cross-coupling reactions that usually require harsh conditions. In addition, the stability of Ni^{II} intermediates towards decomposition to Ni^{I} species may improve catalytic reactions proceeding through $\text{Ni}^0/\text{Ni}^{\text{II}}$ pathways and are intolerant to the presence of Ni^{I} species.

These Ni^0 and Ni^{II} catalytic systems as well as the progressive mechanistic studies enlightened and opened the way for the mono-selective α -arylation of acetone to be implemented for

several other transformations like Ni-catalyzed cascade amination-arylation cross-couplings (**Scheme 3-a**) and remote functionalization (**Scheme 3-b**). These transformations were already established in catalysis but will be very interesting to test with acetone using the nickel/Josiphos catalytic system.^{2,3}



Scheme 3: Outlook for some possible interesting transformations using our developed system.

Unfortunately, our preliminary tests with the developed catalytic systems was not very effective for asymmetric induction. This is probably because of the high bulkiness of the Josiphos ligand and its bulky P(Ph)₂ and P(Cy)₂ substituents that acts as a shield preventing the stereogenic center from interacting with the enolate during the transition state. However, the development of a stereoselective arylation system might be possible by designing and screening similar chiral ligands having chiral centers that are directly connected to the metallic center or by using a less bulkier P(R)₂ groups that have a lower shielding effect and could be more efficient in inducing stereoselectivity.

References

- (1) Abou Derhamine, S.; Krachko, T.; Monteiro, N.; Pilet, G.; Schranck, J.; Tlili, A.; Amgoune, A. Nickel-Catalyzed Mono-Selective α -Arylation of Acetone with Aryl Chlorides and Phenol Derivatives. *Angew. Chem. Int. Ed.* **2020**. Early view (DOI: 10.1002/anie.202006826)
- (2) Fu, W. C.; Zheng, B.; Zhao, Q.; Chan, W. T. K.; Kwong, F. Y. Cascade Amination and Acetone Monoarylation with Aryl Iodides by Palladium/Norbornene Cooperative Catalysis. *Org. Lett.* **2017**, *19* (16), 4335–4338.
- (3) Li, Y.; Luo, Y.; Peng, L.; Li, Y.; Zhao, B.; Wang, W.; Pang, H.; Deng, Y.; Bai, R.; Lan, Y.; et al. Reaction Scope and Mechanistic Insights of Nickel-Catalyzed Migratory Suzuki–Miyaura Cross-Coupling. *Nat. Commun.* **2020**, *11* (1), 1–13.

Résumé

La recherche présentée ci-après intitulée "Couplages croisés catalysés au nickel : activation de liaisons carbone-oxygène et α -arylation de l'acétone" visait à développer et comprendre de nouvelles réactions de formation de liaisons carbone-carbone par catalyse au nickel. Ce travail se décompose en deux parties. La première partie se concentre sur l'activation de liaisons C_{Ar}-O des éthers aryliques et leur couplage avec divers nucléophiles organométalliques et non organométalliques (alcènes, alcynes... etc).

Dans la deuxième partie, nous avons exploré l' α -arylation mono-sélective de l'acétone avec des chlorures d'aryle et des dérivés de phénol catalysée par le nickel. Nous avons pu découvrir un système catalytique permettant le couplage d'une large sélection de chlorures d'aryle, ainsi que de dérivés de phénol. Nous avons ensuite entrepris des études mécanistiques approfondies qui nous ont permis de valider un processus redox à deux électrons Ni⁰/Ni^{II}, expliquer la sélectivité observée et vérifier toutes les voies d'inhibition et de désactivation possibles. Finalement, nous avons développé des performances catalytiques améliorées avec des catalyseurs de Nickel(II) stables à l'air et disponibles dans le commerce.

Abstract

The research presented hereafter entitled "Development of nickel-catalyzed cross-coupling methodologies for the activation of carbon-oxygen bonds and α -arylation of acetone" aimed to develop and understand the formation of new C-C bonds under Ni-catalysis. It was decomposed in two parts. The First part focuses on the activation of C_{Ar}-O bonds of aryl ethers and coupling them with several organometallic and non-organometallic nucleophiles (alkenes, alkynes...etc).

In the second part, we explored the Nickel-catalyzed mono-selective α -arylation of acetone with aryl chlorides and phenol derivatives. We were able to discover a catalytic system allowing the coupling of a wide selection of aryl chlorides, as well as phenol derivatives. We then conducted an in-depth mechanistic studies that allowed us to validate a two-electron redox Ni⁰/Ni^{II} process, explain the observed selectivity and verify all the possible inhibition and deactivation pathways. Finally, we discovered an improved catalytic performance with an air-stable and commercially available Nickel(II) catalyst.